CATALYST DISPERSION AND ACTIVITY UNDER CONDITIONS OF TEMPERATURE-STAGED LIQUEFACTION

DOE/PC/89877--T1

DE93 012402

Final Report

by

Alan Davis, H.H. Schobert, G.D. Mitchell

and L. Artok

PENNSTATE

1855

Coal and Organic Petrology Laboratories

(814) 865-6544

Pennsylvania State University

University Park, PA 16802

ABSTRACT

This research program involves the investigation of the use of highly dispersed catalyst precursors for the pretreatment of coals by mild hydrogenation. During the course of this effort solvent preswelling of the coal was evaluated as a means of deeply impregnating catalysts into coal, active phases of catalysts under reaction conditions were studied and the impact of these techniques were evaluated during pretreatment and temperature-staged liquefaction.

Two coals, a Texas subbituminous and a Utah high volatile A bituminous, were used to examine the effects of solvent swelling pretreatment and catalyst impregnation on conversion behavior at 275°C, representative of the first, low-temperature stage in a temperature-staged liquefaction reaction. Ferrous sulfate, iron pentacarbonyl, ammonium tetrathiomolybdate, and molybdenum hexacarbonyl were used as catalyst precursors. Without swelling pretreatment, impregnation of both coals increased conversion, mainly through increased yields of preasphaltenes. Methanol, tetrahydrofuran, tetrabutylammonium hydroxide, and pyridine were used as swelling agents. In the absence of catalyst, swelling the subbituminous coal before reaction improves conversion by enhancing oil and gas yields; the effectiveness of the solvents in enhancing conversion is in the same order as their swelling ratios. Swelling with methanol or pyridine has little effect on reaction of the bituminous coal, but both tetrahydrofuran and tetrabutylammonium hydroxide treatments increase conversion as a result of higher preasphaltene yields. The combined effect

of catalyst addition and swelling enhances conversion, as much as two-fold, of the subbituminous coal and increases yields of all products. On the other hand, little benefit was obtained by combining catalyst addition and swelling for the bituminous coal, though it is possible to effect changes in the relative amounts of the various products. Tetrabutylammonium hydroxide not removed from the coal after pretreatment appears to decompose to the good solvent tributylamine, suggesting the possibility of using swelling agents as "solvent precursors," first swelling the coal and then thermally decomposing to a strong solvent that is emplaced inside the coal. The action of iron pentacarbonyl is sensitive to the reactive gas atmosphere used; in hydrogen it decomposes to an oxide that mainly facilitates hydrogenation of the heavy products to lighter oils, whereas in hydrogen sulfide / hydrogen mixtures the iron pentacarbonyl is sulfided and mainly facilitates depolymerization of the coal to heavy products. This finding suggests the possibility of tailoring the behavior of the catalyst by appropriate selection of catalyst precursor and reactive atmosphere.

The same two coals impregnated with ferrous sulfate were subjected to temperature-staged liquefaction (30 minutes each at 275° and 425°C) in hydrogen and hydrogen sulfide / hydrogen atmospheres. Addition of H_2S to the reaction gas increased the conversion of both coals, through higher asphaltene yields from the bituminous coal and higher yields of all liquid products from the subbituminous coal. Generally the addition of ferrous sulfate to the coals, followed by liquefaction in hydrogen, had about the same effect as addition of H_2S to the gas, though the systems with added $FeSO_4$ had lower yields of preasphaltenes than obtained by use of H_2S:H_2.

The addition of H_2S to the gas combined with impregnation with $FeSO_4$ provided significant enhancement of conversion of both coals. For both coals the effect of using the two additives together was to enhance the asphaltene yields. The results of this work suggest the possibility of selectively tailoring the behavior of the catalyst in different stages of the liquefaction process by selecting the appropriate gaseous atmosphere.

The two coals were also used to examine the effects of solvent swelling and catalyst impregration on behavior in temperature-staged reactions in H_2 and 5:95 H_2S:H_2 atmospheres. Methanol, pyridine, tetrahydrofuran, and tetrabutylammonium hydroxide were used as swelling agents. Molybdenum-based catalyst precursors were ammonium tetrathiomolybdate, molybdenum trisulfide, molybdenum hexacarbonyl, and bis(tricarbonylcyclopentadienylmolybdenum). Ferrous sulfate and bis(dicarbonylcyclopentadienyliron) served as iron-based catalyst precursors. In addition, ion exchange was used for loading iron onto the subbituminous coal. For most experiments, liquefaction in H_2S:H_2 was superior to that in H_2, regardless of the catalyst precursor. The benefit of the H_2S was greater for the subbituminous, presumably because of its higher iron content relative to the hvAb coal. Tetrabutylammonium hydroxide was the only swelling agent to enhance conversion of the hvAb coal significantly; it also caused a remarkable increase in conversion of the subbituminous coal. The combined application of solvent swelling and catalyst impregnation also improves liquefaction, mainly through increased oil yields from the hvAb coal and increased asphaltenes from the subbituminous coal.

Optical and electron microscopy techniques are employed to evaluate the influence of swelling solvents on coals and the interrelationships between catalysts and coals in the presence and absence of preswelling solvents. These studies help to identify the fact that swelling solvents such as tetrahydrofuran, pyridine and tetrabutylammonium hydroxide can lead to different degrees of coal particle agglomeration, which in turn can negatively affect catalyst dispersion and coal hydrogenation under pretreatment conditions. In the case of tetrabutylammonium hydroxide, reaction products form during contact with the bituminous coal that adversely influence catalyst dispersion and lower conversion. In addition, under two specific conditions catalyst precursors and/or the catalyst active phase is seen to be dispersed at a submicron level and in each of these occurrences conversion and product yields are maximized for the particular catalyst, i.e. ion-exchanged iron on the subbituminous coal and ammonium tetrathiomolybdate added to pyridine preswollen coal. For most other combinations of catalysts and preswelling solvents, the catalyst precursors are found as discrete particles loosely held to the exterior surface of coal particles, or following pretreatment or temperature-staged liquefaction are found as discrete particles either intimately associated with the organic residue fraction or as individual particles. The use of optical techniques to describe catalyst/coal associations, the influence of preswelling agents and the distribution of active catalyst materials throughout liquefaction residues provides the need evidence of the value of catalyst impregnation/distribution on the efficiency of liquefaction.

Finally, cooperative research with Wilsonville and Hydrocarbon Research Incorporated provided study samples from larger scale liquefaction units. In particular, the Wilsonville samples demonstrated that finely divided iron oxide catalyst produce large pyrrhotite aggregates that remain in the reactor section as plugs and wall scales. This serves as a warning that other finely dispersed iron catalysts may contribute to the same problem. Characterization of the HRI and Wilsonville samples showed the propensity for solid carbon formation (mesophase and pyrolytic) during the use of low-rank coals.

TABLE OF CONTENTS

SUMMARY

This program of research was undertaken to investigate whether mild catalytic hydrogenation which results in limited coal solubilization is an advantageous pretreatment for coal liquefaction. Emphasis was placed on the improvements and chemical reactions that may occur during the low-temperature pretreatment stage (275°C). Of particular interest was investigation of the use of highly dispersed catalysts for the pretreatment of coal by mild hydrogenation, the testing and evaluation of methods for improved catalyst impregnation/dispersion that included the use of preswelling solvents, the identification of the active forms of the catalysts under reaction conditions and the establishment of the relative impact on conversion and product yields obtained during temperature-staged liquefaction for two different rank coals (DECS-1, a Texas subbituminous C coal and DECS-6, a Utah high volatile A bituminous coal).

During this study, swelling reagents (methanol, tetrahydrofuran (THF), pyridine and tetrabutylammonium hydroxide (TBAH)) were employed to expand the coal macromolecular network phase during a period when catalyst precursors were added to the system. It was thought that this approach would allow for improved impregnation/dispersion. Molybdenum- and iron-based, water- and organic-liquid soluble catalysts were used including ammonium tetrathiomolybdate (ATTM) [also insoluble molybdenum trisulfide], molybdenum hexacarbonyl, bis(tricarbonylcyclopentadienylmolybdenum) (CPMC), ferrous sulfate, iron pentacarbonyl and bis(dicarbonylcyclopentadienyliron)

(CPIC). Both pretreatment (275°C, 30 min) and temperature-staged (275°C, 30 min; 425°C, 30 min) liquefaction experiments were conducted in hydrogen and/or hydrogen sulfide:hydrogen (5:95) atmospheres.

The physical effect of preswelling solvents on each coal was studied by optical techniques and showed that methanol had no or little influence. However, preswelling with THF and pyridine (being stronger solvents) resulted in separation of solvent-soluble fractions that were found as coatings on coal-particle surfaces and that were responsible for some level of particle agglomeration. A greater amount of extract was produced from the bituminous coal using pyridine and the least amount produced from the subC coal when THF was used. The use of 10% TBAH with the subC coal provided the only evidence of true large-scale swelling of a coal, corresponding with the highest swelling ratio measured. For the hvAb coal, optical microscopy revealed that TBAH reacted with the outer edges of the coal particles (vitrinite) leaving behind a tacky, pitch-like reaction product that promoted significant agglomeration. Particle agglomerates were observed in most of residues following pretreatment catalytic liquefaction. Agglomerate particles which endured the preswelling/ impregnation procedure may have negatively influenced catalyst dispersion as well as mass transport of hydrogen during the reaction.

In the case where swelling solvents were not employed, impregnation of both coals with catalyst precursors increased conversion at 275° mainly as a result of increased preasphaltenes yield. Catalyst precursors that were not sulfided before impregnation were less effective in a hydrogen

atmosphere compared to when H_2S was added to the system. The molybdenum catalyst typically outperformed the iron catalyst during pretreatment liquefaction, except in the case of $Fe(CO)_5$ in an $H_2S:H_2$ atmosphere for the subC coal. The reason for this response was that ferrous sulfate, and to some degree $Fe(CO)_5$ did not convert to an active sulfide phase in H_2 at 275°C. For the molybdenum catalyst, $Mo(CO)_6$ in $H_2S:H_2$ performed better than ATTM. In the absence of catalyst, swelling of the subC coal before liquefaction improved conversion, with the increase resulting mainly from additional oil+gas yield. The relative effectiveness of various solvents for improving conversion was in the same general order as their effectiveness in swelling the coal. Preswelling with methanol or pyridine had little effect on pretreatment liquefaction of hvAb coal, but both THF and TBAH provided increased conversion as a result of improved preasphaltene yields. With this coal, the effectiveness of solvents at improving liquefaction was not in the same order as their ability to swell the coal, perhaps a direct result of the higher level of particle agglomeration experienced with the hvAb coal. The combined effect of catalyst addition and swelling with TBAH was to double the conversion of the subC coal. The yields of all products also were enhanced. In contrast, little improvement in total conversion of the hvAb coal was obtained by combining catalyst impregnation and solvent swelling, but changes in the relative proportions of the products were obtained.

The results with $Fe(CO)_5$ in the different gas atmospheres were noteworthy because they suggested the possibility of tailoring the catalyst

action to the characteristics of the coal and the kind of transformations desired. With impregnated $Fe(CO)_5$, an H_2 atmosphere promoted the hydrogenation of asphaltenes and preasphaltenes to oils, whereas use of a H_2S:H_2 atmosphere increased conversion to asphaltenes and preasphaltenes. Thus, the choice of atmosphere (H_2 vs H_2S:H_2) provides the opportunity of generating an active catalyst that acts either for coal breakdown or for shifting the product slate to lighter materials.

Investigation of catalyst impregnation of solvent-swollen or moist coals with SEM demonstrated that ferrous sulfate and ATTM form only surface dispersions. Pretreatment in methanol or THF appeared to have little influence on improved impregnation. Impregnation with ATTM before and after solvent swelling with methanol and THF resulted in a surface dispersion. Aggregates of small crystals were observed on the surface of single particles and on particulate samples. Molybdenum and sulfur peaks were not detected in areas where these crystals were absent. Molybdenum was found to be dispersed on a submicron level following preswelling of both coals with pyridine and impregnation with ATTM. A uniform dispersion of molybdenum was latter confirmed in the residues from temperature-staged liquefaction. The positive influence of pyridine on the dispersion of molybdenum catalysts may be the reason for some improvement in conversion with the subC coal. Particle agglomeration resulting from pyridine preswelling may have reduced conversion for the hvAb coal under pretreatment conditions.

Another benefit of solvent swelling could be the formation of good solvent inside the coal. In most cases, preswelling in TBAH greatly influenced conversion of the subC coal with all catalysts and was unpredictable with the hvAb coal, probably owing to the severe particle agglomeration it caused. During this investigation it was found that thermal decomposition of TBAH resulted in the formation of tributylamine which, as with other amines, may be a very good promoter of coal liquefaction. The use of a good swelling agent as a "solvent precursor", with subsequent in-situ generation of a good extractive solvent, could increase the amount of mobile phase moving out of the coal and reduce its viscosity. In addition, combining an excellent hydrogen donor (tetrahydroquinoline) into the same molecular species as a catalyst precursor facilitates hydrogenation by keeping the donor in, or near, the catalyst. Hence the prospect exists for future developments of combined "solvent-and-catalyst precursors".

It is important to recognize that the first-stage liquefaction may produce changes in coal structure or behavior that significantly enhances conversion in the second, high-temperature stage, but which are not necessarily evident in the macroscopic characteristics of the products of the first stage. That is, a particular coal-catalyst-solvent combination may provide small conversions or yields of soluble products at the end of the first stage, yet may have experienced subtle changes of structure which then facilitate significant conversion in the second stage. Hence the ultimate assessment of the utility of catalyst impregnation, solvent

swelling, or both in improving liquefaction behavior in temperature-staged processes is through determination of conversions and product yields at the end of the second stage.

Generally, results from temperature-staged liquefaction of two coals of different rank, two gas atmospheres, seven catalyst precursors, and four swelling solvents demonstrates that the key to high conversion, and high oil yield, was to increase hydrogen utilization. The effect of sulfided catalysts in temperature-staged liquefaction was mainly to increase conversion via formation of relatively heavy liquids (asphaltenes and preasphaltenes), whereas hydrogenation catalysts had little effect on conversion, but rather facilitated conversion of those liquids which did form into lighter products.

For the bituminous coal, high conversions were attained by impregnating the coal with a molybdenum-based catalyst precursor. If the precursor was already sulfided (ATTM), a hydrogen atmosphere was adequate. However, if the precursor was not sulfided, then liquefaction in a H_2S:H_2 atmosphere was necessary. Although solvent pretreatment did not dramatically increase conversion relative to untreated samples, it was sufficient to gain an extra ≈5% in conversion, especially when using pyridine as the treatment solvent. For the subC coal, the highest conversions (89%) were obtained with ATTM impregnation and solvent pretreatment with pyridine or TBAH, enhancing conversion by ≈10% relative to otherwise similar experiments performed without solvent pretreatment. Also, the nitrogen-containing solvents seemed effective at suppressing

formation of CO_x gases. In contrast to the bituminous coal, the organometallic molybdenum-containing precursors gave very good conversions (84–86%) without using H_2S.

For the bituminous coal, the conditions favoring high oil yields were essentially those that also favored high conversions,i.e., molybdenum-based precursors, either already sulfided or reacted in H_2S:H_2 and with solvent pretreatment. The use of organic solvents enhanced oil yields by up to 10% relative to reaction at the same conditions without solvent. The highest oil yields, 42–43%, were obtained with pyridine pretreatment and ATTM in H_2 or CPMC in H_2S:H_2. Little or no benefit was observed for oil yields by solvent pretreatment of the subC coal. Sulfided molybdenum catalysts were generally best at providing high oil yields.

Remnants of ATTM were found as large discrete particles following temperature-staged runs where no swelling solvents were employed. However, swelling in pyridine had a significant influence on catalyst dispersion during temperature-staged reaction. X-ray maps of the remnants of organic agglomerates in the bituminous coal residues showed a uniform submicron distribution of Mo and S. With respect to MoS_2 the catalyst was deficient in sulfur. Finely dispersed Mo was also observed in a temperature-staged residue of the unswollen hvAb coal reacted in the presence of $Mo(CO)_6$ and H_2S:H_2. Microanalysis of areas within the remnant organic fraction suggested that the Mo was fully sulfided to MoS_2, demonstrating the importance of the presence of H_2S during liquefaction.

Although total conversion was not quite as high, reaction of the subC coal with ion-exchanged iron in $H_2S:H_2$, gave an oil yield quite comparable to those obtained with molybdenum catalyst precursors. Inspection of the ion-exchanged coal using X-ray mapping techniques showed that iron was uniformly dispersed and impregnated throughout most coal particles. This observation provides clear evidence of the positive benefits of uniform catalytic dispersion/impregnation upon liquefaction. The level of ion-exchange attained by simple contact of the moist subC coal with a ferrous sulfate solution was not as effective, and conversion and product yield suffered.

As with $Fe(CO)_5$ during pretreatment liquefaction, our results with ferrous sulfate suggest a strategy for tailoring the activity of the impregnated catalyst for temperature-staged liquefaction. Liquefaction in H_2 with $FeSO_4$ provided little improvement in conversion but rather increased yields of lighter products. For a coal which easily undergoes decomposition to liquids even in the absence of catalysts, the H_2-$FeSO_4$ combination improved the product slate. On the other hand, coals which require a dissolution catalyst to facilitate decomposition to liquids, the addition of small amounts of H_2S to the gas phase, in concert with impregnated $FeSO_4$, can significantly improve conversion relative to that obtained with $H_2S:H_2$ or with $FeSO_4$ alone. The effect of H_2S is not only to promote liquefaction itself; it is also effective in transforming catalyst precursors to their active forms. $FeSO_4$ is quite stable, and it can not be decomposed up to 540°C in N_2. H_2 alone is unable to transform it

completely to pyrrhotite at typical liquefaction temperatures. The additional sulfur made available to the reaction system from the added H_2S may be necessary to transform $FeSO_4$ completely to pyrrhotite, which is believed to be the active catalyst, at these conditions.

Because increases in conversion and product yields clearly result from addition of $FeSO_4$ in either a H_2 or H_2S:H_2 atmosphere, the $FeSO_4$ precursor converts to a catalytically active species in either case. However, the specific behavior of the resulting catalytically active species is different, depending on the chosen gas atmosphere. Thus with H_2, large increases in conversion were not obtained, but there seemed to be a shift in the product slate to favor lighter materials. The ability to tailor the effect of impregnated $FeSO_4$ by sulfiding or not sulfiding, suggests that some benefits might also be realized by having the catalyst in different forms in the different stages of liquefaction.

Another facet of our investigation was designed to promote cooperation between our program and other Advanced Research and DOE-sponsored research efforts in catalytic coal hydrogenation. Through this cooperative effort our program contributed microscopic characterization techniques for those contractors involved in generating materials in larger scale hydrogenation experiments than our own, i.e., Wilsonville and Hydrocarbon Research, Inc. (HRI).

As part of our cooperative research effort, samples of vessel plug and reactor deposit materials were obtained from the Wilsonville Pilot Plant. These deposit samples accumulated during Runs 258 and 260 in which

subbituminous coals (Spring Creek and/or Black Thunder) and a disposable iron oxide catalyst with sulfiding reagents were being fed to the reactor. Accumulation of materials in the thermal reactor, the interstage separator vessel and the pipe connecting the two vessels caused unscheduled outages during Run 258 and extensive clean-up following Run 260.

Our investigation showed that the deposits formed during operation with Spring Creek coal resulted from the deposition of process-derived calcium carbonate (calcite), whereas materials from operations with the Black Thunder coal resulted from a combination of mesophase-derived carbon and calcium carbonate. One common mineral phase observed in all samples was pyrrhotite ($Fe_{1-x}S$), which was found in slightly lower or equal concentration to the carbonate phase. Pyrrhotite was observed in both individual (<2 μm) particles as well as aggregates (reactor solids) exceeding 140 μm. The origin of this pyrrhotite was most certainly from sulfidization of the disposable iron oxide catalyst as analysis of the feed coals showed less than 0.1% pyritic sulfur. The change in mass during sulfidization and the tendency for aggregation of the sulfide suggests a mechanism for pyrrhotite retention in the reactor and interstage separator vessel. The tendency for iron-based catalysts to aggregate into large particles capable of remaining in the reactor section during continuous-flow liquefaction is an important problem which has yet to be addressed.

Deposits also accumulated during Run 260 in which the subbituminous Black Thunder mine coal was being reacted in a catalytic/thermal mode with lower first-stage and higher second-stage temperatures. Materials only

accumulated in the second-stage thermal reactor at the bottom and as deposits on the wall and the outside and inside of the ebullating suction line. We found that the deposits were mainly formed as a result of the formation and accretion or deposition of calcium carbonate with the other available process- and coal- derived inerts. Formation of mesophase-derived carbon was minimized, but there was a proportionally greater amount of secondary vitroplast observed. This suggests that the process conditions selected by Wilsonville to eliminate retrogressive coking reactions were effective in reducing mesophase production, but did not totally alleviate the production of insoluble organic inerts. Furthermore, the larger problem of the formation of process-derived calcium carbonate may not be addressed by altering process conditions, but may require the reduction of organically bound calcium ions before liquefaction.

Additional petrographic work also was completed for HRI in two specific studies that included analysis of feed coals and residues from Illinois #6 which had been cleaned using an oil agglomeration technique and evaluation of the nature of deposit materials taken from a recycle gas-feed line.

Petrographic analysis of the feed coals and residues of HRI Run CC-6 indicated that very little reactive material (vitrinite) remained unconverted following runs with uncleaned Illinois #6 feed coal, with feed coal cleaned by oil agglomeration, or under more severe processing conditions. Reduction in the proportion of lowest reflecting residual material following the more severe processing conditions may indicate that

not only had the vitrinite undergone a slightly improved dissolution, but also that some of the lower reflecting semifusinite may have undergone hydrogenation.

With regard to the deposit material, the question posed by HRI was, "is the deposit a coke material carried from the recycle gas preheater or a coal derived material back-washed from the reactor?" About 60% for the material appeared to be coal derived whereas the remainder was anisotropic carbons that could have been derived by coking of liquid products. It is also possible that some unknown portion may also represent pyrolytic carbon formation, and that some direct coking of undissolved coal particles may have been involved.

In summary, this research program has shown a profound influence of swelling reagents on catalytic and non-catalytic pretreatment and temperature-staged liquefaction of two different rank coals. However, the investigation has demonstrated that improvements in conversion and product yields were not totally in response to coal swelling and deep impregnation of catalyst, but, in some cases, resulted from the physical effects of the solvent on the coals and catalysts, i.e., separation of solvent-soluble fractions, solvent-precursor materials, influence of solvents on the catalyst materials, etc. In other cases, it was shown that solvent interaction was detrimental to improved liquefaction, such as enhanced particle agglomeration in preswollen coals. In a number of specific liquefaction tests, we were able to demonstrate the relative benefits of catalyst impregnation on conversion. For individual catalysts, the best

liquefaction results were obtained when the catalysts were dispersed at a submicron level before or after reaction. In addition, there was some evidence that a uniform surface dispersion of fine catalyst particles resulted in better performance than a heterogenous dispersion of large catalyst particles. However, as suggested from our evaluation of Wilsonville deposit materials, no matter how finely dispersed a catalyst may be, during continuous-flow liquefaction they may tend to aggregate and ultimately become a detriment to operations.

1. INTRODUCTION

The benefits of liquefaction catalysts have been well documented [Anderson et al. 1985; Tomlinson et al. 1985], and include improvement in overall levels of conversion, increased yields of distillates and reduction of asphaltenes and gases, lower viscosity of the products, and reduction in severity of operating conditions. However, there is much about catalyst activity and reactivity that is unknown, particularly when combined with coal. Derbyshire [1988] has divided liquefaction catalysts into two classes, eg., dissolution and supported. Dissolution catalysts (used in this project) are employed to promote the breakdown of the coal structure to liquid products, whereas the supported catalysts are used predominantly for upgrading the dissolution products.

Various types of molybdenum- and iron-based dissolution catalysts have been used in the role of catalyst precursors to effect improvements in coal conversion and product yields. The precursors are catalyst materials which when added to coal may have little inherent activity, but under coal liquefaction conditions undergo chemical changes along with the coal to develop activity with regard to hydrogenation and prevention of condensation and aromatization. One of the most important properties of precursor catalysts is their solubility in water or organic liquids such that they can be readily dispersed onto or impregnated into coal surfaces. Studies by Weller and Pelipetz [1951] and Shibaoka et al. [1980] clearly demonstrated the advantages of having metal salts impregnated into the coal rather than admixed as a powder during coal hydrogenation. However, this

has lead to the untested assumption that slurrying coal in aqueous catalysts results in effective penetration of the coal pore structure. Davis et al. [1989] provided evidence that aqueous "impregnation" of a thiomolybdate catalyst on coals only caused a surface dispersion that could be mechanically stripped from the surface during processing.

The effectiveness of catalyst precursors is not only dependent upon the degree of dispersal and association with coal surface, but on the final stoichiometric form, as well as the time and temperature regime under which the catalyst becomes active. Examples are given in the literature regarding the transformation of thiomolybdate salts or molybdenum carbonyl to molybdenum disulfide (MoS_2) and the conversion of sulfates, oxides or carbonyl of iron to pyrrhotite ($Fe_{1-x}S$) during hydroliquefaction. Transformation of these precursors require the presence of a source of sulfur (either added or derived from sulfur in the coal) and is usually accompanied by an increase in the partial pressure of H_2S in the offgas. Work in this laboratory [Garcia and Schobert, 1989] showed that an imperfectly sulfided ammonium molybdate acted as a better catalyst than "reagent grade" ammonium tetrathiomolybdate (ATTM) or powdered MoS_2. Derbyshire [1988], citing other workers, concluded that the active form for molybdenum may not be MoS_2, but it could be a non-stoichiometric form, the exact composition of which is influenced by the partial pressure of H_2S. Previous work in this laboratory suggested an incomplete conversion of ATTM to MoS_2 which resulted in an excess of sulfur under the reaction conditions used during coal hydrogenation. The work of Cypres et al. [1981] suggested

that neither pyrite or pyrrhotite, an already non-stoichiometric form of iron sulfide, could dissociate hydrogen under liquefaction conditions leading Lambert [1982] to the conclusion that H_2S was responsible for the observed catalytic effects. Therefore, for both catalyst precursors some doubt remains regarding the activity of the resultant catalyst sulfide. It may be that the intermediate products during catalyst conversion or their interaction with H_2S during the conversion result in more activity than the beginning or final forms.

Temperature-staged liquefaction using catalyst precursors is another technique which has been shown to improve net conversion of coal to liquids and gases [Comolli et al. 1985]. This strategy seeks to accommodate the known structure of coal and the capabilities and limitations of the catalyst by hydrogenating coal at two temperatures; a low-temperature stage of 275-375°C followed by a high-temperature stage at 375-450°C. Derbyshire [1986a] suggested that during the low temperature stage coal structure could be partially broken down, increasing the content of extractable liquids which could act as potential H-donor species during the high-temperature stage. Weaker bonds also might be broken and stabilized by H-transfer at low temperature, thus reducing the potential for condensation reactions during subsequent higher severity reactions. The combination of low-temperature catalytic reaction followed by the high-temperature catalytic reaction had the greatest influence in improving both product selectivity and conversion [Derbyshire 1986b]. However, in spite of the apparent advantages of using a catalytic low-severity pretreatment stage,

few chemically significant changes have been observed in the residues [Davis et al. 1988].

With these thoughts in mind, the experimental program covered by this project has focused upon the development of more effective methods of impregnating coal with catalysts, evaluating the conditions under which the catalysts are most active and establishing the relative impact of improved impregnation on conversion and product yields obtained from temperature-staged liquefaction. However, emphasis has been placed on the improvements and reactions occurring during the low-temperature, pretreatment stage (275°C). To achieve these goals our general objectives have been 1) to investigate the use of highly dispersed catalysts such as ammonium tetrathiomolybdate, molybdenum hexacarbonyl, iron sulfate, iron pentacarbonyl for the pretreatment of coal by mild hydrogenation, 2) to develop and evaluate methods for improving catalyst impregnation that includes the use of preswelling solvents (methanol, tetrahydrofuran, pyridine and tetrabutylammonium hydroxide), 3) to identify the active forms of the catalysts under reaction conditions and 4) to clarify the mechanisms of catalysis. Therefore, the ultimate objective was to ascertain if mild catalytic hydrogenation resulting in very limited coal solubilization is an advantageous pretreatment for the transformation of coal into transportable fuels.

2. COAL SELECTION

Coal samples selected for this study from the Penn State Sample Bank were to have high vitrinite content and low ash and sulfur values. The coals were to be of relatively low and different rank, i.e., lignite and high volatile C bituminous. An initial set of coals [PSOC-1503, Blind Canyon, Utah hvBb; PSOC-1444, Texas lignite] were selected based on these limitations and because they were schedule to be freshly re-collected as part of another DOE project [DECS-6, Blind Canyon hvAb; DECS-1, Texas subC]. Detailed physical, chemical and elemental characteristics of the four coals are given in Appendix A and are summarized in Table 1.

Comparison of analytical data between the old and freshly collected samples revealed differences in the ASTM rank and petrographic composition for both coals even though the new samples were collected from the same seam and general locality. ASTM apparent rank is determined using moist mineral-matter free calorific value calculated using as-received moisture. When searching for coals from the Sample Bank, the calorific value determined using equilibrium moisture was employed for rank determination. Differences in ASTM apparent rank and the rank determined by using the equilibrium moisture value accounted for the freshly collected Blind Canyon sample having a rank of hvAb and the lignite having a rank of subC (Appendix A).

Petrographic composition also varied for both samples; the original Blind Canyon sample (PSOC-1503) contained slightly more than 91% vitrinite whereas the new sample (DECS-6) had about 69%. In part, this significant

Table 1. Coal properties

Penn State Sample Number	PSOC-1503	DECS-6	PSOC-1444	DECS-1
Seam	Blind Canyon	Blind Canyon	Unnamed	Bottom
State	Utah	Utah	Texas	Texas
ASTM Apparent Rank	hvBb	hvAb	Sub C (lignite)	Sub C
Date Sampled	10/11/85	6/7/90	3/30/85	12/11/89
Mean-Maximum Reflect. of Vitrinite, $R_o max$, %	0.62	0.66	0.45	0.35
Ultimate Analysis (%daf)				
Carbon	80.41	81.28	74.29	74.27
Hydrogen	6.14	6.24	4.85	5.64
Oxygen	11.34+	10.50+	18.07+	17.45+
Nitrogen	1.54	1.55	1.38	1.46
Total Sulfur	0.56	0.42	1.41	1.18
Proximate Analysis (a.r.%)				
Moisture	10.35	4.73	31.91	30.00
Volatile Matter	41.89	42.40	29.55	33.18
Fixed Carbon	44.25	47.31	27.07	25.75
Ash	3.51	5.56	11.47	11.07
Petrographic Composition (mineral-free, % vol)				
Vitrinite	91.1	69.1	84.7	78.4
Liptinite	1.2	17.3	1.5	14.9
Inertinite	7.7	13.6	13.8	6.7
Gieseler Fluidity				
Maximum Fluidity (ddpm)	2	3	No Fluidity	No Fluidity
Fluid Range	39	38		
Initial Softening T°C	400	400		
Resolidification T°C	439	438		
Maximum Fluidity T°C	422	419		

+ By difference

discrepancy results from a more accurate determination of the liptinite content (using blue-light microscopy), and in part because the new sample had a higher inertinite content resulting from local variation in composition. For the Texas subC sample, a significantly greater amount of liptinite (proportionally less inertinite) was found in the new sample (DECS-1) and the huminite (vitrinite) maceral shifted from being predominantly ulminite in the PSOC-1444 to humodetrinite in the DECS-1 sample. These changes in petrographic composition are not expected to influence total conversion of either coal during catalytic liquefaction, but the higher liptinite content may result in slightly different product yields.

3. SWELLING PRETREATMENT OF COALS FOR IMPROVED CATALYTIC LIQUEFACTION

3.1. INTRODUCTION

It has been known for some time that improvements in catalytic liquefaction can be obtained by having the catalyst or catalyst precursor (i.e., a compound that would decompose to an active catalyst under reaction conditions) impregnated into the coal rather than simply mixed with the coal as a powder [Weller and Pelipetz, 1951]. Having catalyst particles present at the sites of bond cleavage in the coal structure facilitates hydrogenation; away from the vicinity of the catalyst both carbonization and cracking to gases will be favored [Hawk and Hiteshue, 1965]. Hence both the total liquid yield and product quality improve as the extent of catalyst dispersion improves. The use of red mud and supported cobalt-molybdenum catalysts in liquefaction of bituminous coals was effective only when there was a rapid plasticizing of the coal and generation of hydrogen donor species, because these catalysts could not be effectively dispersed through the coal [Bodily et al., 1981]. Prior work in these laboratories has demonstrated the effectiveness of impregnating a water-soluble sulfided ammonium molybdate into coal before liquefaction [Terrer and Derbyshire, 1986; Stansberry and Derbyshire, 1988]. Impregnated ammonium thiomolybdates were more effective catalysts for liquefaction and hydrodesulfurization of Spanish lignite than admixed molybdenum disulfide, a fact attributed to the superior dispersion of the soluble molybdenum salts relative to that obtained from the insoluble disulfide [Garcia and Schobert, 1989].

Hawk and Hiteshue [1965] cited results in which ammonium molybdate was effective for liquefaction of Wyoming subbituminous coal regardless of whether it had been dispersed in aqueous solution or not. In this case the liquefaction solvent could itself act as the vehicle for impregnating the catalyst, even though the salt would be essentially insoluble in the organic solvent. Dispersal of the catalyst by the vehicle has been invoked as a reason for the improved activity (though it must be recognized that solvent-catalyst interactions may also be an important factor). The dispersal of metal halide catalysts was achieved more effectively with methanol and acetone than with aqueous solutions [Bodily and Wann, 1986]. A further approach to improve catalyst dispersion involves using metal salts of organic compounds or organometallic compounds. Thus oil-soluble metal naphthenates were very effective catalysts even at quite low (e.g., 0.01%) metal loadings [Hawk and Hiteshue, 1965]. Iron pentacarbonyl, which is soluble in organic media, is considered to penetrate readily the pore structure of coals and decompose to finely dispersed metallic iron or iron sulfide [Suzuki et al., 1985; Watanabe et al., 1984; Tierney et al., 1988].

Besides affecting catalyst behavior by dispersion, the activity of a catalyst may be varied by structural modification of the coal. In this way, the hydrogenation and dissolution activity of the catalyst can be promoted, because the weakened structure could be more susceptible to hydrogenation and depolymerization reactions. One way to modify coal structure is solvent swelling. The coal network can be swollen using appropriate solvents, leading to expansion of the pores. Swelling may

facilitate impregnation of catalysts or their precursors and diffusion of reagents to the reactive sites of coal. Therefore, it can be presumed that swelling as a pretreatment operation may increase conversion and quality of yield obtained from liquefaction. Rincon and Cruz [1988] found that the conversion of a Colombian coal increased when it was swollen with tetrahydrofuran (THF). Joseph [1991] determined a direct correlation between the extent of preswelling and the conversion of coal under liquefaction conditions. Baldwin and co-workers [1991] also confirmed the beneficial effect of solvent swelling on coal liquefaction by obtaining better yield quality for the THF-swollen Illinois No. 6 coal.

Temperature-staging of liquefaction involves reaction at two temperatures, an initial low-temperature (275-350°C) stage, followed by further reaction at higher temperature (375-450°C). The first, low-temperature stage is sometimes considered to be a pretreatment, since most of the desirable liquid products are still formed in the higher temperature stage. This strategy is known to improve net conversion to liquids, relative to operation at a single temperature, and selectively improves the yield of oils at the expense of asphaltenes without an attendant increase in gas production [Comolli et al., 1985]. During the low-temperature stage, partial depolymerization of the coal could increase the amount of extractable liquids and the coal fluidity [Derbyshire et al., 1986a]. Weaker bonds might be broken and stabilized by hydrogen transfer at low temperature, reducing the potential for retrogressive condensation reactions at higher temperature. Thus effective hydrogenation at the mild

reaction conditions of the first stage may minimize condensation reactions. With low-rank coals, improvement in conversion to soluble products is also aided by the loss of carboxyl groups without formation of crosslinks [Solomon et al., 1991]. Combination of a low-temperature catalytic liquefaction step with a higher temperature catalytic reaction significantly improved product selectivity concomitant with attaining the highest conversion [Derbyshire et al., 1986b]. Although a catalytic low-severity first stage, using an impregnated molybdenum catalyst, provided processing advantages relative to single-stage reactions, few chemically significant changes were detected in the residual materials [Davis et al., 1988].

In this section, we report results of the use of various types of iron and molybdenum catalyst precursors. This aspect of the study involved an examination of the effects of impregnation of the catalyst onto the coal, the effects of swelling the coal prior to reaction, and the combined effects of swelling and catalyst impregnation. The focus of the work discussed in this section was on improvements to be obtained in the first, low-temperature (or pretreatment) stage; consequently all results reported in the first section of this report are for reactions at a pretreatment temperature of 275°C. In succeeding sections we will discuss results obtained from temperature-staged reactions.

3.2. EXPERIMENTAL

3.2.1. Coal Sampling and Initial Swelling Ratio Determination

The coals were chosen from recent additions to the DOE/Penn State Coal Sample Bank and Data Base. Samples of Blind Canyon high volatile

bituminous coal (PSOC-1503 and DECS-6) and a Texas subbituminous C (PSOC-1444 and DECS-1) were used. For both of the coals, the respective PSOC and DECS samples were collected at different dates. The sources and analyses of the coals are given in Table 1 and Appendix A. The coals were ground without drying to minus 60 mesh and stored under a N_2 atmosphere. One gram of air-dried coal (PSOC-1444 and PSOC-1503) was placed in a 15 mL conical graduated screw-top centrifuge tube and centrifuged at 2900 rpm for 10 minutes. The height of the coal in the tube was recorded in mL/g. Twelve mL of solvent (methanol, pyridine, tetrahydrofuran, or tetrabutylammonium hydroxide) was added to the coal in two increments. The first 6 mL was combined with the coal and the mixture was stirred carefully until all the coal particles were wetted, then the remaining solvent was added and the tube was sealed with a cap. After 6-30 h, the tube was centrifuged again at 2900 rpm for 10 min and the height was recorded. The volumetric swelling ratio is defined as $Q = h_2/h_1$, where h_1 = height of unswollen coal and h_2 = height of swollen coal. (It should be noted that the solvent swelling studies were performed on the older, PSOC coals, while the reactivity experiments, discussed below, were performed using newer, DECS samples (also see Section 6.3.1).)

3.2.2. Swelling of Coals Prior to Liquefaction

The coal samples (DECS-1 and DECS-6) were swollen using methanol, pyridine, THF and 10% tetrabutylammonium hydroxide (TBAH) solution (1:1 (w/w) ratio water:methanol mixture). The coal samples, which were predried at 110°C in vacuum, were mixed with the swelling reagent to give a solvent-

to-coal ratio of about 3:1 and were stirred for 6 h under N_2. The solvent was removed and dried at 50°C in vacuum, except in the case of pyridine, where the sample was dried at 100°C in vacuum in an attempt to remove pyridine completely. Based on the increased nitrogen content of the samples after pyridine treatment, the pyridine incorporation after drying was in the range of 2-10%. For TBAH swelling, a TBAH solution was added to undried coal and only methanol and water of the mixture were removed, so that TBAH was retained in the swollen coal.

3.2.3. Catalyst Preparation and Testing

Ammonium tetrathiomolybdate, $(NH_4)_2MoS_4$ (ATTM), was synthesized in our laboratory following the procedure of Naumann [1981]. In summary, 20 g ammonium heptamolybdate, $(NH_4)_6Mo_7O_{24}\cdot 4H_2O$ and 20 mL NH_4OH are added to 100 mL deionized water and cooled to ≈5°C in an ice bath. H_2S is bubbled through the solution until an initial yellow precipitate turns red; the flow is continued for an additional 30 min. The precipitate is filtered, washed with EtOH, and dried in vacuum at room temperature. MoS_3 was prepared by acidifying an aqueous solution of ATTM with HCOOH, followed by washing and drying the precipitate at 110°C in a vacuum oven. $FeSO_4\cdot 7H_2O$, $Mo(CO)_6$, and $Fe(CO)_5$ were purchased as reagent-grade chemicals and used without further treatment.

Thermogravimetric analysis of ATTM was performed using a Perkin Elmer model TGA-7 thermal analyzer at a heating rate of 20°C/min in N_2. Sulfur analyses were performed by the Penn State Materials Characterization Laboratory using a Leco iodimetric titration sulfur analyzer or in the Penn

State Combustion Laboratory using a Leco Model SC-132 sulfur analyzer. Carbon, hydrogen, and nitrogen analyses were performed using a Leco Model CHN-600 elemental analyzer. Molybdenum, iron and water (by the Karl Fisher method) analyses were performed by Galbraith Laboratories, Inc. Elemental values and water content of synthesized molybdenum compounds are given in Table 2.

Catalyst precursors were reacted in a microautoclave at 7 MPa (cold) H_2 or H_2S:H_2 mixtures at 275°C for one hour (Tables 2 and 3). In experiments with ATTM and $FeSO_4 \cdot 7H_2O$, a 5:95 ratio of H_2S:H_2 was used; for molybdenum hexacarbonyl the ratio was 13.6:86.4, and for iron pentacarbonyl, 18:72. These ratios were chosen in order to maintain a constant sulfur:metal ratio of ?.5 during the reactions. X-ray diffraction measurement of the products (XRD) were made using Cu-K_α radiation with Rigaku equipment and operated at 40 kV and 20 mA.

3.2.4. Impregnation of Swollen and Unswollen Coals with Catalyst Precursors

The catalyst precursor was loaded onto the coal in an amount based on 1% molybdenum or 0.59% iron (as the metal, not the metal compound) on a dry, ash- free (daf) basis regardless of whether the coal had been swollen or not. Unswollen coals were impregnated with a water solution of ATTM, $FeSO_4 \cdot 7H_2O$ or suspension of MoS_3 and with a pentane solution of $Fe(CO)_5$ and $Mo(CO)_6$. The pentane was removed from carbonyl-impregnated coals by treatment in vacuum at room temperature for 10 min. Because of the

Table 2. Elemental analysis of ATTM, MoS_3 and the product obtained from microautoclave reaction of ATTM at 7MPa psi (cold) hydrogen gas at a temperature of 275°C

Catalyst	%N	%H	%Mo	%S	$\%H_2O$	nS:nMo
ATTM	10.81	3.10	37.01	49.15	ND	3.98
MoS_3	ND	ND	44.45	50.50	1.39	3.41
HATTM*	3.26	1.40	49.74	39.40	6.36	2.38

ND: Not determined
* Reacted ATTM in 7 MPa (cold) H_2 at 275°C.

Table 3. Elemental analysis of products obtained from microautoclave reaction of $Mo(CO)_6$ and $Fe(CO)_5$ at 7MPa of H_2 and $H_2S:H_2$ (5:95) at 275°C

Catalyst Precursor	Reaction Gas	%Mo	%Fe	%S	%C
$Mo(CO)_6$	H_2	40.77	—	—	24.50
$Mo(CO)_6$	$H_2S:H_2$	57.35	—	32.90	0.87
$Fe(CO)_5$	H_2	—	71.70	—	3.99
$Fe(CO)_5$	$H_2S:H_2$	—	60.63	37.6	0.22

volatility of carbonyls, the possibility exists that a portion of the carbonyl originally added may have been removed subsequently during the drying.

With swollen coal, the swelling reagent (except TBAH) was removed in vacuum at room temperature. While the coal was still wet with swelling reagent, enough ATTM solution (which had been prepared by dissolving ATTM in 1:1 (v/v) ratio methanol:water mixture) to give solution-to-coal ratio of 1:1 was added to the coal and stirred for 30 min. For TBAH, the ATTM was dissolved in a 10% TBAH solution of a 1:1 ratio (w/w) water:methanol mixture; then this solution was added to undried coal and stirred for 6 hours in order to give enough time for the swelling of coal under nitrogen. After stirring, excess solvent was removed at room temperature under vacuum during continuous stirring. Finally, vacuum drying was applied at 50°C for the coals swollen with methanol, THF or TBAH, or at 100°C for pyridine-swollen coal. TBAH was allowed to remain in the coal. When carbonyl compounds were used as catalyst precursor, THF and methanol were removed in vacuum at 50°C, and pyridine was removed in vacuum at 100°C prior to impregnation with pentane solution. Again, any residual TBAH was allowed to remain in the coal. The TBAH content of samples, whether catalyst-impregnated or not, was calculated from the increase of the nitrogen content of the TBAH-treated material relative to that of the untreated coals.

3.2.5. Examination of Catalyst Dispersion

To establish the physical relationship between catalysts and coal surfaces following impregnation, the interfaces were studied by scanning electron microscopy (SEM) to determine whether catalyst materials are deeply impregnated into the coal structure or whether they form only surface dispersions (also see Section 7). Two types of samples were prepared from the Texas lignite/subC (PSOC-1444 and DECS-1) and Blind Canyon bituminous coal (DECS-6), particulate (-60 mesh) samples, and single particles of about 5x20 mm embedded in plastic and polished to expose the bedding plane structures of the coal. The particulate samples were impregnated with catalyst or solvent swollen, or both, as described above, and were coated with gold for observation with an ISI model SX-40A SEM. $FeSO_4 \cdot 7H_2O$ and ATTM catalysts were impregnated into methanol- and THF-swollen coals and moist coals. An energy dispersive spectrometer (EDS) was used for qualitative analysis of elements greater in atomic number than sodium. The single-particle samples were stored under high humidity or were soaked in methanol for 48 h. Without allowing the polished surface to dry, ferrous sulfate (≈1 mg) or ATTM (≈0.5 mg) in the appropriate solvent (i.e., water or methanol) was applied in drops to the surface. Samples were then dried in vacuum at 25°C for 48 h and coated with carbon for SEM examination. (The SEM photomicrographs are discussed throughout the text. At the bottom of each photomicrograph, reading from the left, are the electron beam voltage, total magnification, the size in microns of the white scale bar, and a photograph number.)

3.2.6. Liquefaction Reactions and Product Work-up

The liquefaction reactions were performed in horizontal microautoclave reactors (tubing bombs) of nominal 25 mL capacity. The procedure was the same for both preswollen and unswollen coals and also the same whether they had been impregnated with a catalyst or not.

Five grams of each prepared coal sample and 5 g of phenanthrene were placed in the reactor. After the contents were mixed with a spatula, the reactor was sealed, pressurized to 7 MPa with N_2 and checked for leaks. The depressurized reactor was twice purged with H_2. Subsequently, the reactors were pressurized to 7 MPa (at room temperature) with H_2 or H_2S:H_2 (5:95) and were attached to a fluidized sand bath which was heated to 283°C. Immediately after the reactors were placed in the sand bath, the thermostat was reset to 275°C, which was the desired pretreatment temperature. The reactors attained a temperature of 275°C in about 30 s. The reaction time was 30 min. During this period, the reactors were oscillated through an amplitude of 2 cm at 350 cycles/min. All the pretreatment experiments were done in duplicate. For experiments in these reaction systems we have determined, in a collateral study on bituminous coal liquefaction, that the relative standard deviation (i.e., the standard deviation expressed as a percentage of the mean) of conversion results is 7-12% for six sets of results obtained by three independent experimenters each performing duplicate tests (see Section 9). Relative standard deviations for asphaltene yields are typically 12-13%.

At the end of the reaction, the reactors were rapidly quenched to room temperature by immersion in cold water. After venting the gas, the contents of each reactor were quantitatively washed into a tared ceramic thimble using toluene and then Soxhlet-extracted with toluene under N_2 until the solvent appeared colorless. The toluene extract was concentrated to 10–20 mL by rotary evaporation. The extract was diluted with 400 mL of hexane. The mixture was stirred for 1 h and asphaltenes were allowed to settle overnight and separated with a 0.45 mm filter. The filtrate, containing hexane-solubles, was treated by rotary evaporation to remove the hexane. Toluene- insolubles were Soxhlet-extracted with THF to separate preasphaltenes and the solid residue under N_2 atmosphere. THF was removed from the extract by rotary evaporation. Preasphaltenes, asphaltenes and residue were dried overnight in vacuum at 110°C. The conversion was calculated by subtracting the residue weight (corrected as appropriate for the weight of added catalyst) from the weight of coal and dividing by the daf weight of the coal. It was assumed that in the liquefaction system the catalyst precursors transformed to the same materials as they did in reactions in the absence of coal in hydrogen or H_2S:H_2 at 275°C (Table 2 and 3).

3.3. RESULTS AND DISCUSSION

3.3.1. Swelling of Coals

Solvent swelling ratios as a function of contact time for four different solvents are given in Tables 4 and 5 for the Texas lignite (PSOC-1444) and the Blind Canyon hvCb (PSOC-1503), respectively. The maximum

Table 4. Change in solvent swelling ratio (Q) with time for the Texas Lignite (PSOC-1444)

Methanol		THF		Pyridine		TBAH	
Time (h)	Q	Time (h)	Q	Time (h)	Q	Time (h)	Q
5.0	1.1	6.0	1.2	6.5	1.6	6.0	2.6
11.5	1.1	16.5	1.2	21.5	1.6	14.5	2.6
23.0	1.1	22.0	1.3	42.0	1.6	24.5	2.7
27.5	1.1	28.0	1.3				

Table 5. Change in solvent swelling ratio (Q) with time for the Blind Canyon bituminous coal (PSOC-1503)

	Methanol	THF	Pyridine	TBAH (10%)
Time (h)	Q	Q	Q	Q
6.0	1.2	1.9	2.4	1.2
10.0	1.3	1.8	2.3	1.2
20.0	1.3	1.8	2.2	1.2
26.0	1.3	1.8	2.3	1.2

level of swelling was attained within 6 h; additional solvent-coal contact in excess of 26 h did not significantly increase the swelling ratio. The swelling experienced by each coal was slightly different with respect to the individual solvents. For the Texas lignite, swelling increased in order: methanol < THF < pyridine < 10% TBAH; for the Blind Canyon, the order was: 10% TBAH < methanol < THF < pyridine. The extent of the swelling in the different solvents is rank-dependent. Lignites are more crosslinked than bituminous coals. Therefore, lignites give less swelling and extractability in methanol, THF and pyridine than do bituminous coals. Lignites have higher concentrations of acidic phenolic hydroxyl and carboxylic groups than bituminous coals; therefore, swelling of lignite increases with increasing basicity of solvents. TBAH is quite basic and reacts strongly with the types of oxygen functionalities in most lower rank coals [Liotta et al., 1981]. Our results with the Blind Canyon bituminous coal differ from those of Joseph [1991], who determined for Illinois No. 6 bituminous coal that the highest swelling was obtained with 15% TBAH (compared with THF and methanol). This difference can be explained, at least in part, by the higher oxygen functionality of the Illinois No. 6 coal compared to that of the Blind Canyon coal and by the tendency for TBAH to react with these functional groups [Liotta et al., 1981].

3.3.2. Comparison of Molybdenum and Iron Catalyst Precursors for Pretreatment

In this subsection, we discuss results obtained without swelling. Table 6 shows conversion data for thermal (non-catalytic) reactions and

Table 6. Comparison of molybdenum and iron catalysts on the liquefaction of Texas subbituminous (DECS-1) and Blind Canyon bituminous coals (DECS-6)

Coal	Catalyst	React. Gas	Conversion% (daf)			
			Total	Preasph	Asphalt	Oil+Gas
DECS-1	None	H_2	7	3	2	2
DECS-1	None	$H_2S:H_2$	9	4	2	2
DECS-1	$FeSO_4$	H_2	6	2	2	2
DECS-1	$Fe(CO)_5$	H_2	6	2	2	2
DECS-1	$Fe(CO)_5$	$H_2S:H_2$	11	4	4	4
DECS-1	ATTM	H_2	9	4	4	2
DECS-1	MoS_3	H_2	7	4	2	2
DECS-1	$Mo(CO)_6$	H_2	7	3	2	2
DESC-1	$Mo(CO)_6$	$H_2S:H_2$	9	4	3	2
DECS-6	None	H_2	18	11	2	5
DECS-6	None	$H_2S:H_2$	18	10	2	7
DECS-6	$FeSO_4$	H_2	17	9	3	5
DECS-6	$Fe(CO)_5$	H_2	17	8	2	7
DECS-6	$Fe(CO)_5$	$H_2S:H_2$	23	14	3	6
DECS-6	ATTM	H_2	25	15	3	7
DECS-6	MoS_3	H_2	27	19	3	5
DECS-6	$Mo(CO)_6$	H_2	16	8	2	7
DECS-6	$Mo(CO)_6$	$H_2S:H_2$	27	16	3	7

reactions with catalyst impregnation. Higher conversion was obtained from Blind Canyon hvAb coal than from Texas subC when catalyst was not used (18% vs 7%). A major contribution to the higher conversion of Blind Canyon is the greatly increased yield of preasphaltenes (11 vs 3%). This may indicate a greater liberation of mobile phase from the bituminous coal. A greater oil+gas yield is also noted for Blind Canyon (5 vs 2%). Experiments in H_2S:H_2 (5:95) show increased conversions relative to H_2. This is more noticeable for the subC than for the bituminous coal. This behavior is attributed to the well-known role of H_2S as a liquefaction catalyst. The greater improvement for the subbituminous relative to the bituminous coal, may indicate H_2S interactions with oxygen functional groups.

The conversions of both coals impregnated with sulfided catalysts are greater than those obtained without catalyst. With Texas subC, ATTM improves conversion slightly (9% vs 7%). The increased conversion is due to increased asphaltenes and preasphaltenes. MoS_3 also improves conversion slightly, via increased preasphaltenes (3% vs 4%). With Blind Canyon, impregnation with ATTM increased conversion from 18% to 25%, mainly as a result of increased preasphaltenes. Oil yield also increased slightly (7% vs 5%). MoS_3 does even better (27% conversion), by nearly doubling the yield of preasphaltenes (19% vs 11%). However, the oil yield was not improved with MoS_3. Utz and co-workers [1989] have shown that the conversion of Illinois No. 6 coal with MoS_3 was comparable to that obtained with ATTM. This entire body of results with ATTM and MoS_3 is in general

agreement with our previous findings, which suggested that the principal role of sulfided catalysts in liquefaction is to increase conversion via breakdown of the macromolecular structure of the coal, and hence the predominant contribution to enhanced conversion comes from greater yields of preasphaltenes and asphaltenes [Burgess et al., 1991].

The similarity of results obtained using ATTM and MoS_3 can be explained by the decomposition behavior of ATTM in the reaction system. Thermal analysis of ATTM showed two regions of decomposition (Figure 1). The first occurs around 160°C with loss of 24.5% weight (for the conversion of ATTM to MoS_3, the calculated weight loss is 26.15%). The second occurs around 370°C and the total weight loss was 38.8% (from ATTM to MoS_2 the theoretical weight loss is 38.46%). ATTM was reacted at 275°C in H_2 (7MPa cold) without coal to determine the fate of ATTM in the preliquefaction conditions. Elemental analysis of the product shows that ATTM transforms to MoS_{2+x} which contains 3.26% of nitrogen (Table 2). The slightly different activities of these two molybdenum-based catalysts with both coals may be due to a difference in catalyst dispersion and on the negative effect of ammonia (released from decomposition of ATTM) on the activity of the molybdenum sulfide catalyst derived from the ATTM.

$FeSO_4 \cdot 7H_2O$ produces no change in conversion or product slate for liquefaction of the Texas subC. Also, it is not an active catalyst for liquefaction of the bituminous coal at 275°C. XRD of the product of heating $FeSO_4 \cdot 7H_2O$ in a microautoclave in the absence of coal showed mono- and tetrahydrated ferrous sulfate phases as the primary products at 275°C.

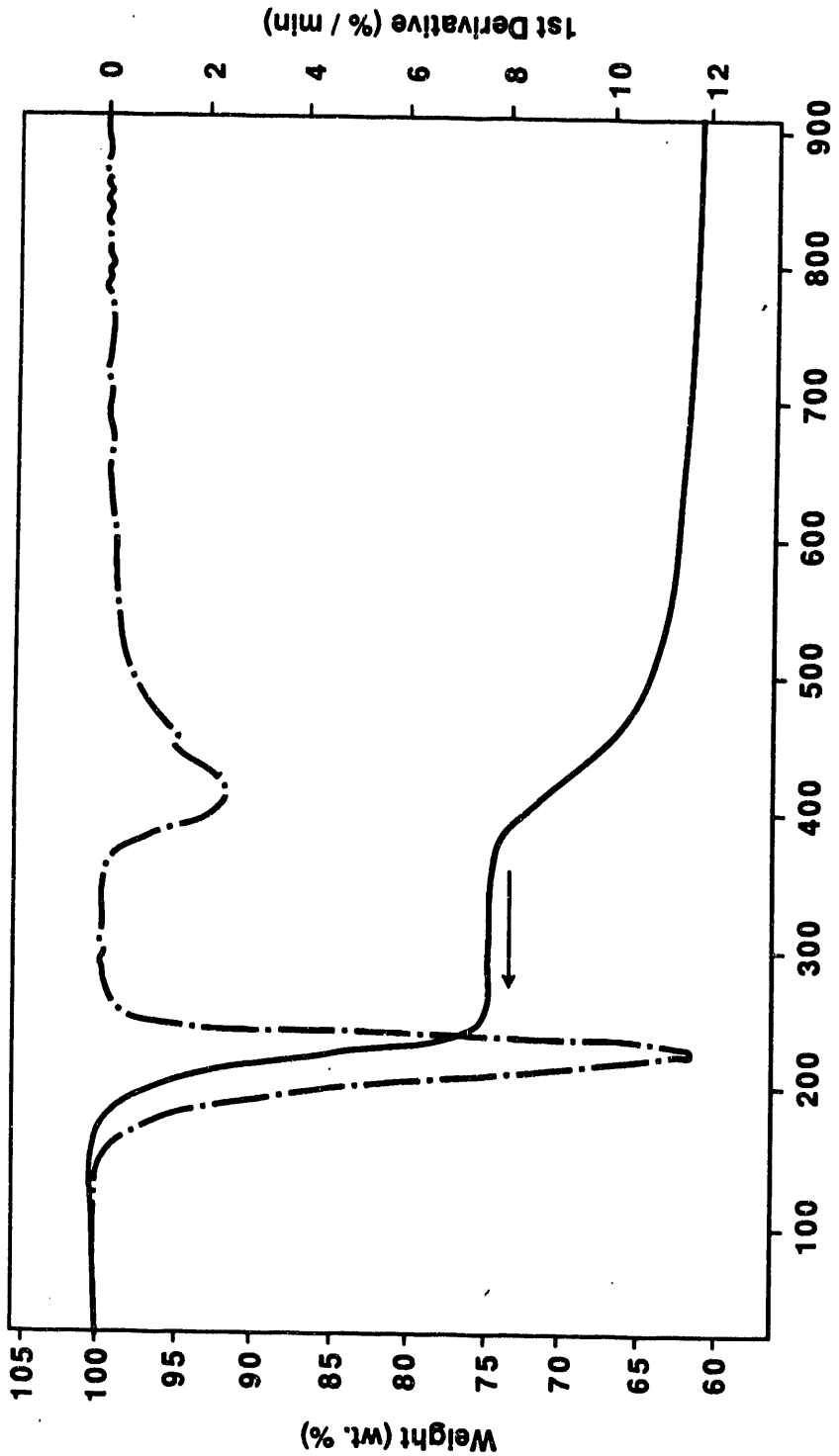

Figure 1 Thermogravimetric and Differential Thermogravimetric Analyses of Ammonium Tetrathiomolybdate

Conversion of $FeSO_4$ to an active sulfide phase was achieved only above 350°C. In Section 4 of this report we will discuss in more detail aspects of the use of ferrous sulfate as a liquefaction catalyst precursor.

Single-particle impregnation studies [discussed in Section 7] using a methanol-pretreated or moist surface of the Texas subC indicate that a good surface dispersion of ferrous sulfate was achieved (Plate IIIc and d, respectively). Plate IIIc illustrates the two crystal types found; one occurred as large prismatic crystals ranging in size from 100 to 300 mm, and the other type occurred as acicular crystals that were distributed as 30 mm size clusters across the coal surface. EDS examination revealed that the larger crystals were ferrous sulfate, whereas the more highly disseminated acicular form was calcium sulfate. At higher magnification (Plate IIId), the needle-like clusters of calcium sulfate were found to be associated with a core of ferrous sulfate. When ferrous sulfate in aqueous or methanol solution is applied to a moist coal surface, ion exchange of iron with organically associated calcium may be promoted. (The calcium content of DECS-1 is 0.7% on a dry basis.) Blind Canyon has less calcium (0.5%, dry coal basis), but some acicular crystals were observed on the single-particle surfaces among crystals of ferrous sulfate.

Both calcium and iron sulfate particles were observed on surfaces in the particulate samples impregnated with ferrous sulfate in aqueous solution (Plate Vb). Different concentrations of iron and calcium sulfates observed between the two coals closely follow those seen with the single-particle samples. However, a much better dispersion of sulfate crystals

was observed in the Blind Canyon sample. EDS examination showed that one particle in five had an iron peak or had recognizable crystalline material. A similar analysis of the Texas subC particulate sample demonstrated that sulfate materials were not as uniformly dispersed, most being found in large deposits not associated with the coal.

Impregnated $Fe(CO)_5$ provided no change in conversion of the Texas subC in a H_2 atmosphere, but slight increases in asphaltene and oil+gas yields (and thus decreased preasphaltenes) were observed. However, in $H_2S:H_2$, $Fe(CO)_5$ provides an increase in conversion (11% vs 7%), with a doubling of preasphaltenes and increased asphaltenes and oil+gas. For the bituminous coal reacted in H_2, $Fe(CO)_5$ does not enhance conversion, but shifts the product slate toward lighter materials at expense of preasphaltenes and asphaltenes. In $H_2S:H_2$, $Fe(CO)_5$ enhances total conversion (23% vs 18%), mainly via increased preasphaltenes (14% vs 11%). Elemental and XRD analyses revealed that $Fe(CO)_5$ transforms to iron oxides (FeO and Fe_3O_4) with accumulated carbon in H_2 and transforms to pyrrhotite in $H_2S:H_2$ (Table 3 and Figure 2). Thus the behavior of the catalyst can be influenced by the choice of atmosphere. In the absence of H_2S, the catalyst is not sulfided, and appears to have no effect on facilitating the breakdown of the coal structure, because the conversion is essentially unchanged. However, in this system the catalyst does facilitate hydrogenation of the heavier fractions of the subC coal. In $H_2S:H_2$, an increase in conversion (9% vs 7%) results, primarily from increased asphaltenes and preasphaltenes.

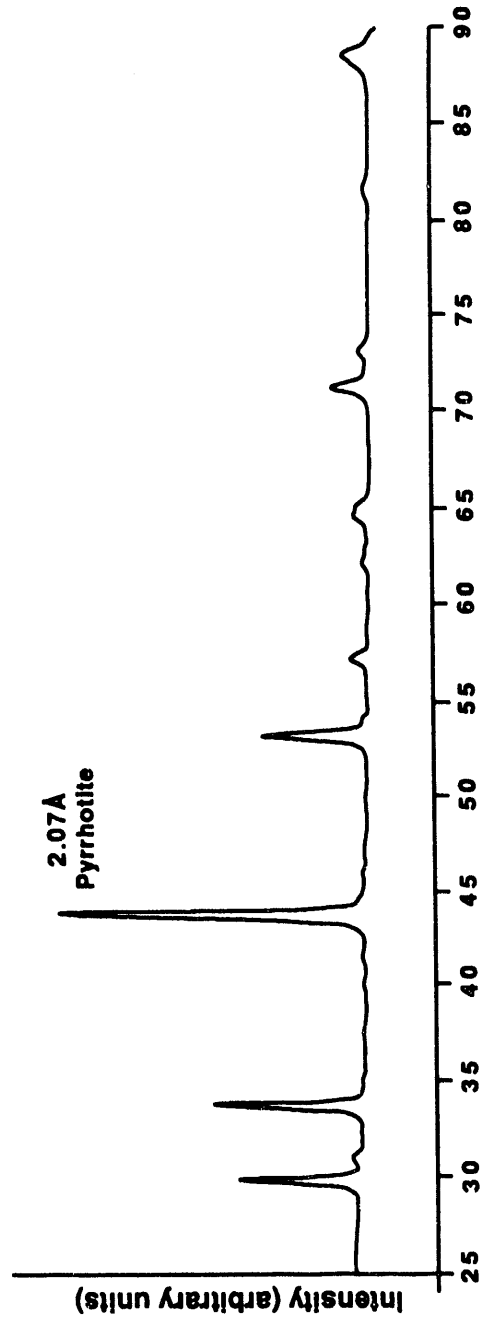

Figure 2 - XRD Spectrum of Products Obtained from $Fe(CO)_5$ in H_2S:H_2 Gas Mixture

Most prior work on iron oxide formation from catalyst precursors and its subsequent effect on liquefaction has been at temperatures much higher than our work. Impregnation of Victorian (Australia) brown coals with ferrous acetate and subsequent reaction initially formed hydrated iron oxides and iron humates [Cook and Cashion, 1987a]. At temperatures ≥380°C in H_2, the iron remaining in the liquefaction residue was present as a mixture of magnetite and troilite [Cook et al., 1988]. The magnetite can be converted to iron, which is subsequently transformed to the carbide [Cook and Cashion, 1987b]. Above 400°C, improved conversion obtained by addition of iron compounds occurs in the form of increased oil yields [Cassidy et al., 1982]. In comparison, several other groups have shown that iron present in a sulfided form helps convert the coal to asphaltenes, but does not facilitate conversion of asphaltenes to oils [Cook et al., 1988; Larkins et al., 1984; Pradhan et al., 1991].

Similar to the findings with $Fe(CO)_5$, $Mo(CO)_6$ in H_2 does not affect conversion of Blind Canyon, but shifts products to lighter materials. This suggests that $Mo(CO)_6$, or its thermal decomposition products, is effective in catalyzing the hydrogenation of preasphaltenes and asphaltenes to oil at 275° in a low-sulfur medium. (No significant beneficial effect was observed with the Texas subC.) In H_2S:H_2, conversion is enhanced, mainly via formation of more preasphaltenes. In the absence of coal, $Mo(CO)_6$ is largely, but not entirely, unreactive in H_2, but transforms to a sulfided catalyst in H_2S:H_2 (Table 3). Reaction of $Mo(CO)_6$ in H_2 at 275° yields a product having the empirical formula (based on elemental analysis) $Mo(CO)_5$.

XRD of this product shows only $Mo(CO)_6$ as an identifiable material, along with some broad peaks indicative of poorly crystalline material. Since $Mo(CO)_6$ readily sublimes at 110°, the amount of hexacarbonyl remaining in the reaction product can be estimated easily by thermogravimetric analysis. For reaction of $Mo(CO)_6$ in H_2 at 275°, the product contains 88% unreacted $Mo(CO)_6$, as estimated by TGA. (It should be noted that a mixture of 83.3% $Mo(CO)_6$ and 16.7% Mo would have an elemental composition consistent with an empirical formula $Mo(CO)_5$, in good agreement with the TGA result of 88% $Mo(CO)_6$.) A small amount of hydrocarbon gases was detected after reaction, suggesting some interaction of CO released by thermal decomposition of the carbonyl with H_2, in a Fischer-Tropsch-like reaction. Reaction of $Mo(CO)_6$ in H_2S:H_2 at 275° gives a product having elemental composition consistent with the empirical formula $MoOS_2$, mixed with small amounts of carbon, although we have not unequivocally identified a specific compound of this formula in the product.

Sulfided molybdenum catalysts are well known to be active for hydrogenation. Hydrogen absorption from the gas phase is approximately 18 mg with sulfided molybdenum catalyst at 275°C, while it was almost zero without catalyst for both coals. The gaseous product of the reaction at 275° is only CO_2, and varies in the range 0.3-0.6% for Blind Canyon and 1.3-2.5% for the Texas subC.

3.3.3. The Effect of Preswelling on Non-catalytic Liquefaction

Conversions of solvent-swollen coals without catalyst impregnation are given in Table 7. Treatment with methanol enhanced oil formation,

Table 7. Effect of preswelling treatment on liquefaction of Texas subbituminous (DECS-1) and Blind Canyon bituminous (DECS-6) coals at 275°C

Coal	Solvent	Conversion % (daf)			
		Total	Preasph	Asphalt	Oil+Gas
DECS-1	None	7	3	3	2
DECS-1	Methanol	8	2	2	4
DECS-1	THF	7	3	1	4
DECS-1	Pyridine	10	2	2	6
DECS-1	TBAH	18	5	4	8
DECS-6	None	18	11	2	5
DECS-6	Methanol	20	12	2	6
DECS-6	THF	22	11	2	9
DECS-6	Pyridine	16	6	1	8
DECS-6	TBAH	24	15	4	5

decreased preasphaltenes and asphaltenes for the Texas subC (DECS-1); and enhanced oils and preasphaltenes and decreased asphaltenes for the Blind Canyon coal (DECS-6).

THF is the least effective swelling reagent for the liquefaction of the subC, but it provided improved conversion, commensurate with its good swelling ability, for Blind Canyon (Q = 1.9). THF pretreatment increased the total conversion of Blind Canyon from 17.7% to 22.1% and oil formation from 4.9% to 9.2%. Its effect on formation of preasphaltenes and asphaltenes was not significant.

Pyridine pretreatment provided greater total conversion and oil formation for the subC than those obtained from methanol and THF treatment. However, this treatment diminished the formation of preasphaltenes from this coal. Pyridine treatment of Blind Canyon decreased conversion from

18% to 16%. A significant reductions in the yield of preasphaltenes, from 11% to 6%, and some decrease in the yield of asphaltenes, from 2% to 1%, were observed. However, the yield of oils increased from 5% to 9%.

TBAH treatment provided the highest conversion for both coals relative to the other solvents, even though a 10% TBAH solution in a 1:1 water:methanol mixture swelled Blind Canyon least. There are two likely reasons for the high conversion with TBAH addition to coals. The first is increased swelling that may result when the carrier solvent is evaporated. Evaporation of methanol and water from the coal-solvent-TBAH mixture increases the concentration of TBAH in the coal. The TBAH, thus concentrated by evaporation, can increase the swelling of the coal. Second, in a reaction of 40% TBAH in a microautoclave at the same reaction conditions as used for the pretreatment experiments (but without coal), butane and butene were observed in the gaseous products. It can be expected that TBAH likely transformed to amines, such as tributylamine. Therefore, TBAH can be envisioned to act as a "solvent precursor," in that the TBAH remaining in the coal after the swelling procedure can undergo thermal decomposition to compounds that are good solvents for coal. Amines are very good promoters for coal liquefaction [Kazimi et al., 1985; Tagaya et al., 1987; Miller et al., 1990]. The nitrogen contents of residue, preasphaltenes and asphaltenes were higher for TBAH-swollen coal than those of unswollen coal. This increase is attributed to the incorporation of amines. Assuming that TBAH transformed to tributylamine, the amount of tributylamine incorporated in residue, asphaltenes and preasphaltenes can

be determined from the difference between the nitrogen contents of these materials and those of the respective products from unswollen coal. The incorporation of amine compound in these products varied between 2-9%. Addition of TBAH provided the highest increase in yields of preasphaltenes, asphaltenes and oil for the subC compared to those of coals swollen with other solvents. For Blind Canyon, TBAH addition provided the greatest conversion, yields of preasphaltenes and asphaltenes, but a lower yield of oil relative to those for coals swollen with the other solvents.

For the subC, conversion of solvent-pretreated samples without catalyst increased in the order of none ≈ THF < methanol < pyridine << TBAH. TBAH and pyridine are the most effective swelling agents, and provide highest conversions of swollen samples. Furthermore, these two solvents also provided the highest oil + gas yields. For Blind Canyon, conversion without catalyst increased in the order of pyridine < none < methanol < THF < TBAH. The behavior of the bituminous coal, with respect to conversion, is quite different from that of the subC, since in this case pyridine was the most effective swelling solvent, yet pyridine pretreatment actually suppressed conversion. However, the two best swelling solvents, pyridine and THF, produced the highest oil+gas yields. The extractive ability of a particular solvent is related to the swelling effect of that solvent for a particular coal. A good extractive solvent can disrupt weak bonds in the coal network or in material trapped in the coal structure. Therefore, molecules released by this disruption and the weakened structure can be reacted at less severe conditions.

3.3.4. Combined Effects of Swelling and Catalyst Impregnation

Comparative conversion data for ATTM-impregnated swollen Texas subC and Blind Canyon bituminous coal are given in Table 8. A comparison of the

Table 8. Effect of preswelling on liquefaction of Texas subbituminous (DECS-1) and Blind Canyon bituminous (DECS-6) coals with ATTM catalyst at 275°C

Coal	Solvent	Conversion % (daf)			
		Total	Preasph	Asphalt	Oil+Gas
DECS-1	None	9	4	4	2
DECS-1	Methanol	10	3	2	4
DECS-1	THF	9	3	3	3
DECS-1	Pyridine	12	3	2	6
DECS-1	TBAH	19	6	5	8
DECS-6	None	25	15	3	7
DECS-6	Methanol	25	15	2	7
DECS-6	THF	25	12	2	10
DECS-6	Pyridine	27	15	3	10
DECS-6	TBAH	24	14	4	6

results presented in Tables 7 and 8 shows that, for the subC swollen with any given solvent, addition of ATTM improved conversion relative to that obtained for experiments without catalyst. The increase in conversion obtained by adding ATTM is about the same for all samples, suggesting that the effects of swelling and catalyst impregnation are independent. However, the improvement in conversion obtained by combining ATTM impregnation and swelling is less than that obtained by adding ATTM to

unswollen subC coal. For example, impregnation with ATTM increased conversion from 7% to 9% when the subC was not pretreated with solvent, but for the solvent-treated samples the conversions increased only by 1-2%. The oil+gas yields are essentially unchanged (relative to the solvent-pretreated samples without catalyst) on adding ATTM, with the increase in conversion obtained via increased yields of preasphaltenes and asphaltenes. Since sulfided molybdenum catalysts appear to act mainly to increase the yields of these two products from unswollen coals, this observation further corroborates the suggestion that the effects of catalyst and swelling solvent are independent. If the effects of swelling and catalyst impregnation are compared with results for catalyst impregnation without swelling, it can be seen that solvent treatment increases conversion, and that generally the yields of preasphaltenes and asphaltenes are reduced relative to the case without solvent treatment. Hence solvent swelling facilitates shifting the product slate toward lighter materials. The greatest conversions and formation of all types of products were obtained with TBAH addition. In this case, the TBAH was by far the most effective solvent pretreatment, because the conversion doubled, relative to the unswollen subC, and yields of all products were increased significantly. The order of conversion can be given as none $\approx$ THF $\approx$ methanol $<$ pyridine $\ll$ TBAH for the subC. This is essentially the same as the order obtained without ATTM.

For Blind Canyon, the results are not as consistent as in the case of the subC. Addition of ATTM increased conversions for solvent-treated

samples, relative to comparable samples without ATTM, except with TBAH-treated coal. In fact, TBAH addition seemed to decrease the activity of the molybdenum sulfide catalyst, because the conversion of TBAH-treated coal was slightly less than that of the unswollen coal (also see Sections 6.3.2. and 8.3.1.). Again the increased conversion is mainly in the form of enhanced yields of preasphaltenes and asphaltenes. For this coal, the effects of solvent pretreatment on conversion at 275° are negligible, but THF, pyridine, and TBAH effect slight changes in the product distribution. THF and pyridine treatments increase oil and gas yields at the expense of preasphaltenes and asphaltenes. TBAH treatment increases asphaltene yield while decreasing preasphaltenes.

One reason for improved conversion and product yield for THF-treated Blind Canyon coal is suggested by Plate Ic. This SEM micrograph shows the surface of several coal particles coated with hemispherical bodies following swelling in THF and impregnation with ATTM. These bodies were easily destroyed by a focused electron beam and are carbon-rich. We conclude that this material was part of the THF-soluble fraction that was extracted from the coal during swelling and that was subsequently redeposited on the coal surface when the THF was evaporated before catalyst impregnation. The benefit of this removal and redeposition of THF-solubles could arise in two ways. First, the separation of the THF-soluble material from the coal during swelling could have created more surface area for catalyst deposition (although we have not measured the surface areas before and after swelling). Second, conversion of bituminous coals in short

contact time, low-temperature liquefaction has been shown to depend on the mobility of the solvent-extractable portion of the coal and its ability to reach catalyst particles on the coal surface [Chamberlin and Schobert, 1991]. THF bringing some of this mobile material to the coal surface should make it easier for this material to contact the dispersed catalyst. The significant increase in oil+gas yield (Table 7) suggests that by improving access of the THF-soluble fraction to the hydrogenation environment may be beneficial. The improved oil+gas yields and reduced preasphaltene and asphaltene yields shown in Table 8 imply that the increased surface area for catalyst/coal contact resulting from swelling in THF has little influence on conversion of the THF-insoluble fraction of this coal under pretreatment conditions. Improved access of catalyst to the THF-soluble coal fraction does not significantly increase yield relative to the non-catalytic reaction, but may improve overall product quality.

Addition of ATTM in water:methanol solutions was studied for both coals using single particles as well as particulate samples. The distribution of catalyst was the same regardless of the coal or whether the samples were pretreated in methanol. As shown in Plate VIb and Plate VIId, when the solvent was evaporated most of the ATTM aggregated in clusters on the coal surface. For the single coal particles (Plate VIb), the clusters were generally large. Individual 10 μm platelets of ATTM occurred in some areas of the sample. Coal surfaces in close proximity to the clusters gave no molybdenum or sulfur peaks using the EDS, suggesting that ATTM forms a

deposit only on the exterior surface of the coal and does not penetrate deeply into the interior of the particles. In the particulate sample (Plate VIId), clusters of ATTM were not found uniformly on all particles, and they were typically much smaller (<5 μm).

Using $Mo(CO)_6$ in H_2S:H_2, little is gained by solvent treatment for Blind Canyon (Table 9). Increased conversion with pyridine is mainly a result of increased asphaltenes. For the Texas subC, similar trends are observed as were seen with ATTM and in the non-catalytic reactions. The principal effect of solvent pretreatment is an increase in oil+gas yield. Conversion of this coal increases in the order none ≈ THF < methanol < pyridine < TBAH. With $Fe(CO)_5$ in H_2S:H_2 (Table 10), only TBAH provided higher conversion for the subC, and increases the yields of all products. Other solvent treatments did not enhance conversion. Pyridine treatment caused an increase of oil+gas yield, and a decrease of preasphaltenes. Solvent treatment provided little improvement in conversion of Blind Canyon. TBAH and pyridine pretreatment slightly increased conversion via an increase of oil+gas yields.

3.4. CONCLUSIONS

Without swelling pretreatment, impregnation of both coals with catalyst precursors increased conversion at 275°. Increased conversion was mainly a result of an increased yield of preasphaltenes. In the absence of catalyst, swelling the subC coal before liquefaction improves conversion, with the increase mainly a result of additional oil+gas yield. The

Table 9. Effect of preswelling on liquefaction of Texas subbituminous (DECS-1) and Blind Canyon bituminous (DECS-6) coals with $Mo(CO)_6$ at 275°C

Coal	React. Gas	Solvent	Conversion (%)			
			Total	Preasph	Asphalt	Oil+Gas
DECS-1	H_2	None	7	3	2	2
DECS-1	$H_2S:H_2$	None	9	4	3	2
DECS-1	$H_2S:H_2$	Methanol	11	3	2	5
DECS-1	$H_2S:H_2$	THF	9	3	3	3
DECS-1	$H_2S:H_2$	Pyridine	14	3	4	7
DECS-1	$H_2S:H_2$	TBAH	15	4	4	7
DECS-6	H_2	None	16	8	2	7
DECS-6	$H_2S:H_2$	None	27	16	3	8
DECS-6	$H_2S:H_2$	Methanol	26	16	4	6
DECS-6	H_2	THF	15	7	1	7
DECS-6	$H_2S:H_2$	THF	27	17	4	6
DECS-6	$H_2S:H_2$	Pyridine	28	16	6	6
DECS-6	$H_2S:H_2$	TBAH	26	16	6	4

Table 10. Effect of preswelling on liquefaction of Texas subbituminous (DECS-1) and Blind Canyon bituminous (DECS-6) coals with $Fe(CO)_5$ in $H_2S:H_2$ (5:95) at 275°C

Coal	Solvent	Conversion% (daf)			
		Total	Preasph	Asphalt	oil+gas
DECS-1	None	11	4	4	4
DECS-1	Methanol	10	2	4	4
DECS-1	THF	11	4	2	5
DECS-1	Pyridine	11	2	3	6
DECS-1	TBAH	24	8	10	6
DECS-6	None	23	14	3	6
DECS-6	Methanol	20	10	2	8
DECS-6	THF	20	10	3	7
DECS-6	Pyridine	24	12	3	9
DECS-6	TBAH	26	12	4	10

relative effectiveness of various solvents for improving conversion is in the same general order as their effectiveness at swelling the coal. Preswelling with methanol or pyridine has little effect on liquefaction of Blind Canyon, but both THF and TBAH provide increased conversion as a result of improved preasphaltene yields. With this coal, the effectiveness of solvents at improving liquefaction is not in the same order as their ability to swell the coal. The combined effect of catalyst addition and swelling is to enhance conversion of the subC coal, with a doubling of conversion obtained by impregnation with catalyst and swelling by TBAH. The yields of all products are enhanced by this pretreatment. In contrast, little improvement in total conversion of the Blind Canyon coal is obtained by combining catalyst impregnation and solvent swelling, but changes in the relative proportions of the products can be obtained.

Investigation of catalyst impregnation of solvent-swollen or moist coals with SEM demonstrates that ferrous sulfate and ATTM form only surface dispersions. Pretreatment in methanol or THF appears to have little influence on impregnation. Impregnation with ATTM before and after solvent swelling results in a surface dispersion. Aggregates of small crystals were observed on the surface of single particles and on particulate samples. Molybdenum and sulfur peaks were not detected in areas where these crystals were absent.

The results with $Fe(CO)_5$ in the different gas atmospheres are noteworthy because they suggest the possibility of tailoring the catalyst action to the characteristics of the coal and the kind of transformations

desired. We have shown elsewhere that sulfided catalysts generally seem to intervene in the initial breakdown of the coal, producing preasphaltenes and asphaltenes [Burgess et al., 1991]. For coals which do not have a high inherent reactivity, a catalyst facilitating breakdown of the structure may be very useful. On the other hand, some coals appear to undergo a facile thermal depolymerization even in the absence of catalyst, and in such cases a catalyst that acts mainly to help hydrogenate heavier products to oils might be preferable. With impregnated $Fe(CO)_5$ the choice of atmosphere (H_2 vs H_2S:H_2) provides the opportunity of generating an active catalyst that acts either for coal breakdown or for shifting the product slate to lighter materials. It is interesting to speculate that one could, for example, use a H_2S:H_2 atmosphere to provide a sulfided, dissolution catalyst for the first stage, re-impregnate with $Fe(CO)_5$ between stages, and use a H_2 atmosphere in the second stage to enhance hydrogenation of the preasphaltenes and asphaltenes.

An added benefit of solvent swelling could be the formation of good solvent inside the coal, as in the case of the thermal decomposition of TBAH to tributylamine. Previously we have shown that the transport of the mobile phase to catalyst particles on the surface of the coal is an important factor in short-contact time liquefaction of bituminous coals [Chamberlin and Schobert, 1991]. The use of a good swelling agent as a "solvent precursor", with subsequent in-situ generation of a good extractive solvent, could increase the amount of mobile phase moving out of the coal and reduce its viscosity. In addition, combining an excellent

hydrogen donor (tetrahydroquinoline) into the same molecular species as a catalyst precursor facilitates hydrogenation by keeping the donor in, or near, the catalyst [Burgess and Schobert, 1991]. Hence the prospect exists for future developments of combined "solvent-and-catalyst precursors".

It is important to recognize that the first-stage liquefaction may produce changes in coal structure or behavior that significantly enhance conversion in the second, high-temperature stage, but which are not necessarily evident in the macroscopic characteristics (e.g., formation of soluble materials) of the products of the first stage. That is, a particular coal-catalyst-solvent combination may provide small conversions or yields of soluble products at the end of the first stage, yet may have experienced subtle changes of structure which then facilitate significant conversion in the second stage. Hence the ultimate assessment of the utility of catalyst impregnation, solvent swelling, or both in improving liquefaction behavior in temperature-staged processes is to determine conversions and product yields at the end of the second stage. This is the topic of the next two sections.

4. TEMPERATURE-STAGED LIQUEFACTION OF COALS IMPREGNATED WITH FERROUS SULFATE

4.1. INTRODUCTION

Iron compounds are attractive catalysts for coal liquefaction due to their relatively low cost, hydrogenation activity and the potential of soluble iron compounds to be dispersed on or impregnated into the coal. One of the earliest large-scale direct liquefaction operations, the Bergius - IG Farben process, used a disposable iron oxide catalyst [Probstein and Hicks, 1982]. In many liquefaction systems the addition of sulfur, or the sulfiding of the iron catalyst, improves the activity of the iron [Jackson and Larkins, 1991]. The active form of iron catalyst is considered to be an iron sulfide [Garg and Givens, 1982]. The non-stoichiometric iron sulfides, such as pyrrhotite, play an especially important role in coal liquefaction [Montano and Granoff, 1980; Brooks et al., 1983; Bommannavar and Montano, 1983]. The Fe/S atomic ratio in the non-stoichiometric sulfides which provides maximum liquefaction conversion is in the range 0.5-1.0 [Yokoyama et al., 1986]. In addition, a synergism exists between pyrrhotite and H_2S for hydroliquefaction [Baldwin and Vinciguerra, 1983]; indeed, in some cases it is thought that pyrrhotite is catalytically active only in the presence of H_2S [Narain et al., 1987; Lambert et al., 1980].

It is now generally appreciated that beneficial effects can be obtained in liquefaction by achieving good dispersion of the catalyst on the surface of the coal particles. Catalyst dispersion increases the number of catalyst particles in close proximity to sites at which reaction

is occurring, and the dispersion of catalyst as fine particles increases the amount of active catalyst surface area available in the reactor (relative to using the same quantity of catalyst, but in larger, less dispersed particles). An approach to achieving catalyst dispersion is to employ a liquid vehicle as the medium for dispersing the catalyst. Unfortunately, several of the compounds of interest as liquefaction catalysts, such as pyrrhotite, pyrite, and molybdenum disulfide, are insoluble in all common solvents. Consequently, a strategy of using "catalyst precursors" has been developed, in which the precursor is a soluble compound that may not itself be catalytically active, but transforms at elevated temperature into an active catalyst. For example, moderately soluble ammonium tetrathiomolybdate, which decomposes to molybdenum disulfide at typical reaction temperatures, has been used as a precursor to obtain a good dispersion of the disulfide.

A variety of iron compounds are soluble in water or organic solvents, and have been investigated as prospective catalyst precursors for direct liquefaction and for co-processing. The compounds used in this application have included iron(II) acetate [Cook and Cashion, 1987], iron pentacarbonyl [Cook and Cashion, 1987a; Suzuki, et al., 1985; Hirschon and Wilson, 1991; Herrick et al., 1990; Pradhan et al., 1991], dithiodiiron hexacarbonyl [Hirschon and Wilson, 1991], iron(III) acetylacetonate [Kamiya et al., 1988], and iron(III) nitrate [Yamashita et al., 1989]. The compound used in our present work is iron(II) sulfate, or ferrous sulfate. Watanabe et al. [1984] and Suzuki et al. [1984] reported using ferrous sulfate as a

catalyst precursor. In their work, addition of ferrous sulfate did not promote conversion of low-sulfur coals. It is likely that ferrous sulfate did not completely transform to an active catalyst during liquefaction. Rahimi and co-workers [1986] examined the effect of H_2S, $FeSO_4$, and both H_2S and $FeSO_4$ together on coprocessing of coals with heavy oils. They showed that an H_2S:H_2 atmosphere is superior to the addition of $FeSO_4$ in a H_2 atmosphere at low and moderate severity conditions, but at high severity the $FeSO_4$ addition is superior to use of H_2S. Their results may reflect the transformation of $FeSO_4$ to the catalytically active pyrrhotite at high-severity reaction conditions.

H_2S and organosulfur compounds are known to convert various iron compounds to the sulfide under reaction conditions similar to those in the present work. Mills [1950] showed that Fe_2O_3 is converted to the sulfide during catalytic cracking of sulfur-rich feeds. Impregnation of Morwell (Victorian) brown coal with iron(II) acetate resulted in the initial conversion of the precursor to iron(III) oxide and iron (II) humate [Cook and Cashion, 1987b], with subsequent conversion, in hydrogen, of the added iron to magnetite, troilite [Cook et al., 1988] and cementite [Cook et al., 1987a]. However, reacting a high-sulfur, iron-treated coal or adding sulfur to coal treated with iron carbonyl resulted in all of the iron being converted to pyrrhotite [Suzuki et al., 1985].

The work reported in this section is part of a follow-up to the investigation of catalytic pretreatment, as we have described in the previous section and have published elsewhere [Artok et al., 1992]. Staged

processes have been of interest for some time, because they offer the prospect of improving process flexibility, increasing process efficiency, and optimizing the use of hydrogen [Znaimer et al., 1983]. Hydrogen utilization may be fairly easy, and with low requirements for gas-phase hydrogen, up to about 20% conversion [Grainger and Gibson, 1981]. The concept of temperature-staging involves reaction first at a low temperature, e.g. 275-350°C, followed by a second reaction at a higher temperature more typical of direct liquefaction processing, e.g., 375-450°. This technique can provide significant benefits, particularly in conversion to soluble oil products [Derbyshire et al., 1986a; Derbyshire et al., 1986b]. The efficient use of hydrogen in the milder, low-temperature stage could minimize retrogressive condensation reactions [Solomon et al., 1991], combined with a partial depolymerization of the macromolecular structure of the coal [Derbyshire et al., 1986b]. Particularly for low-rank coals, the improved conversion may be facilitated by the loss of carboxyl groups without subsequent retrogressive crosslinking at the reactive sites made available by decarboxylation [Solomon et al., 1991]. Use of catalysts in the two stages can offer enhanced product selectivity in conjunction with high conversions [Derbyshire et al., 1986a].

It was not a goal of our work to optimize reaction conditions, but rather to explore the changes in product distribution resulting from impregnation of two coals of different rank with the precursor of interest, $FeSO_4 \cdot 7H_2O$. Hence we selected a temperature-staging regime of 275°/425° mainly to ensure commonality with prior work and collateral work to be

reported in the following section, eventually to develop comparisons of the benefits of using this catalyst precursor with those obtained from other precursors at comparable reaction conditions.

4.2. EXPERIMENTAL

The coals used for this work were Blind Canyon (Utah) high volatile A bituminous coal and a Texas subbituminous C coal. Proximate and ultimate analyses of these coals are given in Table 1. The coals were impregnated with $FeSO_4 \cdot 7H_2O$ (0.59% iron, expressed as elemental iron, not the ferrous sulfate salt, on a daf coal basis) in the following way: the iron salt was dissolved in sufficient distilled water to give an approximate water-to-coal ratio of 1:1 (v/w). Usually a single batch of 30 g of coal was impregnated at a time, enough for several experiments. The solution was added to coal in a flat-bottom flask and the mixture was stirred for 30 min, then excess water was removed under vacuum at room temperature. The mixture was continuously stirred during this procedure. While the coal was still wet with water, the mixture was quenched in a dry ice-acetone bath until frozen and was then freeze dried, followed by vacuum drying at room temperature. This low-temperature drying of the coal-catalyst slurry has been shown to improve conversion, presumably by an improvement in catalyst dispersion [Stansberry and Derbyshire, 1988]. For thermal (non-catalytic) hydrogenation, the coals were dried overnight at 100°C.

Liquefaction experiments were carried out using horizontal microautoclave reactors (tubing bombs) with a 25 mL capacity. Five grams of each prepared sample and 5 g of phenanthrene were placed in the tubing

bomb and mixed with a spatula. Then the reactor was sealed and air was removed by repetitive pressurizing to 7 MPa, once with N_2, twice with H_2. Subsequently, the reactor was pressurized to 7 MPa (cold) with H_2 or H_2S:H_2 (5:95). The reactor was immersed in a preheated sand bath. Temperature-staged reaction conditions were 275° for 30 min and at 425° for 30 min. Hydrogen pressures were in the range 10.5-14 MPa at reaction temperature. The reactor was oscillated vertically through 2.5 cm at 350 cycles/min. At the end of each stage, the reactor was plunged into cold water to quench the reaction, then the volume of the product gas was measured by water displacement. The water was saturated with NaCl to prevent CO_2 dissolution. Gas samples were collected for analysis. CO, CO_2, C_1-C_2 determinations were performed using a packed Carbosieve column with thermal conductivity detector. C_1-C_5 determinations were performed using a Chemipack C18 column (connected to a flame ionization detector) on a Perkin Elmer model gas chromatograph. Details of the separation and calculation of yields were given in the previous section. Briefly, preasphaltenes are THF-soluble, toluene-insoluble; asphaltenes are toluene-soluble, hexane-insoluble; and oils are hexane-soluble. Total conversion is determined from the weight of THF-insolubles. Hydrogen absorption was calculated as the difference between the amount of hydrogen initially charged to the reactor and that found by gas chromatographic analysis of the gas after reaction.

To determine the fate of ferrous sulfate itself at these reaction conditions, the salt was reacted in microautoclaves at 7 MPa (cold) N_2, H_2

or $H_2S:H_2$ (5:95) at temperatures of 275, 350 and 425°C for one hour. X-ray diffraction (XRD) measurements of the products were made using Cu-K_α radiation with Rigaku equipment and operated at 40 kV and 20 mA. Sulfur and iron analyses were performed by Galbraith Laboratories, Inc. Thermogravimetric analysis of $FeSO_4 \cdot 7H_2O$ was performed using a Perkin Elmer model TGA-7 in N_2.

4.3. RESULTS AND DISCUSSION

4.3.1. Reaction Chemistry of Ferrous Sulfate

Thermal analysis of ferrous sulfate in N_2 indicated three regions of decomposition. First, a decomposition takes place around 140°C and represents loss of water of hydration. The product in this stage is $FeSO_4 \cdot H_2O$. The second decomposition begins at 230°C and is completed at 260°C. The product of this stage is $FeSO_4$. Final decomposition of the anhydrous ferrous sulfate is effected at temperatures > 575°C, and the product of this stage is hematite (Fe_2O_3). In each of these cases, the identity of the product was verified by XRD. By examining the products obtained in microautoclave reactions of ferrous sulfate in N_2, H_2 and $H_2S:H_2$, it was determined that ferrous sulfate is stable at 425°C in nitrogen and is stable at least to 350°C in either H_2 or $H_2S:H_2$ (5:95). However, it decomposed at 425°C in H_2 and $H_2S:H_2$ (5:95). XRD of the product obtained at 425°C in H_2 showed the presence of troilite and pyrrhotite phases (Figure 3), whereas only the pyrrhotite phase was observed when ferrous sulfate reacted in a mixture of H_2S and H_2 at 425°C (Figure 4). The elemental composition of the stoichiometric ferrous

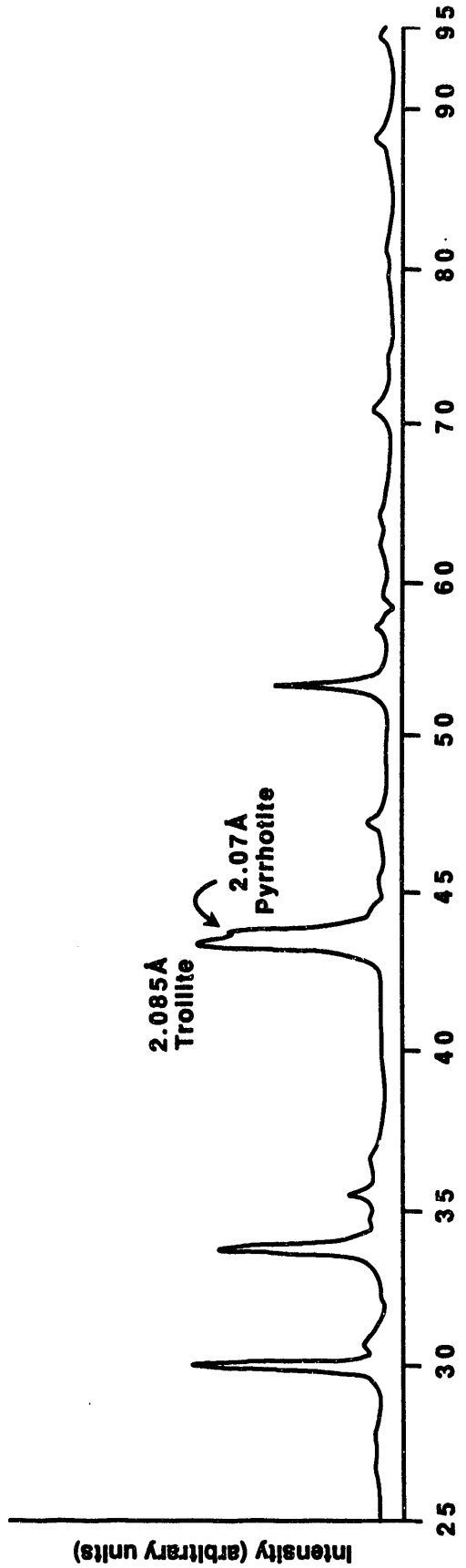

Figure 3 X-Ray Diffractogram of Products Obtained from Reaction of Ferrous Sulfate in Hydrogen Atmosphere at 425°C

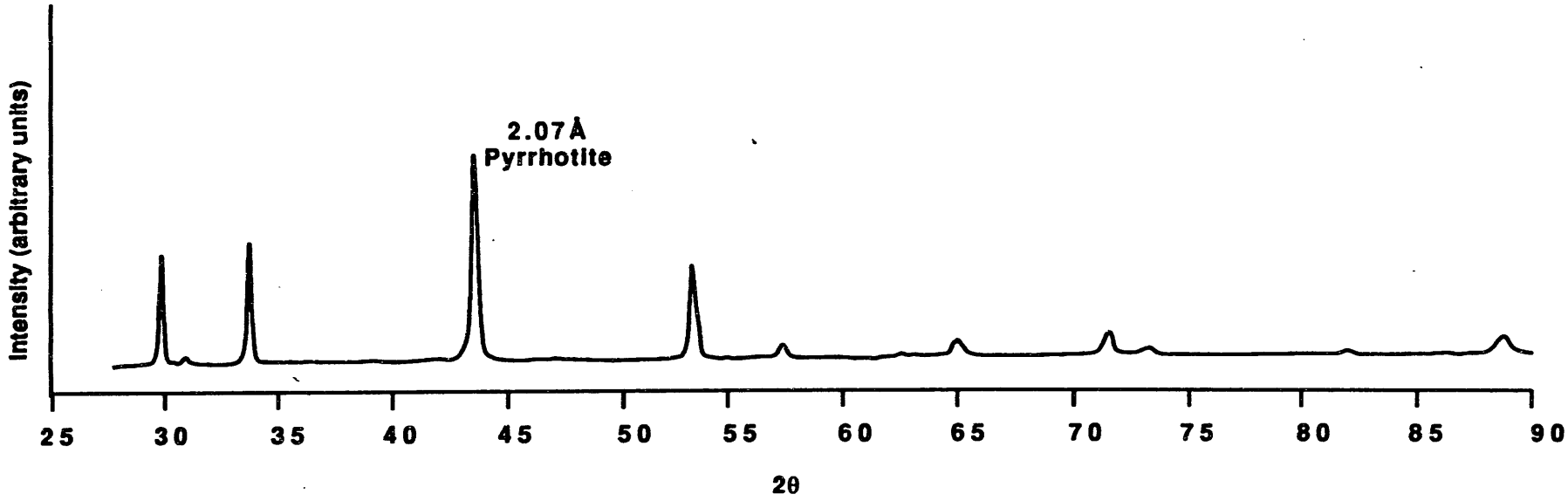

Figure 4 X-Ray Diffractogram of Products Obtained from Reaction of Ferrous Sulfate in 5:95 H_2S:H_2 Atmosphere at 425°C

sulfide is 63.6 Fe, 36.4 S. By comparing the elemental composition of the products (50.0 Fe, 32.8 S in H_2 and 57.5 Fe, 37.8 S in H_2S:H_2 at 425°C), it can be seen that the H_2S:H_2 gas mixture is superior for the transformation of ferrous sulfate to pyrrhotite.

4.3.2. Reactions of Coals Impregnated with Ferrous Sulfate

A comparison of conversion data from liquefaction of Blind Canyon and Texas subC coals in H_2 and H_2S:H_2 (5:95) with and without $FeSO_4$ is given in Tables 11 and 12. For reaction without added $FeSO_4$, hydrogen sulfide addition to the reaction gas increased the total conversion of both coals. The increased conversion came mainly via greater formation of asphaltenes for the Blind Canyon coal. The yields of all liquid products—oils, asphaltenes, and preasphaltenes—were increased for the Texas subC, but the most significant increase was in the oils. Absorption of H_2 from the gas phase also increased by addition of H_2S. These findings agree with the well-known observation that H_2S is beneficial for the liquefaction of coals due to enhancing of hydrogen transfer reactions (hydrogen shuttling), to cleavage of certain types of bonds, and to sulfiding iron species which are already present in coal, producing iron sulfide active for hydrogenation of coal [Baldwin and Vinciguerra, 1983; Murakami et al., 1986; Anderson and Bockrath, 1984; Satterfield and Gultekin, 1981; Willson et al., 1985; Trewhella and Grint, 1987]. H_2S improves conversions of both bituminous and lignitic coals, regardless of whether an iron-containing catalyst is present [Youtcheff and Given, 1982]. One of the properties of H_2S that makes it useful in this regard is the lower dissociation energy of an H-S

Table 11. Conversion and product yields from liquefaction of Blind Canyon bituminous coal with and without $FeSO_4$ catalyst precursor in different atmospheres

Gas Atm.	Catalyst	H_2 Abs. from Gas mg, and (%daf)	Conversion % (daf)					
			Total	Preasp.	Asph.	Oils	CO_x	C_1-C_5
H_2	No	26.0 (0.56)	48.0	12.3	8.5	21.9	3.1	2.2
H_2S:H_2	No	45.4 (0.97)	58.2	12.1	17.2	22.3	2.8	3.8
H_2	Yes	37.2 (0.83)	52.4	10.2	15.4	21.0	3.3	2.5
H_2S:H_2	Yes	71.2 (1.58)	78.5	15.5	29.2	27.5	2.9	3.4

Table 12. Conversion and product yields from liquefaction of Texas subbituminous C coal with and without $FeSO_4$ catalyst precursor in different atmospheres

Gas Atm.	Catalyst	H_2 Abs. from Gas mg, and (% daf)	Conversion % (daf)					
			Total	Preasp.	Asph.	Oils	CO_x	C_1-C_5
H_2	No	25.3 (0.61)	53.1	8.2	10.9	21.2	9.9	2.9
H_2S:H_2	No	47.0 (1.17)	66.7	11.2	13.9	28.1	10.0	3.5
H_2	Yes	50.6 (1.26)	61.2	6.7	13.0	27.2	12.0	2.3
H_2S:H_2	Yes	57.4 (1.43)	71.5	5.1	24.4	27.7	10.2	4.1

bond relative to an H-H bond (i.e., in H_2), making H_2S a better hydrogen donor than H_2 [Stenberg et al., 1982].

The use of $FeSO_4$ (in H_2) slightly increases conversion from 48.0% (daf basis) to 52.4% for Blind Canyon, and from 53.1% to 61.2% for Texas subC. In the liquefaction of Blind Canyon, the major increase in conversion with added $FeSO_4$ is a result of increased asphaltene yield; in contrast, the major increase in conversion of Texas subC is via increased oil yield. In this respect, impregnation of coal with $FeSO_4$ followed by temperature-staged liquefaction in a hydrogen atmosphere has nearly the same effect as liquefaction of the same coal at the same conditions in a H_2S:H_2 atmosphere but without added ferrous sulfate. For both coals, the principal distinction of reaction in the $FeSO_4$: H_2 system relative to the H_2S:H_2 case is that the ferrous sulfate addition provides a lower yield of preasphaltenes than does reaction in H_2S:H_2.

Although the two coals provided similar conversions when liquefied in H_2 without added catalyst, the improvement in conversion obtained by addition of $FeSO_4$ is much greater for the Texas subC than for the Blind Canyon bituminous coal. We attribute this difference to the higher oxygen content of the former coal. Iron catalysts have been shown in several investigations to facilitate carbon-oxygen bond cleavage [Larkins et al., 1984; Cebolla et al., 1991]. Furthermore, the hydrogen uptake nearly doubles in the case of the Texas subC (from 25.3 mg without added $FeSO_4$ to 50.6 mg with $FeSO_4$), whereas a much smaller increase (26.0 mg to 37.2 mg) was observed in comparable experiments with Blind Canyon bituminous coal.

Previous workers have indicated that iron catalysts facilitate conversion of coal to asphaltenes, but do not significantly improve hydrogen uptake [Cook and Cashion, 1987; Herrick et al., 1990]. Our work substantiates this observation for the bituminous coal, but certainly not so for the subbituminous coal.

The H_2S:H_2 atmosphere in combination with impregnated $FeSO_4$ was quite beneficial for conversion of these coals. Addition of H_2S to the reaction gas atmosphere combined with impregnation with $FeSO_4$ significantly promoted conversion of both coals. With Blind Canyon, enhancement of the conversion in H_2S:H_2 with impregnated ferrous sulfate is mainly via greater formation of asphaltenes. For this coal, treatment with either H_2S or $FeSO_4$ used singly produced, in both cases, a near doubling of the asphaltene yield (that is, from 8.5% to 17.2% by addition of H_2S, and from 8.5% to 15.4% by impregnation with $FeSO_4$). The use of the two additives together appeared to have a synergistic effect, resulting in a greater than three-fold increase in asphaltene yield. (The synergy is also quite evident by comparing conversions; for Blind Canyon, for example, the conversions are increased by ≈10% with added H_2S and ≈4% with added $FeSO_4$, but by ≈30% when using the two additives together.) It is also noteworthy that use of H_2S and $FeSO_4$ in combination increased the oil yield as well. The observed H_2 absorption increased from 37.2 mg for reaction in H_2 to 71.2 mg for reaction in H_2S:H_2 (5:95) with $FeSO_4$. With the Texas subC, addition of H_2S or ferrous sulfate singly increased the yields of all of the liquid products, relative to liquefaction in H_2 only, but the most significant

increase was in the oil yield. The use of these two additives together had no additional affect on oil yield, but produced a marked increase in asphaltenes. Hydrogen uptake increased from 50.6 mg to 57.4 mg, compared to the reaction in H_2 with $FeSO_4$. When comparing the amounts of H_2 consumed for the two coals, it is important to recognize that there is less carbonaceous coal substance in the reactor with the Texas subC than with Blind Canyon, because of the higher mineral matter content of the former. To compare the results of one coal with respect to the other, we show in Tables 11 and 12 the H_2 consumptions corrected to a daf basis.

When the coals are impregnated with $FeSO_4$ and liquefied in H_2 (with no added H_2S), there is little increase in conversion relative to the reaction without $FeSO_4$. However, there is a marked shift in the product slate toward lighter products. For example, the asphaltene/preasphaltene ratio for Blind Canyon liquefaction increases from 0.69 without impregnated $FeSO_4$ to 1.51 with $FeSO_4$. Thus a major effect of the addition of $FeSO_4$ to Blind Canyon is catalysis of hydrogenation of preasphaltenes to asphaltenes. The corresponding change for Texas subC is 1.33 to 1.94, again demonstrating that the preasphaltene-to-asphaltene conversion has been facilitated by addition of $FeSO_4$. Even though the initial product slate (that is, as obtained for liquefaction by H_2 without either $FeSO_4$ or H_2S addition) is different for the two coals, as indicated e.g. by the significantly different asphaltene/preasphaltene ratios, added $FeSO_4$ appears to intervene in the same way for both coals. A distinction between the behavior of the two coals impregnated with $FeSO_4$ and reacted in H_2 is the significant

difference in hydrogen utilization. For Blind Canyon, H_2 absorption increased from 26.0 to 37.2 mg upon addition of $FeSO_4$. However, for the subC, H_2 uptake doubled, from 25.3 to 50.6 mg, accompanied by an increase in asphaltenes and a significant increase in oils. Texas subC has about three times the sulfur content of Blind Canyon (1.18% vs 0.42%), and this difference in coal behavior may reflect an *in situ* sulfiding of the $FeSO_4$ by H_2S generated from the coal.

The data in Tables 11 and 12 have been plotted as Figure 5, showing the total conversion, asphaltene yield, and oil yield as functions of the H_2 consumption. Results for both coals, reaction with and without catalyst, and in both H_2 and H_2S:H_2 atmospheres are incorporated as a single data set. It is noteworthy that the lines (obtained by linear least squares regression) have similar slopes for the conversion and asphaltene yields as functions of H_2 consumption, while the slope of the oil yield vs H_2 consumption line is closer to zero. This observation suggests that the principal role of hydrogen absorbed from the gas phase is to participate in the depolymerization of the coal to relatively heavy products (i.e., asphaltenes) and not in the hydrogenation of the asphaltenes to oils.

It must be recognized that a possible side reaction in this liquefaction system is hydrogenation of the liquid vehicle, phenanthrene. Suzuki and co-workers [1984] have demonstrated the use of pyrrhotite to hydrogenate phenanthrene. Thus some of the observed H_2 uptake in our experiments could reflect the hydrogenation of phenanthrene. The hydrogenation product, 9,10-dihydrophenanthrene, is a very good hydrogen

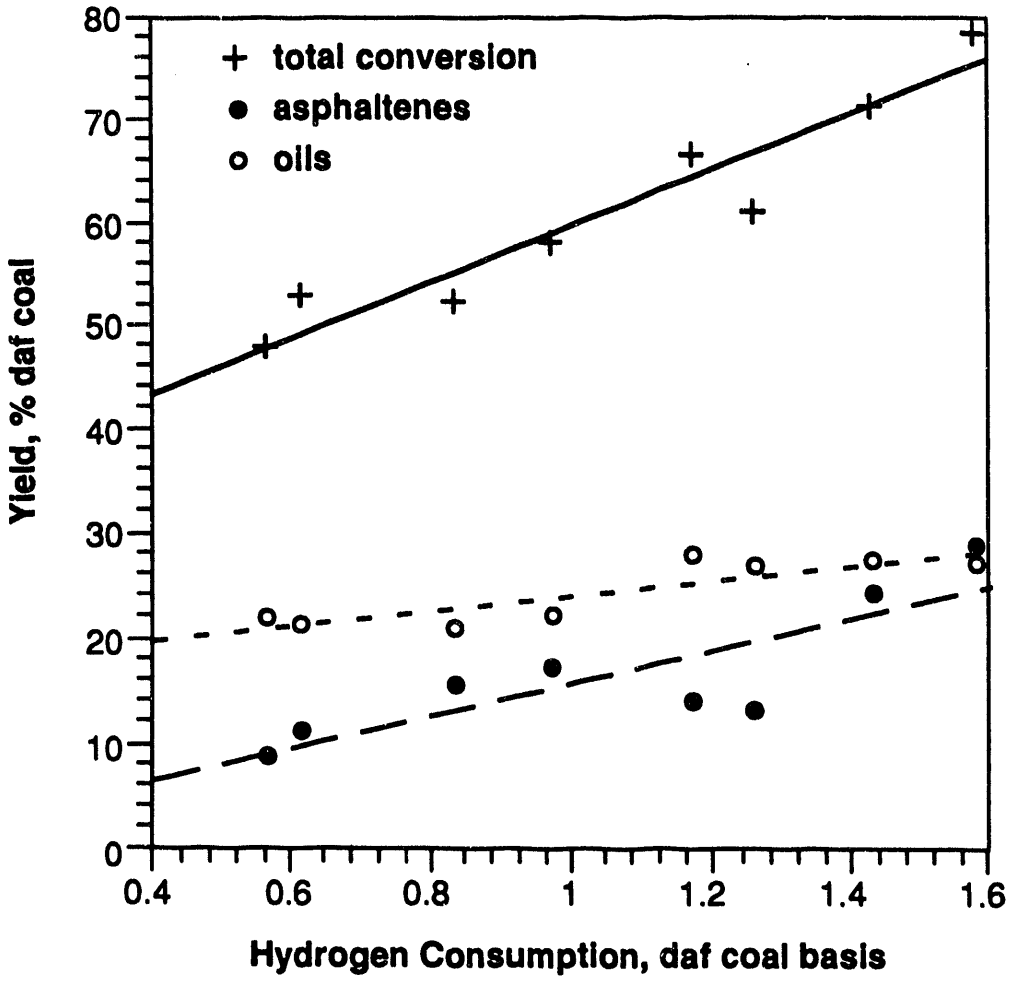

Figure 5 The Dependence of Total Conversion, Asphaltene Yield and Oil Yield on Hydrogen Absorption from the Gas

The data plotted include the results for both coals, with and without $FeSO_4$ impregnation and in H_2 and 5:95 H_2S:H_2 atmospheres.

donor. Thus it was of concern to check the possibility that our conclusions of the behavior of added H_2S, $FeSO_4$, or both, were not confounded by the hydrogenation of phenanthrene and the reaction of the resulting 9,10-dihydrophenanthrene with the coal. Gas chromatographic analysis of the hexane-soluble products showed that less than 2% of the phenanthrene was hydrogenated in our system. Hence we consider that H_2 uptake by phenanthrene and reaction of the 9,10-dihydrophenanthrene with the coal are negligible in this system. Furthermore, since the same quantities of phenanthrene, H_2S, and $FeSO_4$ were used in all experiments, and since the reaction conditions were kept the same, the differences in the extent of H_2 uptake from one experiment to another must incorporate at least some coal-specific effects.

4.3.3. Effect of Reaction Conditions

As noted above, it was not the objective of the present work to examine the effect of various reaction conditions (e.g., changing residence times or temperatures of the stages) or of changing reaction strategies (e.g. the comparative behavior in a single-stage reaction or temperature-programmed reactions). In the previous section we presented results of reaction of both the Texas subC and Blind Canyon coals impregnated with $FeSO_4$ and reacted in H_2 only at the first stage, 275°. We have also presented these results elsewhere [Artok et al., 1992]. In this low-temperature stage no discernable benefit is obtained from adding $FeSO_4$; the conversions of both coals and the yields of various products are virtually identical with results obtained without added catalyst. Indeed, the same

behavior is observed when the two coals are treated with $Fe(CO)_5$ and reacted with H_2 at 275°. We have not investigated the effects of reaction of $FeSO_4$ only in the first stage (275°) in H_2S:H_2. However, the combination of impregnated $Fe(CO)_5$ with a H_2S:H_2 atmosphere resulted in enhanced conversions at 275°. The conversion of the Texas subC increased from 6.6% to 11.2%, mostly via increased yields of preasphaltenes and asphaltenes. The increase in conversion of Blind Canyon, in percentage units, was quite similar, from 17.7% without $Fe(CO)_5$ or H_2S to 22.9% when both additives are used. Again much of the increased conversion was due to enhanced preasphaltene yield.

We have shown elsewhere that temperature programming is an alternative to temperature staging [Song et al., 1991; Huang et al., 1992]. Temperature programming involves a slow heat-up from the low-temperature to the high-temperature stage, in comparison to the relatively quick heat-up normally employed in temperature staging. In the preliminary work done so far, temperature programming without catalyst appears to offer conversions and yields comparable to catalytic temperature-staged liquefaction. However, we have not as yet examined the behavior of Texas subC or Blind Canyon coals and $FeSO_4$ in a temperature-programmed regime.

4.3.4. The Role of the Catalyst in this System

It has long been established that the chemical form of the iron catalyst is an important factor in determining its role in gasification reactions. Several lines of evidence relevant to the present work suggest that the form of the active iron catalyst in temperature-staged

liquefaction also has an effect on its role in these reactions. Iron catalysts derived from organometallic precursors appeared to intervene in single-staged liquefaction of lignite and high volatile C bituminous coal by removing oxygen functional groups [Hirschon and Wilson, 1991]. In H_2, the addition of $FeSO_4$ gives a greater enhancement of conversion for the coal having the higher population of C-O bonds, i.e., the Texas subC. In pyrolysis reactions over heterogeneous iron-containing catalysts, the decomposition of small organic oxygen compounds (e.g., acetone) is inhibited by addition of H_2S to the gas phase [Bennett et al., 1982]. In our work Texas subC shows a smaller enhancement of conversion on addition of $FeSO_4$ and liquefaction in H_2S:H_2 than does the higher rank coal.

Various iron-containing catalysts showed no activity for cleavage of C-C bonds in the model compound 4-(1-naphthylmethyl)bibenzyl [Farcasiu et al., 1991]. Addition of the sulfur to the system facilitated cleavage of the bond between the naphthyl group and methylene carbon. In Blind Canyon, with a higher proportion of C-C bonds than in the Texas subC, the enhancement of conversion on addition of $FeSO_4$ in H_2S:H_2 is much more pronounced relative to liquefaction in H_2. That is, in H_2, the conversion of Blind Canyon coal increased from 48.0% without $FeSO_4$ to 52.4% with this reagent, while in a H_2S:H_2 atmosphere the corresponding conversions were 58.2% without $FeSO_4$ addition and 78.5 with it.

Our observation of the shifting of the product slate to lighter fractions (e.g., enhanced oil yields) with the addition of $FeSO_4$ that is not fully sulfided—that is, without also adding H_2S to the reaction

atmosphere—is in general agreement with results of other investigators on the use of iron-containing catalysts that are not fully sulfided. Morwell (Australian) brown coal treated with iron(II) acetate and reacted at temperatures >405°C showed rather small increases in conversion relative to the coal without iron addition, and the additional conversion was due mainly to increases in lighter products [Cassidy et al., 1982a; Cassidy et al., 1982b]. In related work with the same coal, other investigators confirmed the observation of low increases in conversion, but higher oil yields, using catalysts derived from iron oxide ores [Ogata et al., 1985]. Synthetic iron oxide catalysts also showed the ability to enhance oil yields from French coals [Bacaud, et al., 1990]. In a study aimed at developing an optimum iron/sulfur ratio in liquefaction catalysis, the addition of sulfur to hydrated iron oxide catalysts resulted initially in reduced oil yields (though at high levels of sulfur loadings oil yields eventually increased) [Das Gupta et al., 1991].

Although we have not carried out detailed kinetic studies as part of the present work, the comparison of conversions obtained at comparable reaction times indicates that the activity of the added iron catalyst, with respect to conversion, is much lower when reactions are performed in H_2 relative to H_2S:H_2. The selectivity of the catalyst is changed markedly by choice of atmosphere; for both coals, for example, asphaltene yields with $FeSO_4$ in H_2S:H_2 are double those obtained with added $FeSO_4$ in H_2. Thus the fully sulfided catalyst appears to be very good at hydrogenation, probably supplying hydrogen to cap radicals generated from thermal bond cleavage,

but not having a significant role in hydrocracking or catalytic bond cleavage (i.e., production of lighter products). A comparable observation, based on comparison of FeS_2 with $Fe_2O_3(SO_4)^{-2}$, has recently been reported [Kotanigawa, 1991].

4.3.5. Implications for Liquefaction Processing

We have recently shown that the effect of sulfided catalysts in temperature-staged liquefaction is mainly to increase conversion via formation of relatively heavy liquids (asphaltenes and preasphaltenes), whereas hydrogenation catalysts have little effect on conversion, but rather facilitate conversion of those liquids which do form into lighter products [Burgess et al., 1991]. Collateral work in our laboratory has shown that the efficacy of impregnated nickel sulfate in conversion, liquids yield, and hydrodesulfurization of Mequinenza (Spanish) lignite is directly related to the extent to which $NiSO_4$ has transformed to NiS under a given set of reaction conditions [Garcia and Schobert, 1991].

The results communicated in this section of the report suggest a strategy for tailoring the activity of impregnated $FeSO_4$ for temperature-staged liquefaction. Liquefaction in H_2 with $FeSO_4$ provides little improvement in conversion but rather increased yields of lighter products. For a coal which undergoes facile decomposition to liquids even in the absence of catalysts, the H_2-$FeSO_4$ combination improves the product slate. (An interesting example of such a coal is Gardanne (French) lignite, for which conversions of about 93% in the absence of catalyst are reported [Bacaud et al., 1990].) On the other hand, for those coals which require a

dissolution catalyst to facilitate decomposition to liquids, the addition of small amounts of H_2S to the gas phase, in concert with impregnated $FeSO_4$, can significantly improve conversion relative to that obtained with $H_2S:H_2$ or with $FeSO_4$ alone. The effect of H_2S is not only to promote liquefaction itself; it is also effective to transform catalyst precursors to active forms. $FeSO_4$ is quite stable, and it can not be decomposed up to 540°C in N_2. H_2 is not enough to transform it completely to pyrrhotite at typical liquefaction temperatures. The additional sulfur made available to the reaction system from the added H_2S may be necessary to transform $FeSO_4$ completely to pyrrhotite, which is believed to be the active catalyst, at these conditions.

Because processing improvements (that is, increases in conversion and in asphaltene or oil yield) clearly result from addition of $FeSO_4$ in either a H_2 or $H_2S:H_2$ atmosphere, the $FeSO_4$ precursor converts to a catalytically active species in either case. However, the specific behavior of the resulting catalytically active species is different, depending on the chosen gas atmosphere. Thus with H_2, large increases in conversion are not obtained, but there seems to be a shift in the product slate to favor lighter materials, asphaltenes rather than preasphaltenes, or oils rather than asphaltenes. We speculate that it becomes possible for an investigator to consider at what point (i.e., breakdown of the coal or hydrogenation of the products) in the liquefaction of *a given coal* it is most useful to have the catalyst intervene, and then, by selection of the reactive atmosphere, convert the catalyst precursor into a species active

for catalysis of the desired step. The ability to tailor the effect of impregnated $FeSO_4$ by sulfiding, or not sulfiding as the case may be, suggests that some benefits might also be realized by having the catalyst in different forms in the different stages (i.e., low- or high-temperature) of liquefaction. At present this speculation is based on limited data, but we hope that it will stimulate further investigation of the role of iron catalysts in liquefaction.

5. SWELLING PRETREATMENT OF COALS FOR IMPROVED CATALYTIC TEMPERATURE-STAGED LIQUEFACTION

5.1. INTRODUCTION

Reaction pathways during the initial stages of coal liquefaction are likely to be driven predominantly by thermal reactions. Thermally derived radicals must be stabilized promptly to prevent retrogressive reactions which could lead to the formation of refractory, high molecular weight species. In particular, low-rank coals have a higher tendency to undergo condensation reactions. The large number of oxygen functionalities in low-rank coals is one of the most important factors affecting their tendency to participate in retrogressive reactions. Phenolic and carboxylic functional groups are known to be involved in polymerization reactions. The radicals formed during heat-up of the coal can participate in a number of competing reactions (e.g., hydrogenation and condensation). When a catalyst is not available, gas-phase H_2 is not sufficiently reactive to quench promptly all the radicals formed. Therefore, a good hydrogen-donor solvent, an active catalyst, or both, are necessary to achieve a fast transfer of hydrogen to the reactive sites. A good donor solvent capable of a high degree of contact with the coal surface can limit condensation reactions by donating its own hydrogen to the nascent radicals. However, a solvent itself is not sufficient to drive hydrocracking reactions of asphaltenes to lower molecular weight products in relatively short liquefaction reaction times (1-30 min). A catalyst with high activity (e.g., MoS_2) dissociates molecular H_2 into active hydrogen atoms that stabilize radicals promptly

and facilitate the hydrogenolysis of carbon-carbon and carbon-oxygen bonds. Unfortunately, solid catalysts have the disadvantage of not being accessible to all the reactive sites of the coals. For that reason, coals generally can be solubilized in a good donor solvent (even in the absence of catalyst) to a greater extent than during dry catalytic liquefaction (i.e., liquefaction in the absence of solvent). Nevertheless, a catalyst is essential for the rehydrogenation of dehydrogenated solvent and for facilitating the further reactions which are necessary to obtain liquid yields of high quality, such as hydrocracking, hydrodesulfurization, or hydrodenitrogenation.

Viable alternatives to minimize retrogressive reactions include pretreating the coals before liquefaction experiments and utilizing the catalyst more efficiently by enhancing its dispersion. Pretreatment methods include low-temperature hydrogenation (often carried out as the first stage of temperature-staged liquefaction), chemical treatment methods and solvent swelling techniques. The favorable effect of a low-temperature hydrogenation step on liquefaction has been demonstrated [Derbyshire et al., 1986a; Derbyshire et al., 1986b; Burgess and Schobert, 1991] and was attributed to an inhibition of retrogressive reactions [Solomon et al., 1991]. A recent example of the beneficial effect of chemical treatments is the work of Baldwin et al. [1991], who reported that the alkylation of coals improved liquefaction. Rincon and Cruz [1988] were the first to report the beneficial effect of tetrahydrofuran (THF) preswelling on liquefaction. Later, Joseph [1991a] established a direct correlation

between the extent of preswelling and the conversion of coal under liquefaction conditions. As described in Section 3 of this report, we have also found that preswelling was beneficial for conversion at a pretreatment temperature of 275°C. Our findings have also been documented elsewhere [Artok et al., 1991; Artok et al., 1992].

A more efficient catalyst dispersion (smaller particle sizes and deeper pore penetration) on coal increases the coal-catalyst surface contact per unit catalyst, thus resulting in improved conversion. Weller and Pelipetz [1951] were the first to point out the importance of catalyst dispersion for promoting the conversion of coals under liquefaction conditions. Dispersed-phase catalysts for direct coal liquefaction have been thought to be more efficient than insoluble catalysts [Terrer and Derbyshire, 1986; Stansberry and Derbyshire, 1988; Garcia and Schobert, 1989]. Impregnation of coals using water- or oil-soluble catalyst precursors should enhance their dispersion. The decomposition of these catalyst precursors into a catalytically active form in the initial stage of liquefaction improves conversion [Artok et al., 1991; Artok et al., 1992; Hawk and Hiteshue, 1965; Suzuki et al., 1985; Watanabe et al., 1984; Anderson and Bockrath, 1984; Suzuki et al., 1984]. Cugini et al. [1991] found that it is possible to have a yield of liquids when using a well-dispersed iron catalyst as high as obtained with a molybdenum catalyst. The extent to which catalysts can be dispersed on coal is highly dependent on the properties of the coal (e.g., surface functionalities and porosity), and on the type of catalyst precursor used. As we have indicated in

Section 3 and elsewhere [Artok et al., 1992], impregnation techniques can be accompanied by an undesirable agglomeration of the catalyst particles during the removal of the impregnation solvent, and by inability of the catalyst precursor to penetrate the pores within coal structure. In this regard, oil-soluble organometallic compounds can produce dispersed catalysts of higher activity than water-soluble precursors [Hirschon and Wilson, 1991]. For example, Yamada et al. [1985] determined that as low as 0.1% molybdenum loading on the coal, in the form of $Mo(CO)_6$, is sufficient to obtain a high liquefaction yield. This was attributed to the attainment of smaller catalyst particle sizes with the organometallic precursors. One of the techniques to improve dispersion is the use of reagents known to swell coal as the solvents for impregnation of the coal with the catalyst precursor. An appropriate solvent might open and enlarge pores, thus enabling the precursor to penetrate the coal matrix. Joseph [1991b] confirmed that higher yields could result from the proper combination of swelling solvent and catalyst for the liquefaction of coals. As discussed in Section 3 and elsewhere [Artok et al., 1991; Artok et al., 1992], we also observed this positive effect, even at a pretreatment temperature of 275°C. In contrast, however, Warzinski and Holder [1991] reported that the impregnation of a coal with ammonium tetrathiomolybdate (ATTM) using pyridine (which is a well-known swelling agent) as the solvent gives a performance comparable to that using water as the impregnation vehicle.

In this section of the report, we provide results of an investigation on the effects of the catalyst precursors, impregnation techniques and solvent swelling during temperature-staged liquefaction and the effects on the product slate and composition. This section is an extension of the previous sections, particularly Section 3, in which we reported results of catalyst impregnation and solvent swelling on the same coals only for the first, low-temperature stage. In that section, we demonstrated that, at 275°C, catalyst impregnation without swelling pretreatment improved conversion of two coals, mainly by enhancing preasphaltene yields. In the absence of catalyst, swelling the subbituminous coal with any solvent enhanced conversion as a result of increased oil and gas yields. Only THF and tetrabutylammonium hydroxide (TBAH) increased the conversion of the hvAb coal, by increasing preasphaltenes. Combining catalyst impregnation with solvent swelling enhanced conversion of the subbituminous coal by up to a factor of two, and increased the yields of all products. Little benefit was obtained for the hvAb coal. We now show how temperature staging, with the addition of a second stage at 425°C, extends and modifies the findings discussed in Section 3.

5.2. EXPERIMENTAL

5.2.1. Catalyst Preparation and Testing

Ammonium tetrathiomolybdate (ATTM) and MoS_3 were synthesized as discussed previously and described elsewhere [Artok et al., 1991]. $Mo(CO)_6$, $FeSO_4 \cdot 7H_2O$, bis(tricarbonylcyclopentadienylmolybdenum) (CPMC) and bis(dicarbonylcyclopentadienyliron) (CPIC) catalyst precursors were

purchased from Johnson Matthey/Alfa products and were used without further treatment. One gram samples of ATTM, $Mo(CO)_6$ and $FeSO_4 \cdot 7H_2O$ were reacted in microautoclaves at 7 MPa (cold) N_2, H_2 or $H_2S:H_2$ at temperatures of 275°, 350° and 425°C for 1 h. When $H_2S:H_2$ was the reaction atmosphere, a 5:95 ratio of $H_2S:H_2$ was used for the ATTM and $FeSO_4 \cdot 7H_2O$ experiments, but the ratio was 13.6:86.4 for the $Mo(CO)_6$ to give a sulfide:metal ratio of 2.5. X-ray diffraction analyses (XRD) of the products were made using Cu-K_α radiation with a Rigaku instrument operated at 40 kV and 20 mA. Sulfur analyses were performed using a Leco Model SC-132 Sulfur analyzer and were also obtained from the Penn State Materials Characterization Laboratory using a Leco iodometric titration sulfur analyzer. Carbon, hydrogen and nitrogen analyses were performed using a Leco model CHN-600 elemental analyzer. Molybdenum and water (by the Karl Fisher method) analyses were performed by Galbraith Laboratories, Inc.

5.2.2. Coal Sampling and Characterization

Samples of Blind Canyon (Utah) high volatile A bituminous coal (DECS-6) and a Texas subbituminous C coal (DECS-1) were used in this study. The principal characteristics of these coals are summarized in Table 1 and Appendix A.

5.2.3. Swelling of Coals Prior to Liquefaction

The coal samples were swollen using methanol, pyridine, THF and 10% TBAH solution (in a 1:1 w/w water:methanol mixture). Approximately 30 g of the as-received coal sample were mixed with sufficient swelling reagent to give approximately a solvent-to-coal ratio of 3:1 and were stirred for 6 h

under N_2. This was followed by vacuum drying at room temperature for the methanol-, THF- and TBAH-treated coals (until less than 3% of water remained on each coal) and at 100°C for the pyridine-treated coals (to limit amount of pyridine retained on the coal samples). Residual TBAH was allowed to remain on the coals.

5.2.4. Impregnation of Coals with Catalyst Precursors

Each catalyst precursor was loaded onto batches of coal in an amount based on 1 wt% molybdenum or 0.59 wt% iron (as the metal, not metal compound) on a dry, ash-free (daf) basis regardless of the impregnation method, except for the ion-exchange method discussed below. The different percentages of loaded iron and molybdenum were used in order to provide the same metal loading on a gram-atom basis. Except for MoS_3, experimental conditions were selected to favor the following factors during impregnation of the catalyst precursors onto coal: a) to keep each catalyst precursor in a soluble form during impregnation in order to maximize its dispersion on, and penetration into, the coals; b) to remove the swelling and impregnation reagents efficiently; and c) to keep the coal matrix at a maximum level of swelling during impregnation with the catalyst precursor. Therefore, the selection of both solvent and the method for the impregnation of the catalyst precursor was dependent upon the solubility and volatility of the catalyst precursor and the type of coal used.

When swelling of the coal was not induced, the coal samples were impregnated with a aqueous solution of ATTM or $FeSO_4 \cdot 7H_2O$, an aqueous suspension of MoS_3, a pentane solution of $Mo(CO)_6$, and methanol solutions

of CPIC and CPMC. Undried coal samples were used for impregnation except with $Mo(CO)_6$. In that case it was necessary to dry the coal prior to impregnation, because the prolonged drying of the catalyst-coal mixture after impregnation causes sublimation of $Mo(CO)_6$, even at room temperature. Catalyst-solvent mixtures were added to the coal and stirred for 30 min; then the excess solvent was removed while stirring under vacuum, and the impregnated samples were dried at room temperature in vacuum until the solid contained less than 3% moisture.

ATTM, CPIC and CPMC catalyst precursors were used in the investigation of the effect of swelling on liquefaction. In the case of ATTM, the swelling solvent was added to the undried coal (solvent:coal ratio of 3:1) and stirred for 6 h under N_2. Subsequently, the water-methanol solution of ATTM was added to the coal-solvent mixture (ATTM being soluble in this mixture regardless of the type of solvent used as swelling reagent) and stirred for an additional 30 min under N_2. When TBAH was used as the swelling agent, ATTM was dissolved in a 10% TBAH solution of a 1:1 (w/w) ratio water:methanol mixture (ATTM is insoluble in 10% TBAH solution in water only). This solution was added to coal and stirred for 6 h under N_2. In Section 3 we show that 6 h are enough to reach the maximum level of swelling. Stirring was then followed by the removal of excess solvent at room temperature in vacuum and subsequent drying at room temperature for THF and TBAH, and at 100°C in vacuum for pyridine. TBAH was allowed to remain in the coal. With CPIC and CPMC, the catalyst precursor was dissolved in a swelling agent, and then mixed with the coal and stirred for

6 h. Removing the solvent and drying the coal were done as in the case of ATTM, until the solids contained less than 3% moisture.

For ion-exchange loading of iron, approximately 30 g of as-received Texas subC were slurried in 150 cc of 1M NH_4OAc and stirred for 20 h in N_2 at 65-70°C. Subsequently, the mixture was filtered and washed with 1 L of distilled water. The filtrate solution was monitored for Ca^{2+} content using 0.3 M $(NH_4)_2C_2O_4$. The filtered, washed and ammonium ion-exchanged coal was slurried with 0.05 M of $FeSO_4$. After 20 h of stirring, the mixture was filtered and the filtrate was washed with 1 L of distilled water. The coal ion-exchanged with iron was dried at room temperature in vacuum until it contained less than 3% moisture. The Fe, Ca, Na, K and Mg contents of untreated coal and ion-exchanged coal sample were analyzed by the Penn State Materials Characterization Laboratory.

5.2.5. Liquefaction Experiments and Fractionation of Products

A temperature-staged reaction scheme was applied for the liquefaction experiments, 30 min at 275° followed by 30 min at 425°C. Five grams of coal and 5 g of phenanthrene (as a hydrogen-shuttler vehicle) were used for each experiment. The details of sample loading, reactor preparation and reaction performance at 275°C were given in Section 3. At the end of the 275° first stage, the microreactor was quenched in water. The gas volume was measured by displacement of water (saturated with NaCl in order to limit CO_2 dissolution). When the reaction was performed a H_2S:H_2 mixture, the H_2S content of the gas was absorbed by bubbling the product gas through a $Cd(OAc)_2$ solution before measuring the volume of gas produced. Gas

samples were collected for further analysis. The microautoclave was repressurized to 7 MPa (cold) with the desired gas mixture and heated for 30 min at 425°C in a preheated sandbath. During the reaction period at each stage, the reactor was oscillated through an amplitude of 2 cm at 350 cycles/min. At the end of the reaction, the reactor was quenched to room temperature and the volume of the gas product was measured as explained above, after which portions of gas were taken for analysis.

The fractionation procedure of the products was also described in detail in Section 3. Briefly, the preasphaltenes are THF-soluble and toluene-insoluble, the asphaltenes are toluene-soluble, hexane-insoluble, and the oils are the hexane-solubles. The conversion is determined from the weight of the THF-insoluble residue (corrected as appropriate for weight of added catalyst). The moisture content of the coal sample was corrected for in calculation of yields. Gas chromatographic analyses (GC) were performed for CO and CO_2 using a packed Carbosieve column and thermal conductivity detector, and C_1-C_5 using a Chemipack C18 column with flame ionization detector. H_2 consumption during the reaction was calculated from the difference between the amount of H_2 initially charged to the reactor and that found by gas chromatographic analysis of the gas left after reaction. Analysis of the hexane-solubles revealed that less than 3% of the phenanthrene was transformed to hydrogenated products. Since the amount of hydrogen in the solvent is within the accuracy limits of the measured amount of hydrogen consumed, no attempt was made to correct the amount of calculated H_2 consumption from the gas phase.

5.2.6. Analysis of Liquefaction Products

Saturated fractions of selected samples were eluted as follows; 80 g of neutral alumina (activity Super I, purchased from ICN) and 25 g of silica were wet-packed using hexane on top of a 22 x 500 mm glass column. One gram of sample was impregnated on 10 g of silica using $CHCl_3$ and the sample so prepared was packed on top of the alumina. The sample was eluted with 1100-1300 mL of hexane. The eluted fraction was analyzed by GC with 1-phenyldodecane as an internal standard on a Perkin Elmer model 5800 gas chromatograph equipped with a RTX-50 (0.25 mm x 30 m) column. The column temperature was programmed from 40° to 280°C at a rate of 4°/min and with a hold for 10 min at 280°. Gas-chromatography/mass spectrometry (GC/MS) of saturate fractions was performed on a Hewlett Packard GC/MS Model 5971A instrument operated using 70 eV impact voltage and equipped with a DB-17 (0.25 mm x 30 m) column. The column temperature was programmed in the same fashion as that of the GC analysis. Selected samples of THF-insoluble residues were analyzed by solid state ^{13}C NMR and FTIR, and both asphaltenes and preasphaltenes were analyzed by FTIR. The NMR spectra were recorded on a Chemagnetics M-100 NMR spectrometer by using the cross polarization/magic angle spinning technique (CPMAS).

FTIR spectra were obtained on a Digilab FTS-60A system. Spectra were recorded by coadding 200 scans (interferograms) at a resolution of 2 cm^{-1}. The samples used for FTIR analysis were prepared as KBr pellets. This involved grinding 2±0.02 mg sample with 300±1 mg KBr for 60 s in a Perkin-Elmer Wig-L-Bug and holding under 10 tons of pressure for 5 min in an

evacuated cylinder. The recorded spectra were normalized to 2 mg of sample.

5.3. RESULTS AND DISCUSSION

5.3.1. Catalyst Precursor Transformation

Elemental analysis of the products obtained in microautoclave tests of $Mo(CO)_6$ in H_2, N_2 and H_2S:H_2 are given in Table 13. $Mo(CO)_6$ is largely unreactive at 275°C in H_2 and N_2, as indicated by XRD and elemental analyses. At the higher temperatures, $Mo(CO)_6$ transforms to carbide and oxide forms. The elemental analyses do not concur with any stoichiometric empirical formula, but rather suggest the presence of excess carbon. Leclercq et al. [1989] pointed out that during carbiding of molybdenum by CO, the molybdenum carbides contained free carbon. Optical microscopy of the 275°C products in both H_2 and N_2 revealed a low reflecting, submicron amorphous phase that could be soot.

$Mo(CO)_6$ can be sulfided efficiently at temperatures as low as 275°C. It is likely that sulfidation at low temperatures is more efficient than at higher temperatures, because the rates of oxidation and carbiding increase at the higher temperatures (i.e., 350° and 425°). These competing reactions reduce the formation of sulfided molybdenum, which is the desired form of molybdenum for liquefaction catalysis. XRD of the H_2S:H_2 products (Figure 6) shows peak intensities increasing with increasing reaction temperatures, although no strongly crystalline phases were observed. As the reaction temperature increases, the (hkl) reflections corresponding to

Table 13. Elemental analysis of the products obtained from microautoclave experiments with $Mo(CO)_6$

Reaction Atm.	Reaction Temp.°C	%Mo (wt)	%C (wt)	%S(wt)	100-(%Mo +%C+%S)
H_2	275	40.8	24.5	—	34.7
H_2	350	81.8	3.3	—	14.9
H_2	425	84.7	3.0	—	12.3
N_2	275	40.8	23.3	—	35.9
N_2	350	87.3	4.5	—	8.2
N_2	425	90.3	5.2	—	4.5
$H_2S:H_2$	275	57.4	0.9	32.9	8.8
$H_2S:H_2$	350	69.7	1.3	25.8	3.2
$H_2S:H_2$	425	69.5	1.4	26.5	2.6

Table 14. Elemental analysis of products obtained from microautoclave experiments with $(NH_4)_2MoS_4$ (ATTM)

Reaction Gas	Reaction Temp. °C	%S (wt)	%Mo (wt)	%N (wt)	S:Mo Mol Ratio
H_2	275	39.4	49.7	3.3	2.4
H_2	350	42.7	51.2	1.2	2.5
H_2	425	42.2	53.5	1.0	2.4
N_2	275	48.5	42.1	3.2	3.5
N_2	350	45.5	53.0	0.6	2.6
N_2	425	44.3	52.7	0.6	2.5
$H_2S:H_2$	275	39.7	49.4	3.4	2.4
$H_2S:H_2$	350	42.6	52.3	1.3	2.4
$H_2S:H_2$	425	41.9	53.8	1.0	2.4

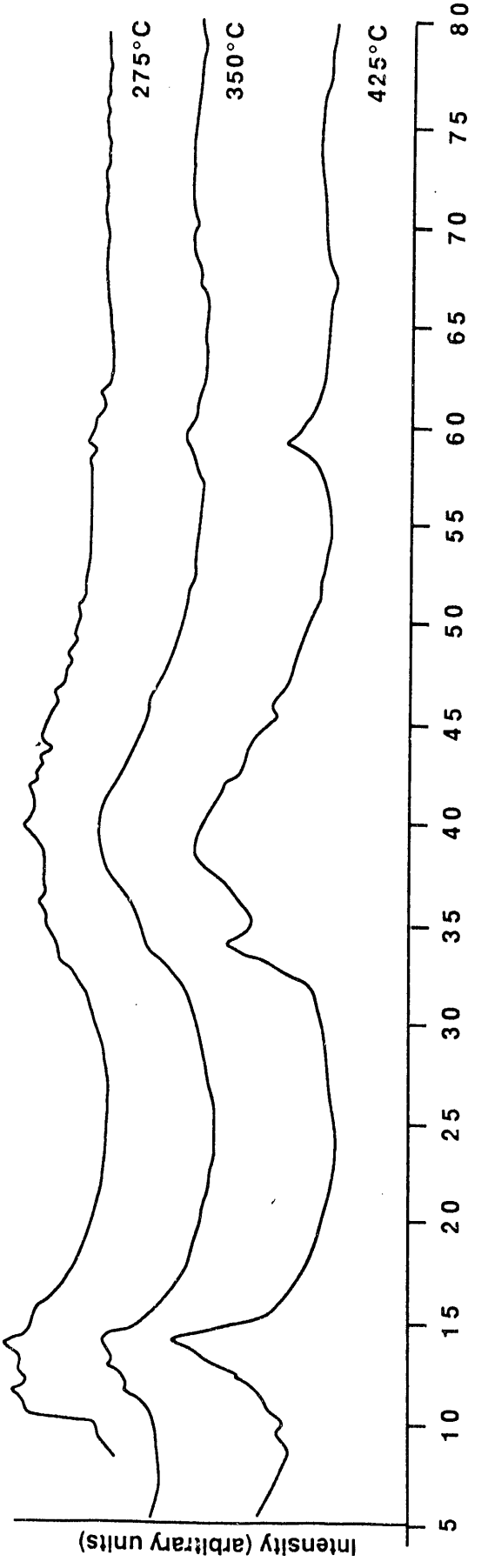

Figure 6 – Comparison of X-ray Diffractograms of Products Obtained from $Mo(CO)_6$ at 275°C, 350°C and 425°C in $H_2S:H_2$

the (002), (101), (103) and (110) planes of hexagonal MoS_2 begin to develop.

Elemental analyses of the products obtained from microautoclave reactions of ATTM in H_2, N_2 and H_2S:H_2 are given in Table 14. The water analysis of the sample (by the Karl Fisher method) obtained from the reaction of ATTM in hydrogen at 275°C gave 6.4%. The samples contain various amounts of nitrogen that gererally decreased with increasing reaction temperature. Since these reactions are carried out in a static reactor without exchange of gas atmosphere, NH_3 formed during the thermal decomposition of ATTM in the reactor might have recombined with molybdenum sulfide. The S:Mo ratios of all the samples are less than 3, except for the sample obtained at 275° in N_2, for which the S:Mo ratio is 3.4, suggesting the presence of MoS_3. Thermogravimetric analysis of ATTM also confirmed the stability of MoS_3 up to 350°C. However, as can be seen in Table 14, H_2 readily reduces MoS_3 to MoS_2 even at 275°. The S:Mo ratio of all samples obtained by reaction in H_2 or H_2:H_2S is greater than 2, suggesting a molybdenum deficiency in the product. As in the case of pyrrhotite, this deficiency might be responsible for the activity of MoS_2. XRD (Figure 7) shows the same trends with increasing temperature for ATTM as those of $Mo(CO)_6$; however, the lines are more intense for the ATTM reaction products than for the $Mo(CO)_6$ products.

5.3.2. Comparison of Catalyst Precursors for the Liquefaction of Coals

The activities of various iron and molybdenum catalyst precursors were compared for the liquefaction of Texas subC (DECS-1) and Blind Canyon

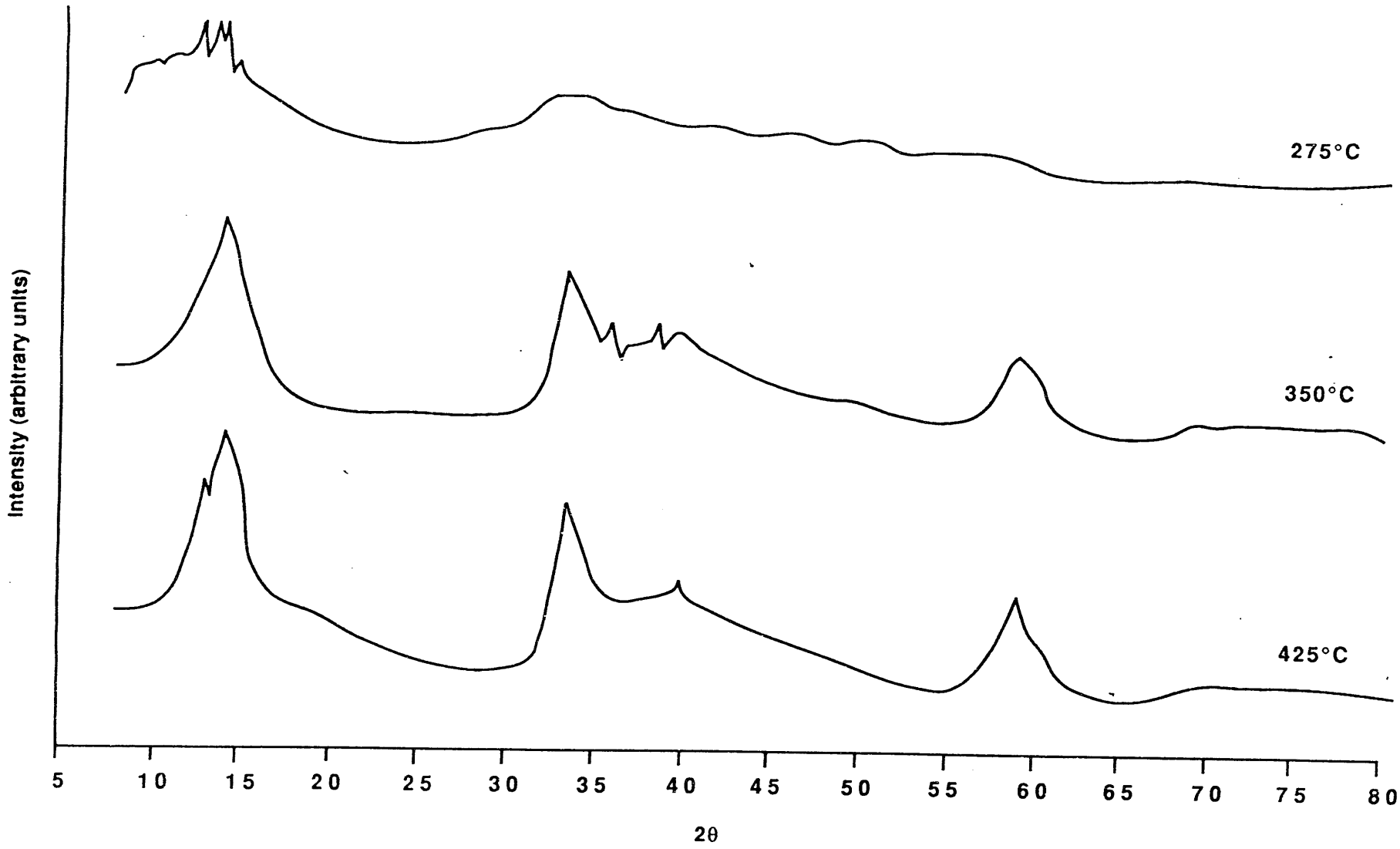

Figure 7 - Comparison of X-ray Diffractograms of Products Obtained from ATTM at 275°C, 350°C and 425°C in H_2

DECS-6) coals in H_2 and H_2S:H_2 (5:95). The results are given in Tables 15 and 16.

We consider first the reactions in H_2. For both coals, addition of any of the catalyst precursors improved hydrogen consumption and conversion of the coal. For Blind Canyon, the molybdenum-containing precursors were, as a group, superior to the iron-containing compounds, with regard to enhancing H_2 consumption, coal conversion, and asphaltene and oil yields. Among the molybdenum compounds, those already sulfided (i.e., ATTM and MoS_3) were superior to the $Mo(CO)_6$; furthermore, the results obtained with the sulfided molybdenum catalyst precursors were generally comparable to each other.

Regardless of which precursor were used, the conversion, asphaltene and oil yields correlate well with hydrogen consumption, as shown in Figure 8. The linear least squares coefficients of determination, r^2, are 0.956 for conversion as a function of hydrogen consumption, and 0.944 and 0.792 for asphaltene and oil yields, respectively. Preasphaltene yields are not plotted in Figure 8 since, as can be seen from Table 15, the yields vary only between 10 and 18% with no evident trend. The relationships shown in Figure 8 indicate that the primary reactions under these conditions are the conversion of coal into soluble materials, and that this conversion is enhanced by increased H_2 consumption.

For the Texas subC in H_2, similar behavior is observed: any catalyst precursor provides improved H_2 consumption, coal conversion, and oil and asphaltene yields relative to a non-catalytic reaction; the molybdenum-

Table 15. Comparison of catalyst precursors for the liquefaction of Blind Canyon bituminous coal (DECS-6)

Catalyst	Gas Atmosp.	H_2 Cons. wt% (daf)[b]	Conversion% (daf)					
			Total	Preas.	Asph.	Oil	CO_x[a]	C_1-C_5
None	H_2	0.56	48.0	12.3	8.5	21.9	3.1	2.2
None	H_2S:H_2	0.97	58.2	12.1	17.2	22.3	2.8	3.8
$FeSO_4$	H_2	0.83	52.4	10.2	15.4	21.0	3.3	2.5
$FeSO_4$	H_2S:H_2	1.58	78.5	15.5	29.2	27.3	2.9	3.6
CPIC	H_2	1.33	69.2	17.7	18.3	26.7	3.3	3.2
CPIC	H_2S:H_2	1.66	76.0	16.2	20.6	31.9	3.8	3.5
ATTM	H_2	2.16	85.1	14.7	32.5	34.9	1.9	2.0
MoS_3	H_2	1.94	86.1	16.9	25.3	38.9	2.3	2.7
$Mo(CO)_6$	H_2	1.74	72.5	11.7	26.9	28.1	1.7	4.1
$Mo(CO)_6$	H_2S:H_2	1.90	86.0	14.2	28.9	36.8	2.9	3.2
CPMC	H_2S:H_2	1.89	88.3	10.9	39.0	32.5	2.6	3.3

[a] Corrected for CO content of CPIC, CPMC and $Mo(CO)_6$
[b] daf basis.

Table 16. Comparison of catalyst precursors for the liquefaction of Texas subbituminous C Coal (DECS-1)

Catalyst	Gas Atmosp.	H_2 Cons. wt%, (daf)	Conversion% (daf) Total	Preas	Asph.	Oil	CO_x[a]	C_1-C_5
None	H_2	0.61	53.1	8.2	10.9	21.2	9.9	2.9
None	H_2S:H_2	1.17	66.7	11.2	13.9	28.1	10.0	3.5
$FeSO_4$	H_2	1.26	61.2	6.7	13.0	27.2	12.0	2.3
$FeSO_4$	H_2S:H_2	1.43	71.5	5.1	24.4	27.7	10.2	4.1
CPIC	H_2	1.53	63.7	11.2	15.6	22.0	11.6	3.3
CPIC	H_2S:H_2	1.87	74.3	9.6	23.2	30.0	8.1	3.4
Fe[b]	H_2S:H_2	2.21	79.3	7.6	23.0	37.0	8.0	3.7
ATTM	H_2	2.42	78.9	10.6	19.3	36.4	10.3	2.3
MoS_3	H_2	2.16	82.4	8.5	21.5	39.3	8.6	4.5
$Mo(CO)_6$	H_2	1.92	86.2	9.3	26.5	36.0	11.0	3.4
$Mo(CO)_6$	H_2S:H_2	2.05	80.1	9.1	18.3	38.7	10.5	3.5
CPMC	H_2	2.03	84.5	7.0	31.4	34.1	8.0	4.0
CPMC	H_2S:H_2	1.82	79.2	20.5	18.6	27.5	7.0	5.6

[a] Corrected from CO content of CPIC, CPMC and $Mo(CO)_6$.
[b] Ion-exchanged

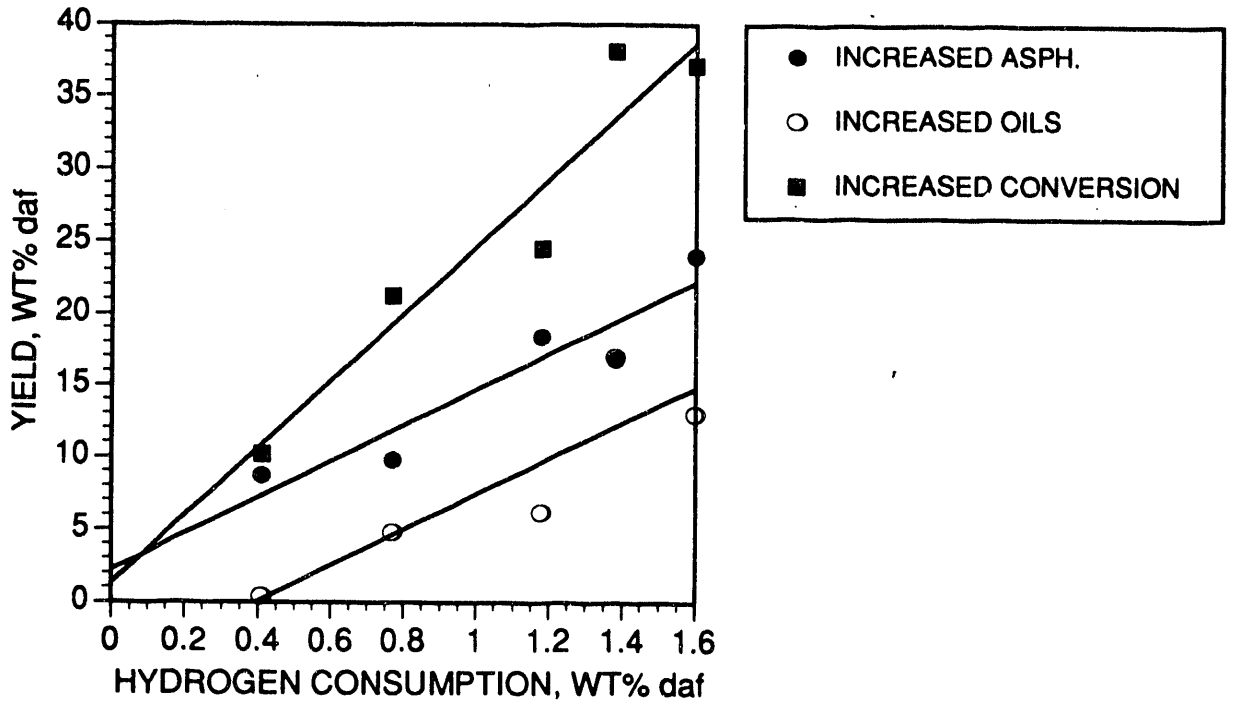

Figure 8 - The Dependence of Conversion, Asphaltene yield, and Oil Yield on Hydrogen Consumption for Liquefaction of Blind Canyon Bituminous Coal (DECS-6), in Non-catalytic Experiments and with $FeSO_4$, CPIC, ATTM, MoS_3, and $Mo(CO)_6$ Catalyst Precursors

containing precursors are superior to the iron compounds; and, among the molybdenum compounds, those that are sulfided are superior to those that are not. Also, conversion, asphaltene yield, and oil yield all show linear relationships with hydrogen consumption, although in this case the correlations are not as good (e.g., r^2 of 0.792 for the dependence of conversion on hydrogen consumption). Again similar to the results with Blind Canyon, the preasphaltene yields are low (5-11%) and show no evident trends.

The apparent lack of dependence of preasphaltene yield on H_2 consumption has at least two explanations: First, it may be that, since asphaltene formation appears to depend on H_2 consumption while preasphaltene formation does not, most of the asphaltene yield was produced directly from the coal, rather than from preasphaltenes. This has been observed in a previous study of the liquefaction of Wandoan (Australian) subbituminous coal and up-grading of coal-derived liquids, in which it was suggested that asphaltenes can form directly from the coal [Song et al., 1989]. Second, it may be that preasphaltenes are being hydrogenated to asphaltenes and oils simultaneously with breakdown of the coal structure. To test the second possibility, the following sequence of assumptions and calculations was made: It was assumed that the distribution of products among preasphaltenes, asphaltenes, and oils would have the same proportion in a catalytic experiment as in a non-catalytic experiment. That is, the ratios preasphaltenes/conversion, asphaltenes/conversion, and oils/conversion are assumed be the same for any experiment with a given

coal. Numerical values of these ratios were calculated from the reaction without added catalyst. Then, for any other experiment, the "expected values" of the product yields could be calculated from the experimentally observed conversion and the appropriate values of the ratios. For example, for Blind Canyon, the ratio preasphaltenes/conversion in the non-catalytic experiment is 0.256. For reaction with added ATTM, the observed conversion was 85.1%; thus the expected preasphaltene yield would be 21.8% (i.e., 0.256 • 85.1). Of course, the actual values of the product yields are measured as part of the experiment. Having both the experimentally measured yield and the "expected yield" allows calculation of an "excess yield," from

Excess yield = Experimental yield - Expected yield.

Continuing the example of Blind Canyon with ATTM, the experimentally observed preasphaltene yield was 14.7% (Table 15). Hence the "excess yield" is -7.1%, the negative value indicating that the experimentally observed preasphaltene yield is lower than would have been anticipated on the basis of the yield structure observed in the reaction without catalyst. (A positive value would represent an experimentally observed yield higher than anticipated by extrapolating results of the non-catalytic experiment.) These calculations can be performed for each combination of coal, catalyst precursor, and gas atmosphere, and for each of the products. In Figure 9 we show the relationship between the excess yields of (asphaltenes + oils) and excess yields of preasphaltenes, using data for both coals and all catalyst precursors tested in hydrogen atmosphere. The linear least

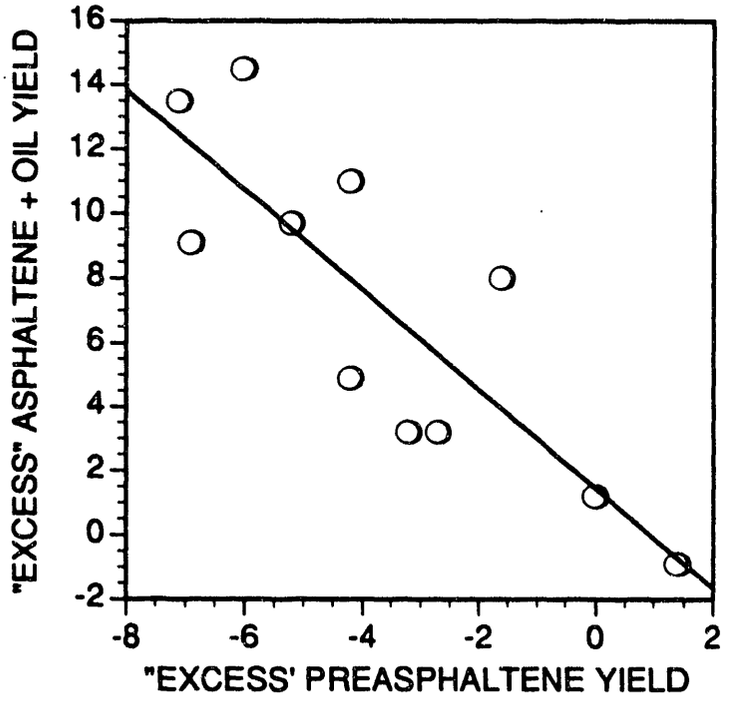

Figure 9 - The Relationship of "Excess" Asphaltenes+Oils with "Excess" Preasphaltene Yields, Using Data for Liquefaction of Both Coals In H_2 with $FeSO_4$, CPIC, ATTM, MoS_3, $Mo(CO)_6$, and CPMC Catalyst Precursors. The "Excess" Yields Represent the Difference Between the Experimentally Observed Yield and that Calculated Assuming that a Catalyst Experiment Would have the Same Relative Proportions of Products as Observed in a Non-catalytic Experiment.

squares coefficient of determination, r^2, for this curve is 0.704. The negative slope, and the fact that asphaltene+oil yields are higher than would be extrapolated from a non-catalytic experiment while the corresponding preasphaltene yields are lower, indicate that preasphaltenes are being converted to the lighter products.

The H_2S:H_2 atmosphere is generally superior to H_2. The beneficial effects of H_2S for liquefaction processing have been documented in the literature [Baldwin and Vinciguerra, 1983; Willson et al., 1985; Murakami et al., 1986]. The promoting effect of H_2S, in the absence of other catalyst precursors, is more pronounced for the Texas subC than for Blind Canyon. This is attributed to the higher iron content of the Texas subC (i. e., 0.50% vs 0.30%, dry basis), because sulfided iron species already in coal can also act as liquefaction catalysts. Ferrous sulfate as a catalyst precursor is the least active in H_2 for both coals, even though it is a sulfur-containing compound. However, in the presence of H_2S, it shows a remarkable activity. It was found that ferrous sulfate is quite stable in H_2, but in the presence of H_2S it completely transforms to an active pyrrhotite phase. The details of these reactions were given in Section 4 of this report.

When the behavior of a H_2S:H_2 atmosphere is combined with an added catalyst precursor, several effects are noted. In all but two cases ($Mo(CO)_6$ and CPMC added to Texas subC) the conversions are higher than attained for the same precursor in a H_2 atmosphere. Usually the enhanced conversion is a result of substantially increased oil yields. Although

molybdenum-containing precursors are still generally superior to iron compounds, the distinction between the two families of compounds is much less in $H_2S:H_2$. For Texas subC, for example, in H_2 the best conversion obtained with an iron compound was 63.7%, while the poorest observed with a molybdenum compound was 78.9%. In $H_2S:H_2$, though, the conversion obtained with ion-exchanged iron, 79.3%, is quite comparable with conversions observed for $Mo(CO)_6$ and CPMC.

The superiority of results in $H_2S:H_2$ relative to those in H_2 alone is attributed to those catalyst precursors not containing sulfur being transformed by H_2S into sulfided compounds which are desirable active phases for liquefaction catalysis. The effect of sulfiding the catalyst precursor by adding H_2S to the gas phase is illustrated by the results for the molybdenum compounds added to Blind Canyon, where similar total conversions are obtained by using sulfided precursors (ATTM or MoS_3) in H_2 and non-sulfided precursors (CPMC or $Mo(CO)_6$) in $H_2S:H_2$. For these four systems, the conversions were all in the range 85-88%, although the distribution of products among preasphaltenes, asphaltenes, and oils varied somewhat for different precursors. Although MoS_3 is not soluble in water or in organic solvents, the conversion obtained using this catalyst precursor was comparable with those obtained with the soluble ATTM, CPMC, and $Mo(CO)_6$. Utz et al. [1989] also reported similar results when comparing MoS_3 with ATTM. The results obtained with Blind Canyon—but not Texas subC—show an apparent synergy between the added catalyst precursor and the H_2S. By comparing the non-catalytic experiments in H_2 and $H_2S:H_2$,

one can determine the enhancement in conversion and product yields due to the added H_2S. Similarly, by comparing a non-catalytic experiment in H_2 with results from using a catalyst precursor in H_2, one can determine conversion and yield enhancements caused by the added catalyst. For Blind Canyon with added $FeSO_4$, CPIC, or $Mo(CO)_6$, the increase in oil yield for reaction in H_2S:H_2 relative to using the same catalyst precursor in H_2 is in all cases greater than the sum of the increases in yield caused by H_2S and the precursors acting alone. This behavior represents another beneficial effect of sulfiding the catalyst. When non-sulfided precursors (i.e., $FeSO_4$, CPIC, or $Mo(CO)_6$) and H_2 are used, the change in oil yields is quite small, in the range -1 to +6%. In comparison, sulfided precursors—ATTM or MoS_3—in H_2 increase oil yields by 13 and 17%, respectively.

With Texas subC coal, the organometallic molybdenum precursors showed more activity in H_2 alone than in H_2S:H_2 or when using sulfur-containing molybdenum compounds. This was not observed for Blind Canyon. Suzuki et al. [1989] reported that a $Mo(CO)_6$-S combination is comparable to $Mo(CO)_6$ alone for hydrocracking C-C and C-O bonds and for hydrogenation of pyrene and phenanthrene. On the basis of those results, one might expect that $Mo(CO)_6$ would exhibit an activity in H_2S:H_2 comparable to that in H_2. In a H_2S:H_2 atmosphere, the $Mo(CO)_6$ and CPMC provide conversions similar to those observed for the sulfided precursors ATTM and MoS_3 in H_2, which would be reasonably expected as a result of sulfidation of the $Mo(CO)_6$ and CPMC by the H_2S. The remarkable feature of the organometallic molybdenum

compounds is that, in H_2, they provide the highest conversions of the subbituminous coal observed for any combination of catalyst precursor and gas atmosphere tested. When reacted in the absence of coal in H_2 at 275°, $Mo(CO)_6$ is largely stable to decomposition, but when the gaseous product was analyzed after reaction of Texas subC impregnated with $Mo(CO)_6$ at 275°C in H_2, the additional CO in the gas was equal to the amount of CO in the added $Mo(CO)_6$. We hypothesize that small, activated arene moieties in the subbituminous coal may participate in CO displacement reactions with the added carbonyl (as are well known for analogous carbonyls, as in the reaction of anisole with $Cr(CO)_6$) [Yamamoto, 1986], possibly leading to better dispersed and more active Mo species.

For the iron-containing precursors, the presence of H_2S allows their transformation to a more active phase. With Texas subC, ion exchange provided a highly active iron-based catalyst, probably due to its success in providing a better dispersion of iron throughout the coal. The conversions and oil yields are very similar to those obtained with ATTM and MoS_3 in H_2. The change in inorganic composition of the subbituminous coal after ion exchange is shown in Table 17. Figure 10 illustrates the FTIR

Table 17. Inorganic elemental analyses of original and iron ion-exchanged Texas subbituminous C coal (DECS-1) (wt%, dry basis)

Sample	Fe	Ca	Mg	Na	K
Raw	0.32	1.47	0.19	0.05	0.04
Ion-Exch.	2.54	0.28	0.02	<0.01	0.04

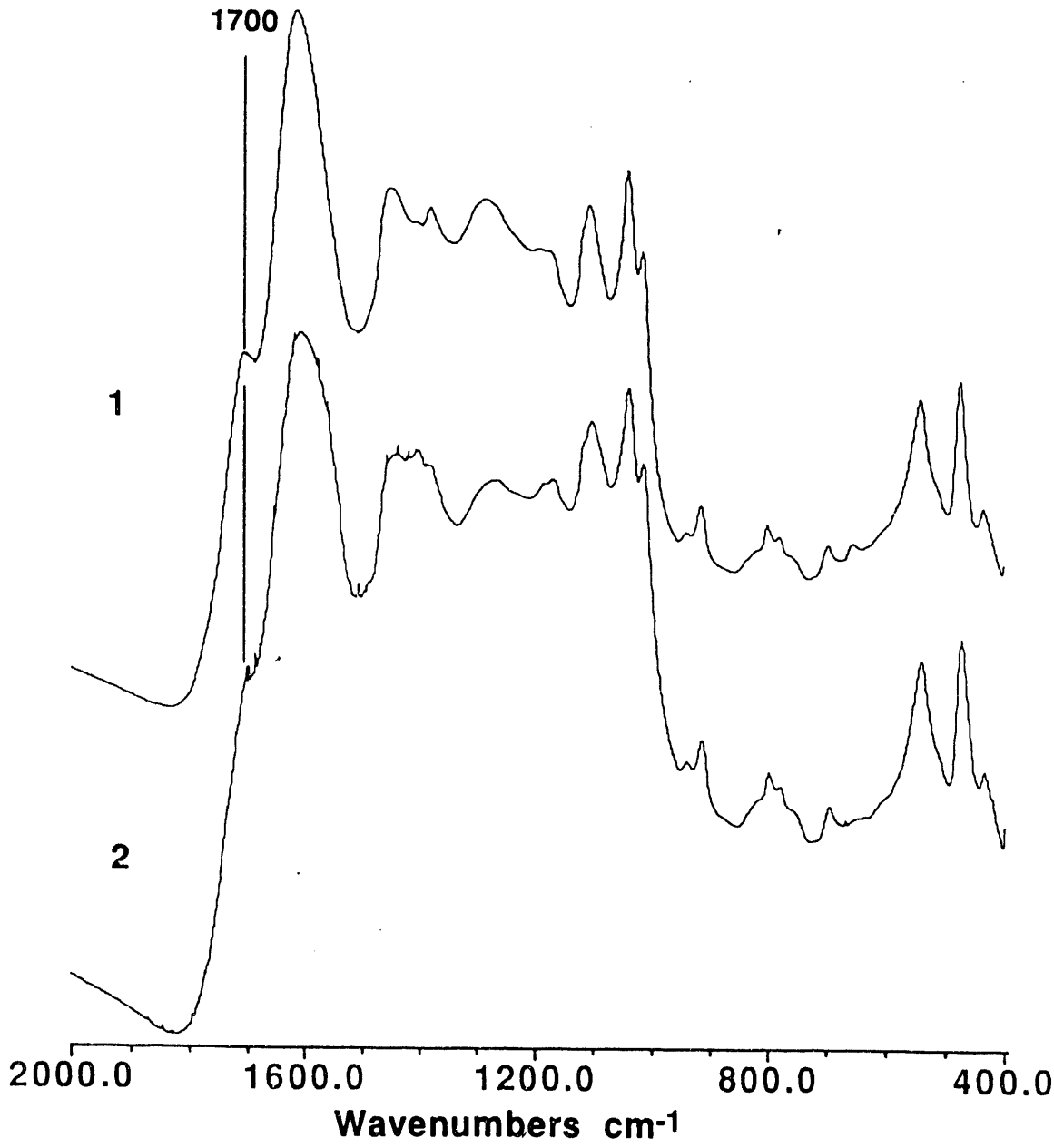

Figure 10 - Comparison of FTIR Spectra of Untreated Texas Subbituminous C Coal (DECS-1) and Texas SubC Ion-exchanged with Iron. 1) Untreated Coal, 2) Ion-exchanged

spectra of the coal with iron (ion exchanged) and in its original form. The shoulder near 1700 cm^{-1} becomes more distinguishable after ion exchange. This finding is in contrast with the FTIR results of Ohtsuka and Asami [1991]. However, the Loy Yang brown coal used by Ohtsuka and Asami had a mineral matter content of only 0.5% (dry basis). Hence, most of the carboxylic groups of the Loy Yang coal were already in the acid (i.e., -COOH), rather than the salt form. A partial combination of H^+ ions from the mildly acidic (pH 4.2) iron solution used for ion exchange with the carboxylic groups causes an increase in the intensity of the absorbance band near 1700 cm-1.

As in H_2, a relationship between the "excess yield" of asphaltenes+oils and the "excess yield" of preasphaltenes is also observed in the H_2S:H_2 atmosphere, as illustrated in Figure 11. For the linear fit of these data, r^2 is 0.916. The negative slope and the fact that asphaltene+oil yields are higher than would be expected from a non-catalytic reaction while preasphaltene yields are lower again implies that preasphaltenes are being hydrogenated to lighter products.

5.3.3. Effect of Preswelling on Liquefaction

The degree of swelling of the two coals by various solvents has been discussed in Section 3. THF and pyridine are effective swelling agents for Blind Canyon, while pyridine and TBAH are effective swelling agents for Texas subC.

Table 18 provides the results from non-catalytic liquefaction of Blind Canyon and Texas subC with and without preswelling. Treatment of

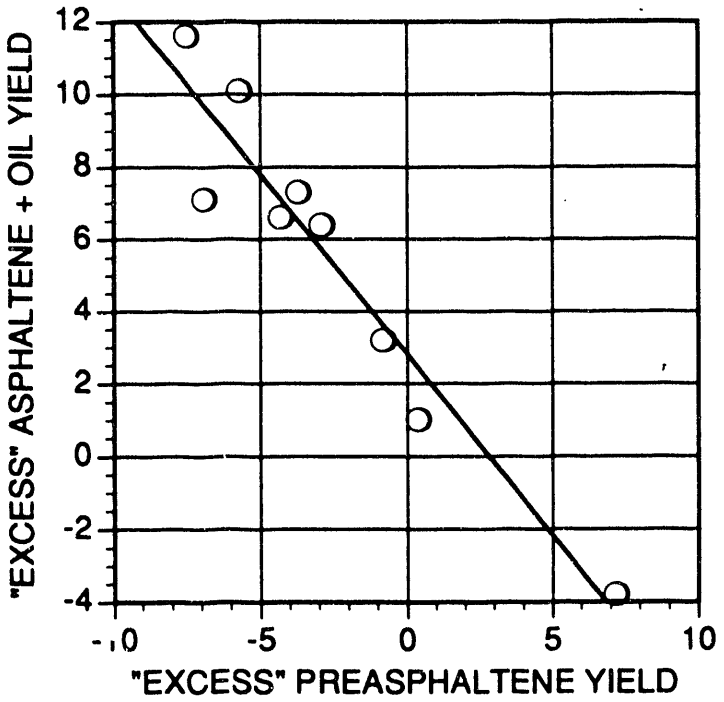

Figure 11 - The Relationship of "Excess" Asphaltenes+Oils with "Excess" Preasphaltene Yields, Using Data for Liquefaction of Both Coals in H_2:H_2S with $FeSO_4$, CPIC, Ion-exchanged Fe, ATTM, MoS_3, $Mo(CO)_6$, and CPMC Catalyst Precursors. "Excess" Yields Determined as in Figure 9

Table 18. Effect of preswelling on the liquefaction of Blind Canyon bituminous (DECS-6) and Texas subbituminous C (DECS-1) Coals

Coal	Solvent	H_2 Cons. wt%(daf)	Conversion (daf) Total	Preas.	Asph.	Oil	CO_x	C_1-C_5
DECS-6	None	0.54	48.0	12.3	8.5	21.9	3.1	2.2
DECS-6	CH_3OH	0.50	46.7	7.2	10.1	22.6	3.8	3.0
DECS-6	THF	0.50	49.7	9.8	12.0	20.5	3.6	3.8
DECS-6	Pyridine	0.54	51.6	7.3	11.3	26.5	3.7	2.8
DECS-6	TBAH[a]	0.60	58.7	9.9	17.3	21.8	5.7	4.0
DECS-1	None	0.61	53.1	8.2	10.9	21.2	9.9	2.9
DECS-1	Pyridine	0.73	60.1	9.2	9.7	29.5	9.3	2.4
DECS-1	TBAH[a]	0.97	72.1	10.9	24.3	25.8	6.9	4.2

[a] Hydrocarbon content of the yield corrected using the gas analysis result of TBAH obtained by hydrogenating TBAH at liquefaction condition without coal.

Canyon with methanol, THF, or pyridine provides essentially no improvement in hydrogen consumption or conversion. The principal effect of these solvents is to shift the product distribution slightly, enhancing the formation of lighter products at the expense of preasphaltenes. Both of these consequences of solvent pretreatment were also observed for reaction only at 275°, although of course conversions and yields were much lower, as we showed in Section 3.3.3. The shift to lighter products is illustrated in Figure 12, which shows the relationship between product yield and solvent swelling ratio. Generally, the better the swelling ability of the solvent used for pretreatment, the lower the preasphaltene yield and the higher the yields of the asphaltenes, oils, and gases. This suggests that

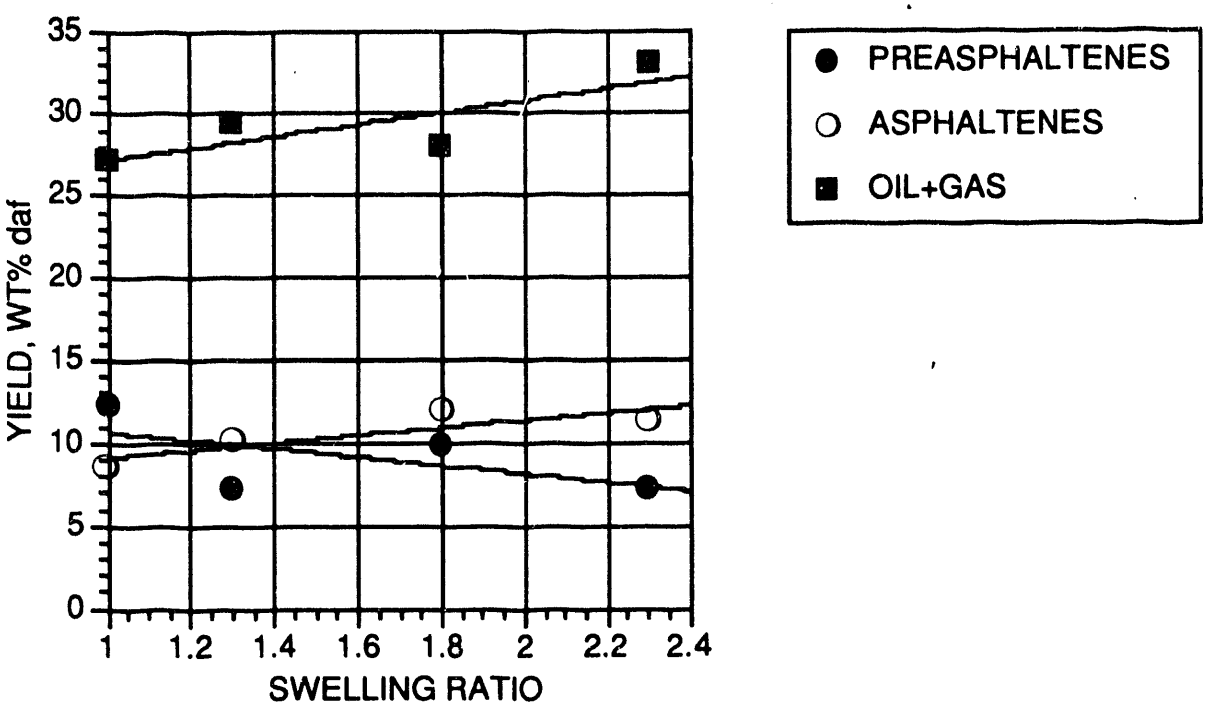

Figure 12 - The Change in Liquefaction Product Slate with Preswelling of Blind Canyon (DECS-6) Coal. Solvents Used Include None, Methanol, THF, and Pyridine

a "loosening" of the structure as a result of swelling may provide better access of the liquefaction vehicle into the coal or easier egress of products. TBAH must be considered a separate case, because its effect on enhancing conversion of Blind Canyon is disproportionate to its rather modest swelling ratio (1.2) for this coal. We have discussed previously in Section 3 that residual TBAH remaining after solvent treatment decomposes to amines (mainly tributylamine) during reaction, and have suggested that tributylamine generated *in situ* acts as a very effective solvent for dissolving coal and possibly facilitating transport of products out of the coal particles. Physical evidence for a TBAH reaction product is discussed in Section 6.3.2.

The beneficial effects of preswelling are more pronounced for the Texas subC. As shown in Section 3, for reaction at 275°, conversions of the subbituminous coal are lower than those of the bituminous coal. For example, without solvent pretreatment, the conversion of Texas subC is 6.6% as compared to 17.7% for Blind Canyon; with pyridine swelling, the respective conversions are 10.0% and 16.0%. However, with temperature-staging and solvent pretreatment, conversion, asphaltene yields and oil yields are now higher from the subbituminous than from the bituminous coal treated with the same solvent. Again the best results are obtained with TBAH pretreatment, although in this case TBAH had by far the highest swelling ratio (2.6) of any of the solvents.

The highly beneficial effect of treating the subbituminous coal with pyridine or TBAH may result from several factors. The nitrogen-containing

basic compounds may interact with acidic oxygen functionalities, such as -COOH and -OH functional groups, to limit retrogressive cross-linking reactions. As we will explain below, additional evidence for this interaction is the reduced yields of CO_x gases and changes in the FTIR spectra of preasphaltenes and asphaltenes from pyridine- or TBAH-treated coals. TBAH might also alkylate the coal, possibly in the course of the first-stage reaction [Anderson and Winans, 1991]. Alkylation of coals may be beneficial for liquefaction [Baldwin et al., 1991]. As noted previously, TBAH decomposes to amines during liquefaction; amines are known to be good promoters for coal liquefaction [Kazimi et al., 1985; Tagaya et al., 1987; Miller et al., 1990].

Swelling agents were used to impregnate ATTM, CPIC and CPMC to investigate the combined effect of solvent treatment and catalyst impregnation of these precursors. With ATTM, using THF and pyridine as impregnation solvents enhanced the total conversion of Blind Canyon from 85.1% to 88.0% and 90.3%, respectively (Table 19). The beneficial effect of swelling was seen mainly in the formation of oils. Oil production increased from 33.9% to 41.9% with the THF and to 43% with pyridine. Improved conversions were consistent with a higher consumption of hydrogen. In contrast, TBAH addition was slightly detrimental for liquefaction of Blind Canyon with ATTM, decreasing both the conversion and oil yield, though increasing the asphaltene yield. We have shown elsewhere that tetrahydroquinoline may convert to propylcyclohexylamine in the presence of a sulfided molybdenum catalyst and poison the catalyst [Burgess and

Table 19. Effect of preswelling on the liquefaction of Blind Canyon bituminous (DECS-6) and Texas subbituminous C (DECS-1) coals with ATTM

Coal	Solvent	H_2 Cons. wt%(daf)	Conversion% (daf) Total	Preas.	Asph.	Oil	CO_x	C_1-C_5
DECS-6	Water	21.6	85.1	14.7	32.5	33.9	1.9	2.1
DECS-6	THF	22.2	88.0	13.4	28.1	41.9	1.7	2.9
DECS-6	Pyridine	24.4	90.3	9.4	33.7	43.0	0.8	3.3
DECS-6	TBAH[a]	22.4	81.7	9.5	45.9	26.3	2.6	4.0
DECS-1	Water	24.3	78.9	10.6	19.3	36.4	10.3	2.3
DECS-1	Pyridine	28.4	88.8	10.9	30.1	37.4	5.6	4.3
DECS-1	TBAH[a]	25.4	88.9	8.9	35.6	34.6	6.3	4.2

[a] Hydrocarbon content of yield corrected using the gas analysis obtained by hydrogenating TBAH at the same liquefaction conditions but in the absence of coal.

Schobert, 1991]; butylamines generated from TBAH may do the same again in the present system. The use of swelling solvents for impregnation of ATTM on Texas subC increased conversions even more than was observed for Blind Canyon, about 10% for both pyridine and TBAH. This increase was mainly reflected in the production of asphaltenes. In addition, both TBAH and pyridine treatments reduced the formation of CO_x gases. The improvements in conversion and oil and asphaltene yields are attributed to an improved catalyst dispersion resulting from better impregnation of the catalyst precursor. The swelling of the coal by the organic impregnation solvent may allow the precursor to penetrate into the coal.

The effectiveness of solvent swelling on liquefaction with CPIC in H_2S:H_2 is not pronounced (Table 20). Using THF as impregnation solvent

Table 20. Effect of solvent swelling on liquefaction of Blind Canyon (DECS-6) and Texas (DECS-1) coals with CPIC in $H_2S:H_2$

Coal	Solvent	H_2 Cons. wt%(daf)	Conversion% (daf) Total	Preas.	Asph.	Oil	CO_x[a]	C_1-C_5
DECS-6	CH_3OH	1.7	76.0	16.2	20.6	31.9	3.8	3.5
DECS-6	THF	1.8	80.0	17.0	25.2	28.9	4.8	4.1
DECS-6	Pyridine	1.5	69.1	8.8	25.5	27.4	3.3	4.1
DECS-1	CH_3OH	1.9	74.3	9.6	23.2	30.2	8.0	3.4
DECS-1	Pyridine	2.1	73.6	6.2	24.0	30.2	8.7	4.5
DECS-1	TBAH[b]	1.9	80.22	11.3	29.8	24.6	9.0	5.5

[a] Corrected for the CO content of CPIC
[b] Hydrocarbon content of yield corrected using the gas analysis from TBAH, obtained by hydrogenating TBAH at the liquefaction conditions in the absence of coal.

Table 21. Effect of solvent swelling on liquefaction of Blind Canyon bituminous (DECS-6) and Texas subbituminous C (DECS-1) coals with CPMC in $H_2S:H_2$

Coal	Solvent	H_2 Cons. wt% (daf)	Conversion% (daf) Total	Preas.	Asph.	Oil	CO_x[a]	C_1-C_5
DECS-6	CH_3OH	1.89	88.3	10.9	39.1	32.5	2.6	3.3
DECS-6	THF	2.00	87.7	8.3	35.6	37.0	3.1	3.7
DECS-6	Pyridine	2.75	91.6	7.9	35.4	42.1	1.8	4.4
DECS-1	CH_3OH	1.82	79.2	20.5	18.6	27.5	7.0	5.6
DECS-1	Pyridine	2.13	75.3	6.3	19.7	38.7	5.0	5.6
DECS-1	TBAH[b]	1.97	78.0	8.6	28.8	25.0	9.6	6.0

[a] Corrected for the CO content of CPMC
[b] Hydrocarbon content of yield corrected using the gas analysis from TBAH, obtained by hydrogenating TBAH at the liquefaction conditions in the absence of coal.

slightly increased the conversion of Blind Canyon from 76% to 80%, with a higher formation of asphaltenes. However, when pyridine was used, conversion and H_2 consumption both decreased. The residual pyridine content, calculated from the increase in nitrogen content of the pyridine-treated coal compared to untreated coal, was 2-4% for Blind Canyon. (The calculation of yields of pyridine-treated coals was corrected for residual pyridine content.) Pyridine may have interrupted the transformation of CPIC to pyrrhotite, the active catalyst for hydrogenation. Addition of TBAH increased the conversion of Texas subC to 80.2%, but this increase was a result of an increase of asphaltenes and preasphaltenes, and reduction of oil yield.

With CPMC, THF and pyridine treatments were beneficial for liquefaction of both coals, mainly by shifting the product slate to favor enhanced oil yields (Table 21). Swelling with pyridine provided a slight increase in total conversion of Blind Canyon. Particularly, using pyridine gave a ≈10% increase in oil yield for both coals. In general a higher amount of H_2 consumption occurred, concomitant with a higher formation of oil. Another effect of pyridine treatment was a decrease in the formation of CO_x gases.

5.3.4. Characterization of Selected Products

To begin an investigation of the effects of catalyst addition and solvent treatment on modification of the structure of the liquefaction products, selected products were subjected to ^{13}C solids NMR spectroscopy (THF-insoluble residues), to FTIR spectroscopy (residues, asphaltenes and

preasphaltenes), and to GC and GC/MS analysis (saturated fractions of hexane-solubles).

Tables 22 and 23 compare f_a values of the residues calculated from ^{13}C NMR spectra. It is noteworthy that there is a significant increase in f_a of the residue from non-catalytic reactions relative to the unreacted coal, even though these reactions attained only ≈50% conversion and consumed relatively little H_2. Further increase in f_a, accompanying an increase in conversion to ≈90% and a quadrupling of H_2 consumption, is relatively small. These results suggest that the early stage of reaction, in which half (or perhaps even less) of the coal is converted to soluble products, leaves a highly aromatic material as residue; further hydrogenation, facilitated by addition of a catalyst, swelling solvent, or both, essentially "nibbles away" molecular fragments of the residue and converts them to soluble products. From our present experiments we cannot say whether the highly aromatic residue at ≈50% conversion represents the less-reactive aromatic material originally present in the coals, or is a result of retrogressive crosslinking reactions inadvertently accompanying the early stages of liquefaction.

Figure 13 illustrates the FTIR spectra of THF-insolubles obtained from the Texas subC coal. The aliphatic C-H stretching bands between 2700 and 3000 cm^{-1} are less intense in the residue than in the unreacted coal. With higher conversion, the contribution of the organic phase to the spectrum decreases, and the absorbance bands from minerals become more noticeable. Similarly, the intensities of aliphatic C-H stretching bands

Table 22. f_a Values of THF-insoluble residues of Blind Canyon coal (DECS-6)

Solvent	—	None	None	pyridine
Catalyst	—	No	ATTM	ATTM
f_a	0.598*	0.891	0.850	0.871

* Parent coal

Table 23. f_a Values of THF-insoluble residues of Texas subbituminous C coal (DECS-1)

Solvent	—	None	None	Pyridine	TBAH
Catalyst	—	No	ATTM	ATTM	ATTM
a					

* Parent coal

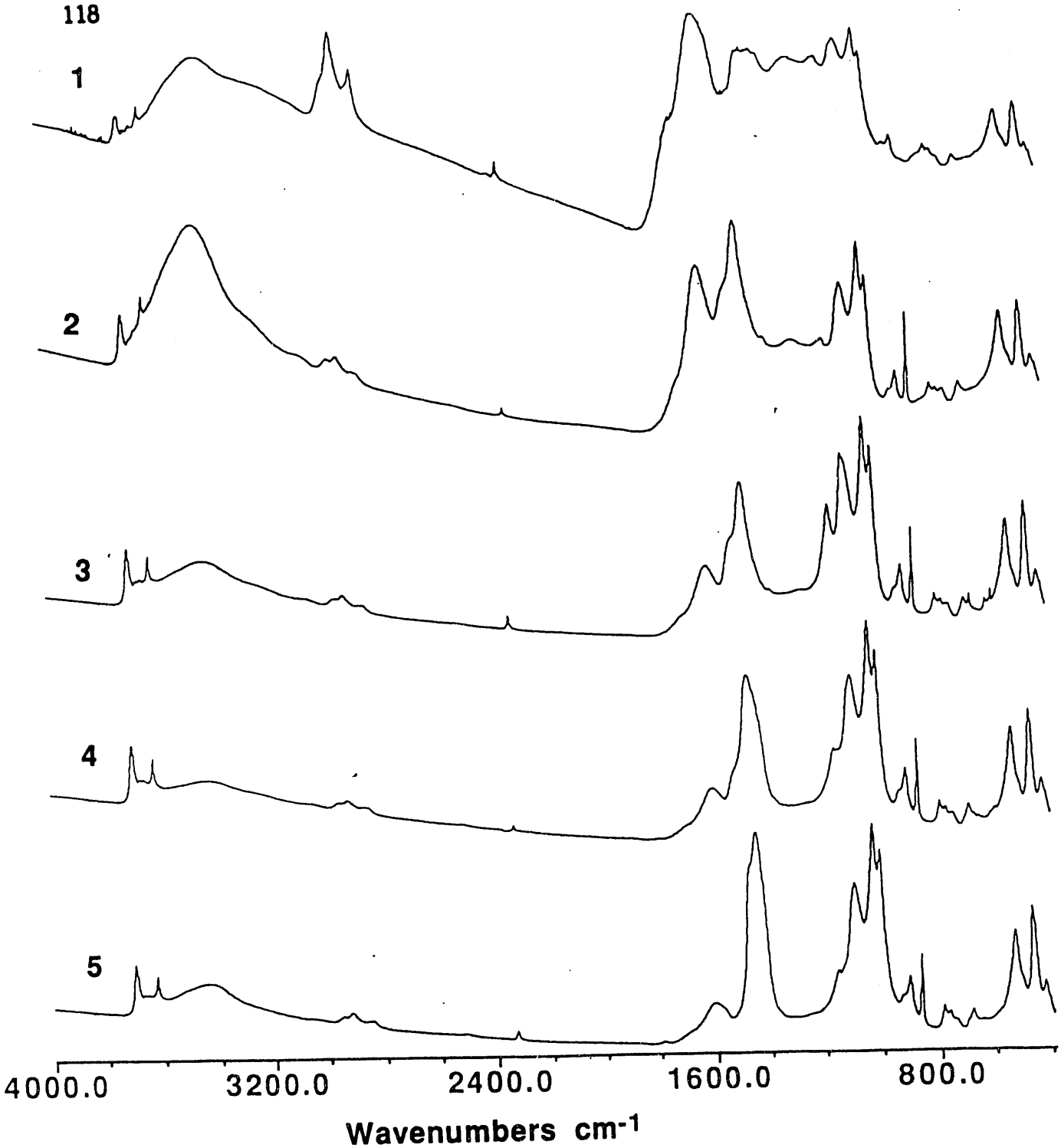

Figure 13 - Comparison of FTIR Spectra of The Texas Subbituminous Coal (DECS-1) and THF-Insoluble Liquefaction Residue. 1) Untreated Coal, 2) Residues from Non-catalytic Reaction, 3) Residue from Reaction with ATTM, 4) Residue from Reaction of Pyridine-treated Coal with ATTM, 5) Residue from Reaction of TBAH-treated Coal with ATTM

in the spectra of residues from Blind Canyon is always less than those in the original coal (Figure 14).

Selected asphaltene and preasphaltene fractions were also examined by FTIR. Generally, slight differences can be seen in the region between 1150 cm^{-1} and 1300 cm^{-1}. The unresolved absorption bands in this region can be attributed to aryl C-O (stretching) aromatic ethers and phenols and to C-O-H deformation bands [Painter and Coleman, 1979; Painter et al., 1981; Bellamy, 1975]. The peak at 1035 cm^{-1} may be due to C-O vibrations of aryl-alkyl ether [Briggs et al., 1957]. Figure 15 illustrates the spectra of asphaltenes obtained from Texas subC. The spectrum of asphaltenes produced in the non-catalytic reaction exhibits two maxima in the region representing C-O groups, at 1267 and 1225 cm^{-1}, and a shoulder at 1700 cm^{-1} assigned to C=O stretching. The spectrum of asphaltenes produced in catalytic reactions spectrum did not differ from that of the non-catalytic experiment. For the pyridine-treated subbituminous coal, the intensity of the 1267-1225 cm^{-1} region decreased slightly. The most notable distinction was in the spectrum of asphaltenes from the catalytic reaction of TBAH-treated coal. The maximum at 1225 cm^{-1} disappeared and the relative intensity of the band at 1267 cm^{-1} was lowered. A decrease in O-H stretching at 3400 cm^{-1} was observed (although there is a contribution from water to this region). In addition, the distribution of aliphatic hydrogens is different from that of other asphaltenes obtained from this coal, owing to a higher proportion of methyl groups absorbing at 2956 cm^{-1}, and similarly for methylene groups (2925 cm^{-1}). The proportion of bands

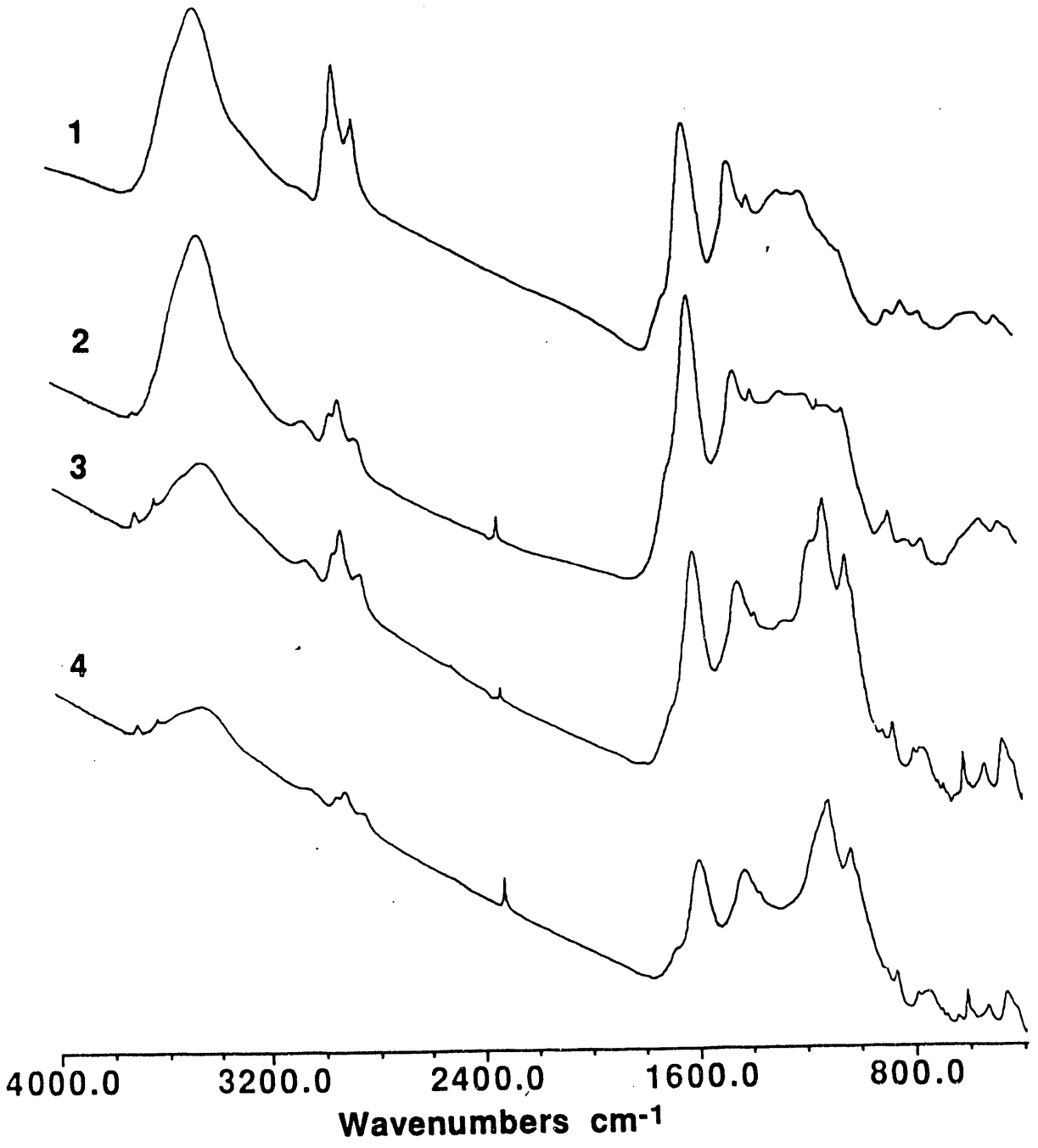

Figure 14 - Comparison of FTIR Spectra of Blind Canyon (DECS-6) Bituminous Coal and THF-insoluble Liquefaction Residues. 1) Untreated Coal, 2) Residue from Non-catalytic Reaction, 3) Residue from Reaction with ATTM, 4) Residue from Reaction of Pyridine-treated Coal with ATTM

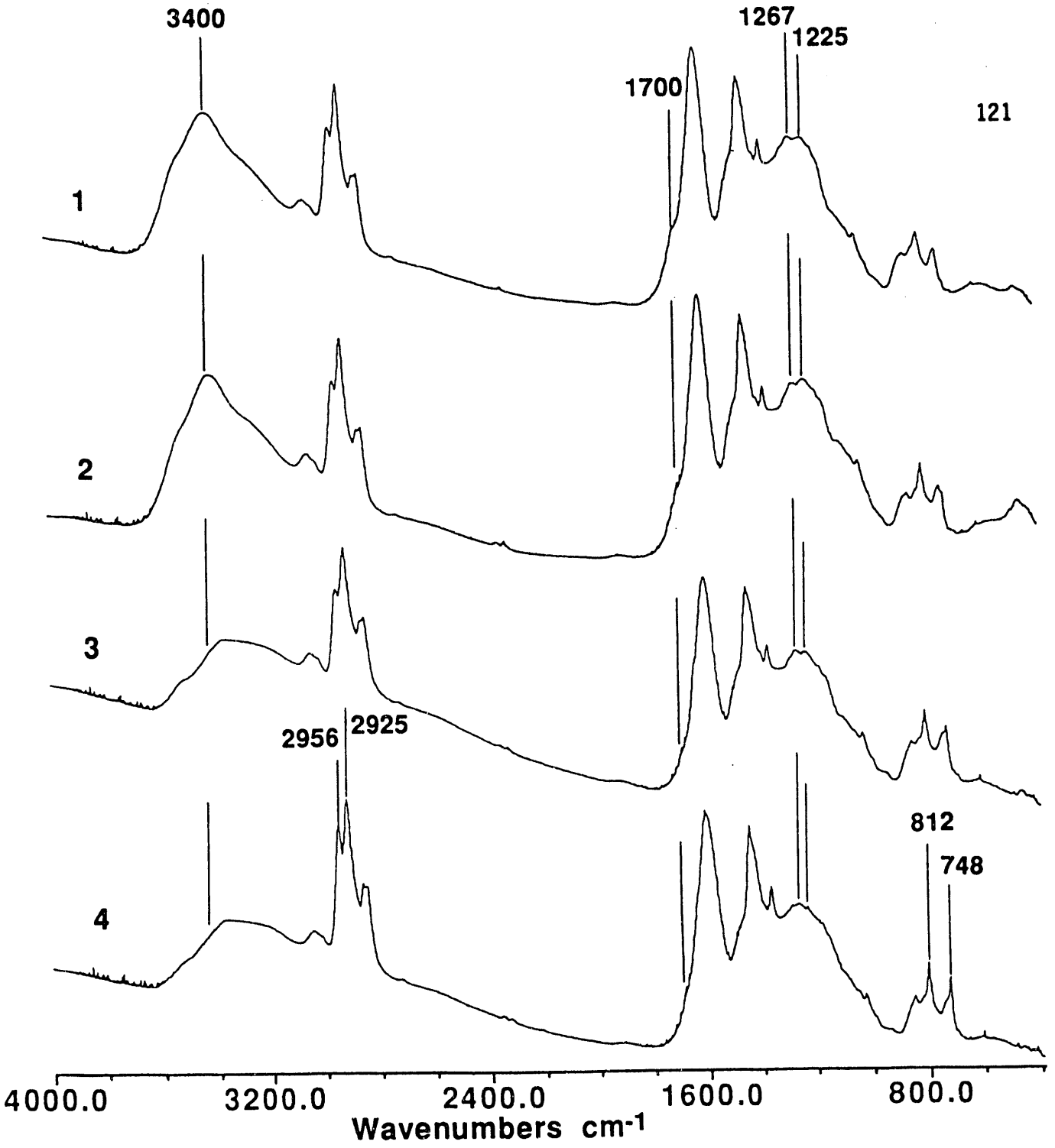

Figure 15 - Comparison of FTIR Spectra of Asphaltenes from Liquefaction of Texas Subbituminous Coal (DECS-1). 1) Asphaltenes from Non-catalytic Reaction, 2) Asphaltenes from Reaction with ATTM, 3) Asphaltenes from Reaction of Pyridine-treated Coal with ATTM, 4) Asphaltenes from Reaction of TBAH-treated Coal with ATTM

between 700 and 900 cm^{-1} (aromatic C-H out-of-plane bending) also differed from those of other asphaltene. That the proportion of the bands at 748 (four neighboring H) and 812 cm^{-1} (two neighboring H) increased relative to the absorption band at 850 cm^{-1} (isolated H band) suggests that the asphaltene sample from the TBAH-treated Texas subC is less substituted and contains less condensed aromatic species. (It should be noted that, not only are there apparent chemical differences in the asphaltenes from TBAH-treated Texas subC vis-a-vis the other asphaltenes from this coal, but also TBAH treatment—with or without added catalyst—invariably led to the highest yields of asphaltenes.) For asphaltenes from Blind Canyon, no difference in the C-H stretching region was observed, nor was there any remarkable difference among samples in the range between 1150-1300 cm^{-1}. The use of catalyst did not affect the intensity of the C=O and C-O group bands. However, after pyridine treatment the carbonyl peak intensity was weakened.

FTIR spectra of preasphaltenes obtained from the Texas subC coal show no differences in the aliphatic C-H stretching region, regardless of the use of catalyst or preswelling (Figure 16). The intensity of the peaks at 1230 and 1190 cm^{-1} is less for the preasphaltene obtained from the catalytic experiment. Pyridine treatment resulted in a decrease in the maxima at 1230, 1190 and 1267 cm^{-1}. The spectrum of the preasphaltene sample obtained from TBAH-treated coal does not show peaks at 1230 and 1190 cm^{-1}. Use of a catalyst seems not to affect the carbonyl peak (1700 cm^{-1}), but solvent treatment caused a significant decrease. In the case of preasphaltenes from Blind Canyon, the band at 3400 cm^{-1} is more intense

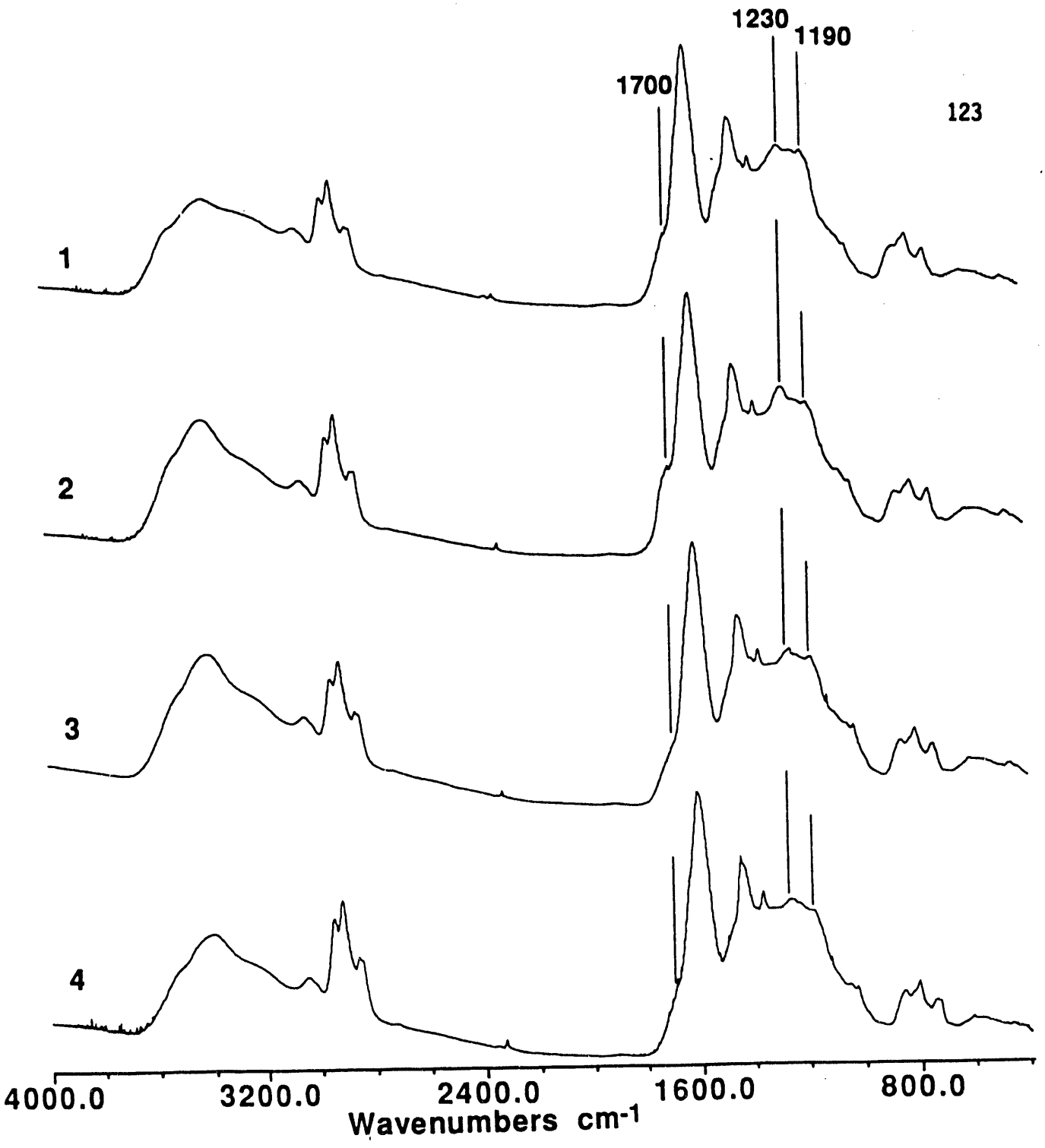

Figure 16 - Comparison of FTIR Spectra of Preasphaltenes from Liquefaction of Texas Subbituminous C Coal (DECS-1). 1) Preasphaltenes from Non-catalytic Reaction, 2) Preasphaltenes from Reaction with ATTM, 3) Preasphaltenes from Reaction of Pyridine-treated coal with ATTM, 4) Preasphaltenes from Reaction of TBAH-treated Coal

when catalyst is used, regardless of whether the coal had also been treated with a swelling solvent (Figure 17). Since in the presence of catalyst the absorbance peak at 1184 cm^{-1} decreased, and with pyridine treatment the maxima at 1184 and 1225 cm^{-1} disappeared, it is likely that the increase of the 3400 cm^{-1} peak is due to water. The oxygen content of the asphaltenes and preasphaltenes, shown in Table 24, are consistent with FTIR results. The nitrogen content of samples obtained from TBAH- and pyridine-treated coals are higher than that of untreated coal. This is attributed to contribution of nitrogen-containing compounds to asphaltenes and preasphaltenes. In view of all the FTIR results and elemental analyses of asphaltenes and preasphaltenes, it can be understood that nitrogen-containing solvents which are capable of swelling coal interact with oxygen functional groups so as to lower their concentration in liquefaction products.

Comparative gas chromatograms of the saturated fractions of oils from Texas subC and Blind Canyon coals are illustrated in Figures 18 and 19, respectively. Smooth distributions of n-alkanes were obtained. The distributions of n-alkanes are more homogeneous for the subbituminous than for the bituminous coal following the non-catalytic reactions. In the non-catalytic reactions, n-alkanes from Texas subC have a maximum at C_{27}, whereas those from the bituminous coal have a maximum at C_{25}. The concentration of saturates was found to be 2.5% (daf) for the subbituminous and 2.7% (daf) for the bituminous coal (Table 25) when no catalyst was used.

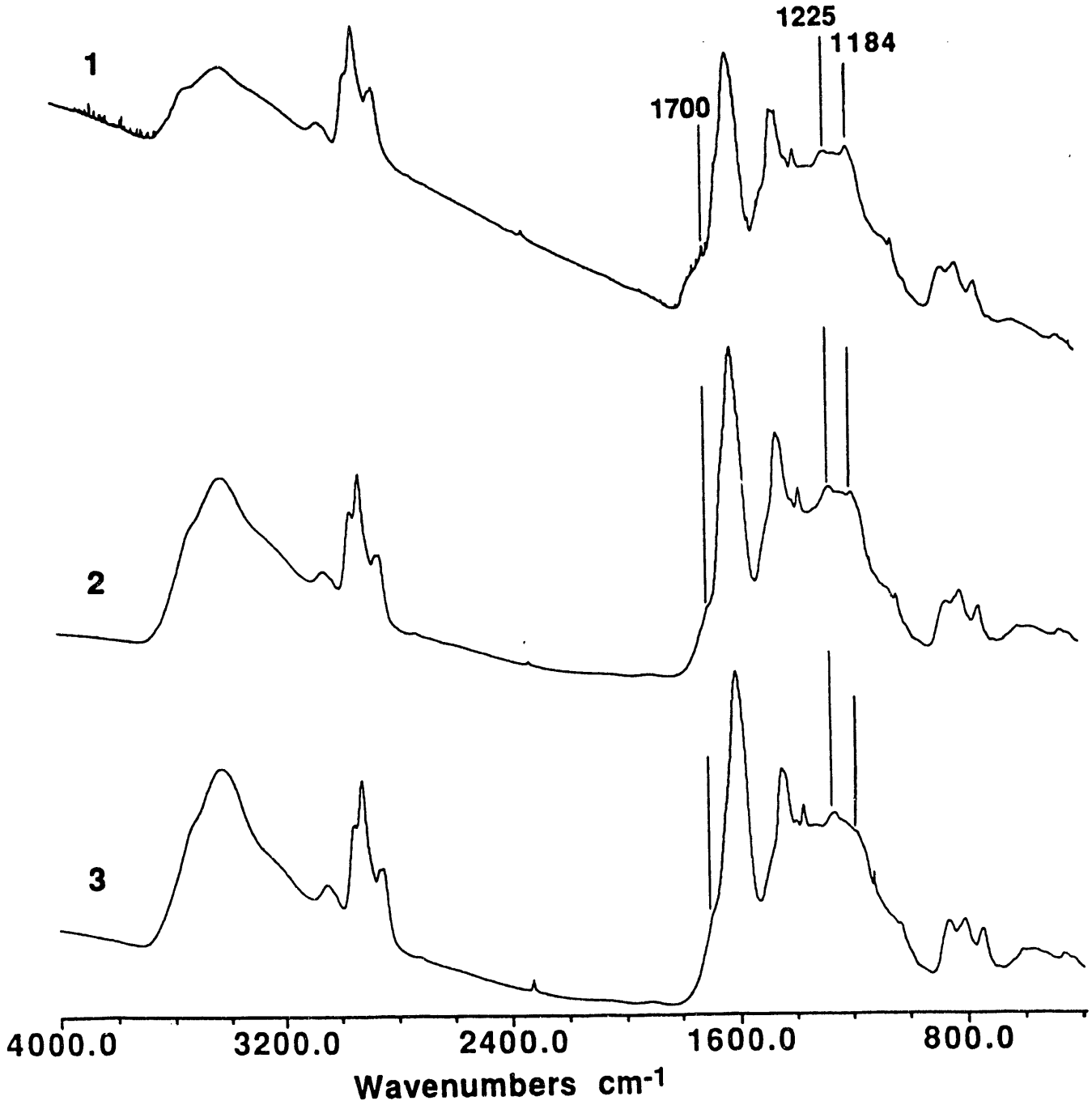

Figure 17 - Comparison of FTIR Spectra of Preasphaltenes from Liquefaction of Blind Canyon Coal (DECS-6). 1) Preasphaltenes from Non-catalytic Reaction, 2) Preasphaltenes from Reaction with ATTM, 3) Preasphaltenes from Reaction of Pyridine-treated Subbituminous Coal with ATTM

Table 24. Elemental analyses of preasphaltenes and asphaltenes.

Sample[a]	Solvent	Catalyst	Element (wt%, daf) C	H	N	O+S
6-AS	—	—	78.8	5.7	1.5	14.0
6-AS	Water	ATTM	83.1	6.1	1.9	8.9
6-AS	Pyridine	ATTM	85.2	6.1	1.9	6.8
6-PAS	—	—	82.5	5.4	2.1	10.0
6-PAS	Water	ATTM	83.6	5.3	2.1	9.0
6-PAS	Pyridine	ATTM	84.4	4.9	2.6	8.1
1-AS	—	—	77.7	5.4	1.7	15.2
1-AS	Water	ATTM	81.1	5.7	2.0	11.2
1-AS	Pyridine	ATTM	82.2	6.1	1.9	9.8
1-AS	TBAH	ATTM	82.3	6.1	2.9	8.7
1-PAS	—	—	80.6	4.9	2.1	12.4
1-PAS	Water	ATTM	81.3	5.0	2.1	11.6
1-PAS	Pyridine	ATTM	81.1	5.0	3.3	10.6
1-PAS	TBAH	ATTM	82.0	5.2	3.0	9.8

[a] 6= DECS-6; 1=DECS-1; AS=Asphaltene; PAS=Preasphaltene.

Table 25. Percentage of saturated fraction of oil yields from Texas (DECS-1) and Blind Canyon (DECS-6) coals and pristane-phytane ratios in each related saturate fraction.

Coal	Catalyst	Solvent	Pri./Phyt.	Sat.% (daf)
DECS-6	None	None	7.1	2.7
DECS-6	ATTM	Water	5.2	3.4
DECS-6	ATTM	Pyridine	6.1	4.0
DECS-1	None	None	5.4	2.5
DECS-1	ATTM	Water	5.4	4.1
DECS-1	ATTM	Pyridine	5.3	4.4
DECS-1	ATTM	TBAH	5.4	4.2

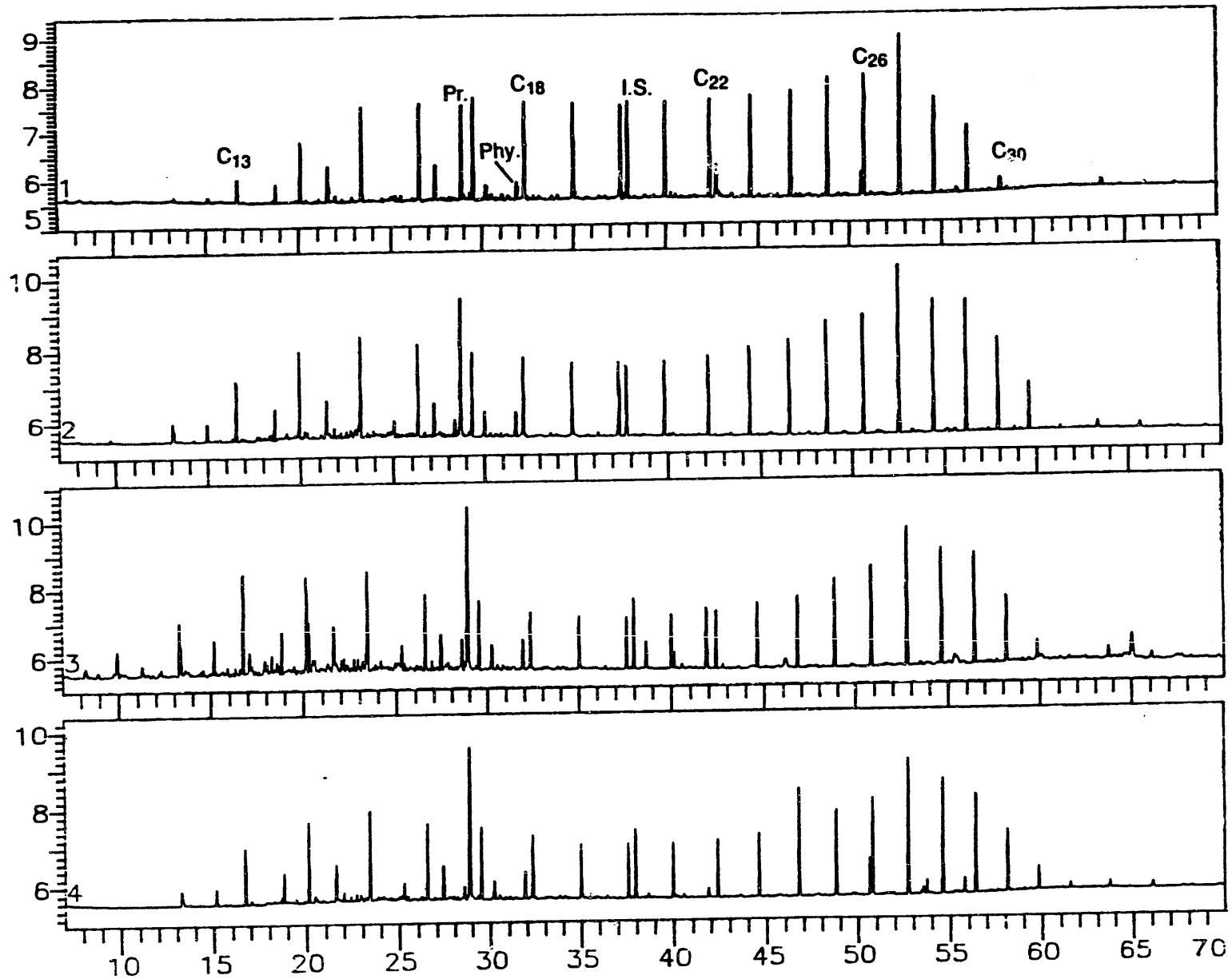

Figure 18 – Comparison of Gas Chromatograms of Saturated Fractions from Liquefaction of Texas Subbituminous C Coal (DECS-1). 1) Saturates from Non-catalytic Reaction, 2) Saturates from Reaction with ATTM, 3) Saturates from Reaction of Pyridine-treated Coal with ATTM, 4) Saturates from Reaction of TBAH-treated Coal with ATTM. Phy – pristane, Phy – phytane, IS – internal standard

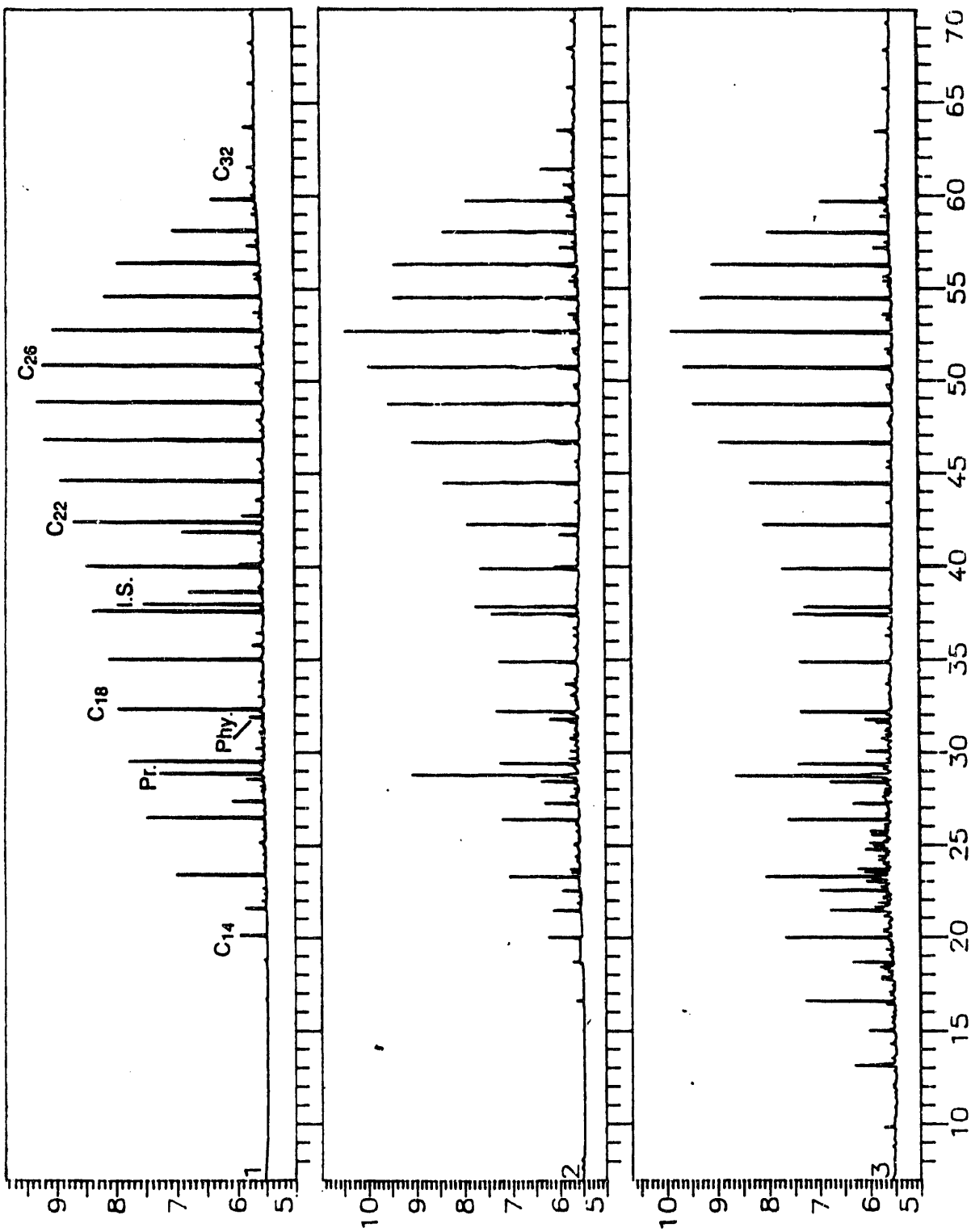

Figure 19 - Comparison of Gas Chromatograms of Saturated Fractions from Liquefaction of Blind Canyon Coal (DECS-6). 1) Saturates from Non-catalytic Reaction, 2) Saturates from Reaction with ATTM, 3) Saturates from Reaction of Pyridine-treated Coal with ATTM, 4) Saturates from Reaction of TBAH-treated Coal with ATTM. Phy - pristane, Phy - phytane, IS - internal standard

When ATTM was used, higher concentrations of bicyclic terpenes and monoaromatic hydrocarbons contributed to the chromatograms. For Blind Canyon, the maximum in the n-alkane distribution shifted to C_{27} for reaction in the presence of the catalyst. With pyridine swelling pretreatment, the concentration of n-alkanes increased slightly and the alkanes exhibit two maxima, at C_{27} and C_{15}. For Texas subC with pyridine pretreatment, n-alkanes exhibit maxima at C_{13}-C_{15} and C_{27}. TBAH treatment yielded maxima at C_{15} and C_{27}. The concentration of saturates increased upon catalyst addition for both coals. Solvent treatments increased the concentration of saturates only slightly for Blind Canyon, and there was no difference in the case of the subbituminous coal.

Various ideas have been offered to account for the origin of alkanes in coal liquefaction products. It has been proposed that alkanes are absorbed physically in the coal matrix [Bartle et al., 1975; Bartle et al., 1979]; that alkanes derived from hydrocarbons present in the pore structure or from the decomposition of alkyl chains bonded to the coal matrix [Snape et al., 1981; Mashima et al., 1984]; or that at least part of the n-alkanes derive from hydrogenation of occluded esters, alcohols, or acids [Mudamburi and Given, 1985; Dong et al., 1986; Dong et al., 1987]. The most noticeable effect of the added catalyst is a substantial increase in the concentration of pristane and phytane. The pristane-to-phytane ratio in products from the Texas subC was ≈5.4 regardless of the use of catalyst during liquefaction or of preswelling. For Blind Canyon, this ratio was more variable, being 7.1 in products from reaction without catalyst, 5.2

for catalytic reactions, and 6.1 in products from pyridine-treated coal. These results raise the possibility that, at least in part, isoprenoids are bonded to the coal matrix.

Pristane is thought to be formed from the oxidation and decarboxylation of pristol; phytane is formed by the hydrogenation and dehydration of phytol [Philp, 1985]. The source of phytol may be the side chain of chlorophyll. Dihydropythyl- and phytyl-containing components (vitamin E and vitamin K1, for example) might be possible alternative precursors [Dong et al., 1987]. On the basis of extraction and hydrogenation of Wandoan (Australian) coal, Dong et al. [1987] proposed that part of the n-alkane content in the fractions was produced by the reduction of methyl and ethyl esters of straight-chain carboxylic acids. Isoprenoids (e.g., pristane and phytane) linked by ether bonds to the coal matrix are the possible precursors, and they may be derived from pristol or phytol skeletons. Both our and Dong's findings support the idea that pristane and phytane are bound, at least in part, to the coal matrix.

5.4. SUMMARY AND CONCLUSIONS

The experimental findings are summarized in Figure 20, which is a plot of the conversions and oil yields from all of the experiments described in this section of the report. Although there is certainly some scatter in the data, we consider the linearity remarkable, considering that the Figure incorporates 51 sets of data derived from liquefaction of two coals of different rank, two gas atmospheres, seven catalyst precursors,

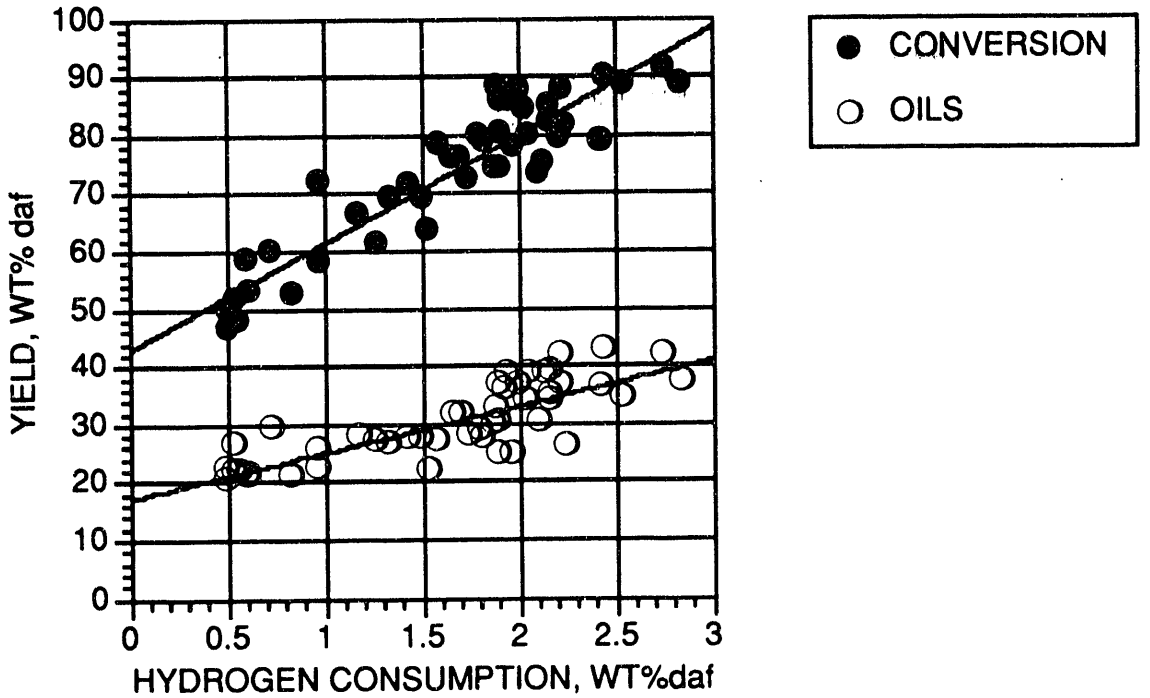

Figure 20 - Dependence of Conversion and Oil Yield on Hydrogen Consumption, Combining all Data Reported in this Section, for 51 Temperature-staged Liquefaction Reactions Involving Two Coals, Two Gas Atmospheres, Seven Catalyst Precursors, and Four Swelling Solvents

and four swelling solvents. Clearly the key to high conversion, and high oil yield, is to increase hydrogen utilization.

For Blind Canyon bituminous coal, high conversions (i.e., in the 85-91% range) are attained by impregnating the coal with a molybdenum-based catalyst precursor. If the precursor is already sulfided, e.g. ATTM, a hydrogen atmosphere is adequate; if, however, the precursor is not sulfided, then liquefaction in a $H_2S:H_2$ atmosphere is desirable. Although solvent pretreatment does not provide dramatic increases in conversion relative to untreated samples, it is sufficient to gain an extra ≈5% in conversion, especially when using pyridine as the treatment solvent. This "extra" 5% conversion is, however, enough to raise conversion from ≈85% to ≈90%. The highest conversion observed for this coal, 91.6%, was obtained by a combination of pyridine pretreatment, impregnation with CPMC, and liquefaction in $H_2S:H_2$. For the Texas subbituminous C coal, the highest conversions (89%) were obtained with ATTM impregnation and solvent pretreatment with pyridine or TBAH. Pretreatment of the subbituminous coal enhances conversions by ≈10% relative to otherwise similar experiments but without solvent pretreatment, and the nitrogen-containing solvents seem effective at suppressing formation of CO_x gases. In contrast to Blind Canyon bituminous coal, the organometallic molybdenum-containing precursors gave very good conversions (84-86%) without using H_2S. The marked difference in behavior of these precursors with subbituminous and bituminous coals merits further investigation.

The slopes of the curves plotted in Figure 20 are not parallel; the

oil yield increases less rapidly with increased hydrogen consumption than does conversion. The results suggest that if it were possible to attain 100% conversion, the oil yield would be about 45%. Consequently, if one were to envision a process designed around the reaction conditions reported here, some down-stream hydrotreating of preasphaltenes and asphaltenes would be necessary if the goal were to obtain very high oil yields.

For Blind Canyon bituminous coal, the conditions favoring high oil yields are essentially those that also favor high conversions: molybdenum-based precursors, either already sulfided or reacted in $H_2S:H_2$; and solvent pretreatment. The use of organic solvent can enhance oil yields by up to 10% relative to reaction at the same conditions without solvent. The highest oil yields, 42-43%, were obtained with pyridine pretreatment and ATTM in H_2 or CPMC in $H_2S:H_2$. Little or no benefit is observed for oil yields by solvent pretreatment of the subbituminous coal. Sulfided molybdenum catalysts are generally best at providing high oil yields. However, it is noteworthy that ion-exchanged iron, with reaction in $H_2S:H_2$, gave an oil yield from the subbituminous coal quite comparable to those obtained with molybdenum catalyst precursors, although the total conversion was not quite as high. Ion-exchange impregnation of catalyst precursors into low-rank coals also merits further investigation.

Finally, it should be understood that throughout the course of this work the temperatures, reaction times, and vehicle were not varied, nor was the overall reaction strategy (i.e. comparison with single-stage reaction or temperature-programmed reactions). All of these factors are well known

to affect the course of liquefaction reactions. Although we have demonstrated approaches to achieve ≥90% conversions with ≥40% oil yields, further experimentation that involves changing one or more of these factors could offer potential improvements in reduction of reaction severity, increase of yields of specific desired products, or both.

6. COAL-SOLVENT INTERACTIONS

6.1. INTRODUCTION

Impregnation or dispersion of catalyst in or onto coals using a variety of solvent vehicles was one of the primary objectives of this research. Measurement of the solvent swelling ratio was used to provide the relative increase in coal particle size in the presence of specific solvents [Dryden, 1951; Green et al., 1984]. This measurement was usually performed on coals that were first exhaustively Soxhlet extracted in pyridine. Although Cody et al., [1988] have determined that unextracted coal thin sections yield similar swelling volumes as pyridine-extracted coals, our objective here was to study techniques for catalyst impregnation of whole coals. Consequently, some alteration of the solvent swelling technique was necessary. Using the revised procedure, preliminary experiments were completed to determine the volumetric swelling of the two coals selected for this investigation in four different solvents, i.e., methanol, THF, pyridine and 10% tetrabutylammonium hydroxide (0.385 M TBAH). During the course of this project, solvent swollen and sometimes catalyst impregnated coals were observed using optical and electron optical techniques to determine the physical influence of each solvent on the different coals.

6.2. EXPERIMENTAL

As employed in this study, volumetric swelling ratio was determined by adding 1.00 g of -60 mesh (<0.25 mm), air-dried coal in a 15 mL graduated screwtop centrifuge tube. The coal was then centrifuged at 2900

rpm for 10 min and the height of the coal in the tube recorded in mL/g. Twelve mL of solvent were added in increments to the coal. First, 6 mL were combined with the coal and stirred carefully until all the coal particles were wetted, then the remaining solvent was added and the tube sealed with the cap. After a period of time the tube was centrifuged again at 2900 rpm for 10 min and the height recorded. The volumetric swelling ratio was defined as,

$$Q = h_2/h_1$$

where h_1 = height of unswollen coal and h_2 = height of swollen coal.

To obtain a better understanding of the rate of swelling for unextracted coals, a number of experiments were conducted using the Texas lignite (PSOC-1444). For each solvent, one tube was centrifuged at regular time intervals, the coal height (h_2) recorded, and then shaken and allowed to stand until tested again. Results from this test sample were compared with samples that remained undisturbed for the same total time interval. Because no significant difference was found for the swelling ratios when the samples were intermittently centrifuged, this procedure was adopted as standard practice with the Blind Canyon sample (PSOC-1503).

Another problem to be addressed was the difficulty in measuring the coal-solvent horizon when there was a high concentration of solvent-soluble material in the coal, i.e., THF, pyridine and TBAH. This problem was overcome by back lighting or by inverting the centrifuge tube after centrifugation. Back lighting was preferred and could be used with THF and

pyridine. Tube inversion was required with TBAH, particularly with the lignite which reacted strongly with the base.

6.3. RESULTS AND DISCUSSION

6.3.1. Solvent Swelling

Solvent swelling ratios with contact time for four different solvents are given in Tables 26 and 27 (also given in Tables 4 and 5, Section 3.3.1.) for the Texas lignite and the Blind Canyon hvBb coals, respectively. In general, some interesting observations can be made regarding solvent swelling without prior extraction or drying of the coal. In nearly every case, the maximum level of swelling was attained within 6 h; additional solvent-coal contact in excess of 26 h did not produce a significant increase in swelling ratio. These findings corresponded to results given by Matturro et al. [1985] for the rate of swelling of extracted Illinois #6 in different molar concentrations of TBAH. They found that the rate of increase in bulk swelling diminished after 3 h.

As discussed in Section 3.3.1., the level of swelling experienced for each coal was slightly different with respect to the individual solvents. For the lignite (PSOC-1444), swelling increased in the order: methanol < THF < pyridine < 10% TBAH; for the Blind Canyon hvBb coal, the order was: 10% TBAH < methanol < THF < pyridine. Note that the level of swelling for different solvents was rank dependent. THF and pyridine extractability and swelling of coal is typically higher for bituminous coals and increases with increasing rank to medium volatile. Therefore, swelling was greater for the Blind Canyon coal compared to the lignite using these solvents. On

Table 26. Change in solvent swelling ratio (Q) with time for the Texas lignite (PSOC-1444)

Methanol		THF		Pyridine		TBAH (10%)	
Time (h)	Q	Time (h)	Q	Time (h)	Q	Time (h)	Q
5.0	1.1	6.0	1.2	6.5	1.6	6.0	2.6
11.5	1.1	16.5	1.2	21.5	1.6	14.5	2.6
23.0	1.1	22.0	1.3	42.0	1.6	24.5	2.7
27.5	1.1	28.0	1.3				

Table 27. Change in solvent swelling ratio (Q) with time for the Blind Canyon hvBb coal (PSOC-1503)

Time (h)	Methanol Q	THF Q	Pyridine Q	TBAH (10%) Q
6.0	1.2	1.9	2.4	1.1
10.0	1.3	1.8	2.3	1.2
20.0	1.3	1.8	2.2	1.2
26.0	1.3	1.8	2.3	1.2

the other hand, TBAH has been shown to react strongly with the types of oxygen functionalities found in most lower rank coals (carboxylic and phenolic hydroxyl; [Liotta et al., 1981]). Consequently, swelling was enhanced for the lignite compared to the Blind Canyon. From consideration of the solvent effects, pyridine and TBAH appeared to be the swelling solvent of choice for the lignite, and pyridine and THF were most effective with the hvBb coal.

6.3.2. Microscopy of Solvent-Swollen Coals

During the course of this study, subsamples of solvent-swollen coals, some impregnated with catalyst, others not, have been prepared for inspection using optical and electron optical microscopy to determine the physical influence of the different solvents on the Texas subC (DECS-1) and Blind Canyon hvAb (DECS-6) coals. Optical microscopy was performed on polished surfaces of solvent swollen coals mounted in epoxy resin, whereas particulate samples were evaluated using the SEM.

Inspection of coal samples that had been swollen in methanol revealed no discernable influence of the solvent on either coal. Some very minor fracturing was observed in the Texas subC coal contacted with methanol, but this could not be wholly attributed to the solvent as these samples were dried to <3% moisture. This conforms to the relatively low swelling ratios found with methanol for the two older coal samples (PSOC-1444 and -1503).

Polar solvents such as THF and pyridine are often used to extract varying amounts of solvent-soluble fractions from coals of different rank. From our swelling study these solvents were found to have a low to moderate

influence on the Texas lignite, but a fairly significant effect on the Blind Canyon sample. Inspection of the Texas subC coal following swelling in these solvents showed that a majority of the coal particles were apparently unaffected by the solvents. However, in the pyridine swollen sample evidence was found for agglomeration of coal particles presumably by the once-soluble extract. As seen in Plate Ia, larger coal particles were cemented together in a matrix material of slightly lower reflectance. Although a THF swollen sample was not viewed under the optical microscope, inspection of a particulate sample in the SEM showed small, ≈10 μm size particles adhering to the surfaces of larger coal particles and may suggest the same, but more limited agglomeration as observed with pyridine.

THF and pyridine extractability are presumably much greater for the hvAb Blind Canyon sample and therefore agglomeration of coal particles was expected to be more advanced. In the case of THF swollen DECS-6 some agglomerated particles were observed, but most of the particles were found with coatings of the extractable materials on their outer surfaces, as shown in Plate Ib. These coating were also observed in the SEM. Plate Ic shows the surface of several coal particles coated with hemispherical bodies. These bodies were easily destroyed by a focused electron beam and were carbon-rich. We have concluded that this material was part of the THF-soluble fraction that was extracted from the coal during swelling and subsequently redeposited on the coal surface following evaporation of the THF before catalyst impregnation.

Pyridine, being a stronger solvent than THF, resulted in more particle agglomeration with the swollen Blind Canyon hvAb sample. Plate Id shows numerous coal particles cemented by a granular matrix of slightly lower reflectance than the vitrinite. Shibaoka et al. [1979] showed that pyridine treatment of hvAb coals resulted in the swelling and microbrecciation of vitrinite (along the particle edges) which could be the origin of the fine-particle matrix. Although many more of these agglomerates were found compared with THF, many individual particles with coatings also were seen, like those in Plate IIa. The deposition of solvent-soluble components onto the surface of coal particles and their subsequent agglomeration could significantly influence catalyst impregnation, total conversion and product yields during liquefaction. Coatings and agglomeration may restrict access of the catalyst to some of the internal porosity of a large number of coal particles, thus reducing the effectiveness of catalytic hydrogenation. On the other hand, concentration of solvent-soluble fractions of coal at the coal surface may enhance product yield of lighter fractions by virtue of their exposure to catalytic hydrogenation.

The influence of TBAH on these coals stands as an enigma in that the Texas lignite was most effected and the Blind Canyon hvBb least effected by the base in terms of pretreatment liquefaction yields (Section 3). During solvent contact the lignite exhibited physical signs of reaction, but inspection of TBAH treated Texas subC coal under the optical microscope revealed no indications of particle agglomeration. What was observed is

PLATE I
FIGURE DESCRIPTION

a. Particle agglomeration exhibited in a pyridine swollen Texas subC (DECS-1) sample that was impregnated with ATTM.

b. Particle of Blind Canyon (DECS-6) showing reaction along the left-hand edge and fine particles adhering to the outer surface of the particle following preswelling in THF.

c. SEM micrograph showing hemispherical THF-soluble deposit on coal surface following preswelling of the DECS-6 coal in THF and subsequent impregnation with ATTM.

d. Agglomeration of Blind Canyon coal particles with a fine particle matrix containing pyridine-soluble fraction of similar reflectance as vitrinite following preswelling in pyridine.

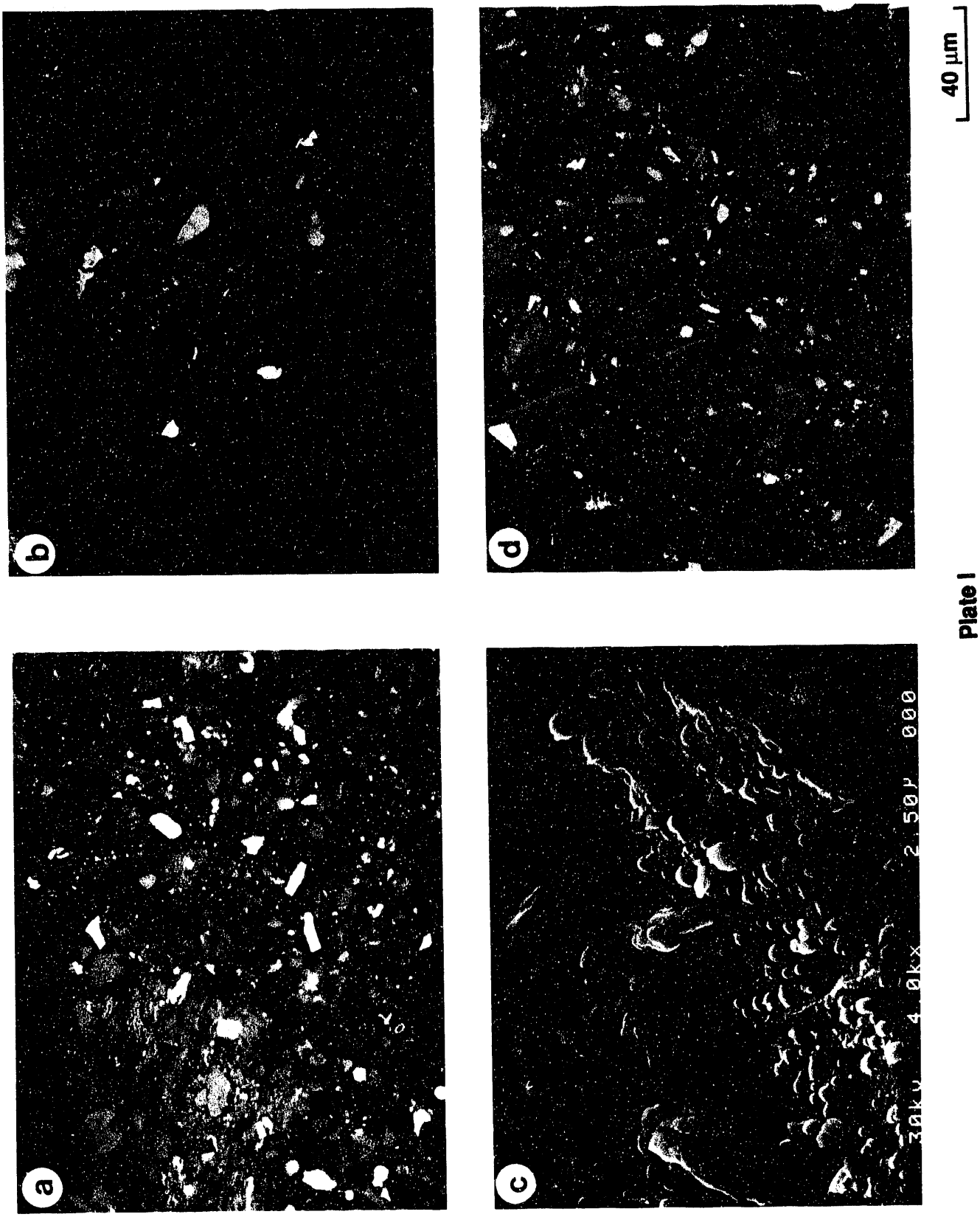

Plate I

PLATE II
FIGURE DESCRIPTION

a. Influence of pyridine preswelling on the Blind Canyon hvab coal. Central and right-hand particles exhibit reaction front or coating of pyridine soluble material of slightly lower reflectance than the vitrinite.

b. Coal particle from the Texas subC coal following preswelling in TBAH exhibiting large-scale fracturing along and perpendicular to the bedding.

c. A group of Blind Canyon coal particles cemented by a low-reflecting reaction product following preswelling in TBAH. Note the intrusion of the reactant into the fractures in the central particle.

d. Particle of Blind Canyon coal preswollen in TBAH showing the low-reflecting reaction product. The central coal particle is well rounded and exhibits clear signs of a reaction front as well as the ability of the reaction product to engage in particle agglomeration.

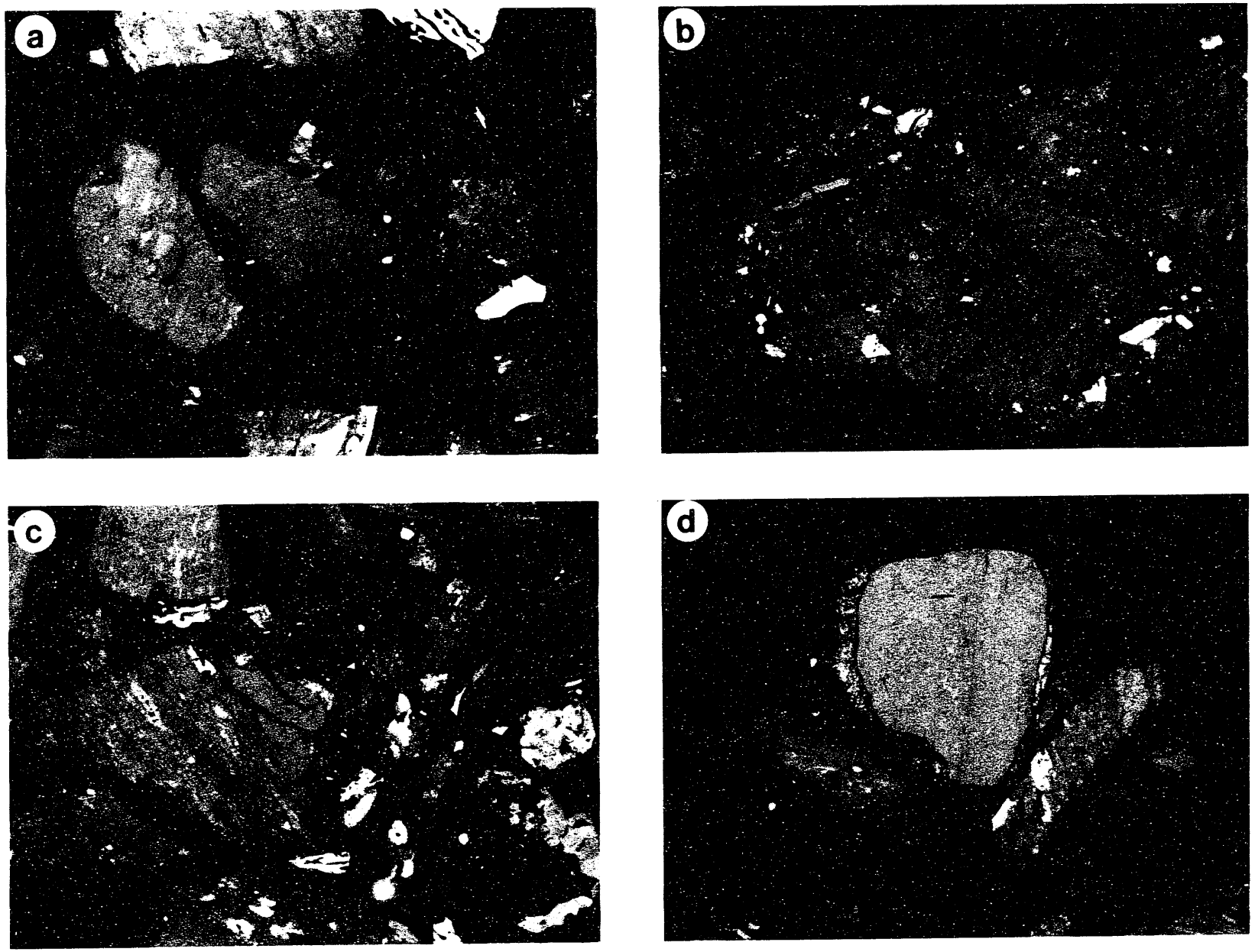

Plate II

poorly during pretreatment liquefaction following impregnation of molybdenum catalysts.

6.4. CONCLUSIONS

The influence of four solvents on the swelling and physical properties of two sets of coals was investigated using quantitative solvent-swelling measurements and optical and electron microscopy. Using one set of coals we found that the swelling ratio for the PSOC-1444 Texas lignite proceeded in the order: methanol < THF < pyridine < 10% TBAH, whereas the PSOC-1503 hvBb Blind Canyon coal proceeded in the order: 10% TBAH < methanol < THF < pyridine. Some of the reasons for this different order are related to coal rank and solvent strength. On the other set of coals, methanol was found to have no or little influence on the physical properties of either coal. However, THF and pyridine being stronger solvents were found to have more influence. The solvent-soluble fractions of each coal were found as coatings on coal particle surfaces and were responsible for some level of particle agglomeration. A greater amount of extract was produced from the Blind Canyon bituminous coal using pyridine and the least amount produced from the Texas lignite/subC coals when THF was used. Pyridine preswelling was beneficial for both coals, whereas THF was only effective for the Blind Canyon coal. The use of 10% TBAH with the Texas subC coal was most beneficial and appeared to provide the only evidence of true large-scale swelling of a coal which corresponded with the highest swelling ratio measured. On the other hand TBAH was apparently ineffective as a swelling agent for the Blind Canyon coal. Optical

microscopy revealed that TBAH reacted with the outer edges of the coal particles (vitrinite) leaving behind a tacky, pitch-like deposit that promotes agglomeration and which may block the coal pore and fracture system.

7. CATALYST DISPERSION ON COALS

7.1. INTRODUCTION

To establish some basic information concerning the dispersion of different catalysts upon coal surfaces, a study of catalyst/coal interfaces was undertaken. As part of this investigation we wanted to determine whether a catalyst could impregnate the fine pore structure of coal or whether it formed a uniform surface dispersion. The simplest experimental approach was to place catalyst solutions onto a prepared surface of coal, strip away the solvent and then characterize the interfaces in three dimensions.

Single, small particles of coal were used to study catalyst/coal interfaces by first embedding them in epoxy so that only one surface of the coal was exposed. A catalyst solution was placed on the coal surface, then the solvent was removed (evaporated, vacuum impregnated or freeze-dried) and the resulting surface and cross-sectional areas characterized using electron and optical microscopy. Particulate coals, like those normally used in tubing bomb liquefaction experiments (Section 3.2.), were also studied to determine what degree of dispersion/impregnation was achieved with natural particle surfaces. SEM-EDS and electron microprobe techniques were employed to locate catalyst materials associated with solvent-swollen and non-swollen coal surfaces. In addition, X-ray mapping was used to study the effectiveness of ion-exchanging iron for calcium in the Texas subC sample (see Section 5.2.4.).

7.2. EXPERIMENTAL

Small particles of DECS-1 (freshly collected Texas subC coal) and of DECS-6 (freshly collected Blind Canyon hvAb coal) measuring approximately 5 X 20 mm were embedded in plastic and polished to expose the bedding plane structure of the coals. Two of the particles of each coal were soaked in methanol and one soaked in THF for about 12 h, whereas the remaining particles were stored under high humidity until catalyst solutions were added. Coal particles were soaked in the solvents to swell the coal and to remove some of the inherent moisture.

Solutions of 4.5% $FeSO_4 \cdot 7H_2O$ (≈1.0 - ≈1.7 mg of catalyst per coal particle) and 2.0% ATTM (≈0.5 - ≈1.6 mg per particle) with methanol and 2.3% molybdenum hexacarbonyl ($Mo(CO)_6$, 0.8 mg catalyst) with THF were prepared. Two sample blocks (one soaked in a swelling solvent and one stored under high humidity) were prepared for each catalyst by placing drops of the solution onto the polished surface. Catalyst solutions were applied to soaked coal surfaces without allowing them to dry. As the solvent evaporated, more solution was added until the total amount had been applied to the surface. Each sample was then placed in a vacuum oven at 25°C for up to 48 h to completely remove the solvent and reduce coal moisture. The sample soaked in THF disintegrated and was lost. Individual-particle studies were not performed with the other swelling solvents (pyridine and TBAH) employed in this project because coal-particle disintegration was also anticipated.

Samples were prepared for observation under the scanning electron microscope (SEM) by coating each with a thin layer of carbon. The coating is necessary to prevent heat damage by the electron beam and to eliminate the buildup of surface charges which can interfere with imaging. An ISI-SX-40 SEM was used for imaging only. In subsequent sessions samples were observed in an ISI-SX-40A SEM having a Kevex X-ray energy spectrometer (EDS) for qualitative analysis of elements greater in atomic weight than boron.

Following inspection of the polished surfaces in the SEM, the methanol-soaked samples of the ferrous sulfate and ATTM catalysts were embedded in an iodine-substituted epoxy resin so that the catalyst coal interface could be observed in cross section [Davis et al., 1989]. The coal particles were cut in half to expose a cross-sectional area and were rough ground (600 grit) without the aid of lubricant (water or solvent) so that the catalyst would not dissolve. These sections were also observed in the SEM.

Evaluation of catalyst dispersion on particulate coals was performed on samples prepared for liquefaction, i.e., -60 mesh coal (DECS-1 and 6) was dried at 100°C in vacuum, mixed with a swelling reagent to give a solvent-to-coal ratio of 3:1 (v/w) and stirred for 6 h under nitrogen. Swelling reagents used in this part of the study were methanol, pyridine and THF. Solvents were removed by evaporation at room temperature in vacuum for methanol and THF and at 100°C for pyridine. Aqueous solutions of ferrous sulfate or ATTM were added to each coal sample (0.59 wt.% Fe or

1.0 wt.% Mo) in the manner described in Section 3.2.4. The dry, particulate coal samples impregnated with ferrous sulfate or ATTM were then prepared for study with the SEM and electron microprobe (EP). Samples were carefully (gently) split to about 0.6 g using a micro-riffler and a small subsample mounted on a pedestal for SEM imaging using double-sided tape. For the electron microprobe, samples were dispersed on the pedestal in a cold-setting epoxy resin to eliminate surface charging problems.

Particulate samples were prepared for observation under the SEM by coating each with a thin layer of gold, whereas those for EP analysis were coated with carbon. All samples were coated at the same time to ensure an identical coating thickness. The ISI-SX-40A SEM equipped with a Kevex energy dispersive spectrometer (EDS) was used for imaging and for the qualitative elemental analysis.

An ETEC automated electron microprobe analyzer was employed for quantitative analyses. The PET (Pentaerythritol) crystal spectrometer was used for sulfur and molybdenum analysis, whereas other elements were monitored with an attached EDS system. Spectrometer wavelengths were calibrated using pyrite (FeS_2) as a standard for sulfur and 99.95% pure molybdenum metal for the molybdenum. The accelerating voltage was set at 15 keV and the data were reduced by the ZAF method using various internal software packages. The $S_{K\alpha}$ (5.392 Å) peak was used for sulfur, while the $Mo_{L\alpha}$ (5.407 Å) peak was used for molybdenum.

To evaluate the effectiveness of the iron ion-exchange for calcium in the Texas subC coal (DECS-1) a Cameca Camebax SX50 electron microprobe was

used for X-ray mapping and quantitative analysis. A coal sample that had been ion-exchanged as discussed in Section 5.2.4 was embedded in iodine-substituted epoxy and polished surfaces prepared and coated with carbon.

7.3. RESULTS AND DISCUSSION

7.3.1. Ferrous Sulfate Catalyst

Plate III illustrates the differences in affinity of ferrous sulfate (dissolved in methanol) to methanol-soaked and moist surfaces of the Texas subC coal. At the bottom of each SEM micrograph the numbers indicate the electron beam operating voltage, total magnification, number of microns represented by the white bar, and the photograph number. Plate IIIa shows the fractured, methanol-soaked coal surface to the left and the plastic embedding agent to the right. As can be seen, the plastic was heavily coated with crystalline ferrous sulfate, whereas the coal surface appeared to be devoid of catalyst. Using the EDS system the coal surface was tested for the presence of iron but no significant accumulations were detected. This result signifies that deposition of iron sulfate may be so evenly distributed as to give iron concentrations below the detection limits of the spectrometer or that the methanol-soaked and dehydrated surface of this subbituminous coal may repel iron sulfate.

In contrast, Plate IIIb and c show what appears to be ferrous sulfate catalyst distributed evenly across the coal and plastic surfaces of the sample that was stored under moist conditions. At higher magnification (Plate IIIc), two crystal types were observed; one occurred as large

crystals ranging in size from 100-300 μm, and the other type occurred as acicular crystals that were distributed as 30 μm size clusters across the coal surface. Inspection of this sample using the EDS system revealed that the large crystals were ferrous sulfate and the acicular crystals were calcium sulfate. As demonstrated in Plate IIId, the needle-like crystals of calcium sulfate were embedded and presumably growing from a central area containing ferrous sulfate. These observations clearly show that when ferrous sulfate in solution with methanol was applied to a moist coal surface, ion exchange of iron was promoted with the exchangeable and organically bound calcium present in high concentration in the subC coal [Ca = 0.7 wt. % of dry coal, Appendix A].

Differences between the methanol-soaked and moist samples were observed during application of the catalyst solution. After about 25 min, the soaked sample appeared dry, with a uniform dull luster, whereas the moist sample remained moist and uneven. Because of these observations and the apparent differences in coal/catalyst surface affinity between the samples, we speculate that the ability of a coal to absorb/adsorb iron from the ferrous sulfate onto internal surfaces might be greater for the soaked sample. In other words, ion exchange of iron from ferrous sulfate in the presence of water may be promoted at the coal surface, whereas removal of water by presoaking in methanol may inhibit ion exchange. This may or may not allow iron to penetrate deeply into the coal fracture system.

To test this hypothesis, a cross-sectional area of the methanol-soaked sample was prepared. Plate IVa shows the fractured coal in the

PLATE III
FIGURE DESCRIPTION

a. SEM micrograph showing coal to left and mounting plastic to the right. The Texas subc (DECS-1) was soaked in methanol and impregnated with ferrous sulfate. Crystalline ferrous sulfate can be seen clearly on the plastic surface, but not on the coal.

b. SEM micrograph showing relatively large ferrous sulfate crystals on the plastic and coal surface. This sample was stored under moist conditions. Clusters (≈30 μm) of acicular crystals of calcium sulfate are seen evenly distributed across the coal surface.

c. Higher magnification SEM micrograph showing the acicular clusters on the coal surface (Texas subC). The needle-like crystals are calcium sulfate that are intergrown with a central area of ferrous sulfate.

d. Micrograph showing the association of needle-like calcium sulfate clusters growing from a core of ferrous sulfate after the impregnation of a moist surface of DECS-1 subC with ferrous sulfate.

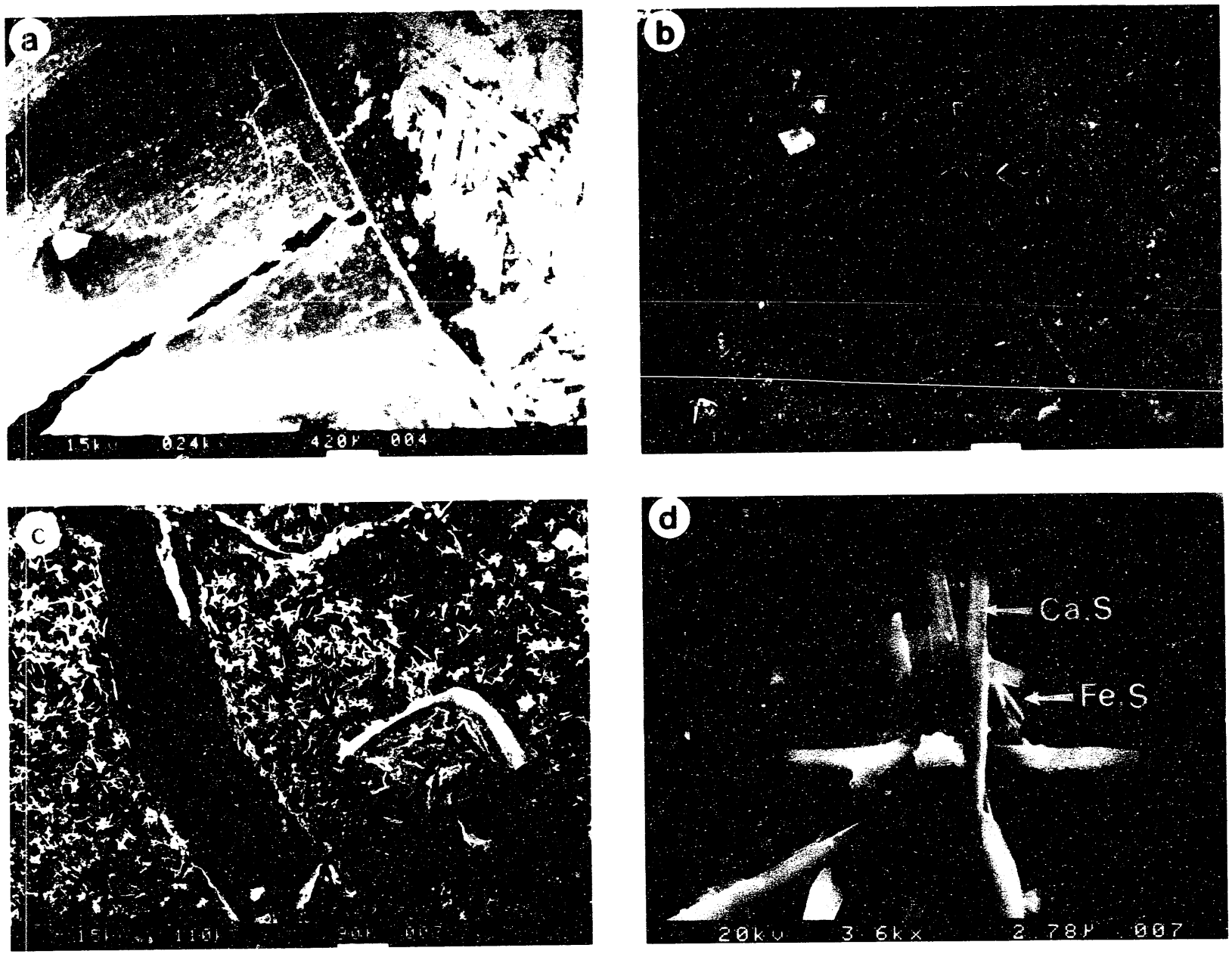

Plate III

PLATE IV
FIGURE DESCRIPTION

a. Cross-sectional area of the Texas subC coal particle that was soaked in methanol and impregnated with ferrous sulfate. High-resolution epoxy is seen in the bottom half intruding into the coal in the upper half of this SEM micrograph. The high-contrast regions along coal fractures are from iodine and not from the deposition of ferrous sulfate.

b. SEM micrograph of moist Blind Canyon (DECS-6) coal particle impregnated with ferrous sulfate. Large crystals (200-450 μm) of $FeSO_4$ seen on the coal surface with some smaller acicular crystals of calcium sulfate.

c. High magnification micrograph of acicular clusters of $CaSO_4$ on the same sample as described in (b).

d. Cross-sectional area of iron and calcium sulfate coated DECS-6 particle. The upper portion is high-contrast epoxy, the horizontal line of high contrast is the catalyst and the lower half is coal. Strong Fe and S peaks were obtained from the vertical line of high contrast (arrow), which is presumable catalyst filling a fracture in the coal.

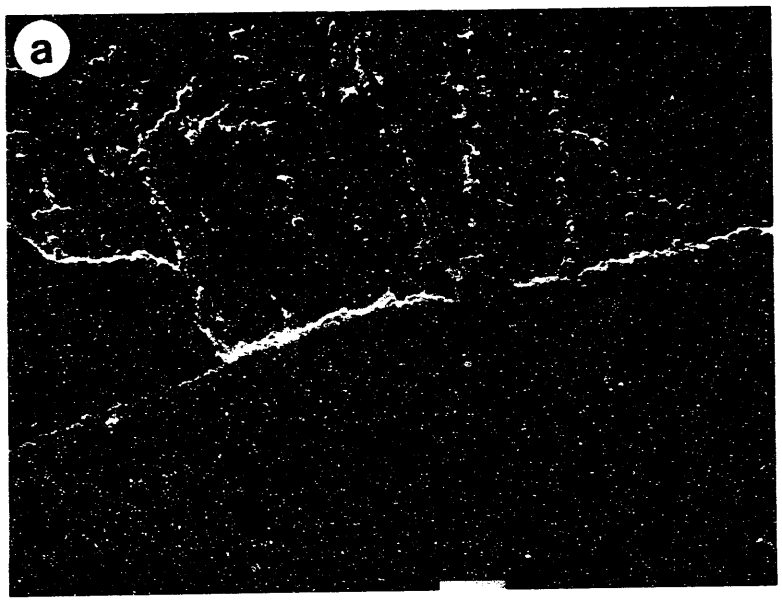
a

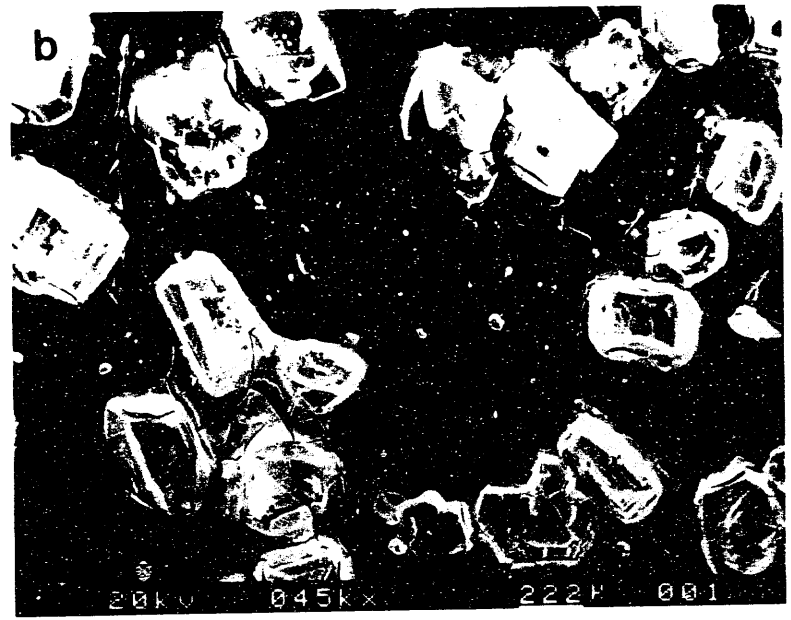
b
20kV 045kx 222µ 001

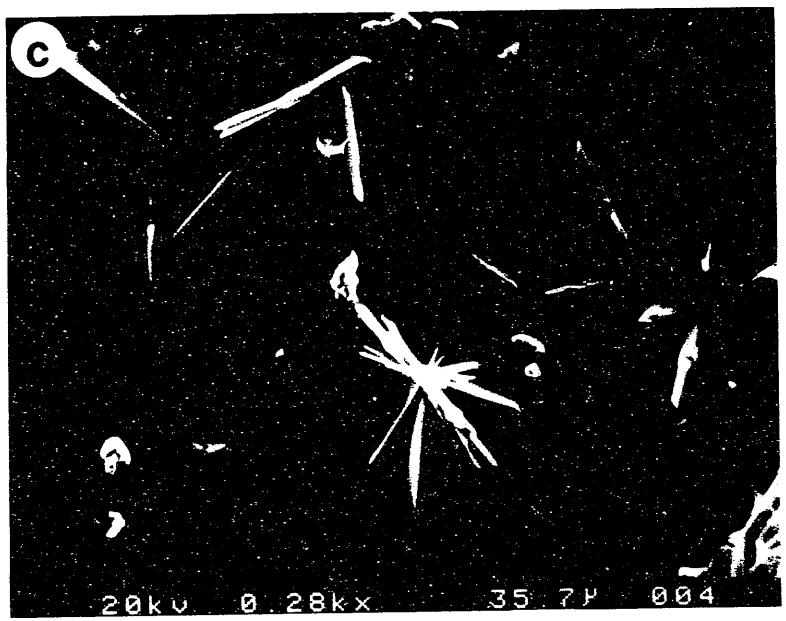
c
20kV 0.28kx 35.7µ 004

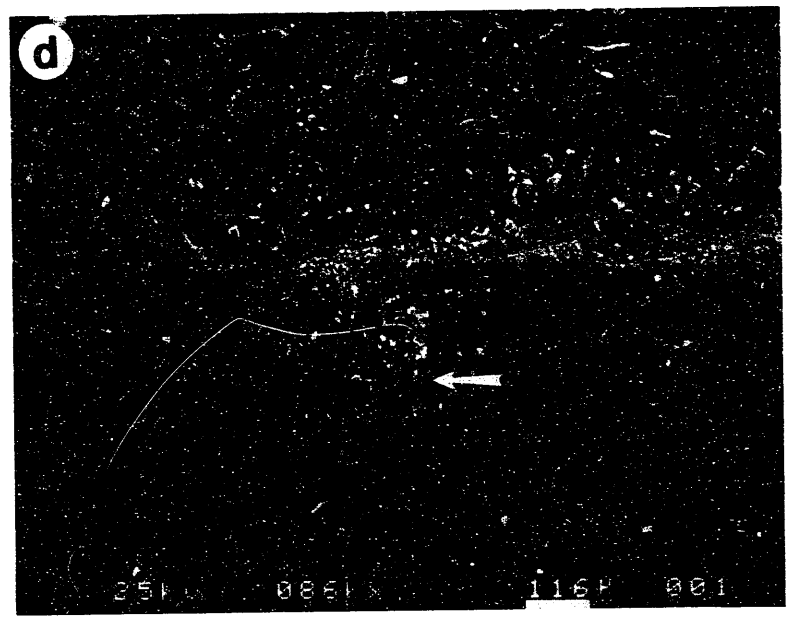
d
25kV 086kx 116µ 001

Plate IV

upper half of the micrograph and the high-contrast epoxy in the lower half. As can be seen, the interior fracture surfaces were coated with a high-contrast material. Inspection of the exterior and interior coal surfaces using the EDS system, however, revealed no significant iron peaks. Most of the contrast difference resulted from iodine and chlorine found in the epoxy resin. Thus, it must be concluded that presoaking the subC coal in methanol prior to impregnation of ferrous sulfate not only inhibits ion exchange, but also may inhibit deposition of catalyst on the coal surface.

Plate IV shows the different forms of catalyst material on the polished surface of a single particle of Blind Canyon coal after having been stored under relatively high humidity. Plate IVb shows rather large crystals (200 - 450 μm) of iron sulfate grouped together on the coal surface as was observed for the Texas subC coal, but in much higher concentration. At higher magnification (Plate IVc), clusters of much smaller acicular crystals of calcium sulfate can be observed, some of which also give a fairly strong iron peak.

In comparison to the Texas subC coal, there was less calcium sulfate observed with the Blind Canyon sample which corresponds with its lower calcium content [Ca = 0.5 wt. % of dry coal, Appendix A] as well as a presumed lower calcium exchangeability. Although we are certain that the presence of calcium sulfate is evidence of a calcium/iron ion exchange, we have been unable to locate significant iron peaks from any of the exposed surface of these two coals. It may be that the sites of ion exchange were so widely dispersed that our spectrometer was unable to register

significant counts.

Investigations of the methanol-soaked coal particles of DECS-6 coated with iron sulfate was not completed. However, a cross-sectional area of the sample stored under humid conditions was studied. Plate IVd shows the epoxy layer above and the coal in the lower part of the SEM micrograph separated by a distinct layer of mixed iron and calcium sulfate. Also, some minor intrusion of iron sulfate (at arrow) into a coal fracture can be seen. Penetration of catalyst materials was not observed with the methanol-soaked subC (DECS-1) sample and we suspect that the same may be true for the Blind Canyon coal.

The association of the iron sulfate catalyst with particulate (-60 mesh) coal is illustrated in Plate V for both coals. Plate Va shows numerous small particles of Blind Canyon coal resting on the substrate. Intermixed with these particles a number of needle-like calcium sulfate crystals were observed which appeared mostly separated from the coal surfaces. Inspection of about 50 individual coal particles using the EDS system revealed no significant Fe or Ca peaks, demonstrating that the catalyst was not evenly dispersed on coal surfaces. It is possible that our specimen handling procedure caused catalyst materials to be loosened from the surfaces. Less often, coal particles were observed with a large volume of catalyst concentrated in one area. Plate Vb shows a coal particle with a mass of mixed calcium and iron sulfate crystals on the surface. The crystal shapes and concentration are very similar to what has been observed from studies of individual coal particles.

PLATE V
FIGURE DESCRIPTION

a. Acicular $CaSO_4$ crystals (arrows) found in close proximity but not intimately associated with Blind Canyon (DECS-6) coal particles after impregnation with iron sulfate.

b. A large cluster of both iron and calcium sulfate crystals seen in intimate association with a Blind Canyon coal particle following impregnation with iron sulfate.

c. Calcium sulfate crystals observed in close association with the Texas subC (DECS-1) coal following impregnation with ferrous sulfate.

d. Most of the calcium sulfate found in the particulate subC sample following impregnation with iron sulfate was observed in very large clusters (>300 μm long) such as the one seen in this SEM micrograph.

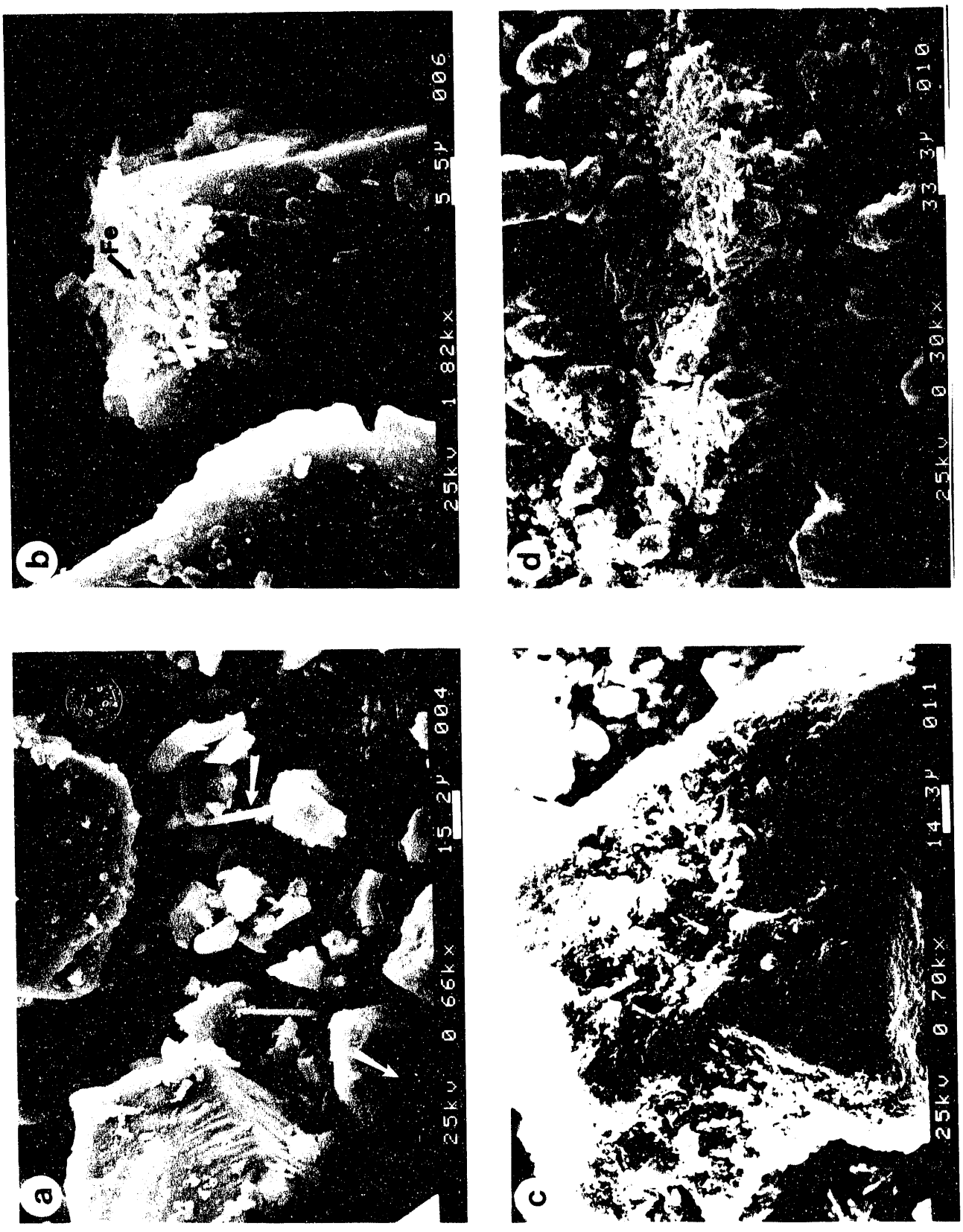
a
25kv 0 66kx 15 2μ 004
b
Fe
25kv 1 82kx 5 5μ 006
c
25kv 0 70kx 14 3μ 011
d
25kv 0 30kx 33 3μ 010

Plate V

Plate Vc and d show areas of calcium sulfate observed after impregnation of the Texas subC coal (DECS-1); no iron sulfate was found. Also, most of the coal particles tested with the EDS system gave no Ca, Fe or S peaks. Although a few particles were observed with associated calcium sulfate (Plate Vc), most of the material was found in large concentrations like that seen in Plate Vd. These observations suggest that catalyst dispersion may be less effective with this coal than with the Blind Canyon. However, ion exchange clearly has been demonstrated to be far superior with the subC coal and therefore dispersion of iron must be greater. As found during our study of individual coal particles, problems were experienced locating significant concentrations of iron in proximity to coal surfaces.

7.3.2. Ion-exchanged Iron Catalyst

Ion-exchange of iron for organically bound calcium in the Texas subC coal has been demonstrated as a mechanism occurring during impregnation of the coal with a ferrous sulfate catalyst. Samples of the Texas subC coal which were ion-exchanged using the method described in Section 5.2.4 (ammonium acetate calcium/iron ion-exchange) were obtained and prepared into a polished section. The sample was evaluated quantitatively using X-ray mapping and microanalysis techniques using the Cameca SX50 electron microprobe. Three separate spectrometers set to the peak wavelengths of sulfur, iron and calcium were employed. X-ray counts were collected for about 10 min to establish the base concentration of the elements associated with the coal particle. Then microanalyses of these elements were

collected on selected (1 μm) areas of the particle interior and near the edge to determine the variation in concentration throughout the particles.

Table 28. Comparison of iron and calcium concentration for raw and ion-exchanged whole coal with electron microanalysis of individual particles (wt %)

Sample	% Fe (wt)	% Ca (wt)
Chemical Analysis		
Raw	0.32	1.47
Ion-Exch.	2.54	0.28
Microanalysis of Ion- exchanged Particles n = 2		
Interior	1.96	0.36
Edge	2.39	0.22

About five recognizable coal particles were selected at random for testing. In all cases similar results to that shown in Figure 21 were obtained. The coal particle is illustrated in the upper left-hand quadrant and the X-ray maps of sulfur (upper right), iron (lower left) and calcium (lower right) are provided. These maps demonstrate that the concentrations of all elements were fairly low and that, relatively, calcium concentration was the lowest. The iron and sulfur maps clearly define the outline of the coal particle, but the calcium is somewhat indistinct at the particle boundary. Microanalysis confirmed a lower calcium concentration at the particle edge as shown in Table 28. These data also suggest that iron may

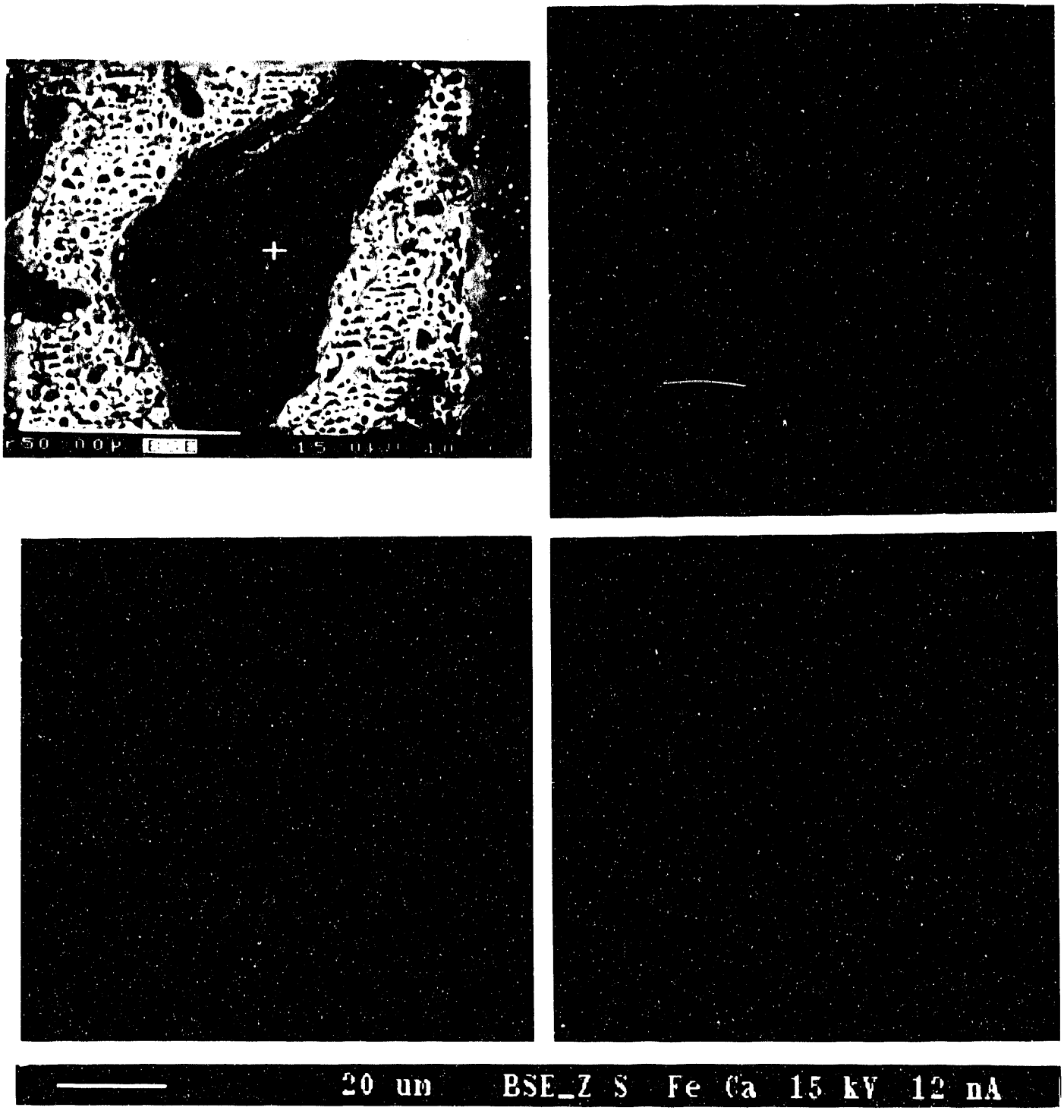

Figure 21 - X-ray Map of the Iron for Calcium Ion-exchanged Texas Subbituminous C Coal. 1) Upper Left-Backscatter Image of Coal Particle, 2) Upper Right-Sulfur Map, 3) lower left-Iron Map, 4) Lower Right-Calcium Map

be slightly higher at the particle edge, thus demonstrating that ion-exchange was not as diffusion limited as may have been the case with our individual particle impregnation work.

7.3.3. Ammonium Tetrathiomolybdate Catalyst

Dispersion of an ATTM solution in methanol onto methanol-soaked and moist surfaces of the Texas subC coal are shown in SEM micrographs in Plate VI. Plate VIa shows the fractured, methanol-soaked coal particle embedded in plastic. Two crystal types of ATTM were observed; a blade-like crystal form was found on the embedding plastic surface only and the other form was found in large clusters (<120 μm) on both the coal and plastic surfaces. At higher magnification (Plate VIb), the clusters were seen to be intergrown crystals of ATTM that appeared to be associated with coal fractures. This suggests that the ATTM/methanol solution may once have been concentrated at the coal fracture, but during evaporation of the solvent and inherent coal moisture under vacuum, ATTM may have been drawn out of the fracture system.

There was some evidence that a more uniform surface dispersion of ATTM may be obtained when applied to a moist coal surface. Plate VIc shows that the blade-like crystals of ATTM have grown across both the plastic and coal surfaces. Also, small crystals of ATTM can be seen in the upper right-hand corner of Plate VIc. Plate VId shows these ≈10 μm plate-like crystals scattered about the surface individually or in small clusters. This suggests that the moist surface of coal may have a greater potential for surface dispersion than a methanol soaked and preswollen coal surface.

PLATE VI
FIGURE DESCRIPTION

a. SEM micrograph of methanol-soaked Texas subC coal impregnated with ATTM. The blade-like crystal form of ATTM can be seen on the mounting plastic (lower left corner) and relatively large crystalline clusters of ATTM are distributed unevenly on the coal surface.

b. High-magnification micrograph of the methanol-soaked subC coal showing that the intergrown crystals of ATTM are associated with a coal fracture.

c. When the coal is stored under moist conditions, blade-like crystals of ATTM are seen growing across the plastic and coal surfaces. Also, there are individual ≈10 μm plate-like crystals of ATTM distributed across the coal surface, as seen in the upper right corner.

d. High-magnification SEM micrograph showing the plate-like crystals of ATTM distributed on the coal surface as described for Plate VIc.

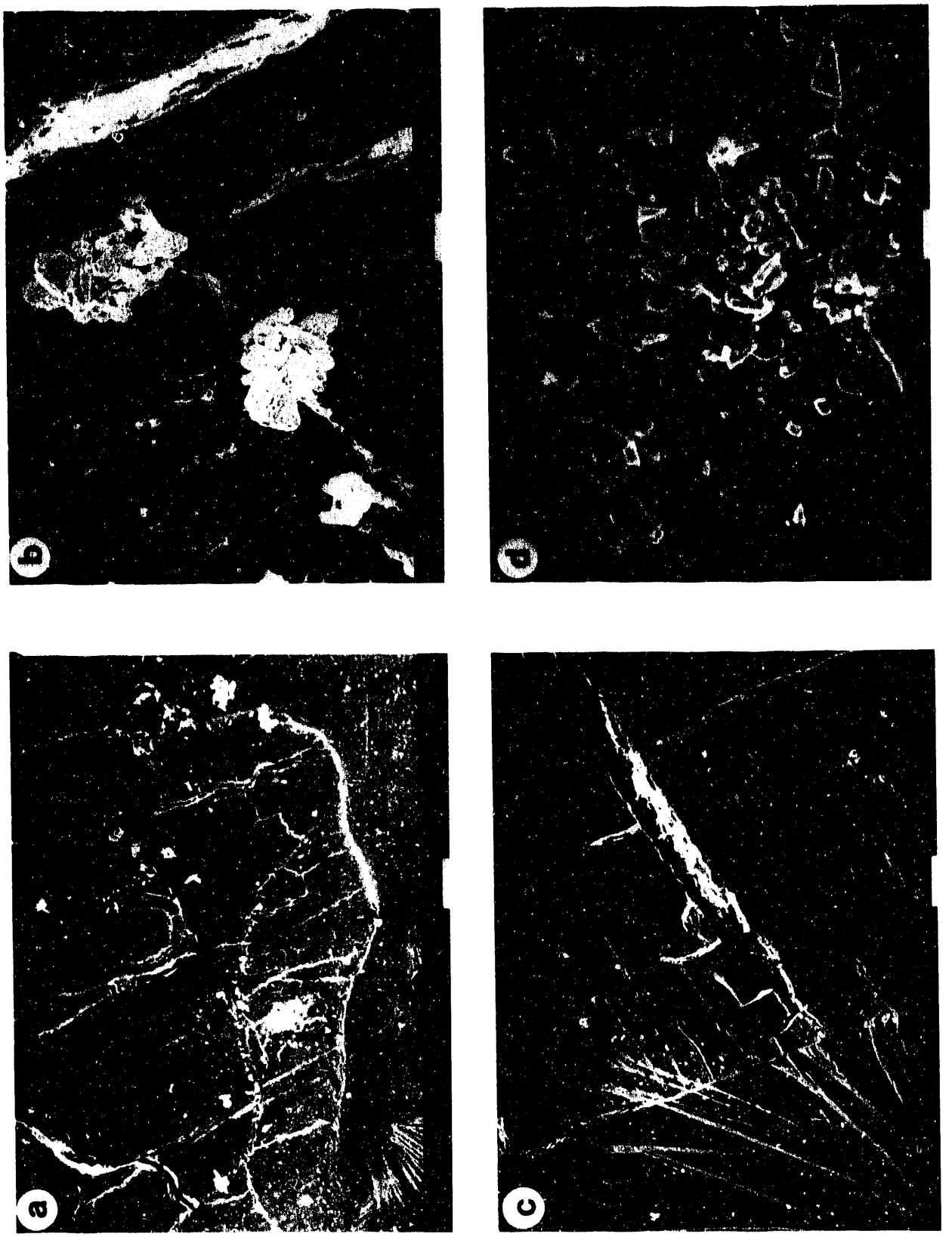

Plate VI

A cross-sectional area of the soaked sample with ATTM catalyst also was prepared for inspection in the SEM. As observed with the ferrous sulfate sample, no molybdenum or sulfur peaks were detected on either interior of exterior surfaces of the coal. From this we conclude that the ATTM - methanol solution does not effectively penetrate a methanol-soaked preswollen surface of the Texas subC coal.

The dispersion/impregnation of ATTM in methanol on individual particles of Blind Canyon coal also was studied. However, the batch of ATTM prepared in-house had altered to some degree and was no longer completely soluble in methanol. Plate VIIa shows that when ATTM was added to a methanol soaked surface of Blind Canyon, large crystals (20 - 80 μm) of the insoluble fraction of ATTM were cemented in place by clusters of very fine ($\approx$0.2 μm) particles of what presumably had been the soluble fraction of ATTM. Inspection of the cross-sectional area prepared from this sample showed that the catalyst was mainly associated with the exterior coal surface; no penetration of the catalyst into fracture system was observed.

Plate VIIb through d illustrates the degree of dispersion of ATTM on the surface of particles of the subC coal (DECS-1) that were prepared for liquefaction. Plate VIIb and c are micrographs of the same coal particle which gave a relatively strong Mo and S peak with the EDS. Arrows in each illustration show the exact location of small (<5 μm), plate-like crystals of ATTM attached to the coal surfaces. These crystal forms and that seen in Plate VIId are very similar to those shown from individual coal

particles (Plate VI). Most of the particles encountered and tested in this sample did not give Mo or S peaks, suggesting that ATTM probably forms a wide dispersion of discrete particles that are loosely held to the surface of coal. Even so, conversion and product yield has been improved as suggested by the pretreatment data in Table 6.

Particle mounts of an unswollen Blind Canyon sample (DECS-6) impregnated with ATTM were evaluated using the SEM in a similar manner as described for the Texas subC coal. The whole sample was scanned and individual particles tested at random for the presence of sulfur and molybdenum peaks using the EDS system. This procedure required approximately 1 h per sample and must be considered qualitative at best. As demonstrated in Figure 22, the X-ray energies of molybdenum, sulfur and gold (coating material) overlap between about 2.0-2.5 keV. Therefore, some interpretative difficulty arises as to whether ATTM may be present at any given test point. However, the presence of gold and its relative intensity may be established by the $Au_{L\alpha}$ peak at ≈9.7 keV. In addition, peak broadening and skewness to higher energies of the main S/Mo peak at 2.2 keV can be used as a qualitative indication of the presence of molybdenum for any given sample set.

Figure 23 demonstrates the effective use of the EDS system where several X-ray energy spectra were collected from different areas of a single coal particle shown in the accompanying SEM micrograph. The particle shown is from a Blind Canyon sample impregnated with ATTM, but which had not been preswollen with a solvent. Area and spectrum #1 show a

PLATE VII
FIGURE DESCRIPTION

a. ATTM in solution with methanol was placed on a methanol presoaked surface of an individual particle of Blind Canyon (DECS-6) coal. Large ATTM crystals from a methanol-insoluble fraction are held fast to the coal surface by clusters of submicron-sized crystals of once-soluble ATTM.

b. The central particle of DECS-1 (subC) in this micrograph gives a strong Mo and S peak owing to the presence of crystalline ATTM at the arrow. Sample was impregnated with ATTM from aqueous solution.

c. Higher magnification micrograph of the coal particle surface seen in "b", showing the association of ATTM plate-like crystals with the coal surface.

d. A high-magnification micrograph of an ATTM crystal cluster found on another subC (DECS-1) coal particle following impregnation with an aqueous solution of ATTM.

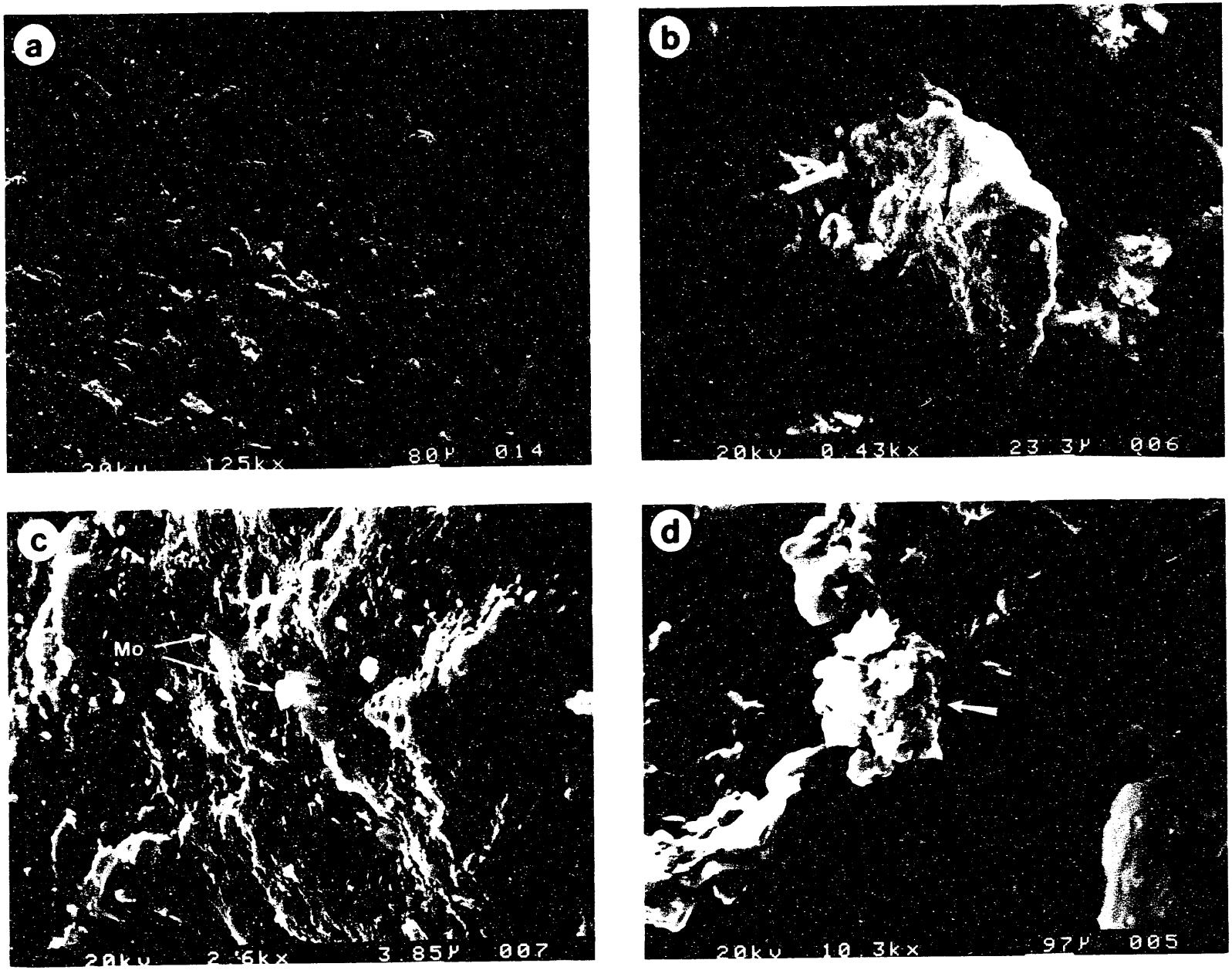
a
125kx
80µ 014
b
20kv 0 43kx 23 3µ 006
c
Mo
20kv 2 5kx 3 85µ 007
d
20kv 10 3kx 97µ 005

Plate VII

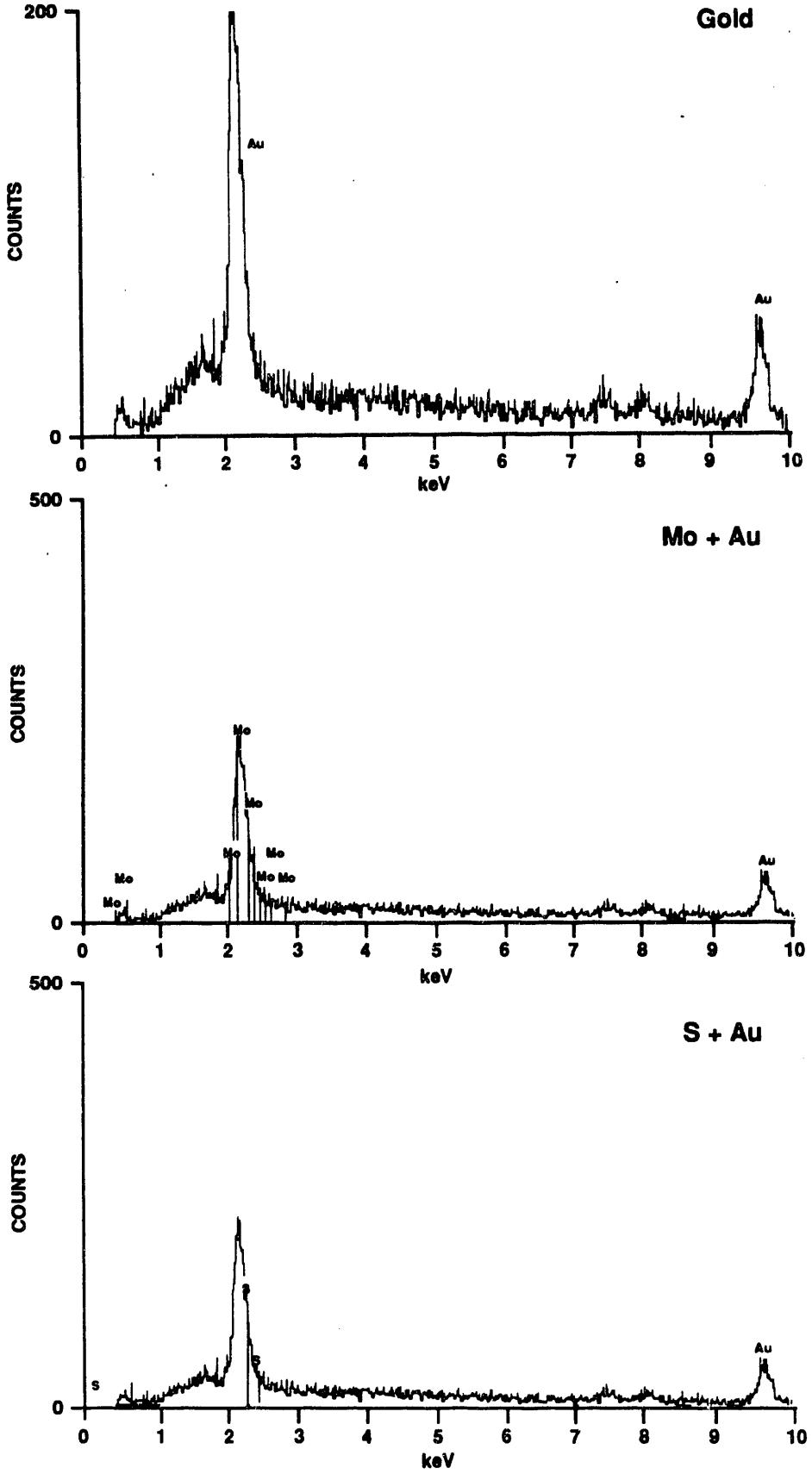

Figure 22 - X-ray Counts Accumulated Over 100 s Showing the Location and Overlap of Gold, Molybdenum and Sulfur Peaks in Unswollen Blind Canyon Sample Following Impregnation with ATTM

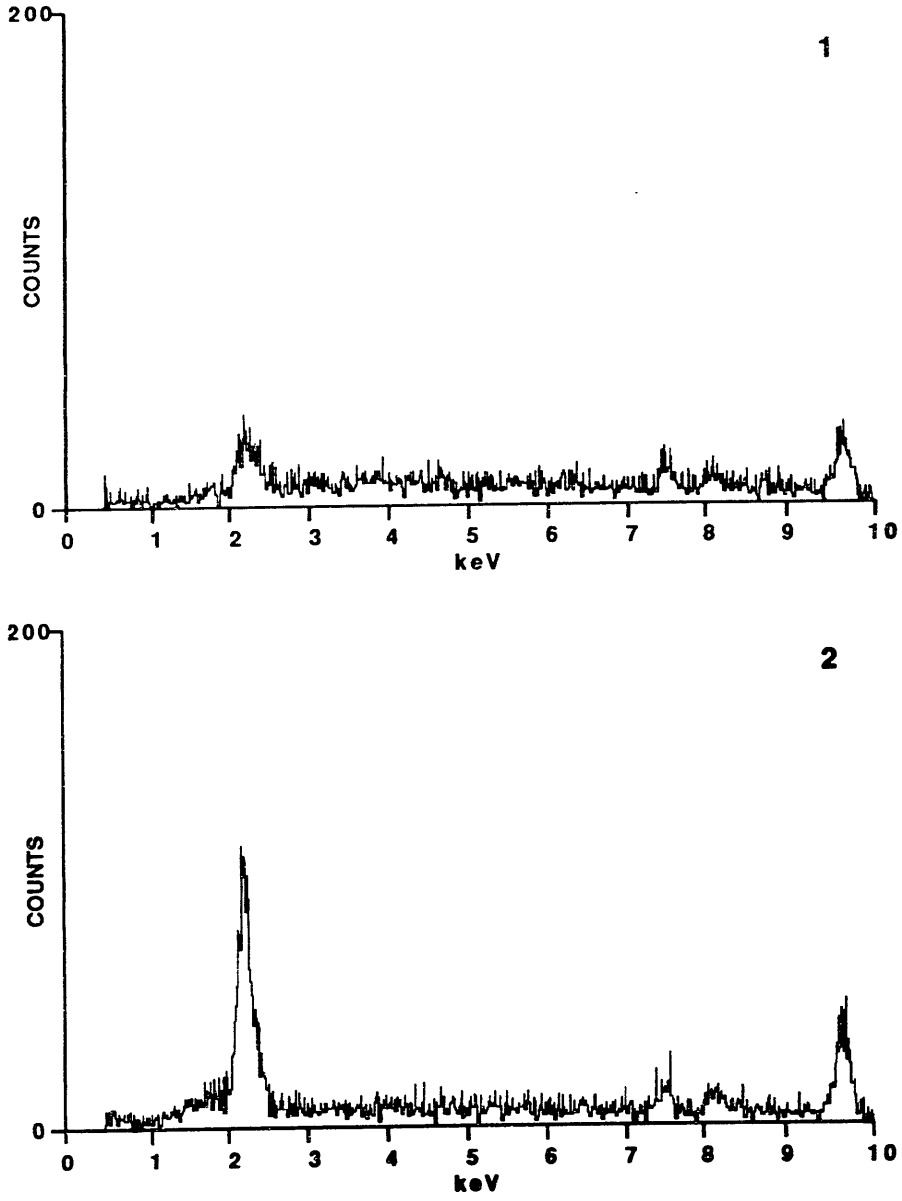

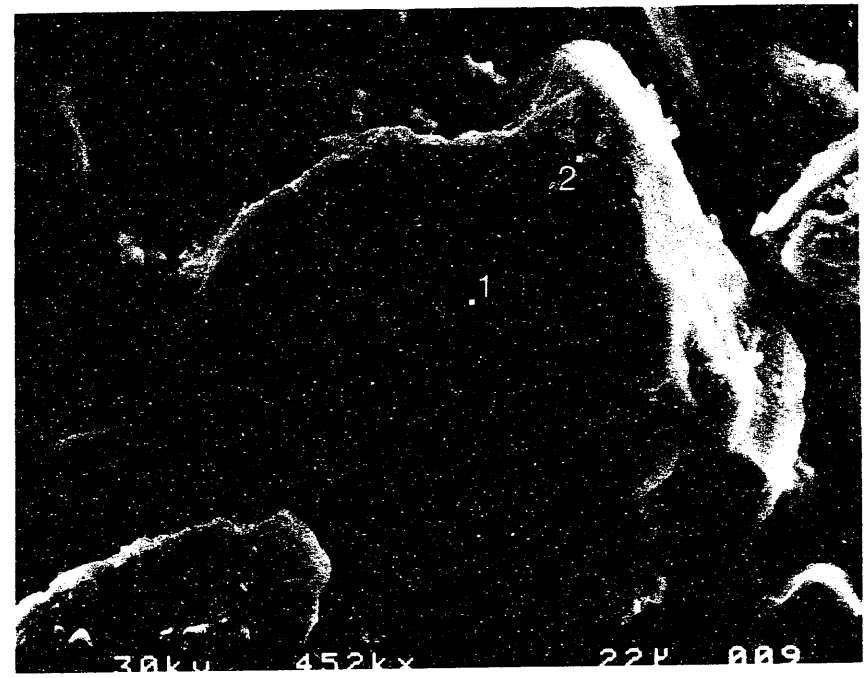

Figure 23 - EDS X-ray Counts Accumulated on Different Areas of a Blind Canyon Coal Particle Impregnated with Aqueous ATTM

relatively weak gold peak and no sulfur peak, suggesting that ATTM may not be present at that site. However, for area and spectrum #2 not only is there a stronger gold peak, but the lower energy peak near 2.2 keV was found to be proportionally higher, thus implying that Mo and/or S may be contributing X-ray energies. In general for this sample, much of the ATTM appeared to be scattered as small discrete particles across the coal surface, much as was shown for the Texas subC sample.

A similar SEM evaluation was conducted for Blind Canyon samples that were first swollen in methanol, pyridine and THF before being impregnated with ATTM. However, location of discrete catalyst particles associated with the coal surface was not altogether successful. As shown in Figure 24 for the coal preswollen in pyridine, energy spectra are very uniform from site to site, with a relatively low gold peak and a large peak in the 2.0-2.5 keV region. From this evaluation we were uncertain whether the low energy peak was being influenced by S or Mo or by both elements. Most of the coal particles in the pyridine-swollen Blind Canyon sample gave these same uniform spectra. On the other hand, spectra collected for the Blind Canyon samples swollen with methanol and THF were not as uniform. In fact, there was some difficulty in locating low-energy X-rays from these samples, suggesting that catalyst dispersion may be heterogeneous, i.e., as discrete particles.

In addition to the Blind Canyon samples two Texas subC particulate samples preswollen in methanol and pyridine and that were impregnated with ATTM were evaluated using the SEM technique. Unfortunately, there was

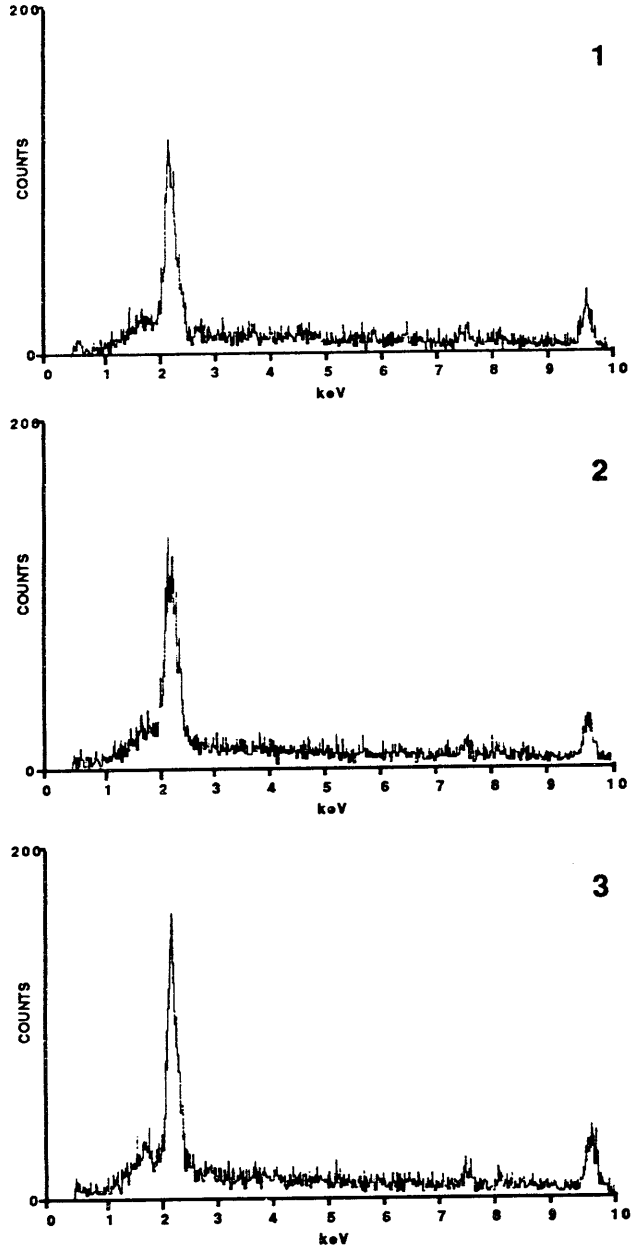

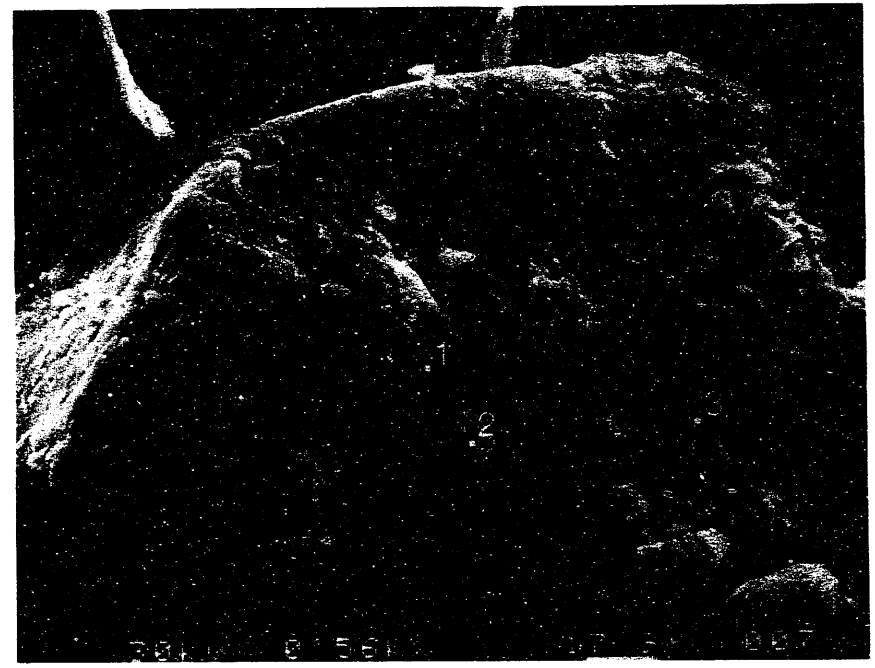

Figure 24 - EDS X-ray Counts Accumulated on Pyridine-Preswollen Blind Canyon Coal Particle Impregnated with ATTM

significant interference from the presence of other elements (Ca, Al, Si, Ti, etc.) such that Mo and S peaks were difficult to locate or interpret. In the case of the pyridine-swollen sample, not a single particle gave a Mo or S peak. Clearly, a more quantitative characterization of these samples was needed and this was the reason the electron microprobe was employed. Consequently, all ATTM impregnated samples were prepared for electron microprobe analysis.

Microprobe measurements were made by identifying an individual coal particle using the probe white-light optics, then impinging the electron beam on the center of the particle and collecting X-ray counts for 20 sec for each element (S and Mo). Between 5 and 8 particles were analyzed in this manner for each sample. This analytical procedure does not provide an indication of catalyst impregnation vs dispersion, but it aids in our determination of whether the catalyst is or is not associated with individual coal particles.

Table 29 lists the results from these analyses and tends to confirm the qualitative evaluation performed using the SEM. For the ATTM-impregnated Blind Canyon samples, molybdenum and sulfur peaks were measured in association with all particles tested (100%) when swelling solvents were not employed. When pyridine was used, about 80% of the particles had a low level of associated molybdenum, whereas most (75%) of the particles tested in the methanol-swollen coal showed no molybdenum peaks. In comparison, particle mounts of the Texas subC sample preswollen in methanol and pyridine showed that about 80% of the methanol sample had associated

Table 29. Electron microprobe results from ATTM-impregnated Blind Canyon hvAb and Texas subC coals

Particle No.	Elements Detected: Mo	S	Other (EDS)	Relative Strength of MO Peak	Relative Strength of S Peak
DECS-6 -- Unswollen					
1	*	*	--	4.8	53.6
2	*	*	Al, Si	6.1	51.6
3	*	*	--	9.1	63.3
4	*	*	--	38.0	170.8
5	*	*	--	7.0	70.0
6	*	*	--	7.7	51.2
DECS-6 -- Pyridine					
1	*	*	--	7.3	39.8
2	*	*	Al, Si, Cl	2.5	20.6
3	None	None	--	--	--
4	*	*	--	3.9	24.7
5	*	*	--	4.3	39.2
DECS-6 -- Methanol					
1	*	*	Al, Si, Ca	11.2	67.7
2	None	None	Al, Si	--	--
3	*	*	Al, Si, Ca	1.1	14.8
4	None	None	--	--	--
5	None	None	--	--	--
6	None	*	Al, Si, S, Ca	--	5.1
7	None	None	Al, Si, Ti, Ca	--	--
8	None	None	--	--	--
DECS-1 -- Methanol					
1	*	*	Al, Si, Ca	6.1	34.6
2	None	*	Al, Si	--	4.2
3	*	*	Al, Si, Ca	5.8	77.4
4	*	*	Al, Si, Ca	6.8	70.2
5	*	*	Al, Si, Ti	5.0	18.6
6	*	*	Ca	4.7	57.6
DECS-1 -- Pyridine					
1	None	*	--	--	4.1
2	None	*	--	--	20.4
3	None	*	--	--	2.6
4	None	*	--	--	2.8
5	None	*	--	--	2.8

* = element present

molybdenum and sulfur, whereas none was detected on the pyridine-swollen coal above about 1000 ppm concentration. The relative intensity of the molybdenum peak presented in Table 29 suggests that in most cases Mo was in fairly low concentration with respect to the mass tested. This could reflect a submicron dispersion of the catalyst in and about the coal particle surface layers. The relative intensity of the sulfur peak was much higher and somewhat more variable, because we have measured the organic sulfur fraction naturally occurring in the coal as well as a somewhat less uniform contribution of sulfur derived from the ATTM catalyst.

7.4. SUMMARY AND CONCLUSIONS

A number of different sample preparation and microscopic techniques were employed in order to characterize the dispersion/impregnation of catalyst onto or into two coals, i.e., Texas subC (DECS-1) and Blind Canyon (DECS-6). The relative influence of various swelling solvents were also investigated. Sample preparation techniques were varied owing to physical limitations of the systems studied. For example, water- and methanol-soluble catalysts could be applied to individual coal particles and effectively studied. However, the use of relatively strong swelling solvents (THF, pyridine and TBAH) caused particle disintegration. Thus, to effectively study coals preswollen in these solvents required the use of particulate samples that were prepared for liquefaction. SEM-EDS evaluation of particulate samples was effective as long as the catalyst was dispersed on the surface as discrete particles. However, when

dispersion/impregnation became more uniform and catalyst concentration decreased with respect to any given particle, the SEM-EDS method became ineffective and the electron microprobe had to be employed. During microanalysis, we sacrifice our ability to view the associations of catalyst with the rough surfaces of coal particles for an ability to measure catalyst concentration.

Solutions of ferrous sulfate and ATTM in methanol were placed on the polished surfaces of methanol-soaked and moist particles of the Texas subC and Blind Canyon hvAb coals and vacuum impregnated. Results from this study showed that iron ion-exchanges with the organically bound calcium (to form calcium sulfate) on a moist surface of the subC, forming a uniform distribution of calcium sulfate and excess ferrous sulfate across the surface. A much greater amount of ferrous sulfate and a lower amount of calcium sulfate was found with the Blind Canyon sample because of a lower content of exchangeable calcium. No evidence was found for ion exchange with the methanol-soaked sample of either coal. When individual particle samples were viewed in cross section, some evidence was found for penetration of the iron sulfate in solution with methanol into the fracture system when moist coal was impregnated.

The same observations were made using particulate coal samples concerning ferrous sulfate dispersion as with individual particle samples. Both test procedures showed that iron sulfate was involved in an ion-exchange process with calcium to form calcium sulfate crystals. As would be expected, calcium sulfate was found in much higher concentration with

the Texas subC than with the hvAb Blind Canyon coal, although it was not as widely dispersed in the subC sample, e.g., the catalyst was found in large aggregates.

To gain a better understanding of the level of iron dispersion that may be achieved during the ion-exchange mechanism, ammonium acetate calcium/iron ion-exchange was performed for the Texas subC coal. Inspection of coal following the procedure showed a very uniform dispersion of iron throughout most coal particles at a relatively low concentration. The study also showed a reduction of calcium ions within coal particles, with the lowest concentration found along the particle perimeter. Presumably, the ion exchange attained by simple contact of the moist subC coal with a ferrous sulfate solution for 6 h would not be as effective.

As discussed in Sections 4 and 5, $FeSO_4$ was not an active catalyst under pretreatment conditions (275°) in the presence or absence of H_2S and was only slightly better than no catalyst addition during temperature-stage liquefaction in H_2. With the addition of H_2S to the reaction gas during temperature-staged processing conversion and product yields were increased marginally. When Fe was uniformly dispersed/impregnated during ammonium acetate ion-exchange for Ca in the subC coal there was a much greater improvement in conversion with H_2S present. We have shown through X-ray mapping the extent to which Fe was widely disseminated throughout subbituminous coal particles and, therefore, have clearly demonstrated the positive benefits of uniform catalytic dispersion/impregnation upon liquefaction. However, under the best conditions of dispersion and

sulfidization the iron-based catalysts are only marginally comparable with molybdenum-based catalyst with respect to conversion and product yields.

ATTM appeared to form a reasonably good surface dispersion on a moist rather than a preswollen coal surface. Examination of cross-sectional areas of the methanol-soaked samples impregnated with ATTM revealed no penetration of the catalyst into the coal fracture system. Dispersion of an aqueous solution of ATTM within a particulate sample of the Texas subC coal demonstrated that ATTM is widely disseminated as discrete crystalline particles that are loosely held to the surface of coal.

Both qualitative SEM and quantitative electron microprobe analyses were performed on Blind Canyon and Texas subC samples that were first swollen in various solvents and then impregnated with ATTM. This investigation showed that pyridine-swollen coals provided a better dispersion of ATTM catalyst on a submicron level on the Blind Canyon coal than when swollen in methanol. When no swelling reagent was used, the catalyst was found as discrete, but uniformly distributed particles on the coal's surface. ATTM was dispersed more evenly on the water and methanol preswollen Texas subC coal than when pyridine was used.

Total conversion of the Texas subC coal was influenced by the use of swelling solvents, with TBAH having the greatest effect and pyridine being a distant second followed by methanol, THF and water under pretreatment conditions. Addition of ATTM only marginally improved conversion under these conditions suggesting that it is ineffective as a pretreatment catalyst for the subC coal. ATTM contributed to an overall greater

conversion during temperature-staged liquefaction, basically following the same order with regard to the swelling solvents (TBAH and pyridine). Methanol and THF were not used as a swelling solvent during temperature-staging because they were mostly ineffective under pretreatment conditions. Our microscopic observations showed that ATTM was distributed uniformly as discrete particles when water and methanol were used, but could not be located in ≈>1000 ppm concentration when pyridine was used. This intimates that the use of pyridine may have resulted in a broad dissemination of molybdenum at the submicron or perhaps angstrom level. Total conversion of pyridine-swollen Texas subC coal under temperature-staged with ATTM was equal to that using TBAH.

Dispersion of the ATTM catalyst on the Blind Canyon hvAb coal was found to be very similar to that described for the Texas subC, although the resulting conversion and product yield information was much less predictable. For example, under pretreatment conditions total conversion decreased in the order: TBAH > THF > methanol > none > pyridine, however, when ATTM was introduced the order changed to: pyridine > methanol = THF = none > TBAH. The changing order of TBAH and pyridine may result from the fact that these solvents have a relatively strong physical influence on the hvAb coal as was discussed in Section 6. The effect of particle agglomeration and reaction with the solvents may interfere with the distribution of the catalyst and its availability to hydrogen during liquefaction. Under temperature-staged conditions total conversion basically followed the order of solvent strength (i.e., TBAH, pyridine,

THF, none and methanol), whereas with the introduction of ATTM, preswelling with pyridine resulted in the highest conversion and TBAH the least. Again, the change in ordering for these reaction conditions may have resulted from the physical interrelationship between solvent-soluble materials and catalyst. However, during temperature-staged liquefaction conversions are higher and particle agglomeration is not as important of a consideration.

8. COAL/SOLVENT/CATALYST INTERACTIONS DURING LIQUEFACTION

8.1. INTRODUCTION

This section of the report is concerned with the investigation of the nature of the organic residues of liquefaction and the association and distribution of catalyst materials with the remaining organic fractions. Residues from pretreatment and two-staged liquefaction have been studied using optical and electron optical techniques in an effort to formulate a more accurate picture of the fate of catalyst material with respect to the reacting coal. Sections 3 and 5 of this report provide information regarding the effectiveness of catalysts and catalyst conversion into an active phase, whereas this section will attempt to explain these results from physical associations remaining following reaction.

A systematic characterization of some 35 THF-insoluble liquefaction residues has been completed using optical or electron optical techniques. The samples were more-or-less equally divided between runs made with Blind Canyon (DECS-6) and the Texas subC (DECS-1) coals. For each coal, residues from runs at pretreatment and temperature-staged conditions were selected based on process conditions and coal treatment, i.e., presence or absence of catalyst, swelling solvents and different gas atmospheres. Residues were chosen in an effort to cover the influences of catalyst, swelling solvents and reaction conditions on different coals.

8.2. EXPERIMENTAL

Table 30 lists the residues that were prepared for microscopy together with pertinent reaction conditions and product yields for each

Table 30. List of samples employed for optical and electron optical characterization and their liquefaction data

Sample	Catalyst	Gas Atmosphere	Reaction Temperature	Swelling Solvent	wt% Total Conversion	Asphaltene	Pre-Asphaltene	Oil & Gas	Oil	Gas
DECS-6										
5	none	H_2	275	none	17.7	2.1	10.7	4.9	--	--
DECS-6, ATTM	ATTM	H_2	275	none	25.0	3.0	15.1	6.9	--	--
DECS-6, $FeSO_4$	$FeSO_4$	H_2	275	none	16.9	2.6	9.2	5.1	--	--
DECS-6, MoS_3	MoS_3	H_2	275	none	23.2	3.3	15.2	4.7	--	--
7	none	H_2	275	THF	22.1	2.2	11.1	9.2	--	--
10	none	H_2	275	TBAH	24.0	3.6	15.1	5.3	--	--
11	ATTM	H_2	275	THF	25.1	2.4	12.4	10.3	--	--
14	ATTM	H_2	275	TBAH	23.7	3.9	13.5	6.3	--	--
3	$Fe(CO)_5$	$H_2S:H_2$	275	Pentane	22.9	2.7	14.1	6.1	--	--
1	$Mo(CO)_6$	$H_2S:H_2$	275	Pentane	26.6	3.3	15.7	7.6	--	--
17	$Mo(CO)_6$	$H_2S:H_2$	275	TBAH	26.4	6.0	16.6	3.8	--	--
15	$Mo(CO)_6$	$H_2S:H_2$	275	Pyridine	28.1	5.7	15.9	6.5	--	--
20	none	H_2	275/425	none	48.0	8.5	12.3	27.2	21.9	5.3
21	none	H_2	275/425	Pyridine	51.6	11.3	7.3	33.0	26.5	6.5
22	none	H_2	275/425	TBAH	58.7	17.3	9.9	31.5	13.4	18.1
24	none	$H_2S:H_2$	275/425	none	58.2	17.2	12.1	28.9	22.3	6.6
23	ATTM	H_2	275/425	none	85.1	32.5	14.7	37.9	33.9	4.0
25	$FeSO_4$	$H_2S:H_2$	275/425	none	78.5	29.2	15.5	33.8	27.5	6.3
26	$Mo(CO)_6$	$H_2S:H_2$	275/425	Pentane	86.0	28.9	14.2	42.9	36.8	6.1
34	ATTM	H_2	275/425	Pyridine	90.3	33.7	9.4	47.1	43.0	4.1

Table 30. List of samples employed for optical and electron optical characterization and their liquefaction data (continued)

Sample	Catalyst	Gas Atmosphere	Reaction Temperature	Swelling Solvent	wt% Total Conversion	Asphaltene	Pre-Asphaltene	Oil & Gas	Oil	Gas
DECS-1										
6	none	H_2	275	none	6.6	2.2	2.8	1.6	--	--
DECS-1, $FeSO_4$	$FeSO_4$	H_2	275	none	6.4	2.2	2.4	1.8	--	--
8	none	H_2	275	Pyridine	10.0	2.0	1.7	6.4	--	--
9	none	H_2	275	TBAH	17.5	3.9	5.2	8.4	--	--
12	ATTM	H_2	275	Pyridine	11.8	2.4	2.9	6.5	--	--
13	ATTM	H_2	275	TBAH	18.7	4.6	6.2	7.9	--	--
4	$Fe(CO)_5$	$H_2S:H_2$	275	Pentane	11.2	3.5	4.2	3.5	--	--
19	$Fe(CO)_5$	$H_2S:H_2$	275	TBAH	23.6	10.0	7.5	6.1	--	--
2	$Mo(CO)_6$	$H_2S:H_2$	275	Pentane	9.1	2.8	4.2	2.2	--	--
16	$Mo(CO)_6$	$H_2S:H_2$	275	Pyridine	13.9	3.6	3.1	7.2	--	--
18	$Mo(CO)_6$	$H_2S:H_2$	275	TBAH	15.3	3.5	4.5	7.3	--	--
27	none	H_2	275/425	none	53.1	10.9	8.2	34.0	21.2	12.8
30	ATTM	H_2	275/425	none	78.9	19.3	10.6	49.0	36.4	12.6
28	none	$H_2S:H_2$	275/425	none	66.7	13.9	11.2	41.6	28.1	13.5
29	$FeSO_4$	$H_2S:H_2$	275/425	none	71.5	24.4	5.1	42.0	27.7	14.3
31	$Mo(CO)_6$	$H_2S:H_2$	275/425	Pentane	80.1	18.3	9.1	52.7	38.7	14.0
32	ATTM	H_2	275/425	Pyridine	88.8	30.1	10.9	47.4	37.4	9.9
33	ATTM	H_2	275/425	TBAH	88.9	35.6	8.9	45.1	34.6	10.5

run. Each THF-insoluble residue was embedded in an iodine-substituted epoxy resin and a polished surface prepared. Optical microscopy was employed to obtain a better understanding of the progressive transformation of the organic fraction of coal with respect to the different treatments, catalysts and reaction conditions, whereas electron microscopy techniques were employed to obtain information on the fate of catalyst materials.

Optical microscopy was performed using a Zeiss Axiophot reflectance microscope at 400X magnification. Reflectance analyses (mean random reflectance) were performed on the vitrinite-derived portion of some residues using a Leitz MPV2 microscope following the general procedures as described in ASTM D5 2798-91. Electron optical equipment used in this study was the same as described in Section 7, i.e., the ISI-SX-40A SEM with Kevex EDS system for qualitative evaluation; the Cameca SX50 was used for X-ray mapping and quantitative analyses.

8.3. RESULTS AND DISCUSSION

8.3.1. Optical Microscopy of Liquefaction Residues

The influence of swelling solvents on the Texas subC and Blind Canyon hvAb coals were characterized in Section 6 and showed that 10% tetrabutylammonium hydroxide (TBAH) and pyridine promoted the greatest effect. As discussed in Section 3, one or the other of these solvents also contributed to significantly greater total conversion and product yields under pretreatment conditions (275°C) when various catalysts were employed.

TBAH markedly improved the conversion of the Texas subC coal with and

without added catalyst. In the absence of catalyst the 275°C residue from DECS-1 exhibited some of the same properties as observed following swelling in the base, i.e., many of the particles were severely swollen and fractured. Following thermal treatment, however, a large portion of the residue had agglomerated into larger particles and, as shown in Plate VIIIa, competent coal particles were cemented together with a fine grained, low-reflecting matrix. The matrix material along with the appearance of some of the vitrinite particles within the agglomerates suggests that minor plasticity had developed during thermal hydrogenation. This same observation was made when a TBAH-swollen subC sample was impregnated with $Mo(CO)_6$ and reacted in H_2S:H_2 at 275°C. As shown in Plate VIIIb, numerous coal particles are cemented together; the low-reflecting matrix found in the residue of the thermal run was not observed following the catalytic run nor were there any fine-particle agglomerates. The more pronounced agglomeration of larger particles and the lack of the low-reflectance matrix may correspond with the fact that this catalytic run showed a lower total conversion compared with the thermal (15.3% vs 17.5%). The low-reflecting matrix material and poor agglomeration of coal particles were observed in the TBAH-swollen Texas subC sample impregnated with $Fe(CO)_5$ and reacted in H_2S:H_2; this run also had the greatest total conversion under pretreatment conditions (23.6%). Similar observations were made with the DECS-1 sample impregnated with ATTM.

As expected, some coal particle plasticity, i.e., particle agglomeration, was observed in the Blind Canyon hvAb coal without prior

solvent or catalyst treatment. However, it was minor compared with the level of plasticity seen when TBAH was employed. Plate VIIIc shows the tattered, thread-like edges of a particle of DECS-6 after thermal pretreatment. These shreds of material appear to be the reacted remnants of the TBAH reaction front illustrated in Plate IIc and d. Note that the TBAH reaction product has about the same reflectance as the coal vitrinite, suggesting that it partially reacted under pretreatment thermal conditions. Reaction of DECS-6 under these conditions resulted in the highest conversion of any solvent alone (24.0%) and was about equal to or slightly lower than any of the catalysts with TBAH (i.e., ATTM=23.7%, $Mo(CO)_6$=26.4% and $Fe(CO)_5$=25.6%). However, in the case of molybdenum catalyst addition, TBAH preswelling adversely influenced conversion of the Blind Canyon coal compared to pyridine or THF. One reason for the apparent inactivity of catalysts may be a function of the TBAH reaction layer blocking the coal porosity. Another may be that the catalyst was mainly in contact with the reaction product and spent before fresh coal surfaces became available. Yet another may be that the catalyst was incorporated in the reaction product and so isolated from hydrogen. Inspection of 275°C residues of coals impregnated with ATTM and $Mo(CO)_6$ catalysts showed nearly the same particle interaction as that shown in Plate VIIIc except that the particle agglomerates had less open porosity. There were also many more fine-grained agglomerates present in the catalytic residues which were typically lower in reflectance than the vitrinite.

PLATE VIII
FIGURE DESCRIPTION

a. Example of particle agglomeration by a fine-particulate matrix following liquefaction of a TBAH preswollen Texas subC at 275°C in the absence of added catalyst.

b. Apparent fusion (plasticity) of coal particles resulting in agglomeration following pretreatment liquefaction (275°C) of the TBAH preswollen Texas subC in the presence of $Mo(CO)_6$ in an $H_2S:H_2$ atmosphere.

c. Weak agglomeration of Blind Canyon coal particles by the TBAH reactant material observed in Plate IIc and d following pretreatment hydroliquefaction (275°C) of the TBAH preswollen DECS-6 coal in the absence of catalyst.

d. Apparent reaction of the pyridine-soluble fraction cementing particles of the Blind Canyon coal following pretreatment liquefaction (275°C) of a pyridine preswollen DECS-6 coal in the presence of $Mo(CO)_6$ in a $H_2S:H_2$ atmosphere.

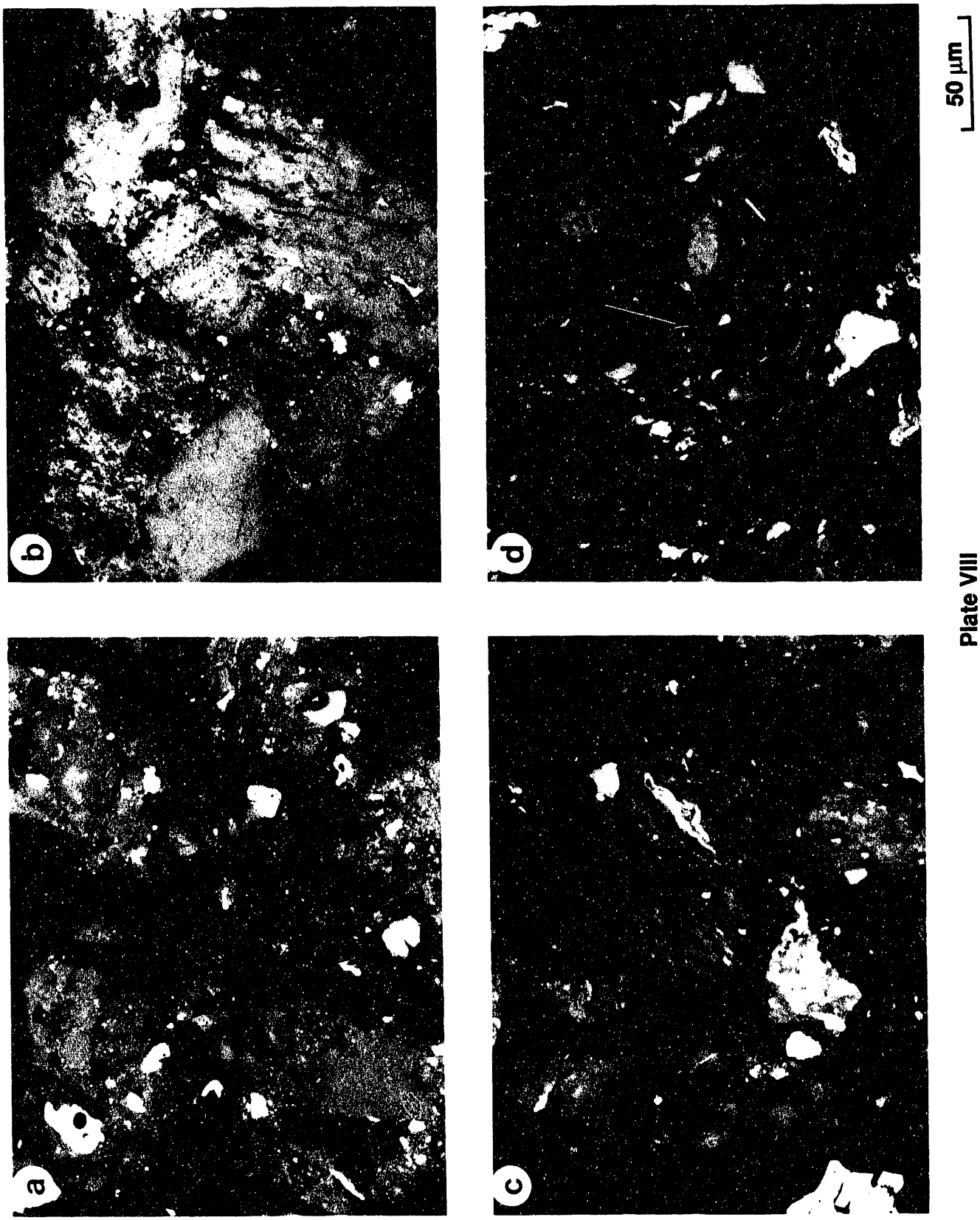

Plate VIII

Pyridine swelling had a much less noticeable influence on the physical characteristics of the residual materials of the subC coal under thermal pretreatment conditions. In comparison with the non-swollen DECS-1 it appeared that particle size was significantly smaller and that the particles were more rounded following contact with pyridine and subsequent reaction. Qualitatively it seemed that many of the remnant particles showed more advanced signs of desiccation (fracturing); otherwise particle agglomeration and signs of plasticity were absent. Similar observations were made regarding pyridine-swollen DECS-1 coal impregnated with $Mo(CO)_6$. Particle size was smaller yet, desiccation slightly more advanced, and some small fine-gained agglomerates were observed. Judging from the residues, pyridine swelling of the subC coal effectively reduced particle size and resulted in little or no agglomeration. All of these factors may have contributed to the fairly strong conversion and product yield attributable to pyridine swelling in the presence and absence of catalysts.

As shown in Plates Id and IIa, pyridine swelling had a much greater influence on the hvAb coal. Although residues from the thermal treatment were unavailable, inspection of a 275°C residue following impregnation with $Mo(CO)_6$ showed nearly the same characteristic agglomeration that was observed after swelling alone. Plate VIIId, showing the agglomeration of numerous coal particles, exhibits a layer of pyridine-soluble cement (arrow) that, following pretreatment reaction, has slightly higher reflectance than the surrounding vitrinite. Just as had been observed earlier with the TBAH reaction product, the increase in reflectance

suggests preferential reaction with the once-soluble component. In this particular case (Plate VIIId), the pyridine-soluble material may have been involved in condensation reactions which is generally associated with increased reflectance [Davis et al., 1989]. However, in most of the agglomerates the cement had about the same reflectance as the surrounding vitrinite. From data presented in Section 3, the combination of preswelling in pyridine and impregnation with catalysts (ATTM, $Mo(CO)_6$ or $Fe(CO)_5$) had a profound positive influence on conversion of the hvAb coal under pretreatment conditions.

Temperature-staged reaction (275°C, 30 min; 425°C, 30 min) of the two coals under the various reaction conditions (preswelling and presence or absence of catalysts) resulted in total conversions of >50% to 90%. Qualitative inspection of these residues under the optical microscope revealed little about the interrelationships among different swelling solvents and catalysts.

In general, temperature-staged residues of the subC coal were composed of relatively high reflecting remnants of original coal particles, fine-grained agglomerates and mineral matter. Comparison of residues from the reaction conditions without swelling solvents or catalysts showed similar particle geometries, but the amount of recognizable vitrinite (huminite) decreased with increasing level of conversion. For the residues where molybdenum compounds were used, catalyst materials were not recognized. However, sulfide minerals were observed in abundance when $FeSO_4$ was employed as the catalyst precursor in an H_2S:H_2 atmosphere.

Temperature-staged residues from reactions with the Blind Canyon hvAb coal were much different. Mitchell et al. [1977] showed that coals of bituminous rank generate varying amounts of primary vitroplast, which is the plastically deformed remnant of vitrinite. Vitroplast can act as a matrix material for most of the large particle agglomerates found in the high-temperature residues of liquefaction. As conversion increases, vitroplast concentration typically decreases; any remainder is converted to isotropic or anisotropic semicoke as condensation and aromatization reactions occur. These reactions are accompanied by an increase in reflectance. Inspection of the temperature-staged residues from reactions with the Blind Canyon coal supported these observations.

Qualitative observations suggested that reflectance of the remnant vitrinite and/or vitroplast of both coals may vary slightly with changing reaction conditions. Consequently, a series of residues was selected for the measurement of mean random reflectance. As shown in Table 31, reflectance values are compared with the fraction of aromatic carbon (f_a) determined by ^{13}C NMR as discussed in Section 5.3.4, and with total conversion. For each coal random reflectance values of the unreacted coal are compared with those of thermal pretreatment residues (where no swelling solvents were employed) and then to temperature-staged residues (generated with and without both ATTM and swelling solvents).

The influence of pretreatment conditions on reflectance of the residue from the hvAb coal showed a very slight decrease, whereas a significant increase was observed for the subC coal. Similar observations

Table 31. Mean random reflectance of vitrinite and vitroplast in liquefaction residues from reaction of DECS-6 and DECS-1 coals

Sample #	Catalyst	Atmosphere	Reaction Temperature °C	Swelling Solvent	wt% Total Conversion	wt% f_a ^{13}C nmr	Mean Random Reflectance Ro	Standard Deviation
DECS-6 Blind Canyon hvAb								
DECS-6	unreacted coal				0.0	0.598	0.547	0.038
5	none	H_2	275	none	17.7	—	0.521	0.041
20	none	H_2	275/425	none	48.0	0.891	1.256	0.109
23	ATTM	H_2	275/425	none	85.1	0.850	1.194	0.094
34	ATTM	H_2	275/425	Pyridine	90.3	0.871	1.557	0.183
DECS-1 Texas sub C								
DECS-1	unreacted coal				0.0	0.438	0.335	0.034
6	none	H_2	275	none	6.6	—	0.444	0.041
27	none	H_2	275/425	none	53.1	0.850	1.033	0.112
30	ATTM	H_2	275/425	none	78.9	0.850	0.775	0.130
32	ATTM	H_2	275/425	Pyridine	88.8	0.881	1.350	0.189
33	ATTM	H_2	275/425	TBAH	88.9	0.896	1.362	0.214

have been made previously by Mitchell et al. [1977] and Davis et al. [1989]. Temperature-staged residues provided a different and more interesting comparison. For both coals, reflectance of the vitrinite-derived residue components were slightly higher for the thermal (non-catalytic) runs than for the runs with ATTM-impregnated coal. The f_a of the catalytic runs without preswelling were lower than (for DECS-6) or equal to (for DECS-1) that of the non-catalytic residues. When swelling solvents (pyridine and/or TBAH) were employed and as total conversion increased, reflectance and the f_a increased to a maximum. It must be stressed that ^{13}C NMR measurements of f_a were made on the entire residue material (including inertinite, semicoke and mineral matter), whereas reflectance was measured only on the vitrinite-derived components. Nevertheless, as conversion increases the inert coal macerals are concentrated and the reactive macerals which are not converted to liquid products become more condensed and aromatic. The fact that both aromaticity and reflectance were lower in the temperature-staged residues following impregnation of ATTM, strongly suggests that the catalyst was performing at least one of the function for which it was applied, i.e., preventing aromatic condensation.

8.3.2. Catalyst Dispersion in Liquefaction Residues

Optical microscopy of the liquefaction residues revealed little information about the catalyst materials, i.e., their presence and associations with the organic and inorganic remnants. Clearly, inspection

of the residues to determine these association is the only means possible of determining whether a catalyst remained dispersed, or whether it agglomerated into a solid mass or was incorporated into an organic agglomerate. Any one of these situation could result in a partial loss of catalytic activity during processing. For example, catalyst material could be well dispersed in that portion of the organic residue that had become plastic during reaction, and although the catalyst maintains contact with the organic fraction it may be shielded from the solvent and hydrogen, thus becoming ineffective. Therefore, in this portion of the study both pretreatment and temperature-staged residues were inspected with the SEM and electron microprobe in an attempt to locate catalyst materials.

Residues of both the subC and hvAb coals impregnated with molybdenum catalysts (ATTM and $Mo(CO)_6$) were selected for this investigation (Table 32). Both pretreatment and temperature-staged runs with and without preswelling solvents were evaluated. In general, discrete (≈5 μm) particles of catalyst were found in all 275°C residues of the hvAb coal (DECS-6) regardless of catalyst type or preswelling solvent. As seen in Figure 25, catalyst fragments of ATTM appear to be incorporated within coal particles in the pretreatment residue of DECS-6 that was preswollen in TBAH (sample #14). Catalyst material most probably penetrated into the particle interior during the plastic deformation of the TBAH reaction product. However, catalyst was only found sporadically and unevenly dispersed through the residue during X-ray mapping and SEM-EDS evaluations. When preswelling was not performed, catalyst material also was found as discrete

Table 32. Liquefaction samples selected for SEM-EDS evaluation and electron microprobe analysis

Sample #	Catalyst	Gas Atmosphere	Reaction Temperature	Swelling Solvent	wt% conversion	Mode of Analysis	Summary of Catalyst Distribution
	DECS-6						
1	$Mo(CO)_6$	$H_2S:H_2$	275	none	26.6	EP	Discrete Particles
26	$Mo(CO)_6$	$H_2S:H_2$	275/425	none	86.0	SEM/EP	Even Distribution
14	ATTM	H_2	275	TBAH	23.7	SEM/EP	Discrete Particles
23	ATTM	H_2	275/425	none	85.1	SEM	Discrete Particles
34	ATTM	H_2	275/425	Pyridine	90.3	SEM/EP	Even Distribution
--	ATTM	H_2	275	none	25.0	SEM	Discrete Particles
	DECS-1						
18	$Mo(CO)_6$	$H_2S:H_2$	275	TBAH	15.3	EP/SEM	Even Distribution on Particle Edges
31	$Mo(CO)_6$	$H_2S:H_2$	275/425	none	80.1	SEM	No Mo Found
13	ATTM	H_2	275	TBAH	18.7	EP/SEM	No Mo Found
30	ATTM	H_2	275/425	none	78.9	SEM	Discrete Particles
32	ATTM	H_2	275/425	Pyridine	88.8	EP/SEM	Even Distribution

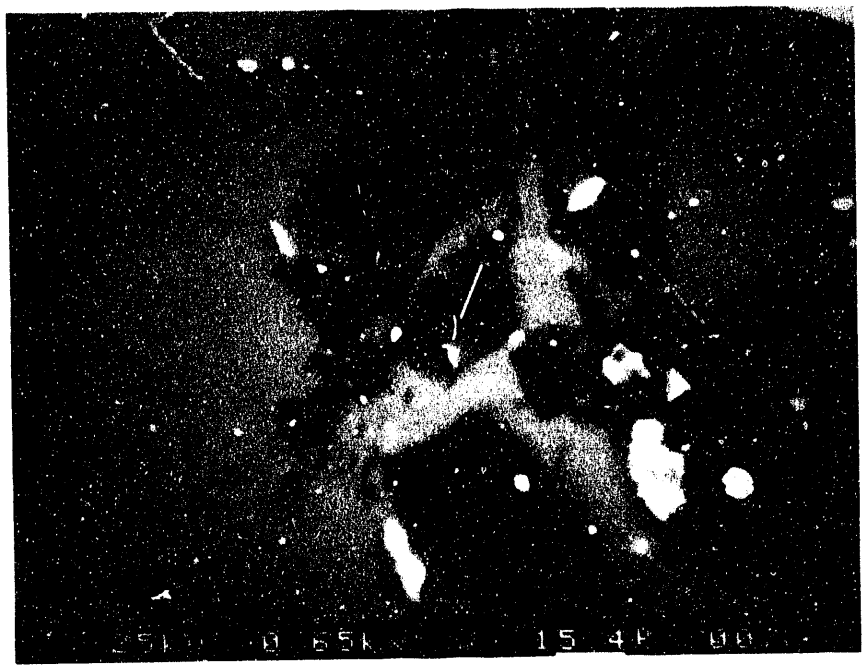

Figure 25 - SEM Micrograph of Metallic Particle (arrow) Giving Strong Mo and S Peaks in the EDS and Embedded within the Boundary of an Organic Residue Particle Following Reaction at 275°C of TBAH-treated, ATTM-Impregnated Blind Canyon Coal

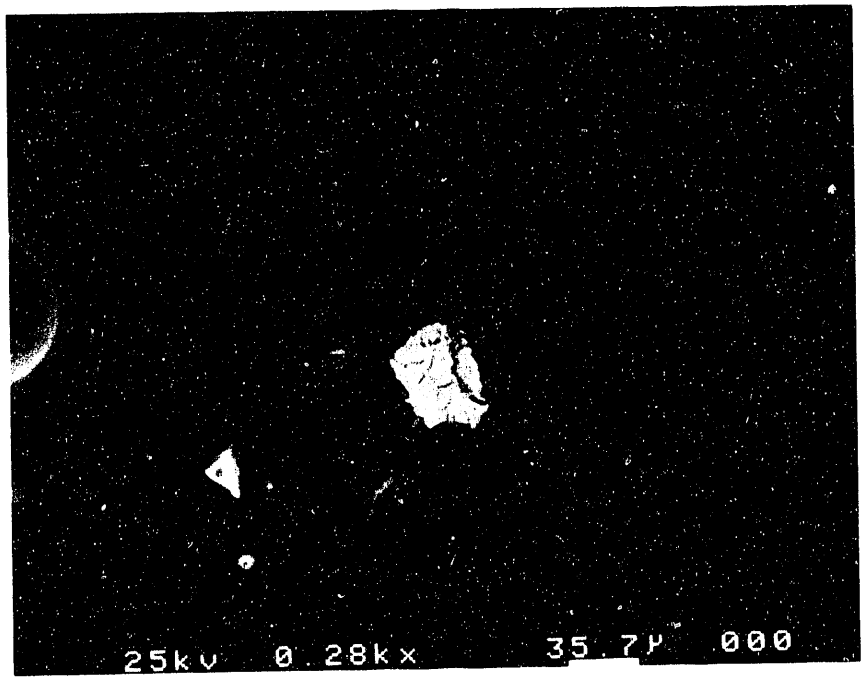

Figure 26 - SEM Micrograph of Central Metallic Particle Giving Only Mo and S Peaks Unassociated with the Organic Residue Following Temperature-staged Reaction of ATTM-Impregnated Blind Canyon Coal

particles, but of perhaps slightly larger particle size (≈10 μm) and either unassociated with coal particles or along particle edges as has been observed previously [Davis et al., 1989]. The same observation was made when $Mo(CO)_6$ was used under pretreatment conditions (sample #1), except catalyst fragments were rounded instead of plate-like (as with the ATTM) and on the order of 5-10 μm.

Residue materials from temperature-staged reaction of the hvAb coal impregnated with ATTM and not preswollen (sample #23) predominantly gave X-ray energy peaks for C, S, Ca, Al, Si and Fe. Broadening of the sulfur peak was minimal, suggesting that Mo was not present or of very low concentration with respect to the residue particle agglomerates. Figure 26 exhibits a 35-40 μm size particle of molybdenum sulfide that was found in this samples. The morphology of the particle was very similar to that observed in other work [Davis et al., 1989] for sulfided ammonium molybdate that had formed as surface deposits during dehydration following coal impregnation. This particle may or may not have been associated with a coal surface, but it definitely represents a very localized occurrence that would have much less catalytic effect on direct coal hydrogenation compared with a more disseminated form.

SEM-EDS examination of the temperature-staged residue of DECS-6 (sample #34) preswollen in pyridine and impregnated with ATTM showed that the groundmass of most particles was carbonaceous with included mineral matter. A relatively high concentration of sulfur with a broad peak was observed for most isolated organic areas, suggesting that Mo may be

present. Figure 29 is an X-ray map of some of the organic matrix from this sample obtained from the EP. It shows the uniform distribution of both Mo and S throughout the matrix and the low concentration of Fe. Quantitative analysis of several organic areas within this sample gave a mean Mo concentration of 10.3 wt.% and of 5.1 wt.% S. With respect to MoS_2, which is the presumed reaction product of ATTM during liquefaction, this sample was deficient in sulfur, i.e., S:Mo atomic ratio of 1.49.

A uniform dispersion of Mo was observed for the temperature-staged reaction of DECS-6 which was unswollen and impregnated with $Mo(CO)_6$ (sample #26). The reaction was conducted in a $H_2S:H_2$ atmosphere. Figure 28 exhibits a somewhat lower concentration of molybdenum throughout the organic matrix than was found for the ATTM/pyridine sample, but dispersion appeared uniform. Measured concentration of Mo (5.8 wt.%) and S (4.0 wt.%) for the organic material under the cross in Figure 28, gives a S:Mo ratio of 2.06, or basically molybdenum disulfide. The full implications of introducing H_2S into the reaction vessel thus is clear, although there can be no real assurance that the Mo and S were directly bonded (Fe or Ca are both present). In fact there is some evidence that radicals formed from H_2S may react with other mineral and organic components. For the DECS-6 sample, SEM-EDS evaluation of the $Mo(CO)_6$ samples showed a relatively large amount of pyrrhotite, suggesting that reaction has occurred with Fe ions associated with the organic portion of the coal or the clays.

In comparison to the hvAb coal, both pretreatment and temperature-staged residues from $Mo(CO)_6$-impregnated Texas subC (DECS-1) coal showed

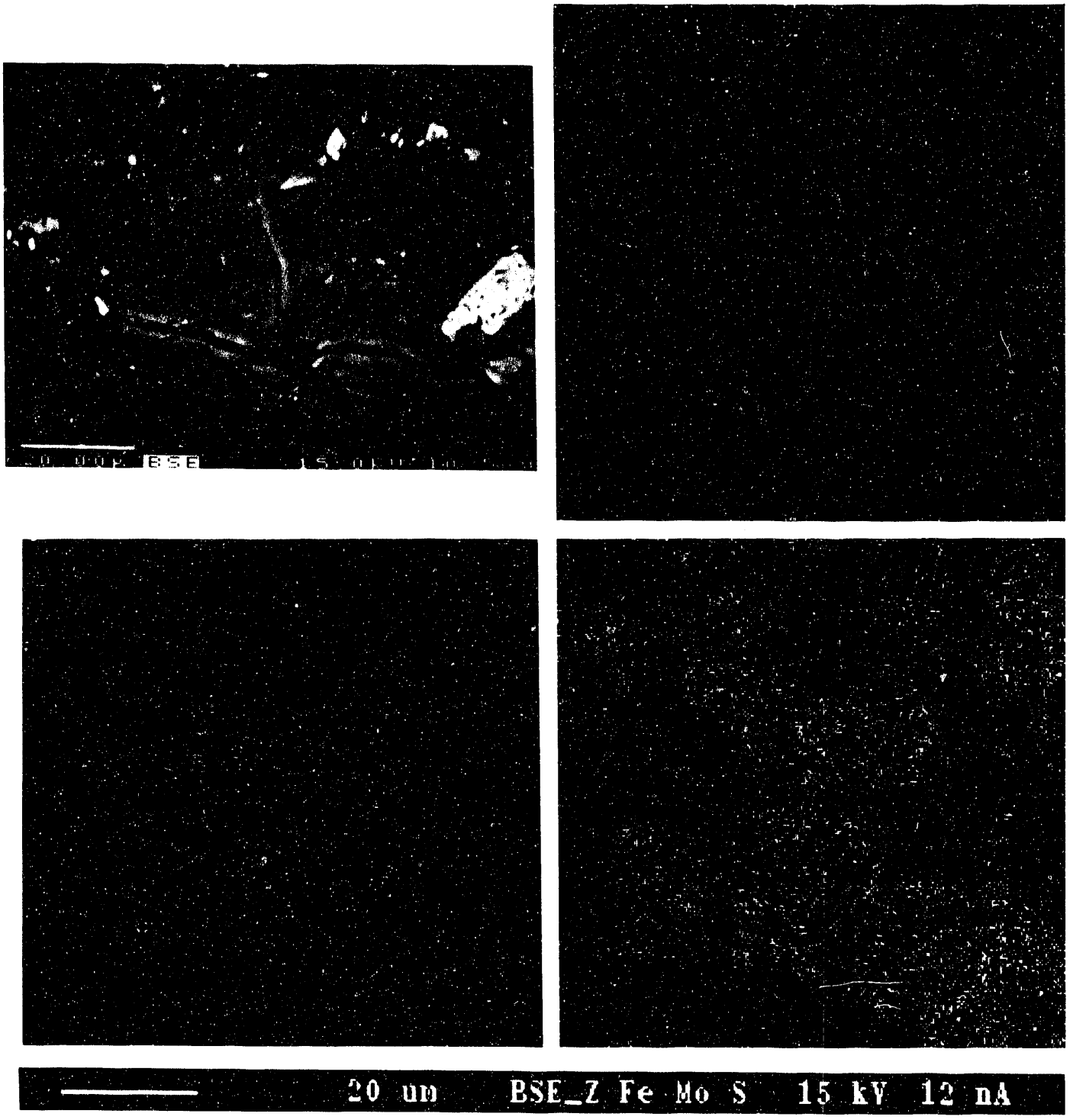

Figure 29 - X-ray Map of Blind Canyon Residue Particle Following Temperature-staged Reaction in Presence of ATTM and Preswollen in Pyridine 1) Upper Left- Backscatter Image of Coal Particle, 2) Upper Right-Iron Map, 3) Lower Left-Molybdenum Map, 4) Lower Right-Sulfur Map

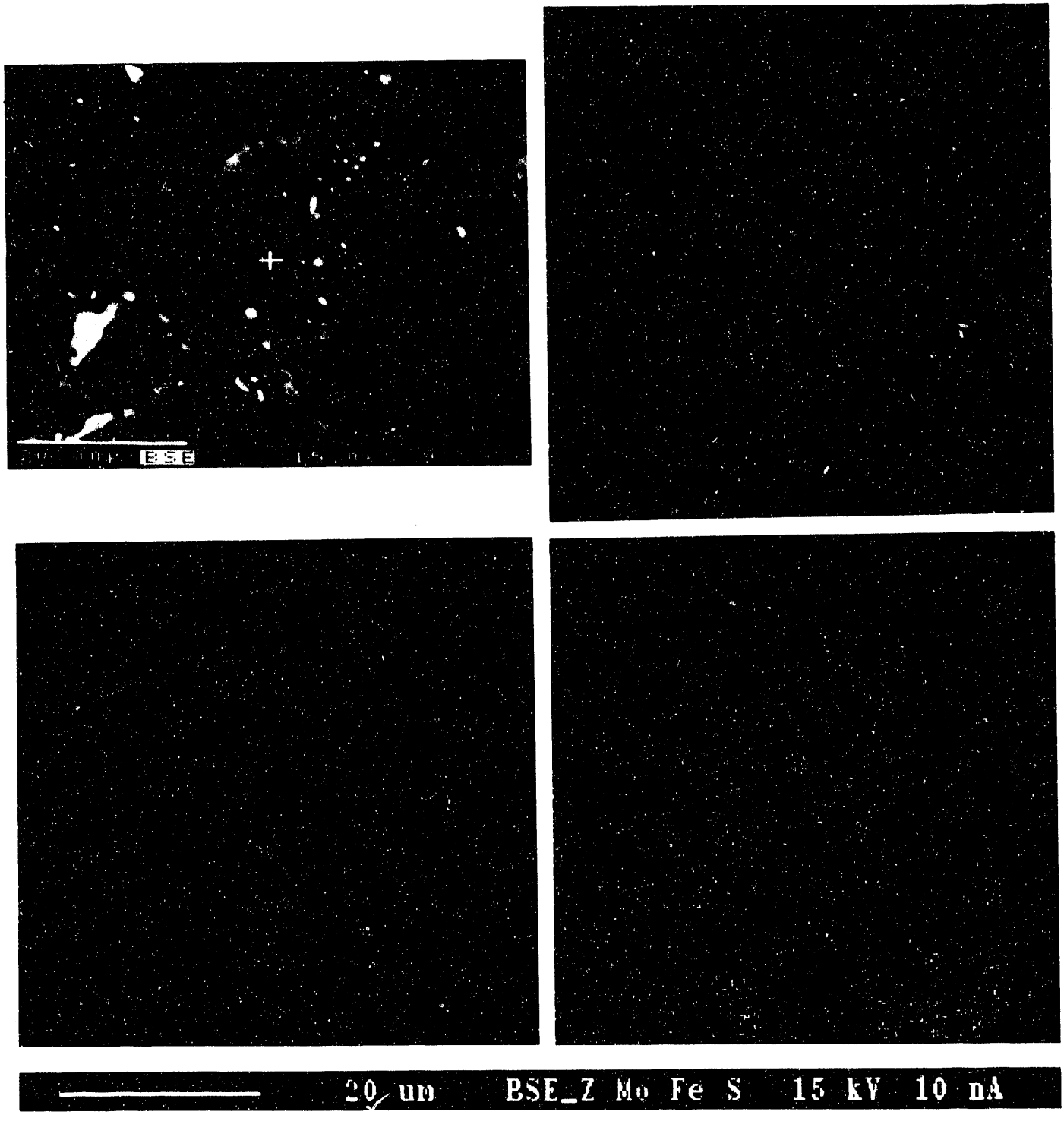

Figure 28 - X-ray Map of Particle of Blind Canyon Residue Following Temperature-staged Reaction in Presence of $Mo(CO)_6$ 1) Upper Left-Backscatter Image of Coal Particle, 2) Upper Right-Molybdenum Map, 3) Lower Left-Iron Map, 4) Lower Right-Sulfur Map

fairly high concentrations of Ca and S in most particles. Particulate $CaSO_4$ was not observed in the pretreatment residues (sample #18) which had been preswollen in TBAH, but remnant coal particles in the residue gave a strong and uniform S peak when tested with EDS. The existence of uniformly high sulfur concentrations was confirmed by X-ray mapping and microanalysis. It was further observed that the catalyst (Mo) had impregnated 3-6 μm into the outer edge of some coal particles, whereas others were devoid of Mo. Microanalyses of Mo and S concentrations at the particle edge compared with the particle interior (1.38 vs 0.27 wt.% Mo and 1.82 vs 0.16 wt.% S, respectively) showed that not only was molybdenum concentration higher, but that there was also a stoichiometric excess of sulfur at the particle edge (3.95 vs 1.83 S:Mo atomic ratio). Thus, it seems reasonable that radicals formed from H_2S may be reacting with some functional groups in the organic fraction of the coal and any available Ca and Fe ions in addition to sulfiding the catalyst.

It is interesting that Mo could not be located in the temperature-staged residue (sample #31) of DECS-1 impregnated with $Mo(CO)_6$; either it formed into relatively large discrete particles which were not located during the investigation or, as suggested in Section 3.2.4, perhaps the catalyst volatilized during removal of the pentane carrier solvent. The groundmass of the large agglomerates found in this residue consistently gave S, Ca, Al and Si peaks. In addition, $CaSO_4$ was commonly found as discrete ≈1 μm size particles within the agglomerates.

As was found with the hvAb coal, impregnation of ATTM with and

without swelling solvents mostly results in discrete particles of catalyst separate from the coal particles in pretreatment runs and bound within particle agglomerates along with coal mineral matter in the temperature-staged residues. However, as with the Blind Canyon coal, the Texas subC that was first swollen in pyridine showed a better distribution of the ATTM catalyst (sample #32). Figure 27 shows the X-ray map of a typical remnant coal particle following temperature-staged liquefaction. The entire coal particle highlighted by the dense distribution of sulfur, whereas the iron and molybdenum maps were sparsely populated. In fact the Mo map only shows clear distribution on three sides and the particle interior has little associated Mo. Thus, although this sample shows evidence of impregnation by the ATTM catalyst, the distribution is uneven. Microanalysis of this particle gave mean concentrations for Mo= 6.60 wt.%, S= 4.45 wt.%, Fe= 1.08 wt.% and Ca= 7.84 wt.%. A S:Mo atomic ratio for this particle has no significance because of the presence of $CaSO_4$.

8.4. SUMMARY AND CONCLUSIONS

THF-insoluble residues from 35 liquefaction runs (pretreatment and temperature-staged) were systematically characterized using optical and electron optical techniques. Qualitative optical microscopy was employed to characterize the effects of run conditions on the organic residues of each coal following pretreatment conditions, whereas (quantitative) reflectance measurements were made on temperature-staged residues for comparison with changes in fractional aromaticity (f_a) determined from ^{13}C NMR (CPMAS). SEM and the electron microprobe were used to identify

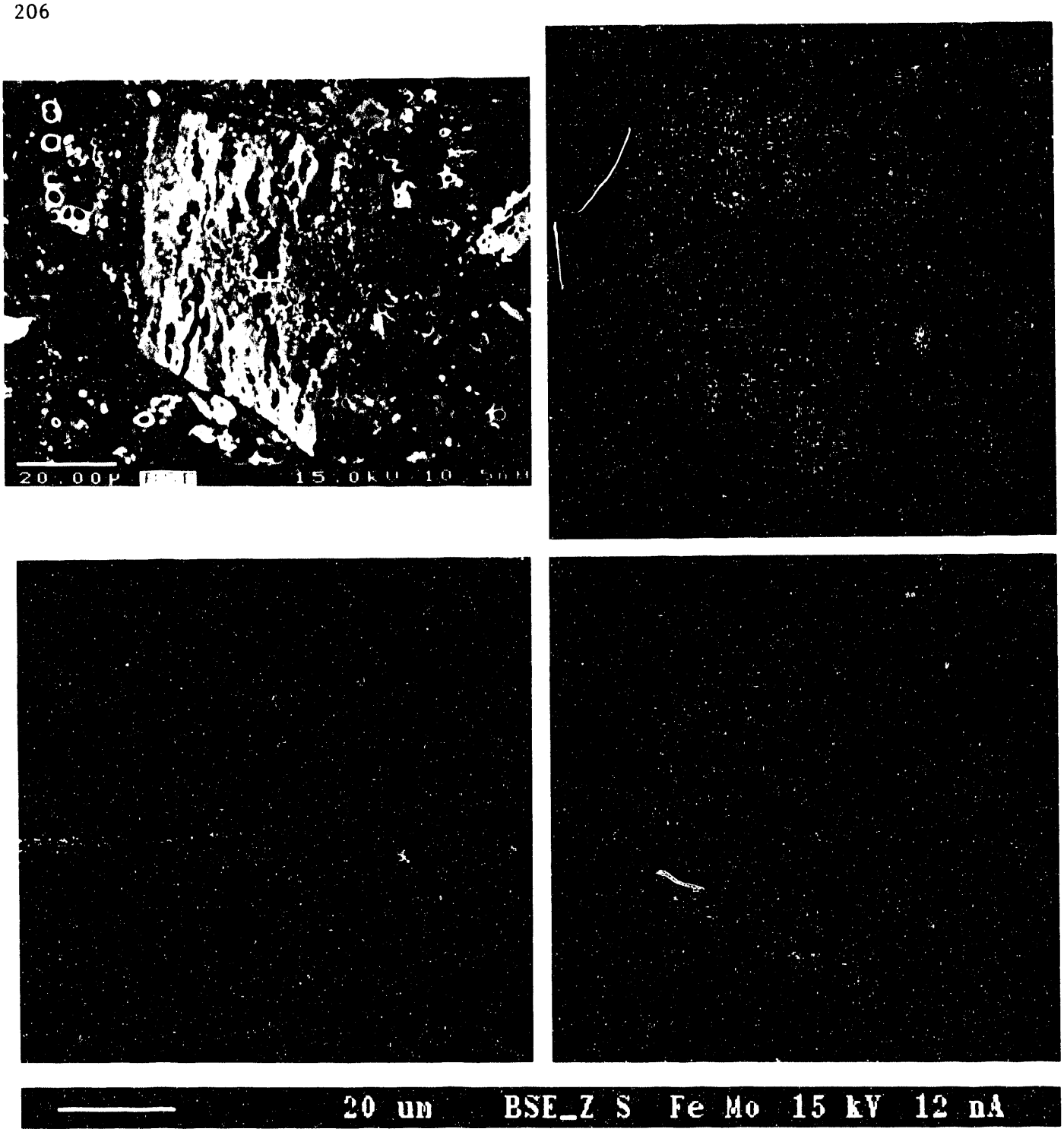

Figure 27 - X-ray Map of Particle of Texas SubC Residue Following Temperature staged Reaction in Presence of ATIM and Preswelling in Pyridine 1) Upper left Backscatter Image of Coal Particle, 2) Upper Right Sulfur Map, 3) lower Left-Iron Map, 4) lower Right Molybdenum Map

catalyst remnants and their associations with the organic portion of residues.

Preswelling solvents TBAH and/or pyridine had the most profound effect on conversion and product yields under pretreatment conditions. Residues of thermal pretreatment runs with the Texas subC coal preswollen in TBAH exhibited large-scale swelling characteristics. However, following reaction, the THF-insoluble residue was composed mostly of large agglomerated particles, cemented by a low-reflecting, fine-grained matrix. Particles were less well agglomerated when $Fe(CO)_5$ was used as a catalyst, perhaps contributing to a relative high total conversion. Addition of the $Mo(CO)_6$ catalyst had little positive effect on conversion compared with thermal pretreatment and was accompanied by an increase in particle agglomeration and absence of the low-reflecting matrix. An intermediate level of agglomeration, presence of the matrix material and total conversion accompanied the use of ATTM. Agglomeration of individual subbituminous coal particles represented some evidence for particle-edge plasticity induced by the use of TBAH.

Particle agglomeration and clear signs of plasticity were observed from thermal pretreatment runs of the Blind Canyon coal. As discussed in Section 6, preswelling the coal in TBAH resulted in particle-edge reactions (reaction front), leaving behind a low-reflecting, pitch-like material responsible for particle agglomeration. During pretreatment liquefaction, the TBAH reaction product caused particle agglomeration. When molybdenum catalysts were employed agglomeration was enhanced. With

respect to other swelling solvents, TBAH with molybdenum catalysts gave an unpredictably low conversion. This could be in response to the TBAH reaction product inhibiting mass transport, e.g., catalyst impregnation as well as solvent and hydrogen interaction with the reacting coal.

Swelling of the two coals with pyridine resulted in relatively less agglomeration and particle plasticity and resulted in higher total conversion. For the Texas subC coal, the main physical influence of pyridine was a reduction in residue particle size, whereas for the Blind Canyon coal some of the agglomeration from the swelling procedure was maintained in the pretreatment residues. In some cases the original pyridine-soluble fraction was converted to an insoluble component during pretreatment liquefaction.

Because of the relatively high conversion attained during temperature-staged liquefaction, little qualitative information regarding the effects of reaction conditions could be resolved. However, measurement of random reflectance of vitrinite and vitrinite remnants within these residues revealed that those of the thermal non-catalytic runs were slightly higher in reflectance than for runs where ATTM was used, suggesting that the catalyst does indeed reduce aromatic condensation. The fraction of aromatic (f_a, ^{13}C NMR) also increased with increasing reflectance. As swelling solvents were employed, conversion increased and the f_a and reflectance reached a maximum.

Discrete particles of catalysts were found in all pretreatment residues of the Blind Canyon coal regardless of catalyst type (ATTM or

$Mo(CO)_6$) or preswelling solvent (none or TBAH). Molybdenum sulfide particles from ATTM were observed incorporated within the organic matrix when TBAH was used as a swelling solvent, whereas when no solvent was employed catalyst particles were found individually or associated with the edges of remnant coal-particles. Molybdenum sulfide particles were also observed along particle edges when $Mo(CO)_6$ was used under pretreatment conditions, except catalyst particle size was comparatively smaller than those observed from runs using ATTM.

Remnants of ATTM were found as large discrete particles following temperature-staged reaction runs where no swelling solvents were employed. However, swelling in pyridine had a significant influence on catalyst dispersion during temperature-staged reaction. X-ray maps of the remnants of organic agglomerates in the Blind Canyon residues show an even distribution of Mo and S. With respect to MoS_2 the catalyst was deficient in sulfur. Dispersed Mo was also observed in a temperature-staged residue of unswollen Blind Canyon coal reacted in the presence of $Mo(CO)_6$ and H_2S:H_2. Microanalysis of areas within the remnant organic fraction suggests that the Mo may be fully sulfided to MoS_2, demonstrating the importance of the presence of H_2S during liquefaction. Observations of $Fe_{1-x}S$ in the residue also suggests that H_2S radicals may be reacting with free Fe ions within the Blind Canyon coal as well.

Impregnation of the TBAH preswollen Texas subC coal with $Mo(CO)_6$ and subsequent reaction under pretreatment conditions in the presence of H_2S revealed a partial but uneven impregnation of the molybdenum catalyst along

particle edges and possible evidence for reaction of H_2S radicals with functional groups within the organic fraction. Without preswelling, catalyst material was not located in the temperature-staged residues of the Texas subC coal, although significant concentrations of sulfur and calcium sulfate were identified.

Impregnation of the Texas subC coal with ATTM in the presence of TBAH (275°C) or no solvent (275:425°C) resulted in the presence of discrete particles of catalyst separate from coal particles under pretreatment conditions or bound within agglomerates following temperature-staged liquefaction. However, just as was observed for the Blind Canyon coal, when pyridine was introduced as a preswelling solvent, a fairly even distribution of Mo was observed throughout the organic fraction.

9. INFLUENCE OF SAMPLE STORAGE ON LIQUEFACTION PROPERTIES

9.1. INTRODUCTION

Although there are relatively few data on the influence of oxidation during storage upon liquefaction conversion yields and product distribution, the subject is one which has raised concern about the comparability of experimental data obtained over time using stored samples. The samples used in this program have been supplied from the DOE Coal Sample Suite maintained as part of the Penn State Coal Sample Bank under Contract DE-AC22-88PC79997. Monitoring of container atmospheres under that contract revealed that significant amounts of oxygen were leaking into containers which had been sealed under argon. As a result, in December 1989, sample collection and storage procedures were modified. In particular, multilaminate bags were used to store coal samples at all sample sizes instead of plastic bags themselves sealed within metal cans. The multilaminate bags have proved to be very effective in maintaining an inert atmosphere [Davis et al., 1989; Glick et al., 1991].

The work reported here was undertaken to investigate the extent of changes in liquefaction parameters which can occur over relatively long periods of storage.

9.2. EXPERIMENTAL

The coal selected for this study was DECS-12 (PSOC-1549), a hvAb Pittsburgh seam coal from Greene County, PA, collected July 25, 1990.

Liquefaction experiments were undertaken using the same tubing-bomb reactors employed for all of the experimentation performed under this

contract. Details of the equipment and product work-up procedures have been given in Section 3. Runs were made at 350°C for 30 min at 1000 psig hydrogen with tetralin as solvent and approximately 2 g coal. These conditions were deliberately made as simple (single stage, no catalyst) as possible and relatively mild in order to optimize any differences induced by oxidation at normal laboratory temperatures.

An initial liquefaction experiment was performed on September 24, 1990 on minus 60 mesh material which had been sealed until that time in argon in a multilaminate bag. Additional representative splits of material were stored (at minus 20 mesh) until a second period of testing was undertaken; splits stored in argon in multilaminate bags were again tested on January 29, 1991, as were splits which had been exposed to the atmosphere. The initial testing was done in quadruplicate and the January 1991 testing was in duplicate.

9.3. RESULTS AND DISCUSSION

The results are presented in Table 33. They show that there has been no deterioration in total conversion of the coal stored in the foil bags. Over the same period, a sample exposed to the atmosphere in the laboratory had undergone a relatively minor but nevertheless significant decrease in total conversion (from 43.1 to 40.5%). No significant changes in product distribution were noted. Together with the observation cited above [Davis et al., 1989b; Glick et al., 1991], that the multilaminate bags are effective in maintaining an inert atmosphere for stored coal samples, these

results are reassuring that coals stored in this fashion can be used for comparative liquefaction testing over a reasonably extended timeframe.

Table 33. Liquefaction of stored Coals

Experiment	Total Conversion % (daf)	Asphaltene %	Oil + Gas %*
Initial (4/24/90)	43.12 ± 0.58	41.20 ± 0.74	1.92 ± 0.86
Repeat, Stored in Foil Bag (1/29/91)	45.3	41.7	3.6
Repeat, Exposed to Atmosphere (1/29/91)	40.5	42.5	-2.0

*By Difference

10. EVALUATION OF MATERIALS FROM OTHER DOE PROGRAMS

10.1 INTRODUCTION

This facet of our investigation, conducted as Task 6, was designed to promote cooperation between our program and other Advanced Research and DOE-sponsored research efforts in catalytic coal hydrogenation. Through this cooperative effort our program has contributed microscopic characterization techniques for those contractors involved in generating materials in larger scale hydrogenation experiments than our own, or that have been involved in catalyst dispersion/impregnation research.

A dialogue was established with personnel at the Wilsonville Pilot Plant (Mr. Charles Cantrell) and with Hydrocarbons Research Incorporated (Mr. Alfred Commolli, HRI) to learn more about recent and planned operations/experimentation and to investigate the potential for a collaborative effort. Our involvement with Wilsonville concerned problems that occurred during their Runs 258 and 260.

In addition to the aforementioned characterization of Wilsonville materials, three series of samples were submitted to us by Hydrocarbon Research, Inc. (HRI) for evaluation in connection with their CTSL Catalytic two-stage liquefaction process under DOE Contract DE-AC22-88PC88818.

10.2 VESSEL PLUGS AND DEPOSITS FROM WILSONVILLE RUN 258

Run 258 began on May 19, 1989 at the Wilsonville pilot plant in the thermal/catalytic CC-ITSL mode with a feed of Spring Creek subbituminous coal, 4.0 wt% (MF coal) of a disposable Fe_2O_3 catalyst, and with ash recycling [Robbins et al., 1990]. Dimethyldisulfide (DMDS) was injected into both first- (thermal) and second- stage (catalytic) reactors to

provide adequate sulfidization of the disposable (Fe_2O_3) catalyst which circulates throughout the system and for the supported catalyst (Shell 324 1/16" Ni/Mo) found only in the second-stage reactor. The interstage separator (V1258), which is employed to remove light oils and gas before further processing, was used throughout the run. Spring Creek coal (Anderson and Dietz seams) was charged for about three months and then was replaced on September 14, 1989 with the Black Thunder subbituminous coal (Wyodak and Anderson seams). Run 258 was completed on November 8, 1989.

During the course of Run 258 many significant outages were experienced due to plugging of the pipe connecting the thermal reactor (R1235) and the separator vessel (V1258), and to solids build up in these vessels. A plugged separator vessel or pipe restriction led to unscheduled shutdown of the Wilsonville Pilot Plant and resulted in cleaning and maintenance of the entire reactor section.

10.2.1. Results and Discussion

Samples of plug and deposit materials were received at Penn State for characterization by optical microscopy and XRD. Table 34 describes the two feed coals and five deposit samples provided, and gives a brief description of test results. Figure 30 shows the approximate locations of deposit materials removed from the plant. Samples of deposit materials were obtained after about two months of operation with the Spring Creek coal [reactor wall scale (SN97680) and separator vessel plug (SN97678)] and following about two months of operation with the Black Thunder coal [reactor solids (SN2671), separator vessel plug (SN2700) and a pipe restriction sample found between the R1235 and V1258 vessels (SN5134)].

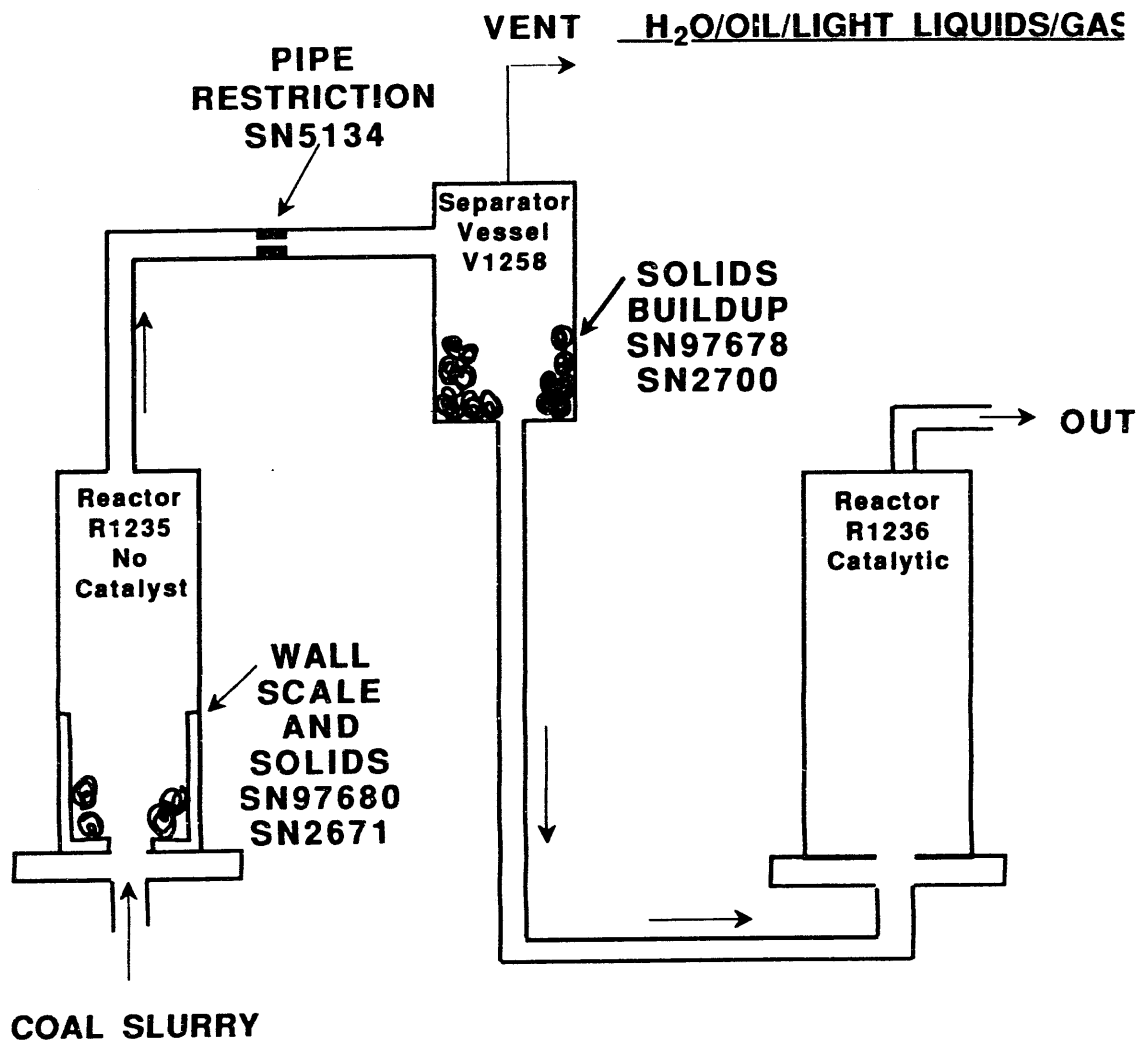

Figure 30 - Schematic Showing Location of Solid Deposits In Wilsonville Pilot Plant During Run 258

Both feed coals were prepared for general qualitative microscopy. The Spring Creek (SN96795) and Black Thunder (SN2053) are fairly typical subbituminous coals in that they are composed predominantly of the huminite (vitrinite) maceral. There is about 2 vol.% inertinite (fusinite, sclerotinite and semifusinite) and <1 vol.% liptinite (mainly sporinite and cutinite). Some minor contamination (<0.1%) of the feed coals with bituminous coals and with coke breeze was observed.

Because most subbituminous coals usually have a high concentration of organically bound calcium, which in the past has contributed to the formation of reactor solids at Wilsonville [Walker et al., 1975], all samples were tested for the presence of calcium carbonate. Table 34 shows the response obtained when -60 mesh (-250 μm) material was reacted with 10% HCl. All of the Spring Creek deposits reacted violently, but only two of the Black Thunder deposits reacted slightly at this particle size. When both of these samples were crushed to -200 mesh (-74 μm) there was a more profuse reaction, suggesting that the calcium carbonate may be incorporated within another phase.

In general, the deposit samples have a high ash content (Table 34). From XRD and optical microscopy pyrrhotite ($Fe_{1-x}S$), calcite ($CaCO_3$), sodium chloride (NaCl), and quartz (SiO_2) are the dominant mineral phases present, although their relative concentrations vary among samples. Minerals that were not observed from XRD include sulfates (anhydrite, bassanite or gypsum), pyrite (FeS_2) or troilite (FeS), vaterite ($CaCO_3$), hematite (Fe_2O_3), or clays. Most of these minerals have been observed in previous investigations of reactor and process solids obtained from Wilsonville

Table 34. Sample description and results

Sample Description	Wilsonville SN	Date Collected	Coal	Reaction to 10% HCl	wt% Ash	X-ray Analysis Major Minerals
Reactor (R1235) Wall Scale	97680	7/18/89	Spring Creek	Profuse	70.6	Calcite > Pyrrhotite > NaCl > +
Vessel Plug (V1258)	97678	7/17/89	Spring Creek	Profuse	86.7	Pyrrhotite > Calcite > Quartz
Reactor (R1235) Solid	2671	11/17/89	Black Thunder	Slight	61.2	Calcite > Pyrrhotite > Quartz
Vessel (V1258) Solid (Plug)	2700	11/17/89	Black Thunder	None	28.5	Pyrrhotite > Quartz
Pipe Plug (between R1235-V1258)	5134	11/17/89	Black Thunder	Slight	57.6	Calcite = Pyrrhotite = NaCl > Quartz
Spring Creek Coal	96795	6/29/89	Spring Creek	None	5.86*	--
Black Thunder Coal	2053	10/27/89	Black Thunder	None	7.17*	--

+ ~10% Unidentified
* Data from Robbins et al., [1990]

[Walker et al., 1975]. The fact that they are not found may be an effect of ash recycling and to more efficient solids separation. The indication of NaCl is perplexing in that both coals used during the run have chlorine levels less than 0.01% [Robbins et al., 1990] and there is no other source for chlorine other than contamination.

Individually, the deposit materials found during operation with the Spring Creek coal are somewhat different than those taken from the Black Thunder operating period. A description of each sample follows.

10.2.1.1. Spring Creek Deposits

A reactor (R1235) wall-scale sample (SN97680) removed during operation with the Spring Creek coal is a rather hard, plate-like material. Several individual plates were mounted and polished to expose a cross-sectional view under the optical microscope. Most of the sample is composed of fine grained particles (<2 μm) which include pyrrhotite, anisotropic semicoke, granular residue (<1 μm), and fragments of coal-derived inertinite in a matrix of process-derived calcium carbonate. There are zones of high carbonate content, like those seen in Plate IXa, which are oriented parallel to the reactor wall and that are separated by the more heterogeneous or granular zones just described.

The separator vessel plug (SN97678) was received in solvent extracted form and contained friable particles of <8mm diameter. This sample consists of rather large (>200 μm) reactor-solid particles (i.e., spherical pellets) which are composed of aggregates and individual particles of pyrrhotite, secondary vitroplast, anisotropic semicoke, coal-derived mineral matter (twinned calcite [Wakeley et al., 1979] and quartz) and

inertinite in a matrix of process-derived calcium carbonate. Pyrrhotite forms a larger proportion of this sample (Plate IXb), and from XRD (Table 34) is present in relatively higher concentration than calcite. Also observed in this sample is a coke breeze contaminant and partially reacted coal particles (mainly huminite). The coke breeze is from metallurgical coke and probably was introduced with the coal feed. This problem has been reported previously for other Wilsonville feed coals [Walker et al., 1975].

From these observations, the deposits formed during operation with the Spring Creek coal appears to be dominated by the presence of calcite. Also, because there is almost no pyrite observed in the Spring Creek coal [Robbins et al., 1990], we conclude that the rather high concentration of pyrrhotite results from the sulfidization and deposition of the disposable Fe_2O_3 catalyst.

10.2.1.2. Black Thunder Deposits

Samples of the reactor (SN2671) and separator vessel (SN2700) deposit materials removed after operations with the Black Thunder coal were received as both large lumps (exceeding 25mm) and fine particles (<1mm). In each case, subsamples of each size class were prepared for optical microscopy.

The reactor deposit sample (SN2671) is dominated by fairly large pyrrhotite aggregates (>50 μm), like that seen in Plate IXc, in a matrix of mesophase-derived semicoke. The pyrrhotite aggregates average about 140 μm and range in size from 40 to 290 μm. Approximately 60% of these aggregates exceed 100 μm, which is much larger than the iron oxide feed material (-74 μm). Their presence suggests a mechanism of aggregation, or

PLATE IX
FIGURE DESCRIPTION

a. Calcium carbonate layer (Ca) separated by heterogeneous layers composed of pyrrhotite and semicoke in a carbonate matrix, as seen in the reactor (R1235) wall-scale deposit (SN97680) formed during operations with Spring Creek coal. Plane polarized reflected light.

b. Relatively large crystals of pyrrhotite associated with carbonate, as observed in the separator vessel deposit (SN97678, Spring Creek coal). Partially crossed-polarized reflected light.

c. Relatively small aggregates of pyrrhotite (reactor solids) embedded in a matrix of mesophase-derived carbon, as seen in the Black Thunder reactor deposit (SN2671). Plane polarized, reflected light.

d. Mesophase-derived carbon with large anisotropic domains apparently cementing two particles of mesophase-derived carbon of smaller mosaic size (SN2700, Black Thunder coal). Partially crossed-polarized reflected light.

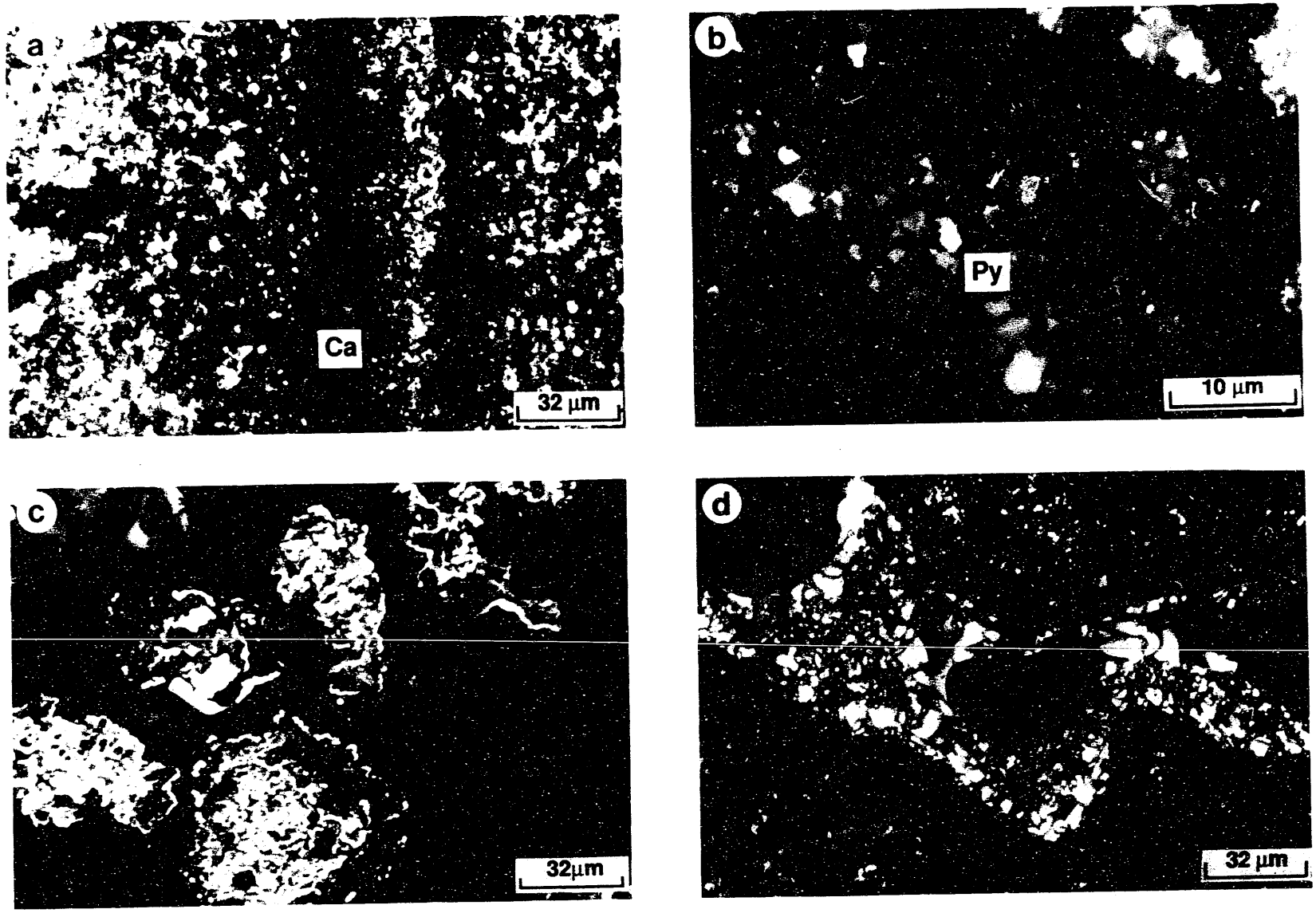

Plate IX

crystallization which can account for their retention in the reactor and separator vessel.

Sizes of individual isochromatic areas within the mesophase-derived carbon matrix range from submicron (common) to 100's of microns (rare). Incorporated into the matrix are coal-derived inertinite and minerals as well as the coke breeze contaminant. Additionally, XRD of this sample shows a fairly high concentration of calcite. However, inspection by optical microscopy failed to locate significant areas of carbonate material like that seen in Plate IXa. This observation and the reaction of this material with 10% HCl at finer particle sizes leads us to suspect that the carbonate, in part, may be intimately associated with the mesophase-derived carbon.

In comparison to previous samples, the Black Thunder separator vessel deposit (SN2700) was found to be of low ash content (28.5%, Table 34) and to consist predominantly of mesophase-derived semicoke. As seen in the top and bottom portions of Plate IXd, the carbon has a mean mosaic size of <3 μm. In the larger particles, this carbonaceous matrix appears to be cemented by a mesophase-derived carbon of much greater mean domain size, as seen in the center of Plate IXd. Also, included within the matrix are pyrrhotite, quartz, secondary vitroplast, inertinite and the coke breeze contaminant. Coke breeze is found in relatively higher concentration (about 2 vol.%) in this sample. Plate Xa shows the much higher reflectance of the coke breeze compared to the mesophase-derived matrix material.

Finally, a section of pipe containing a deposit was received for study. Unfortunately, the restriction material could not be observed in

situ. However, from our optical investigation of material removed from inside the pipe we have been able to identify a sequence of depositional events. As seen in Plate Xb, pyrrhotite crystals compose the initial layer, having been formed in place by sulfidization of the steel pipe or perhaps by deposition. Deposited upon this inner layer is an 85 μm layer of crystalline carbonate (Plate Xb). Growth of the carbonate layer terminates in a heterogeneous layer of submicron isotropic organic material (vitroplast and semicoke) in a carbonate matrix. After this the exact order of deposition becomes difficult to interpret, but subsequent layers are composed of mesophase-derived carbon of various domain sizes ranging from 1-20 μm and with inclusions of coal-derived minerals and organics.

From these observations, the Black Thunder deposit materials appears to have resulted largely from retrogressive reactions in which mesophase-derived carbon was deposited along with process-derived calcite, pyrrhotite aggregates, and coal-derived mineral and organic inerts. There is some evidence of a number of depositional events in which mesophase-derived carbon was produced in the reactor and perhaps carried into the separator vessel. Subsequent formation of mesophase cemented the particulate reactor solids into large deposits within both vessels. A thin layer of carbonate was only observed in the pipe connecting the reactor and separator vessel; however, calcite was detected by XRD in relatively high concentration in both the pipe plug and the reactor deposit. This suggests that the carbonate may be intimately mixed with the organic materials in these samples. The relatively large particle size and mass of the pyrrhotite aggregates and the coke breeze contaminant may be one reason for their

PLATE X
FIGURE DESCRIPTION

a. High-reflecting metallurgical coke-breeze contaminant observed in the matrix of mesophase-derived carbon (SN2700, Black Thunder). Plane polarized reflected light.

b. Apparent contact of restriction deposit (SN5134) within steel pipe. Photomicrograph shows a layer of pyrrhotite crystals growing from the pipe surface into a layer (~85 μm) of carbonate, followed by a heterogenous layer of mixed organic materials in a matrix of carbonate. Plane polarized reflected light.

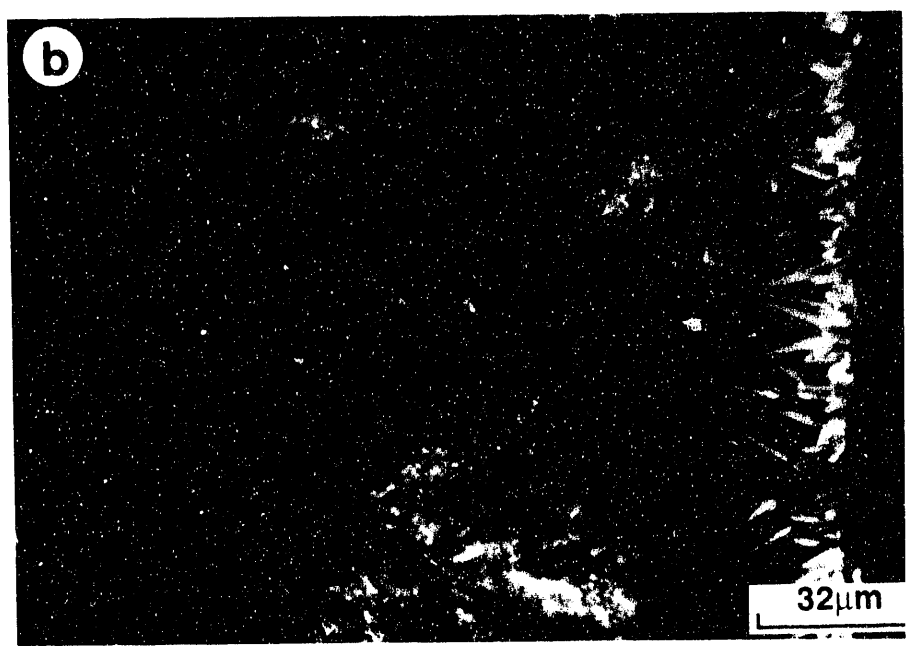

Plate X

retention in the reactor and separator vessels. Consequently, the presence of relatively large inert particles may have adversely effected reactor flow and may have contributed to the deposition of mesophase.

10.2.2. Conclusions

As part of our cooperative research efforts with other DOE contractors, samples of vessel plug and reactor deposit materials were obtained from the Wilsonville Pilot Plant. These deposit samples accumulated during Run 258 in which subbituminous coals (Spring Creek and Black Thunder) and a disposable iron oxide catalyst were being fed to the reactor. Accumulation of materials in the thermal reactor, the interstage separator vessel and the pipe connecting the two units caused significant unscheduled outages during Run 258.

Following characterization of five samples by optical microscopy and XRD, we conclude that deposits formed during operation with Spring Creek coal resulted from the deposition of process-derived calcium carbonate (calcite), whereas materials from operations with the Black Thunder coal resulted from a combination of mesophase-derived carbon and calcium carbonate. One common mineral phase observed in all samples was pyrrhotite ($Fe_{1-x}S$), which was found in slightly lower or equal concentration to the carbonate phase. Pyrrhotite was observed in both individual (<2 μm) particles as well as aggregates (reactor solids) exceeding 140 μm. The origin of this pyrrhotite is most certainly from sulfidization of the disposable iron oxide catalyst as analysis of the feed coals showed less than 0.1% pyritic sulfur. The change in mass during sulfidization and the tendency for aggregation of the sulfide suggests a mechanism for pyrrhotite

retention in the reactor and interstage separator vessel. Calcium carbonate and/or mesophase-derived carbon forms a matrix to cement these particles in place.

We have seen from our tubing bomb experiments that when H_2S is present both ferrous sulfate and iron pentacarbonyl form pyrrhotite. Relatively large aggregates of pyrrhotite have been observed by optical and electron microscopy when ferrous sulfate was used, but the same observation could not be made for iron pentacarbonyl.

10.3. DEPOSITS FROM WILSONVILLE RUN 260

Three additional reactor-solid deposit samples were received from the Wilsonville Pilot Plant on 1-28-91 for optical and mineralogical characterization. These samples had been collected at the plant following the conclusion of run 260 (operating period 7/17 - 11/13/90) which was operated in the catalytic/thermal mode with a feed of Black Thunder mine (Wyodak and Anderson seams) subbituminous coal, at a feed rate of 350 MF lb/h, and using a disposable iron oxide catalyst (Fe_2O_3) added at 2 wt% MF coal with a sulfiding agent (di-tertiary-Nonyl-Polysulfide, $C_9H_{19}S_xC_9H_{19}$) in conjunction with the first stage catalyst (Shell 324, 1/16"). One of the stated objectives of this run was to reduce and/or eliminate the type of reactor deposits that caused operating problems during the Wilsonville run 258 [Southern Clean Fuels, 1991]. In that run (Section 10.2), the system was shut down and the first stage reactor section and interstage separator had to be thoroughly cleaned. Reactor-solid materials provided to Penn State from run 258 revealed that mesophase-derived semicoke was largely responsible for the deposit formed from the Black Thunder coal

(Section 10.2). Thus, run 260 was operated in a catalytic/thermal mode with lower first-stage and higher second-stage temperatures in an attempt to prevent retrogressive reactions and coke formation. However, the generation of solids during the latter run prompted the request for assistance in identifying the nature of the continued solids build-up.

Two of the samples (SN16411, wall deposit and SN16403, reactor bottom solid) received from Wilsonville were saturated with a sticky black resid which had to be removed before analysis. The third sample (SN16413, suction cup line) was a section of pipe containing a hard, dark gray deposit which could be cut away with a knife. The two reactor deposit samples were placed in 150 ml of THF for 15 h, filtered and washed with THF and methanol and dried in a vacuum oven at room temperature for 8 h. All solids were then split into subsamples for the determination of percentage ash content, X-ray diffraction and for optical microscopy.

10.3.1. Results and Discussion

Figure 31 shows the location of each deposit sample within the Wilsonville thermal reactor (R1235), and Table 35 lists the analytical results. Wilsonville reported [Southern Clean Fuels, 1991] that the first-stage catalytic reactor and the downstream line leading to the thermal reactor (R1235) were clean and free of deposits, suggesting that the operating scheme for run 260 caused the deposit problem to be shifted downstream. During inspection of the thermal reactor, considerable deposits were found on both the inside (≈1/4" thick) and outside (≈3/4" thick) of the ebullating pump suction tube (Figure 31) as well as about 132 lbs of material in the bottom of the reactor.

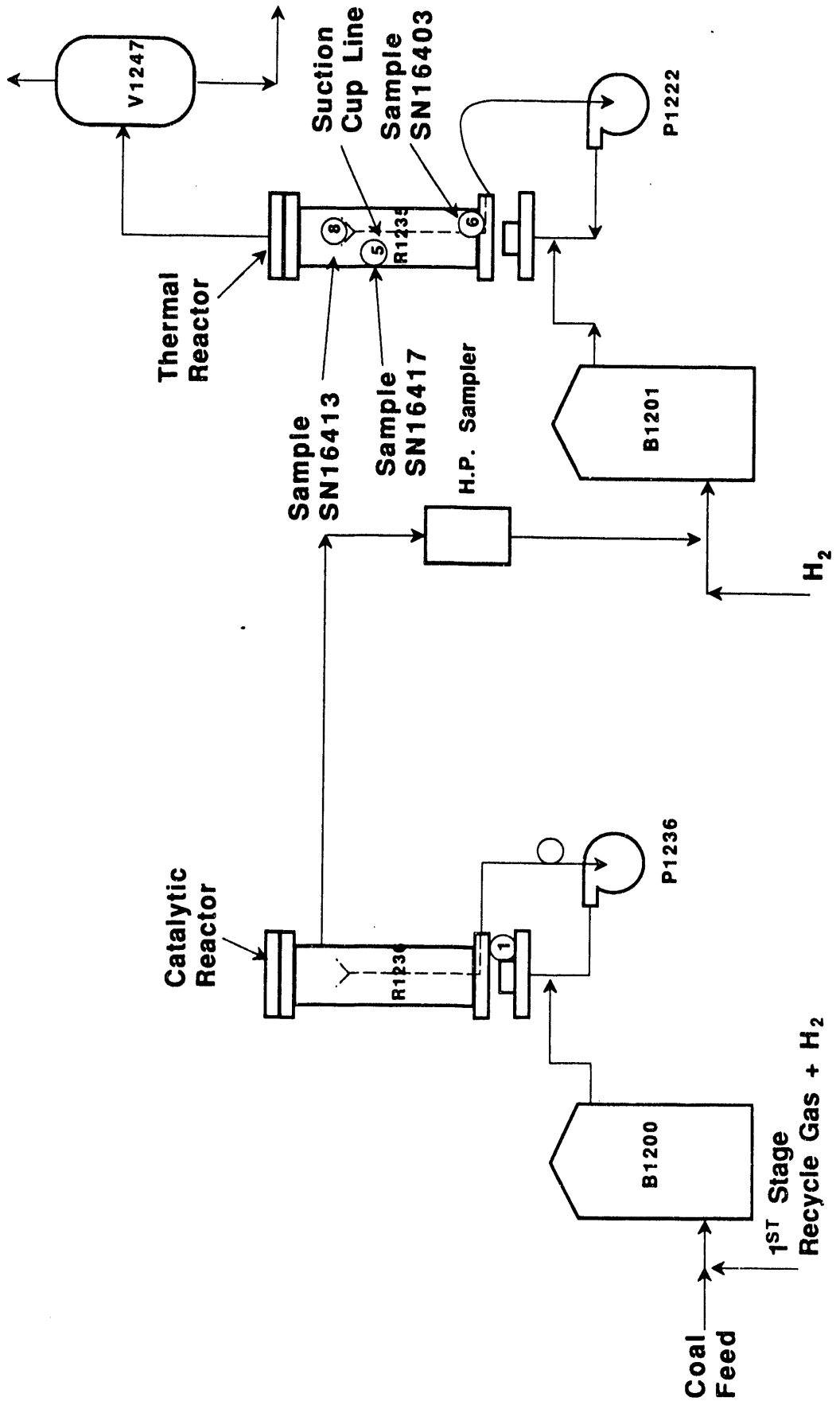

Figure 31 - Location of Reactor Solid Deposit Samples in Wilsonville Pilot Plant Following Run 260

Table 35. Sample description and results

Sample Description	Wilsonville SN	Date Collected	wt% THF-Soluble	wt% Ash Whole Sample	wt% 10M	X-ray Analysis Major Minerals
Solids from Bottom of R1235 Reactor	16403	11/21/90	25.0	67.7	7.3	Calcite > NaCl > Pyrrhotite > Quartz > Spinel
Wall Deposit from R1235 and Outside Suction Line	16411	11/20/90	33.0	41.6	25.4	Calcite > NaCl > Spinel > Pyrrhotite > Quartz
Suction Line Plug	16413	11/26/90	NA	71.8	28.2	Calcite > NaCl > Spinel > Pyrrhotite

Data in Table 35 shows that the reactor bottoms sample (SN16403) has a much lower amount of insoluble organic matter (IOM) than the wall deposit (SN16411) and suction line plug (SN16413) materials, otherwise the high ash content and sample mineralogy were found to be similar. Minerals detected by X-ray diffraction for each sample, which are listed in order of their relative concentrations based on peak intensities, were very similar. Calcite ($CaCO_3$), halite (NaCl) and pyrrhotite ($Fe_{1-x}S$) were the predominate mineral phases found along with spinel ($MgAl_2O_4$) and quartz (SiO_2). Spinel and quartz are coal-derived minerals, whereas the calcite, pyrrhotite (iron oxide catalyst) and perhaps halite are process-derived. The major surprise in this evaluation was to find halite in relatively high concentrations in these solids. Halite was also found in the Black Thunder reactor solids from run 258 even though chlorine levels for the coal were reported to be less than 0.01% (Section 10.2). Again, there can be no plausible explanation for the presence of NaCl other than contamination with the mineral before processing or from the use of a chlorinated chemical during some phase of operations (e.g., cleaning the reactor or lines with HCl).

Optical microscopy of the deposit samples showed that the reactor bottoms sample was mainly composed of calcium carbonate spheres, pyrrhotite aggregates with carbonate rims and coal-derived minerals cemented together with a thin layer of process-derived mesophase. As an example, Figure 32a shows a layer of anisotropic mesophase carbon coating the surface of process-derived vitroplast (isotropic). However, as suggested by the relatively low IOM (Table 35) of this sample, the accretion of calcium

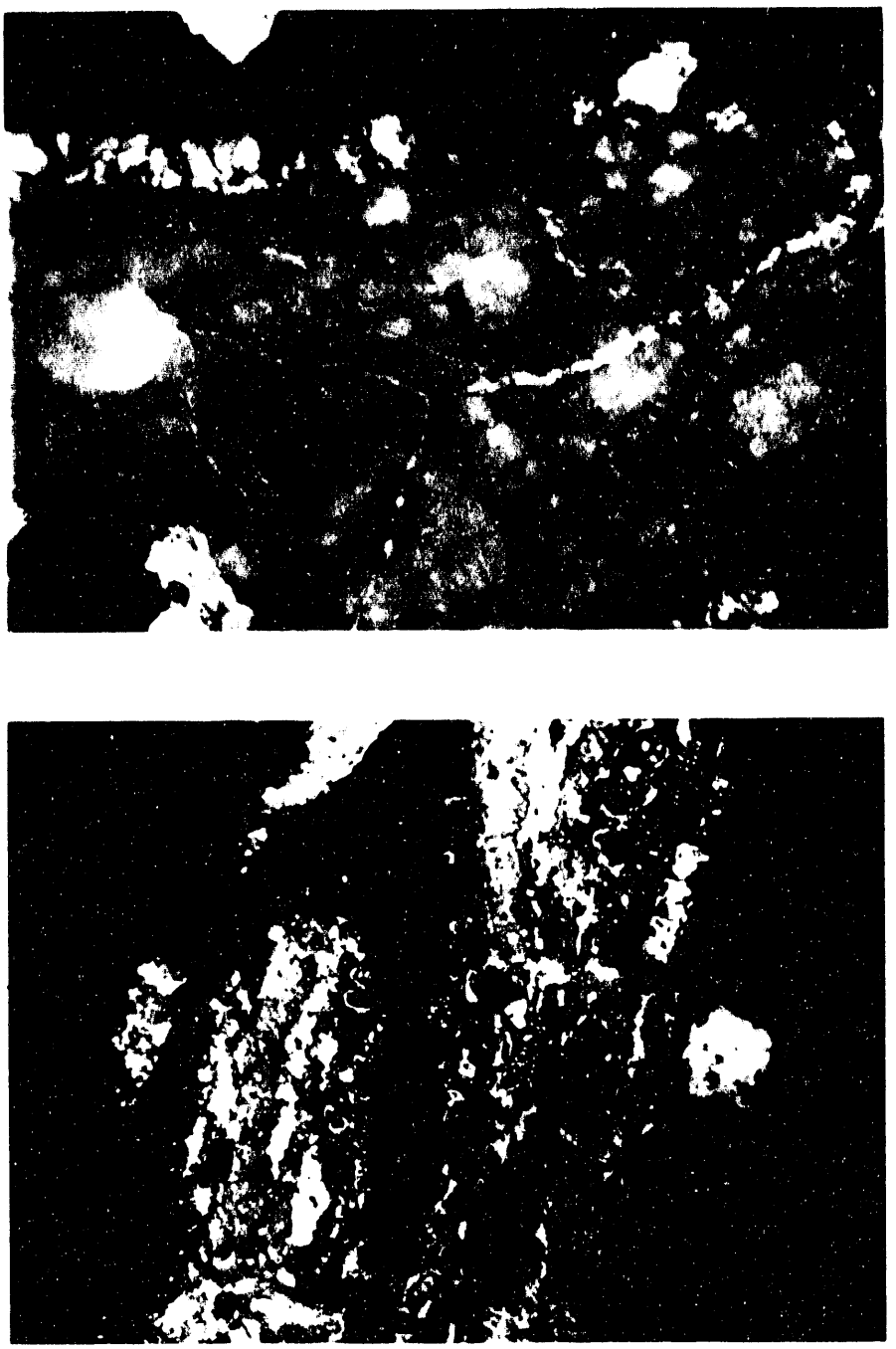

Figure 32 - Wilsonville Reactor Solids Material from Run 260 with Black Thunder Coal,
a.) Particle of Secondary Vitroplast Coated with Mesophase Carbon (SN16403)
b.) Intimate Association of Pyrrhotite, Vitroplast and Carbonate Cement in SN16413

carbonate appeared to be the main cause of the deposit; deposition of mesophase may be only secondary.

The wall deposit and suction line plug samples appeared to be very similar under the optical microscope, in that both samples were composed predominantly of a calcium carbonate cement. Figure 32b shows the interrelationship between some of the organic material (secondary vitroplast), pyrrhotite and the carbonate cement. Most of the IOM in these two samples were found to be isotropic vitroplast and coal-derived inertinite instead of mesophase. This suggests that the process conditions selected by Wilsonville to prevent coking reaction may indeed have been effective. Production of an isotropic carbon was favored instead of an anisotropic organic insoluble material. However, the larger problem of carbonate formation may not be alleviated by altering process conditions, but only be the removal of the organically bound calcium ions prior to liquefaction.

10.3.2. Conclusions

As part of our cooperative research effort with other DOE contractors, samples of reactor deposit materials were obtained from the Wilsonville Pilot Plant. These deposits accumulated during run 260 in which the subbituminous Black Thunder mine coal was being reacted in a catalytic/thermal mode with lower first-stage and higher second-stage temperatures. Materials accumulated solely in the second-stage thermal reactor at the bottom and as deposits on the wall and the outside and inside of the ebullating suction line.

Following the characterization of three samples by X-ray diffraction

and optical microscopy, we conclude that the deposits were mainly formed as a result of the formation and accretion or deposition of calcium carbonate with the other available process- and coal- derived inerts. Formation of mesophase-derived carbon was found to be minimized, but there was a proportionally greater amount of secondary vitroplast observed. This suggests that the process conditions selected by Wilsonville to eliminate retrogressive coking reactions was effective in reducing mesophase production, but did not totally alleviate the production of insoluble organic inerts. Furthermore, the larger problem of the formation of process-derived calcium carbonate has not, and may not be addressed by altering process conditions, but may require the removal of organically bound calcium ions before liquefaction.

10.4. EVALUATION OF THE HRI LIQUEFACTION PROCESSING OF OIL AGGLOMERATION CLEANED ILLINOIS #6 COAL

Hydrocarbon Research, Inc.(HRI) submitted for petrographic evaluation five coal or coal residue samples tested in program Run CC-6, operating identification Run 227-63. The samples were of uncleaned (LO-5466) Illinois #6 feed coal, feed coal cleaned by oil agglomeration (LO-5465), the residue of a CTSL run with uncleaned feed (LO-5464), the residue of a run with oil agglomerated cleaned coal (LO-5462), and the residue of a run under more severe conditions using the same cleaned coal feed. All samples were submitted as oil-free (THF washed) material. At about the same time that the oil-agglomerated samples were submitted for evaluation, a series of eight Otisca micronized cleaned and uncleaned feed materials, refuse and product solids were also submitted; a provisional examination of these

latter samples indicated that no distinct differences existed in the organic fractions of the product solids, so no further work on them was undertaken.

10.4.1. Results and Discussion

Table 36 contains the vol. % mineral-free petrographic analyses of the uncleaned and cleaned feed coals. It is apparent that there is negligible difference in the proportions of the three maceral groups between the two feed samples. So, while the oil agglomeration cleaning was successful in reducing the ash from 15.2 to 4.6%, this operation did not produce any selective separation of macerals.

Figures 33-37 are the printouts of 200-point reflectograms generated on the vitrinite + inertinite components of the five samples. These figures should enable any significant trends in the maceral compositions of the coal and residue samples to be detected. The reflectograms of the two feed samples show that the vitrinite of these samples is concentrated at a reflectance of 0.4-0.7%. Above this range the reflectances show a wide spread of readings for the semi-inertinite (intermediate values) and inertinite (higher values) components. The similarity in the reflectograms of the two feed coals mirrors the very similar petrographic compositions of these samples.

For easier comparison of the reflectance distributions, values have been grouped into four reflectance ranges in Table 36. It is obvious that while most of the vitrinite of the feed samples has reflectance values in the two lowest reflectance groups (82-86%), there is little (8.5-11.5%)

Table 36. Petrographic and reflectance analyses - HRI Run CC-6

	LO-5466 Feed-Uncleaned	LO-5465 Feed-Cleaned	LO-5464 Run-Uncleaned	LO-5462 Run-Cleaned	LO-5463 Run-Cleaned (Severe)
MACERAL ANALYSIS					
Vitrinite, %	88.7	88.7			
Liptinite, %	2.0	2.5			
Semi-Inertinite, %	4.2	3.2			
Inertinite, %	5.1	5.6			
	100.0	100.0			
REFLECTANCE ANALYSIS					
0.00-0.49%	27.0	36.5	8.5	9.0	3.5
0.50-0.99%	59.0	45.5	3.0	4.5	5.0
1.00-1.99%	6.5	8.5	32.5	31.0	31.0
2.00-2.49%	2.0	4.0	14.0	19.0	14.5
2.50-5.00%	5.5	5.5	42.0	36.5	46.0
	100.0	100.0	100.0	100.0	100.0

Figure 33 - Reflectance Distribution for Vitrinite+Inertinite for HRI LO-5466

REFLECTANCE DISTRIBUTIONS FOR VIT+INERT
LO-5466
Mean Random (polariz) Reflectance:

2	0.30	1.00	**
52	0.40	26.00	**********
97	0.50	48.50	**********
12	0.60	6.00	**********
4	0.70	2.00	****
1	0.80	0.50	*
4	0.90	2.00	****
3	1.00	1.50	***
0	1.10	0.00	
3	1.20	1.50	***
1	1.30	0.50	*
1	1.40	0.50	*
0	1.50	0.00	
3	1.60	1.50	***
2	1.70	1.00	**
0	1.80	0.00	
0	1.90	0.00	
0	2.00	0.00	
0	2.10	0.00	
1	2.20	0.50	*
3	2.30	1.50	***
0	2.40	0.00	
0	2.50	0.00	
1	2.60	0.50	*
0	2.70	0.00	
0	2.80	0.00	
0	2.90	0.00	
0	3.00	0.00	
2	3.10	1.00	**
0	3.20	0.00	
2	3.30	1.00	**
0	3.40	0.00	
4	3.50	2.00	****
0	3.60	0.00	
0	3.70	0.00	
0	3.80	0.00	
0	3.90	0.00	
0	4.00	0.00	
1	4.10	0.50	*
1	4.20	0.50	*

Figure 34 - Reflectance Distribution for Vitrinite+Inertinite for HRI LO-5465

REFLECTANCE DISTRIBUTIONS FOR VIT+INERT
HRI LO-5465
Mean Random (polariz) Reflectance:

2	0.30	1.00	**
71	0.40	35.50	**********
81	0.50	40.50	**********
5	0.60	2.50	*****
2	0.70	1.00	**
1	0.80	0.50	*
2	0.90	1.00	**
5	1.00	2.50	*****
2	1.10	1.00	**
0	1.20	0.00	
3	1.30	1.50	***
1	1.40	0.50	*
1	1.50	0.50	*
1	1.60	0.50	*
1	1.70	0.50	*
2	1.80	1.00	**
1	1.90	0.50	*
1	2.00	0.50	*
3	2.10	1.50	***
1	2.20	0.50	*
2	2.30	1.00	**
1	2.40	0.50	*
1	2.50	0.50	*
0	2.60	0.00	
1	2.70	0.50	*
1	2.80	0.50	*
0	2.90	0.00	
0	3.00	0.00	
0	3.10	0.00	
0	3.20	0.00	
3	3.30	1.50	***
0	3.40	0.00	
0	3.50	0.00	
0	3.60	0.00	
0	3.70	0.00	
0	3.80	0.00	
1	3.90	0.50	*
1	4.00	0.50	*
0	4.10	0.00	
1	4.20	0.50	*
1	4.30	0.50	*
0	4.40	0.00	
0	4.50	0.00	
1	4.60	0.50	*

Figure 35 - Reflectance Distribution for Vitrinite+Inertinite for HRI LO-5464

REFLECTANCE DISTRIBUTIONS FOR VIT+INERT
LO-5464
Mean Random (polariz) Reflectance:

4	0.30	2.00	****
13	0.40	6.50	**************
4	0.50	2.00	****
0	0.60	0.00	
1	0.70	0.50	*
1	0.80	0.50	*
0	0.90	0.00	
3	1.00	1.50	***
3	1.10	1.50	***
5	1.20	2.50	*****
5	1.30	2.50	*****
3	1.40	1.50	***
8	1.50	4.00	********
9	1.60	4.50	**********
16	1.70	8.00	**********
6	1.80	3.00	******
7	1.90	3.50	*******
10	2.00	5.00	**********
6	2.10	3.00	******
7	2.20	3.50	*******
2	2.30	1.00	**
3	2.40	1.50	***
4	2.50	2.00	****
2	2.60	1.00	**
5	2.70	2.50	*****
3	2.80	1.50	***
3	2.90	1.50	***
5	3.00	2.50	*****
5	3.10	2.50	*****
3	3.20	1.50	***
6	3.30	3.00	******
4	3.40	2.00	****
5	3.50	2.50	*****
2	3.60	1.00	**
3	3.70	1.50	***
3	3.80	1.50	***
3	3.90	1.50	***
5	4.00	2.50	*****
3	4.10	1.50	***
2	4.20	1.00	**
3	4.30	1.50	***
4	4.40	2.00	****
1	4.50	0.50	*
2	4.60	1.00	**
2	4.70	1.00	**
3	4.80	1.50	***
3	4.90	1.50	***

Figure 36 - Reflectance Distribution for Vitrinite+Inertinite for HRI LO-5462

REFLECTANCE DISTRIBUTIONS FOR VIT+INERT
LO-5462
Mean Random (polariz) Reflectance:

1	0.20	0.50	*
6	0.30	3.00	******
11	0.40	5.50	**********
4	0.50	2.00	****
3	0.60	1.50	***
0	0.70	0.00	
1	0.80	0.50	*
1	0.90	0.50	*
2	1.00	1.00	**
3	1.10	1.50	***
4	1.20	2.00	****
5	1.30	2.50	*****
11	1.40	5.50	**********
8	1.50	4.00	********
8	1.60	4.00	********
8	1.70	4.00	********
7	1.80	3.50	*******
6	1.90	3.00	******
9	2.00	4.50	*********
11	2.10	5.50	**********
9	2.20	4.50	*********
6	2.30	3.00	******
3	2.40	1.50	***
4	2.50	2.00	****
5	2.60	2.50	*****
7	2.70	3.50	*******
2	2.80	1.00	**
1	2.90	0.50	*
8	3.00	4.00	********
4	3.10	2.00	****
7	3.20	3.50	*******
3	3.30	1.50	***
5	3.40	2.50	*****
1	3.50	0.50	*
1	3.60	0.50	*
2	3.70	1.00	**
2	3.80	1.00	**
3	3.90	1.50	***
3	4.00	1.50	***
3	4.10	1.50	***
1	4.20	0.50	*
2	4.30	1.00	**
1	4.40	0.50	*
1	4.50	0.50	*
2	4.60	1.00	**
2	4.70	1.00	**
3	4.80	1.50	***

Figure 37 - Reflectance Distribution for Vitrinite+Inertinite for HRI LO-5463

REFLECTANCE DISTRIBUTIONS FOR VIT+INERT
LO-5463
Mean Random (polariz) Reflectance:

1	0.30	0.50	*
6	0.40	3.00	******
5	0.50	2.50	*****
4	0.60	2.00	****
0	0.70	0.00	
1	0.80	0.50	*
0	0.90	0.00	
1	1.00	0.50	*
7	1.10	3.50	********
1	1.20	0.50	*
6	1.30	3.00	******
4	1.40	2.00	****
7	1.50	3.50	********
8	1.60	4.00	*********
7	1.70	3.50	********
8	1.80	4.00	*********
13	1.90	6.50	**************
7	2.00	3.50	********
3	2.10	1.50	***
10	2.20	5.00	**********
4	2.30	2.00	****
5	2.40	2.50	*****
6	2.50	3.00	******
5	2.60	2.50	*****
6	2.70	3.00	******
1	2.80	0.50	*
6	2.90	3.00	******
7	3.00	3.50	********
4	3.10	2.00	****
1	3.20	0.50	*
7	3.30	3.50	********
6	3.40	3.00	******
4	3.50	2.00	****
7	3.60	3.50	********
4	3.70	2.00	****
2	3.80	1.00	**
0	3.90	0.00	
4	4.00	2.00	****
3	4.10	1.50	***
3	4.20	1.50	***
0	4.30	0.00	
3	4.40	1.50	***
4	4.50	2.00	****
5	4.60	2.50	*****
1	4.70	0.50	*
1	4.80	0.50	*
2	4.90	1.00	**

material with these characteristics remaining in the residues. A small amount of vitrinite has been able to pass unconverted through the reactor. If the run had been entirely successful, none of this material should remain. The reduction in the material reporting to these groups from the residue of run LO-5463 (8.5%) especially in the lowest reflectance group (0-0.49%), indicates that the more severe processing of this run has successfully improved the efficiency of vitrinite conversion. Moreover, the same residue contains the greatest proportion of material in the highest reflectance category (2.50-5.00%). Apparently the residue of the most severe run contains somewhat more condensed material than either of the other residues; this may indicate that not only has the vitrinite undergone more successful hydrogenation, but also that some of the lower reflecting semifusinite may have undergone dissolution.

10.4.2. Conclusions

Petrographic analysis of the feed coals and residues of HRI Run CC-6 indicates that very little reactive material (vitrinite) remains unconverted following runs with uncleaned Illinois #6 feed coal, with feed coal cleaned by oil agglomeration, or under more severe processing conditions. Reduction in the proportion of lowest reflecting residual material following the more severe processing conditions may indicate that not only had the vitrinite undergone a slightly improved hydrogenation, but also that some of the lower reflecting semifusinite may have undergone dissolution.

10.5. EVALUATION OF THE HRI LIQUEFACTION PROCESSING IN PROCESS DEVELOPMENT RUN 260-03

HRI submitted sample LO-6030 on June 23, 1992. This sample represents a deposit found in the recycle gas feed line to the CTSL Coal Liquefaction Process Development Unit Reactor during processing of Black Thunder Mine coal. The specific identification of the sample is LO-6030 Reactor 1 Gas Inlet (Solids Deposit), 6-23-92 0940, 260-03-S/D (Shutdown).

The question posed by HRI was is the deposit "a coke material carried from the recycle gas preheater (because of possible oil inclusion from the recycle gas purification tower), or a coal derived material back-washed from the reactor?"

Our approach to the problem was to examine the material by reflected-light microscopy using oil immersion. The identification of those materials which had been carbonized to yield highly anisotropic products was aided by utilization of crossed polarizers and an accessory mineral plate. A point count of 200 points was undertaken to acquire a semi-quantitative estimate of the proportions of the different organic components present in the deposit.

Because our examination of the deposit revealed the presence of a significant amount of coke, we requested a sample of the feed coal to investigate whether any coke might have been introduced into the reactor as a contaminant within the feed. A sample of Black Thunder Coal 5991 was submitted in response to this request.

10.5.1. Results and Discussion

At least two of the five major organic components are recognizable as being coal-derived. The first category is "Coal Residue", consisting either of coal macerals showing little physical change from the feed coal precursors (and including fusinite, semifusinite, vitrinite and, in some rare instances, even liptinite), or of the same materials showing no change in morphology or anisotropy, but an increase in reflectance in response to the thermal conditions. A semi-quantitative estimate of 20% was obtained for the volume percentage of the unaltered "Coal Residue" component.

The second category of recognizable coal-derived products is "Vitroplast". This low-reflecting (pitch-like and optically isotropic) material is a common component of liquefaction residues and is derived by simple melting or partial hydrogenation of the coal. It is often asphaltenic or preasphaltenic in character, and is solid or semi-solid at ordinary conditions. It may or may not be soluble in solvents such as THF. The semi-quantitative point count gave an estimate of 41% of this material.

Categories three thorough five are somewhat more problematic. It is believed that these have not been derived directly from coal, but probably are the high-temperature cokes derived from the liquid or gaseous products of the process.

The third category, present only in very minor amounts (semi-quantitatively estimated at 3%), is "Pyrolytic Carbon". The well-known spherulitic and highly anisotropic form is easily recognizable as material which is thought to form by the thermal cracking of volatiles, usually at temperatures in excess of 500°C. However, the faint appearance of similar

structures in the carbon forms of categories four and five suggests that at least a part of those materials may have been derived in a similar fashion.

The fourth category is "Coarse Mosaics (including Ribbon Structures)". This type of anisotropic carbon is known to form due to carbonization of the liquid products of hydrogenation. However, as observed above it is possible that some portion of the 6% of this material which occurs in the deposit may be pyrolytic carbon. The fifth category, "Medium and Fine Mosaics" represents a major component (semi-quantitatively judged to be 30%) of the deposit; like the fourth category, it is possible that some part of this may be pyrolytic carbon formed thorough the cracking of gases.

The striking similarity in optical textures of categories four and five to those of metallurgical coke make it necessary to enquire into the possibility that some of the carbonized materials might have been introduced into the reactor as a contaminant with the feed coal. HRI's sample of Black Thunder feed 5991 was examined under the microscope; no coked material was observed. This, and the fact that pyrolytic structures are rare in metallurgical coke led to the conclusion that all of the coke textures originated within the reactor, either from the liquid products or the gases as a result of temperature excursions. The high reflectance of the cokes also suggests that higher than normal temperatures were experienced.

In addition to the organic components, a large amount of inorganic matter is present in the deposit. Minerals observed include pyrite, pyrrhotite, carbonates and sulfates.

10.5.2 Conclusions

About 20% of the organic components of the deposit are relatively unaltered coal maceral materials. A major component (about 40%) consists of 'Vitroplast' which is also coal-derived, but which has undergone melting and/or partial hydrogenation to give a pitch-like material.

Three coked materials are present in the deposit. One, a minor component (about 3%), is obvious pyrolytic carbon, thought to be derived through the cracking of gases. The other two anisotropic cokes (Coarse, and Medium and Fine Mosaics, together totalling about 36%) could have been derived by coking of the liquid products. It is also possible that some unknown portion may also represent pyrolytic carbon formation, and that some direct coking of undissolved coal particles may have been involved.

REFERENCES

Anderson, K. B., and Winans, R. E., 1991. Amer. Chem. Soc. Div. Fuel Chem. Prepr., 36 (2), 765.

Anderson, R.R. and Bockrath, C., 1984. Fuel, 63, 329.

Artok, L., Davis, A., Mitchell, G.D., and Schobert, H.H., 1992. Fuel, 71, 981.

Artok, L., Schobert, H. H., and Davis, A., 1992. Fuel Proc. Technol., 32, 87.

Artok, L., Schobert, H. H., Mitchell; G. D., and Davis, A., 1991. Amer. Chem. Soc. Div. Fuel Chem. Prepr., 36 (1), 36.

Bacaud, R., Charcosset, H., and Jamond, M., 1990. Fuel Process. Technol., 24, 163.

Baldwin, R.M., Kennar, D.R., Nguanprasert, O. and Miller, R.L., 1991. Fuel, 70, 429.

Baldwin, R.M. and Vinciguerra, S., 1983. Fuel, 62, 498.

Bartle, K. D., Jones, D. W., Pakdel, H., Snape, C. E., Calimli, A., Olcay, A., and Tugrul, T., 1979. Nature, 277, 284.

Bartle, K. D., Martin, T. G., and Williams, D.F., 1975. Fuel, 54, 226.

Bellamy, L. J., 1975. "The Infra-red Spectra of Complex Molecules" Chapman and Hall, London, 1975; Part 2.

Bennett, M.J., Chaffey, G.H., Myatt, B.L., and Silvester, D.R.V., 1982. In "Coke Formation on Metal Surfaces" (Eds. L.F. Albright and R.T.K. Baker), American Chemical Society, Washington, Chapter 11.

Bodily, D.M. and Wann, J.P., 1986. Amer. Chem. Soc. Div. Fuel Chem. Prepr., 31 (4), 119.

Bodily, D.M., Shibaoka, M. and Yoshida, R., 1981. Proc. Internat. Conf. Coal Sci., 350.

Bommannavar, A. and Montano, P.A., 1983. Fuel, 62, 932.

Briggs, L. H., Colebrook, L. D., Fales, H. M., and Widmann, W. C., 1957 Anal. Chem. 29, 904.

Brooks, D.G., Guin, J.A., Curtis, C.W. and Placek, T.D., 1983. Ind. Eng. Chem. Process Des. Devel., 22, 343.

Burgess, C.E., Artok, L. and Schobert, H.H., 1991. Amer. Chem. Soc. Div. Fuel Chem. Prepr. 36 (2), 462.

Burgess, C.E. and Schobert, H.H., 1991. Fuel, 70, 372.

Cassidy, P.J., Hertan, P.A., Jackson, W.R., Larkins, F.P., and Rash, D., 1982. Fuel 61, 939.

Cassidy, P.J., Larkins, F.P., and Jackson, W.R., 1982. Amer. Chem. Soc. Div. Fuel Chem. Prepr., 27 (2), 28.

Cebolla, V.L., Diack, M., Oberson, M., Bacaud, R., Cagniant, D., and Nickel-Pepin-Donat, B., 1991. Fuel Process. Technol., 28, 183.

Chamberlin, P.L. and Schobert, H.H., 1991. Fuel Proc. Technol., 28, 67.

Cody, G.D., Larsen, J.W. and Siskin, M., 1988. Energy and Fuels, 2, 340.

Comolli, A.G., MacArthur, J.B. and McLean, J.B., 1985. Proc. EPRI Contractors' Conf. on Clean Liquid and Solid Fuels, 2-1.

Cook, P.S., and Cashion, J.D., 1987a. Fuel 66, 661.

Cook, P.S., and Cashion, J.D., 1987b. Fuel 66, 669.

Cook, P.S., Lim, S.C., Hang, G.S., Jackson, W.R., and Cassidy, P.J., 1988. Fuel 67, 942.

Cugini, A. V.; Utz, B.R.; Krastman, D.; Hickey, R. F., 1991. Amer. Chem. Soc. Div. Fuel Chem. Prepr., 36 (1), 91.

Cypres, R., Ghodsi, M. and Stocq, R., 1981. Fuel, 60, 247.

DasGupta, R., Mitra, J.R., Dutta, B.K., Sharma, U.N., Sinha, A.K., and Mukherjee, D.K., 1991. Fuel Process. Technol., 27, 35.

Davis, A., Derbyshire, F.J. and Schobert, H.H., 1988. U.S. Dept. of Energy Report, No. DOE-DE-FG22-86PC90910-3.

Davis, A., Derbyshire, F.J., Mitchell, G.D. and Schobert, H.H., 1989. U.S. Dept. of Energy Report, No. DE-FG22-86PC90910.

Davis, A., Glick, D.C. and Mitchell, G.D., 1989b, Proc. Direct Liquefaction Contractor's Review Meeting, Pittsburgh, PA, 211.

Derbyshire, F.J., Davis, A., Lin, R., Stansberry, P.G. and Terrer, M.T., 1986a. Fuel Proc. Technol., 12, 127.

Derbyshire, F.J., Davis, A., Epstein, M., and Stansberry, P., 1986b. Fuel, 65, 1233.

Derbyshire, F.J., 1988, Internat. Energy Agency, IEACR/08, London, 69 pp.

Dong, J. Z., Katoh, T., Itoh, H., and Ouchi, K., 1986. Fuel 65, 1073.

Dong, J. Z., Katoh, T., Itoh, H., and Ouchi, K., 1987. Fuel 66, 1336.

Dryden, I.G.C., 1951. Fuel, 30, 145.

Farcasiu, M., Smith, M., Pradhan, V.R., and Wender, I., 1991. Fuel Process. Technol., 29, 199.

Garcia, A.B. and Schobert, H.H., 1989. Fuel, 68, 1613.

Garcia, A. and Schobert, H.H., 1991. Coal Preparation, 9, 185.

Garg, D. and Givens, E.N., 1982. Ind. Eng. Chem. Process Des. Devel., 21, 113.

Glick, D.C., Mitchell, G.D. and Davis, A., 1991. Amer. Chem. Soc. Div. Fuel Chem. Prepr., 36, 861.

Grainger, L. and Gibson, J., 1981. "Coal Utilisation: Technology, Economics, and Policy," Graham and Trotman Ltd., London, Chapter 9.

Green, T.K., Kovac, J. and Larsen, J.W., 1984. Fuel, 63, 935.

Hawk, C.O. and Hiteshue, R.W., 1965. U.S. Bur. Mines Bulletin, No. 622.

Herrick, D.E., Tierney, J.W., Wender, I., Huffman, G.P. and Huggins, F.E., 1990. Energy Fuels, 4, 231.

Hirschon, A.S. and Wilson, R.B., Jr., 1991. In In "Coal Science II" (Eds. H.H. Schobert, K.D. Bartle and L.J. Lynch), American Chemical Society, Washington, Chapter 21.

Huang, L., Song, C., and Schobert, H.H., 1992. Amer. Chem. Soc. Div. Fuel Chem. Prepr., 37, 223.

Jackson, W.R. and Larkins, F.P., 1991. In, "The Science of Victorian Brown Coal" (Ed. R.A. Durie), Butterworth-Heinemann, Oxford, Chapter 10.

Joseph, J.T., 1991a. Fuel, 70, 139.

Joseph, J. T., 1991b Fuel, 70, 459.

Kamiya, Y., Nobusawa, Y. and Futamura, S., 1988. Fuel Process. Technol., 18, 1.

Kazimi, F., Chen, W.Y., Chen, J.K., Whitney, R.R. and Zimny, B., 1985. Amer. Chem. Soc. Div. Fuel Chem. Prepr. 30 (4), 402.

Kotanigawa, T., 1991 Nenryo Kyokaishi, 70, 431.

Lambert, J.M., Jr., Simkovich, G., and Walker, P.L., Jr., 1980. Fuel, 59, 687.

Lambert, J.M., 1982. Fuel, 61, 777.

Larkins, F.P., Jackson, W.R., Rash, D., Hertan, P.A., Cassidy, P.J., Marshall, M., and I.D. Watkins, 1984. In "The Chemistry of Low-Rank Coals" (Ed. H.H. Schobert), American Chemical Society, Washington, Chapter 18.

Leclercq, L., Provost, M., Grimblot, J., Hardy, A.M., and Gengenbre, L., 1989. J. Catal., 117, 371.

Liotta, R., Rose, K. and Hippo, E., 1981. J. Organic Chemistry, 46, 277.

Mashima, K., Kiya, K., Sato, S., Tsuchiya, H., and Ainai, J., 1984. Fuel, 63, 1417.

Matturro, M.G., Liotta, R. and Isaacs, J.J., 1985. J. Org. Chem., 46, 277.

Miller, R. L., Baldwin, R. M. and Kennar, D. R., 1990. Amer. Chem. Soc. Div. Fuel Chem. Prepr., 35 (1), 9.

Mills, G.A., 1950. Ind. Eng. Chem., 42, 182.

Mitchell, G.D., Davis, A., and Spackman, W., 1977. In "Liquid Fuels from Coal", (Ed. R.T. Ellington), Academic Press, 245.

Montano, P.A. and Granoff, B., 1980. Fuel, 59, 214.

Mudamburi, Z., and Given, P. H., 1985. Org. Geochem., 8, 221.

Murakami, K., Yokono, T. and Sanada, Y., 1986. Fuel, 65, 1079.

Narain, N., Cillo, D.L., Steigel, G.J. and Tischer, R.E., 1987. In "Coal Science and Chemistry". (Ed. A. Volborth), Elsevier, Amsterdam, Chapter 4.

Naumann, A.W., 1981. United States Patent, No. 4243554.

Ogata, E., Hatakeyama, K., Tamura, T., Nobusawa, T., Fujimoto, K., Futamura, S., and Kamiya, T., 1985. Proc. Intl. Conf. on Coal Sci., 173.

Ohtsuka, Y. and Asami, K., 1991. Ind. Eng. Chem. Res., 30, 1921.

Painter, P.C., and Coleman, M. M., 1979. Fuel, 58, 301.

Painter, P.C., Snyder, R. W., Starsinic, M., Coleman, M. M., Kuehn, D. H., and Davis, A., 1981. Appl. Spectroscopy, 35, 475

Philp, R.P., 1985. "Fossil Fuel Biomarkers: Applications and Spectra" Elsevier, Amsterdam, Chapter 2.

Pradhan, V.R., Herrick, D.E., Tierney, J.W., and Wender, I., 1991. Energy Fuels 5, 712.

Probstein, R.F. and Hicks, R.E., 1982. "Synthetic Fuels." McGraw-Hill, New York, Chapter 6.

Rahimi, P.M., Fouda, S.A. and Kelly, J.F., 1986. Amer. Chem. Soc. Div. Fuel Chem., Prepr. 31 (4), 192.

Rincon, J.M. and Cruz, S., 1988. Fuel, 67, 1162.

Robbins, G.A., Winschel, R.A. and Burke, F.P., 1990. U.S. Dept. of Energy Report No. DE-AC22-89PC89883.

Satterfield, C.N. and Gultekin, S., 1981. Ind. Eng. Chem. Process Des. Devel., 20, 62.

Shiboaka, M., Stephens, J.F., and Russell, N.J., 1979, Fuel, 58, 515.

Snape, C. E., Stokes, B. J., and Bartle, K. D., 1981. Fuel, 60, 903.

Solomon, P.R., Serio, M.A., Deshpande, G.V., Kroo, E., Schobert, H.H. and Burgess, C.E., 1991. In "Coal Science II" (Eds. H.H. Schobert,

K.D. Bartle and L.J. Lynch), American Chemical Society, Washington, Chapter 15.

Song, C., Hanaoka, K., and Nomura, M., 1989. Fuel, 68, 287.

Song, C., Schobert, H.H., and Hatcher, P.G., 1991. Proc. Intl. Conf. on Coal Sci., 664.

Southern Clean Fuels, 1991. Wilsonville Advanced Coal Liquefaction R & D Facility, Handouts from Technical Meeting, No. 108, Janaury 17, 57 pp.

Stansberry, P.G. and Derbyshire, F.J., 1988. U.S. Dept. of Energy Report, No. DOE-PC-60811-F3.

Stenberg, V.I., Baltisberger, R.J., Ogawa, T., Raman, K., and Woolsey, N.F., 1982. Amer. Chem. Soc. Div. Fuel Chem. Prepr., 27 (3), 23.

Suzuki, T., Osamu, Y., Takahashi, Y., and Watanabe, Y., 1985b. Fuel Process. Technol. 10, 33.

Suzuki, T., Yamada, O., Fujita, K., Takegumi, Y. and Watanabe, Y., 1984. Fuel, 63, 1707.

Suzuki, T., Yamada, H., Sears, P.L. and Watanabe, Y., 1989. Energy Fuels, 3, 707.

Suzuki, T., Yamada, O., Then, J.H. and Ando, T., 1985a. Proc. Internat. Conf. Coal Sci., 205.

Tagaya, H., Sugai, J., Onuki, M. and Chiba, K., 1987. Energy Fuels, 1, 397.

Terrer, M.T. and Derbyshire, F.J., 1986. U.S. Dept. of Energy Report, No. DOE-OC-60811-F1.

Tierny, J.W. and Wender, I., 1988. Proc. DOE Direct Liquefaction Contractors' Review, 39.

Trewhella, M.J. and Grint, A., 1987. Fuel, 66, 1315.

Utz, B.R., Cugini, A.V. and Frommell, E.A., 1989. Amer. Chem. Soc. Div. Fuel Chem. Prepr. 34, 1423.

Wakeley, L.D., Davis, A., Jenkins, R.G., Mitchell, G.D. and Walker, Jr., P.L., 1979. Fuel, 58, 379.

Walker, Jr., P.L., Spackman, W., Given, P.H., White, E.W, Davis, A. and Jenkins, R.G., 1975. EPRI AF417, RP366-1, 102 pp.

Warzinski, R. P., and Holder, G. D., 1991. Amer. Chem. Soc. Div. Fuel Chem. Prepr., 36 (1), 44.

Watanabe, Y., Yamada, O., Fujita, K., Takegami, Y. and Suzuki, T., 1984. Fuel, 63, 752.

Weller, S. W. and Pelipetz, M. G., 1951. Ind. Eng. Chem., 43, 1243.

Willson, W.G., Hei, R., Riskedahl, D. and Stenberg, V.I., 1985. Fuel, 64, 128.

Yamada, O., Suzuki, T., Then, J. H., Ando, T., and Watanabe, Y., 1985. Fuel Proc. Technol. 11, 297.

Yamamoto, A., 1986. "Organotransition Metal Chemistry" Wiley, New York, Chapter 4.

Yamashita, H., Ohtsuka, Y., Yoshida, S. and Tomita, A., 1989. Energy Fuels, 3, 686.

Yokoyama, S., Yoshida, R., Narita, H., Kodaira, K and Maekawa, Y., 1986. Fuel, 65, 164.

Youtcheff, J.S., and Given, P.H., 1982. Fuel, 61, 980.

Znaimer, S., Skinner, R.W., and Phillips, M., 1983. In "Pennsylvania Coal" (Ed. J.K. Majumdar and E.W. Miller) Pennsylvania Academy of Science, Easton, PA, Chapter 11.

APPENDIX A

DETAILED PHYSICAL, CHEMICAL AND ELEMENTAL CHARACTERISTICS OF COALS SELECTED FOR LIQUEFACTION

SAMPLE IDENTIFICATION:

PSU NUMBER	-> PSOC-1503
SEAM NAME	-> BLIND CANYON
ALTERNATE SEAM NAME	->
APPARENT RANK	-> HVB

SAMPLE HISTORY:

SAMPLING DATE & AGENCY	-> 10/ 1/85 ; PSU
SAMPLE TYPE	-> CHANNEL-WHOLE SEAM
ADDITIONAL INFORMATION	->

MINE INFORMATION:

RESERVES	->
ANNUAL PRODUCTION	->

SEAM INFORMATION:

AGE OF SEAM	-> CRET.
GROUP	-> MESAVERDE
FORMATION	-> BLACKHAWK
SEAM THICKNESS	-> 7 FT. 4 IN.

SAMPLE LOCATION:

COUNTRY	-> USA
STATE	-> UTAH
COUNTY	-> EMERY
TOWNSHIP	->
CITY	-> ORANGEVILLE
COAL PROVINCE	-> ROCKY MOUNTAIN
REGION	-> UINTA
MAP REFERENCE: LATITUDE	-> 39 D 19 M 0 S
LONGITUDE	-> 111 D 6 M 0 S
QUADRANGLE	-> HIAWATHA (15')
LIFE EXPECTANCY	->
MINING METHOD	-> UNDERGROUND

** PENN STATE COAL DATA BASE **
** PSOC-1503 **
** 09/14/92 **
** PAGE 1 **

SAMPLE IDENTIFICATION:

PSU NUMBER	-> PSOC-1503
SEAM NAME	-> BLIND CANYON
ALTERNATE SEAM NAME	->
APPARENT RANK	-> HVB

SAMPLE LOCATION:

COUNTRY	-> USA
STATE	-> UTAH

** PENN STATE COAL DATA BASE **
** PSOC-1503 **
** 09/14/92 **
** PAGE 2 **

* * * * * C H E M I C A L D A T A * * * * *

PROXIMATE ANALYSIS	AS REC'D	DRY	DAF	DMMF(PARR)
% MOISTURE	10.35			
% ASH	3.51	3.91		
% VOLATILE	41.89	46.73	48.63	48.39
% FIXED CARBON	44.25	49.36	51.37	51.61

% EQUILIBRIUM MOISTURE = 11.81
MM-FREE = 12.29

ULTIMATE ANALYSIS	AS REC'D	DRY	DAF	DMMF(PARR)
% ASH	3.51	3.91		(4.52%MM)
% CARBON	69.27	77.27	80.41	80.93
% HYDROGEN	5.29 (*)	5.90	6.14	6.18
% NITROGEN	1.33	1.48	1.54	1.55
% TOTAL SULFUR	0.48	0.54	0.56	
% OXYGEN(DIFF)	9.77 (*)	10.90	11.34	11.34

(*)-EXCLUDES MOISTURE

ELEMENTAL ANALYSIS	DRY	DMMF(MOD.P)	DMMF(DIR.)
		(4.46%MM)	(%MM)
% CARBON	77.20	80.80	
% HYDROGEN	5.85	6.12	
% NITROGEN	1.48	1.55	
% ORGANIC SULFUR	0.52	0.54	
% OXYGEN(DIFF)	10.49	10.98	
% MINERAL MATTER (INCL. 0.04% FES2)	4.46		

SULFUR FORMS	% PYRITIC	% SULFATIC	% ORGANIC	% TOTAL
DRY	0.02	0.00	0.52	0.54
DAF	0.02	0.00	0.54	0.56

DRY % CHLORINE = 0.06 DRY % CO2 = 0.26
MOTT-SPOONER DIFFERENCE = -23.

CALORIFIC VALUE (GROSS, BTU/LB)	DRY	AS REC'D MOIST.	EQUIL. MOIST.
MM-CONTAINING	14069.	12613.	12407.
MM-FREE (PARR)	14707.	13120.	12898.
MM-FREE (MOD. P)	14724.	13137.	12914.
NET CV, DMMF BTU/LB	14152.		

ATOM RATIOS (DMMF)	PARR	MOD.PARR	DIRECT
ATOMIC H/C	0.9171	0.9101	
ATOMIC O/C	0.1052	0.1020	

SAMPLE IDENTIFICATION:

PSU NUMBER	-> PSOC-1503
SEAM NAME	-> BLIND CANYON
ALTERNATE SEAM NAME	->
APPARENT RANK	-> HVB

SAMPLE LOCATION:

COUNTRY	-> USA
STATE	-> UTAH

** PENN STATE COAL DATA BASE **
** PSOC-1503 **
** 09/14/92 **
** PAGE 3 **

* * * * * RANK CALCULATIONS * * * * *

APPARENT RANK (AS REC'D MOIST.)	-> HVB	INTERNATIONAL RANK : AS REC'D MOIST.	->
ASTM RANK (EQUIL. MOIST.)	-> HVC	EQUIL. MOIST.	->
REFLECTANCE RANK CATEGORY	-> HVB	REPORTED RANK :	->

* * * * * PETROGRAPHIC DATA * * * * *

MACERAL COMPOSITION (WHITE LIGHT ANALYSIS)

	VITRINITE	PSEUDO-VITRINITE	FUSINITE	SEMI-FUSINITE	MACRINITE	MICRINITE	SCLERO-TINITE	SPOR-INITE	RESINITE	ALGINITE	CUTINITE	
DMMF VOL. %	91.1	0.0	1.3	3.7	0.9	1.5	0.3	1.0	0.2	0.0	0.0	
DRY VOL. %	89.1	0.0	1.3	3.6	0.9	1.5	0.3	1.0	0.2	0.0	0.0	2.2 % MM
DRY WT. %	86.5	0.0	1.4	3.8	0.9	1.5	0.3	0.9	0.2	0.0	0.0	4.5 % MM

REFLECTANCE DATA — VITRINITE : HIGH: 0.68 LOW: 0.53 MEAN-MAX: 0.62

VITRINITE TYPES	V 5	V 6
PERCENT	26.0	74.0

* * * * * CAKING AND MECHANICAL PROPERTIES * * * * *

GIESELER COAL PLASTOMETER:

INIT. SOFTENING TEMP	400
TEMP. MAX. FLUIDITY	422
SOLIDIFICATION TEMP.	439
FLUID TEMP. RANGE	39
MAXIMUM FLUIDITY	2

WASHABILITY DATA AVAILABLE? NO

GRAY-KING COKE TYPE	
HARDGROVE GRINDABILITY	61.5
FREE SWELLING INDEX	2.5
VICKERS HARDNESS NUMBER	

SAMPLE IDENTIFICATION:

PSU NUMBER	-> PSOC-1503
SEAM NAME	-> BLIND CANYON
ALTERNATE SEAM NAME	->
APPARENT RANK	-> HVB

SAMPLE LOCATION:

COUNTRY	-> USA
STATE	-> UTAH

** PENN STATE COAL DATA BASE **
** PSOC-1503 **
** 09/14/92 **
** PAGE 4 **

MAJOR ELEMENT ANALYSIS

% HTA = 3.80

	SIO2	AL2O3	TIO2	FE2O3	MGO	CAO	NA2O	K2O	P2O5	SO3
OXIDE % OF HTA	51.5	12.9	0.85	6.73	0.93	7.56	9.24	0.53	0.07	8.10
	SI	AL	TI	FE	MG	CA	NA	K	P	S
ELEMENT % OF TOTAL DRY COAL	0.9	0.3	0.02	0.18	0.02	0.21	0.26	0.02	0.001	0.54

TRACE ELEMENT ANALYSIS

% HTA = 3.80

	PPM HTA	PPM TOTAL COAL		PPM HTA	PPM TOTAL COAL		PPM HTA	PPM TOTAL COAL	VOLATILES	PPM TOTAL COAL
AG			GE			SN			AS	
B			LA			SR	1350.	51.	BR	
BA	270.	10.	LI			TH			CD	
BE	9.0	0.3	MN	93.	4.	U			CL	600.
BI			MO			V	90.	3.	F	
CE			NB			Y			HG	
CO			NI	80.	3.	YB			SB	
CR	120.	5.	PB			ZN	40.	2.	SE	
CU	190.	7.	RB	20.	1.	ZR	460.	17.		
GA			SC							

SAMPLE IDENTIFICATION:

PSU NUMBER	-> PSOC-1503
SEAM NAME	-> BLIND CANYON
ALTERNATE SEAM NAME	->
APPARENT RANK	-> HVB

SAMPLE LOCATION:

COUNTRY	-> USA
STATE	-> UTAH

** PENN STATE COAL DATA BASE **
** PSOC-1503 **
** 09/14/92 **
** PAGE 5 **

ASH FUSION TEMPERATURES (ALL TEMPERATURES IN DEGREES F)

	REDUCING	OXIDIZING
INITIAL DEFORMATION	1875.	1970.
SOFTENING	2015.	2065.
HEMISPHERICAL	2325.	2420.
FLUID	2440.	2475.

** PENN STATE COAL DATA BASE **
**
** DECS-6 **
**
** 09/14/92 **
** PAGE 1 **

SAMPLE IDENTIFICATION:

PSU NUMBER	-> DECS-6
SEAM NAME	-> Blind Canyon
ALTERNATE SEAM NAME	->
APPARENT RANK	-> HVA

SAMPLE HISTORY:

SAMPLING DATE & AGENCY	-> 6/ 7/90 ; PSU
SAMPLE TYPE	-> CHANNEL-WORKING SECTION
ADDITIONAL INFORMATION	-> TOP 8' OF 8' 6" SEAM

MINE INFORMATION:

RESERVES	->
ANNUAL PRODUCTION	->

SEAM INFORMATION:

AGE OF SEAM	-> U. CRET.
GROUP	-> Mesaverde
FORMATION	-> Blackhawk
SEAM THICKNESS	-> 8 FT. 6 IN.

SAMPLE LOCATION:

COUNTRY	-> USA
STATE	-> UTAH
COUNTY	-> Emery
TOWNSHIP	->
CITY	-> Huntington
COAL PROVINCE	-> ROCKY MOUNTAIN
REGION	-> UINTA
MAP REFERENCE: LATITUDE	-> 39 D 21 M 44 S
LONGITUDE	-> 111 D 10 M 4 S
QUADRANGLE	-> Mahogany Point

LIFE EXPECTANCY	->
MINING METHOD	-> UNDERGROUND

SAMPLE IDENTIFICATION:

PSU NUMBER	-> DECS-6
SEAM NAME	-> Blind Canyon
ALTERNATE SEAM NAME	->
APPARENT RANK	-> HVA

SAMPLE LOCATION:

COUNTRY	-> USA
STATE	-> UTAH

** PENN STATE COAL DATA BASE **
** DECS-6 **
** 09/14/92 **
** PAGE 2 **

* * * * * C H E M I C A L D A T A * * * * *

PROXIMATE ANALYSIS	AS REC'D	DRY	DAF	DMMF(PARR)
% MOISTURE	4.73			
% ASH	5.56	5.84		
% VOLATILE	42.40	44.50	47.26	46.94
% FIXED CARBON	47.31	49.66	52.74	53.06

% EQUILIBRIUM MOISTURE = 4.85
MM-FREE = 5.18

ULTIMATE ANALYSIS	AS REC'D	DRY	DAF	DMMF(PARR)
% ASH	5.56	5.84		(6.53%MM)
% CARBON	72.91	76.53	81.28	81.87
% HYDROGEN	5.60 (*)	5.88	6.24	6.29
% NITROGEN	1.39	1.46	1.55	1.56
% TOTAL SULFUR	0.38	0.40	0.42	
% OXYGEN(DIFF)	9.42 (*)	9.89	10.50	10.27

(*)-EXCLUDES MOISTURE

ELEMENTAL ANALYSIS	DRY	DMMF(MOD.P)	DMMF(DIR.)
		(6.67%MM)	(%MM)
% CARBON	76.27	81.72	
% HYDROGEN	5.80	6.22	
% NITROGEN	1.46	1.56	
% ORGANIC SULFUR	0.37	0.40	
% OXYGEN(DIFF)	9.43	10.10	
% MINERAL MATTER (INCL. 0.04% FES2)	6.67		

SULFUR FORMS	% PYRITIC	% SULFATIC	% ORGANIC	% TOTAL
DRY	0.02	0.01	0.37	0.40
DAF	0.02	0.01	0.39	0.42

DRY % CHLORINE = 0.12 DRY % CO2 = 0.96

MOTT-SPOONER DIFFERENCE = -72.

CALORIFIC VALUE (GROSS, BTU/LB)	DRY	AS REC'D MOIST.	EQUIL. MOIST.
MM-CONTAINING	13923.	13264.	13248.
MM-FREE (PARR)	14874.	14124.	14105.
MM-FREE (MOD. P)	14917.	14163.	14144.
NET CV, DMMF BTU/LB	14333.		

ATOM RATIOS (DMMF)	PARR	MOD.PARR	DIRECT
ATOMIC H/C	0.9228	0.9141	
ATOMIC O/C	0.0942	0.0928	

SAMPLE IDENTIFICATION:

PSU NUMBER	-> DECS-6
SEAM NAME	-> Blind Canyon
ALTERNATE SEAM NAME	->
APPARENT RANK	-> HVA

SAMPLE LOCATION:

COUNTRY	-> USA
STATE	-> UTAH

** PENN STATE COAL DATA BASE **
** DECS-6 **
** 09/14/92 **
** PAGE 3 **

* * * * * RANK CALCULATIONS * * * * *

APPARENT RANK (AS REC'D MOIST.)	-> HVA	INTERNATIONAL RANK : AS REC'D MOIST.	->
ASTM RANK (EQUIL. MOIST.)	-> HVA	EQUIL. MOIST.	->
REFLECTANCE RANK CATEGORY	-> HVB	REPORTED RANK :	->

* * * * * PETROGRAPHIC DATA * * * * *

MACERAL COMPOSITION (WHITE LIGHT AND FLUORESCENCE ANALYSIS)

	VITRINITE	PSEUDO-VITRINITE	FUSINITE	SEMI-FUSINITE	MACRINITE	MICRINITE	SCLERO-TINITE	SPOR-INITE	RESINITE	ALGINITE	CUTINITE	
DMMF VOL. %	69.1	0.0	1.8	5.6	5.3	0.9	0.0	11.1	5.0	0.4	0.8	
DRY VOL. %	66.8	0.0	1.7	5.4	5.1	0.9	0.0	10.7	4.8	0.4	0.8	3.3 % MM
DRY WT. %	64.5	0.0	1.9	5.6	5.3	0.9	0.0	9.7	4.4	0.4	0.7	6.5 % MM

REFLECTANCE DATA ---- VITRINITE : HIGH: 0.82 LOW: 0.58 MEAN-MAX: 0.66

VITRINITE TYPES	V 5	V 6	V 7	V 8
PERCENT	3.0	77.0	19.0	1.0

* * * * * CAKING AND MECHANICAL PROPERTIES * * * * *

GIESELER COAL PLASTOMETER:

INIT. SOFTENING TEMP	400
TEMP. MAX. FLUIDITY	419
SOLIDIFICATION TEMP.	438
FLUID TEMP. RANGE	38
MAXIMUM FLUIDITY	3

WASHABILITY DATA AVAILABLE? NO

GRAY-KING COKE TYPE	
HARDGROVE GRINDABILITY	44.5
FREE SWELLING INDEX	2.0
VICKERS HARDNESS NUMBER	

SAMPLE IDENTIFICATION:

PSU NUMBER	-> DECS-6
SEAM NAME	-> Blind Canyon
ALTERNATE SEAM NAME	->
APPARENT RANK	-> HVA

SAMPLE LOCATION:

COUNTRY	-> USA
STATE	-> UTAH

** PENN STATE COAL DATA BASE **
** DECS-6 **
** 09/14/92 **
** PAGE 4 **

MAJOR ELEMENT ANALYSIS

% HTA = 6.26

	SIO2	AL2O3	TIO2	FE2O3	MGO	CAO	NA2O	K2O	P2O5	SO3
OXIDE % OF HTA	50.3	15.3	0.96	6.88	1.26	12.0	6.91	0.59	0.38	4.80
	SI	AL	TI	FE	MG	CA	NA	K	P	S
ELEMENT % OF TOTAL DRY COAL	1.5	0.5	0.04	0.30	0.05	0.5	0.32	0.03	0.01	0.40

TRACE ELEMENT ANALYSIS

% HTA = 6.26

	PPM HTA	PPM TOTAL COAL		PPM HTA	PPM TOTAL COAL		PPM HTA	PPM TOTAL COAL	VOLATILES	PPM TOTAL COAL
AG			GE			SN			AS	
B			LA			SR	1353.	85.	BR	
BA	1443.	90.	LI			TH			CD	
BE	4.0	0.3	MN	155.	10.	U			CL	1200.
BI			MO			V	140.	9.	F	
CE			NB			Y			HG	
CO			NI	< 25.	< 2.	YB			SB	
CR	95.	6.	PB			ZN	70.	4.	SE	
CU	150.	9.	RB	25.	2.	ZR	470.	29.		
GA			SC							

SAMPLE IDENTIFICATION:

PSU NUMBER	-> DECS-6
SEAM NAME	-> Blind Canyon
ALTERNATE SEAM NAME	->
APPARENT RANK	-> HVA

SAMPLE LOCATION:

COUNTRY	-> USA
STATE	-> UTAH

** PENN STATE COAL DATA BASE **
** DECS-6 **
** 09/14/92 **
** PAGE 5 **

ASH FUSION TEMPERATURES (ALL TEMPERATURES IN DEGREES F)

	REDUCING	OXIDIZING
INITIAL DEFORMATION	1900.	2250.
SOFTENING	2020.	2345.
HEMISPHERICAL	2090.	2400.
FLUID	2240.	2440.

** PENN STATE COAL DATA BASE **
**
** PSOC-1444 **
**
** 09/14/92 **
** PAGE 1 **

SAMPLE IDENTIFICATION:

PSU NUMBER	-> PSOC-1444
SEAM NAME	-> UNNAMED
ALTERNATE SEAM NAME	->
APPARENT RANK	-> SUBBIT C

SAMPLE LOCATION:

COUNTRY	-> USA
STATE	-> TEXAS
COUNTY	-> FREESTONE
TOWNSHIP	->
CITY	-> FAIRFIELD
COAL PROVINCE	-> GULF
REGION	->
MAP REFERENCE: LATITUDE	-> 31 D 49 M 0 S
LONGITUDE	-> 96 D 7 M 0 S
QUADRANGLE	-> YOUNG (7.5')

SAMPLE HISTORY:

SAMPLING DATE & AGENCY	-> 3/30/85 ; PSU
SAMPLE TYPE	-> CHANNEL-WORKING SECTION
ADDITIONAL INFORMATION	-> UNKNOWN AMOUNT(<1')BELOW MINE FLOOR NOT SAMPLED

MINE INFORMATION:

RESERVES	->
ANNUAL PRODUCTION	-> 6000 THOUSAND TONS
LIFE EXPECTANCY	-> 25 YEARS
MINING METHOD	-> STRIP

SEAM INFORMATION:

AGE OF SEAM	-> EOCENE
GROUP	-> UPPER WILCOX
FORMATION	-> UPPER CALVERT BLUFF
SEAM THICKNESS	-> 7 FT. 3 IN.

SAMPLE IDENTIFICATION:

PSU NUMBER	-> PSOC-1444
SEAM NAME	-> UNNAMED
ALTERNATE SEAM NAME	->
APPARENT RANK	-> SUBBIT C

SAMPLE LOCATION:

COUNTRY	-> USA
STATE	-> TEXAS

** PENN STATE COAL DATA BASE **
** PSOC-1444 **
** 09/14/92 **
** PAGE 2 **

* * * * * C H E M I C A L D A T A * * * * *

PROXIMATE ANALYSIS	AS REC'D	DRY	DAF	DMMF(PARR)
% MOISTURE	31.91			
% ASH	11.47	16.84		
% VOLATILE	29.55	43.40	52.19	51.23
% FIXED CARBON	27.07	39.76	47.81	48.77

% EQUILIBRIUM MOISTURE = 33.12

MM-FREE = 37.97

ULTIMATE ANALYSIS	AS REC'D	DRY	DAF	DMMF(PARR)
% ASH	11.47	16.84		(18.83%MM)
% CARBON	42.07	61.78	74.29	76.11
% HYDROGEN	2.74 (*)	4.03	4.85	4.96
% NITROGEN	0.78	1.15	1.38	1.42
% TOTAL SULFUR	0.80	1.17	1.41	
% OXYGEN(DIFF)	10.23 (*)	15.03	18.07	17.51

(*)-EXCLUDES MOISTURE

ELEMENTAL ANALYSIS	DRY	DMMF(MOD.P) (19.09%MM)	DMMF(DIR.) (%MM)
% CARBON	61.66	76.21	
% HYDROGEN	3.81	4.71	
% NITROGEN	1.15	1.42	
% ORGANIC SULFUR	1.10	1.36	
% OXYGEN(DIFF)	13.18	16.29	
% MINERAL MATTER (INCL. 0.09% FES2)	19.09		

SULFUR FORMS	% PYRITIC	% SULFATIC	% ORGANIC	% TOTAL
DRY	0.05	0.01	1.10	1.17
DAF	0.06	0.01	1.32	1.41

DRY % CHLORINE = 0.08 DRY % CO2 = 0.43

MOTT-SPOONER DIFFERENCE = 406.

CALORIFIC VALUE (GROSS, BTU/LB)	DRY	AS REC'D MOIST.	EQUIL. MOIST.
MM-CONTAINING	10810.	7361.	7230.
MM-FREE (PARR)	13246.	8397.	8227.
MM-FREE (MOD. P)	13358.	8458.	8286.
NET CV, DMMF BTU/LB	12896.		

ATOM RATIOS (DMMF)	PARR	MOD.PARR	DIRECT
ATOMIC H/C	0.7835	0.7425	
ATOMIC O/C	0.1727	0.1605	

SAMPLE IDENTIFICATION:

PSU NUMBER	-> PSOC-1444
SEAM NAME	-> UNNAMED
ALTERNATE SEAM NAME	->
APPARENT RANK	-> SUBBIT C

SAMPLE LOCATION:

COUNTRY	-> USA
STATE	-> TEXAS

** PENN STATE COAL DATA BASE **
** PSOC-1444 **
** 09/14/92 **
** PAGE 3 **

* * * * * RANK CALCULATIONS * * * * *

APPARENT RANK (AS REC'D MOIST.)	-> SUBBIT C	INTERNATIONAL RANK : AS REC'D MOIST.	->
ASTM RANK (EQUIL. MOIST.)	-> LIGNITE	EQUIL. MOIST.	->
REFLECTANCE RANK CATEGORY	->	REPORTED RANK :	-> LIGNITE

* * * * * PETROGRAPHIC DATA * * * * *

MACERAL COMPOSITION (WHITE LIGHT ANALYSIS)

	TEXT-INITE	ULM-INITE	HUMO-DETRINITE	GEL-INITE	CORPO-HUMINITE	SPOR-INITE	CUT-INITE	RES-INITE	ALG-INITE	FUS-INITE	SEMI-FUSINITE	MAC-RINITE	SCLERO-TINITE	
DMMF VOL. %	0.1	69.3	11.9	2.8	0.6	1.0	0.0	0.5	0.0	3.9	5.6	3.7	0.6	
DRY WT. %	0.1	56.3	9.7	2.3	0.5	0.8	0.0	0.4	0.0	3.2	4.5	3.0	0.5	18.8 % MM.

DMMF VOL % HUMINITE = 84.7

ULMINITE REFLECTANCE DATA: HIGH: 0.54 LOW: 0.37 MEAN-MAX: 0.45

* * * * * CAKING AND MECHANICAL PROPERTIES * * * * *

GIESELER COAL PLASTOMETER:

- INIT. SOFTENING TEMP
- TEMP. MAX. FLUIDITY
- SOLIDIFICATION TEMP.
- FLUID TEMP. RANGE
- MAXIMUM FLUIDITY

WASHABILITY DATA AVAILABLE? NO

GRAY-KING COKE TYPE

HARDGROVE GRINDABILITY 77.2

FREE SWELLING INDEX 0.0

VICKERS HARDNESS NUMBER

SAMPLE IDENTIFICATION:

PSU NUMBER	-> PSOC-1444
SEAM NAME	-> UNNAMED
ALTERNATE SEAM NAME	->
APPARENT RANK	-> SUBBIT C

SAMPLE LOCATION:

COUNTRY	-> USA
STATE	-> TEXAS

** PENN STATE COAL DATA BASE **
** PSOC-1444 **
** 09/14/92 **
** PAGE 4 **

MAJOR ELEMENT ANALYSIS

% HTA = 13.28

	SIO2	AL2O3	TIO2	FE2O3	MGO	CAO	NA2O	K2O	P2O5	SO3
OXIDE % OF HTA	48.8	12.9	1.12	5.66	3.06	15.2	0.52	0.97	0.08	11.3
	SI	AL	TI	FE	MG	CA	NA	K	P	S
ELEMENT % OF TOTAL DRY COAL	3.0	0.9	0.09	0.53	0.25	1.4	0.05	0.11	0.005	1.2

TRACE ELEMENT ANALYSIS

% HTA = 13.28

	PPM HTA	PPM TOTAL COAL		PPM HTA	PPM TOTAL COAL		PPM HTA	PPM TOTAL COAL	VOLATILES	PPM TOTAL COAL
AG			GE			SN			AS	
B			LA			SR	1690.	224.	BR	
BA	1170.	155.	LI			TH			CD	
BE	4.0	0.5	MN	1410.	187.	U			CL	800.
BI			MO			V	130.	17.	F	
CE			NB			Y			HG	
CO			NI			YB			SB	
CR	85.	11.	PB			ZN	10.	1.	SE	
CU	85.	11.	RB	30.	4.	ZR	370.	49.		
GA			SC							

SAMPLE IDENTIFICATION:

PSU NUMBER	-> PSOC-1444
SEAM NAME	-> UNNAMED
ALTERNATE SEAM NAME	->
APPARENT RANK	-> SUBBIT C

SAMPLE LOCATION:

COUNTRY	-> USA
STATE	-> TEXAS

** PENN STATE COAL DATA BASE **
** PSOC-1444 **
** 09/14/92 **
** PAGE 5 **

ASH FUSION TEMPERATURES (ALL TEMPERATURES IN DEGREES F)

	REDUCING	OXIDIZING
INITIAL DEFORMATION	2135.	2170.
SOFTENING	2160.	2245.
HEMISPHERICAL	2360.	2335.
FLUID	2470.	2485.

SAMPLE IDENTIFICATION:

PSU NUMBER	-> DECS-1
SEAM NAME	-> BOTTOM
ALTERNATE SEAM NAME	->
APPARENT RANK	-> SUBBIT C

SAMPLE HISTORY:

SAMPLING DATE & AGENCY	-> 12/11/89 ; PSU
SAMPLE TYPE	-> CHANNEL-WHOLE SEAM
ADDITIONAL INFORMATION	->

MINE INFORMATION:

RESERVES	->
ANNUAL PRODUCTION	-> 5500 THOUSAND TONS

SEAM INFORMATION:

AGE OF SEAM	-> EOCENE
GROUP	-> Upper Wilcox
FORMATION	-> Upper Calvert Bluff
SEAM THICKNESS	-> 9 FT. 6 IN.

SAMPLE LOCATION:

COUNTRY	-> USA
STATE	-> TEXAS
COUNTY	-> FREESTONE
TOWNSHIP	->
CITY	-> FAIRFIELD
COAL PROVINCE	-> GULF
REGION	->
MAP REFERENCE: LATITUDE	-> 31 D 51 M 10 S
LONGITUDE	-> 96 D 3 M 59 S
QUADRANGLE	-> YOUNG
LIFE EXPECTANCY	-> 25 YEARS
MINING METHOD	-> STRIP

** PENN STATE COAL DATA BASE **
** DECS-1 **
** 10/29/92 **
** PAGE 1 **

SAMPLE IDENTIFICATION:

PSU NUMBER	-> DECS-1
SEAM NAME	-> BOTTOM
ALTERNATE SEAM NAME	->
APPARENT RANK	-> SUBBIT C

SAMPLE LOCATION:

COUNTRY	-> USA
STATE	-> TEXAS

** PENN STATE COAL DATA BASE **
** DECS-1 **
** 10/29/92 **

* * * * * C H E M I C A L D A T A * * * * *

PROXIMATE ANALYSIS	AS REC'D	DRY	DAF	DMMF(PARR)
% MOISTURE	30.00			
% ASH	11.07	15.81		
% VOLATILE	33.18	47.40	56.30	55.52
% FIXED CARBON	25.75	36.79	43.70	44.48

% EQUILIBRIUM MOISTURE = 31.47
MM-FREE = 35.89

ULTIMATE ANALYSIS	AS REC'D	DRY	DAF	DMMF(PARR)
% ASH	11.07	15.81		(17.62%MM)
% CARBON	43.77	62.53	74.27	75.90
% HYDROGEN	3.32 (*)	4.75	5.64	5.77
% NITROGEN	0.86	1.23	1.46	1.49
% TOTAL SULFUR	0.69	0.99	1.18	
% OXYGEN(DIFF)	10.28 (*)	14.69	17.45	16.84

(*)-EXCLUDES MOISTURE

ELEMENTAL ANALYSIS	DRY	DMMF(MOD.P)	DMMF(DIR.)
		(17.97%MM)	(%MM)
% CARBON	62.45	76.13	
% HYDROGEN	4.55	5.54	
% NITROGEN	1.23	1.50	
% ORGANIC SULFUR	0.86	1.05	
% OXYGEN(DIFF)	12.94	15.78	
% MINERAL MATTER (INCL. 0.21% FES2)	17.97		

SULFUR FORMS	% PYRITIC	% SULFATIC	% ORGANIC	% TOTAL
DRY	0.11	0.02	0.86	0.99
DAF	0.13	0.02	1.02	1.18

DRY % CHLORINE = 0.11 DRY % CO2 = 0.29
MOTT-SPOONER DIFFERENCE = -115.

CALORIFIC VALUE (GROSS, BTU/LB)	DRY	AS REC'D MOIST.	EQUIL. MOIST.
MM-CONTAINING	10956.	7669.	7508.
MM-FREE (PARR)	13239.	8709.	8501.
MM-FREE (MOD. P)	13349.	8768.	8558.
NET CV, DMMF BTU/LB	12812.		

ATOM RATIOS (DMMF)	PARR	MOD.PARR	DIRECT
ATOMIC H/C	0.9124	0.8744	
ATOMIC O/C	0.1665	0.1556	

SAMPLE IDENTIFICATION:

PSU NUMBER	-> DECS-1
SEAM NAME	-> BOTTOM
ALTERNATE SEAM NAME	->
APPARENT RANK	-> SUBBIT C

SAMPLE LOCATION:

COUNTRY	-> USA
STATE	-> TEXAS

** PENN STATE COAL DATA BASE **
** DECS-1 **
** 10/29/92 **
** PAGE 3 **

* * * * * R A N K C A L C U L A T I O N S * * * * *

APPARENT RANK (AS REC'D MOIST.)	-> SUBBIT C	INTERNATIONAL RANK : AS REC'D MOIST.	->
ASTM RANK (EQUIL. MOIST.)	-> SUBBIT C	EQUIL. MOIST.	->
REFLECTANCE RANK CATEGORY	->	REPORTED RANK :	->

* * * * * P E T R O G R A P H I C D A T A * * * * *

MACERAL COMPOSITION (WHITE LIGHT AND FLUORESCENCE ANALYSIS)

	TEXT-INITE	ULM-INITE	HUMO-DETRINITE	GEL-INITE	CORPO-HUMINITE	SPOR-INITE	CUT-INITE	RES-INITE	ALG-INITE	FUS-INITE	SEMI-FUSINITE	MAC-RINITE	SCLERO-TINITE	
DMMF VOL. %	0.0	25.4	45.5	0.4	7.1	13.2	0.2	1.5	0.0	1.3	1.8	2.9	0.7	
DRY WT. %	0.0	20.9	37.5	0.3	5.8	10.9	0.2	1.2	0.0	1.1	1.5	2.4	0.6	17.6 % MM.

DMMF VOL % HUMINITE = 78.4

ULMINITE REFLECTANCE DATA: HIGH: 0.51 LOW: 0.20 MEAN-MAX: 0.35

* * * * * C A K I N G A N D M E C H A N I C A L P R O P E R T I E S * * * * *

GIESELER COAL PLASTOMETER:		GRAY-KING COKE TYPE	
INIT. SOFTENING TEMP		HARDGROVE GRINDABILITY	68.2
TEMP. MAX. FLUIDITY		FREE SWELLING INDEX	1.0
SOLIDIFICATION TEMP.		VICKERS HARDNESS NUMBER	
FLUID TEMP. RANGE			
MAXIMUM FLUIDITY			

WASHABILITY DATA AVAILABLE? NO

SAMPLE IDENTIFICATION:

PSU NUMBER	-> DECS-1
SEAM NAME	-> BOTTOM
ALTERNATE SEAM NAME	->
APPARENT RANK	-> SUBBIT C

SAMPLE LOCATION:

COUNTRY	-> USA
STATE	-> TEXAS

** PENN STATE COAL DATA BASE **
** DECS-1 **
** 10/29/92 **
** PAGE 4 **

MAJOR ELEMENT ANALYSIS

% HTA = 17.14

	SIO2	AL2O3	TIO2	FE2O3	MGO	CAO	NA2O	K2O	P2O5	SO3
OXIDE % OF HTA	45.6	17.0	1.26	4.18	2.68	5.50	0.42	0.60	0.23	12.7
	SI	AL	TI	FE	MG	CA	NA	K	P	S
ELEMENT % OF TOTAL DRY COAL	3.7	1.5	0.13	0.50	0.28	0.67	0.05	0.09	0.02	1.0

TRACE ELEMENT ANALYSIS

% HTA = 17.14

	PPM HTA	PPM TOTAL COAL		PPM HTA	PPM TOTAL COAL		PPM HTA	PPM TOTAL COAL	VOLATILES	PPM TOTAL COAL
AG			GE			SN			AS	
B			LA			SR	2960.	507.	BR	
BA	1344.	230.	LI			TH			CD	
BE	5.0	0.9	MN	1239.	212.	U			CL	1100.
BI			MO			V	35.	6.	F	
CE			NB			Y			HG	
CO			NI	< 25.	< 4.	YB			SB	
CR	95.	16.	PB			ZN	50.	9.	SE	
CU	130.	22.	RB	30.	5.	ZR	270.	46.		
GA			SC							

SAMPLE IDENTIFICATION:

PSU NUMBER	-> DECS-1
SEAM NAME	-> BOTTOM
ALTERNATE SEAM NAME	->
APPARENT RANK	-> SUBBIT C

SAMPLE LOCATION:

COUNTRY	-> USA
STATE	-> TEXAS

** PENN STATE COAL DATA BASE **
** DECS-1 **
** 10/29/92 **
** PAGE 5 **

ASH FUSION TEMPERATURES (ALL TEMPERATURES IN DEGREES F)

	REDUCING	OXIDIZING
INITIAL DEFORMATION	1840.	2120.
SOFTENING	2000.	2220.
HEMISPHERICAL	2060.	2280.
FLUID	2100.	2330.

DATE
FILMED
6/4/93